Schistosoma mansoni: Integration of Phosphoproteomics, Kinomics and CaMKII

Natasha Lana Hirst, BSc, MSc

This thesis is being submitted in partial fulfilment of the requirements of Kingston University for the degree of Doctor of Philosophy

July 2019

Acknowledgements

Abstract

Schistosoma mansoni is a parasitic trematode and the causative agent of the debilitating disease human schistosomiasis. This study focused on global signalling processes which occur in the parasite and on Ca^{2+}/Calmodulin Kinase II (CaMKII) signalling. Phosphoproteomics of a mixed population of adult worms was performed, identifying a total of 15,844 phosphopeptides, from 3,176 proteins with 12,936 unique phosphorylation sites. Analysis of the phosphorylated sites/proteins provided valuable insights into the complexities of signalling in this parasite, including insights into overrepresented and novel phosphorylation site motifs, putative upstream protein kinases, molecular function, and interactions between phosphoproteins (1,586 nodes and 12,733 edges). Highly connected interaction clusters highlighted the pivotal role of phosphorylated ribosomal and ribosomal biogenesis proteins, proteasome, and spliceosome proteins within *S. mansoni*. Furthermore, analysis of the protein kinases revealed 808 phosphorylation sites amongst 136 protein kinases representing 54% of the *S. mansoni* kinome. This novel, deep, phosphoproteomic dataset supported the development of the first parasite-specific kinomic array comprising 96 peptides with many upstream kinases predicted. The array was deployed to identify eight peptides (proteins) which were significantly differentially phosphorylated by homogenates from male and female adult worms: the serine/threonine protein kinases CDK/PITSLRE, AMPK, AKT, SmTK4, insulin receptor, protein phosphatase 2c gamma, Rho2 GTPase, and vacuolar protein sorting 26. CaMKII was identified as a protein of interest in the phosphoproteomic analysis, further investigations were carried out. Using anti-phospho-CaMKII antibodies, CaMKII was detected at approximately 57 kDa in cercariae, somules, and adult worms. Activated CaMKII was located visually in the nervous system, excretory system, sensory structures, and the tegument as well as in the female vitellaria. Inhibition assays determined that CaMKII

phosphorylation (activation) in somules could be suppressed by KN93, and further assays found that the anti-schistosomal drug praziquantel had a significant effect on CaMKII activation in *S. mansoni*. Finally, suppression of CaMKII expression by small interfering RNA (siRNA) resulted in a 66% and 52% reduction in males and females respectively. Collectively these studies show that phosphorylation plays a wide reaching and crucial role in the complex signalling pathways that ultimately control *S. mansoni* from highlighting their involvement in reproduction and proliferation, host location and movement to commanding cell death, the elucidation of these phosphorylating pathways are vital to understanding this parasites biology.

Contents

1 Introduction 1

1.1 Schistosomiasis 2

1.2 Epidemiology 3

1.3 Pathogenesis of Schistosomiasis 6

1.4 Control and Prevention of Schistosomiasis 8

1.4.1 Praziquantel 8

1.4.2 Vaccine Development 11

1.5 Life Cycle of Schistosomes 13

1.6 The Biology of Selected Schistosome Life Stages 17

1.6.1 The Cercaria 17

1.6.2 The Somule 18

1.6.3 The Adult Male and Female Worm 20

1.7 Cell Signalling in *S. mansoni* 21

1.7.1 Protein Kinases 22

1.7.2 Protein Kinases in *S. mansoni* 23

2 General Materials and Methods 27

2.1 Reagents 28

2.1.1 Antibodies 28

2.1.2 Immunohistochemistry Reagents 28

2.1.3 Western Blotting Reagents 29

2.1.4 Other Consumables and Reagents 29

2.2 General Methods 30

2.2.1 Ethics 30

2.2.2 SDS-Page and Western Blotting 30

2.2.3 Snail Husbandry 32

2.2.4 Isolation of *S. mansoni* for experiments 33

2.2.5 Statistical Analysis 35

3 Phosphoproteomics of adult *s. mansoni* 36

3.1 Introduction to Phosphoproteomics 37

3.1.1 Phosphoproteomics in Parasites 38

3.1.2 Proteomics and Phosphoproteomics in Schistosomes 39

3.1.3 Aims 40

3.2 Methods 41

3.2.1 Preparation of material for PTM Scan analysis 41

3.2.2 Phosphoproteomic Analysis 42
3.2.3 Bioinformatics – Primary Peptide Scan 44
3.2.4 PTM Scan Bioinformatics – Motif Analysis 45
3.2.5 Upstream Kinase Motif Analysis 46
3.2.6 Gene Ontology 47
3.2.7 GO SLIM 47
3.2.8 Analysis of Protein Kinases 48
3.2.9 STRING Analysis 48
3.2.10 Phosphorylated Protein Interaction Network Analysis 49
3.2.11 KEGG Analysis 49
3.3 Results 50
3.3.1 Initial Bioinformatics 50
3.3.2 Phosphoproteomics of adult *S. mansoni* 51
3.3.3 Depth and Character of the *S. mansoni* phosphoproteome 57
3.3.4 Peptide Classification and Motif Analysis 61
3.3.5 Upstream Kinase Analysis 65
3.3.6 Phosphorylation of Eukaryotic Protein Kinases in *S. mansoni* 68
3.3.7 Gene Ontology 73
3.3.8 Phosphoproteins in the Tegument 80
3.3.9 Protein – Protein Interactions 82
3.3.10 KEGG Analysis 90
3.4 Discussion 93
3.4.1 Protein Kinases and Substrate Motif Analysis 94
3.4.2 Functional Annotation of *S. mansoni* Phosphoproteins 97
3.4.3 The *S. mansoni* Phosphointeractome 99
4 Schistosome specific Peptide array development 101
4.1 Introduction 102
4.1.1 SPOT Technology 102
4.1.2 Array Use in Parasitology 104
4.1.3 Array Use in Schistosomes 105
4.1.4 Kinomics using Peptide Arrays 106
4.1.5 Aims 109
4.2 Methods 110
4.2.1 Array Protocol 110
4.3 Results 117
4.3.1 Schistosome Specific Peptides 117
4.3.2 Preliminary Array Testing 117
4.3.3 Array Results 119

4.3.4 Quantification of Array Results 124
4.4 Discussion 129
4.4.1 Development of the Array 129
4.4.2 Preliminary Array Trials 130
4.4.3 Employment of the Developed Array 132
5 Investigation of Ca2+/Calmodulin dependent protein kinase II (CaMKII) signalling in *Schistosoma mansoni* 137
5.1 Introduction to CaMKII 138
5.1.1 Ca^{2+}/Calmodulin Dependant Protein Kinase II 138
5.1.2 CaMKII Signalling 139
5.1.3 CaMKII in Schistosomes 143
5.1.4 CaMKII Inhibitors 143
5.1.5 Aims 144
5.2 Methods 145
5.2.1 RNAi Reagents 145
5.2.2 Primary Antibodies 146
5.2.3 Lambda Phosphatase Assay 146
5.2.4 KN93 Inhibition Assays 147
5.2.5 Praziquantel Assays 148
5.2.6 Immunohistochemistry 149
5.2.7 RNAi 150
5.2.8 Worm Motility Analysis 151
5.2.9 Statistics 152
5.3 Results 153
5.3.1 Bioinformatics 153
5.3.2 Antibody Validation 156
5.3.3 Detection of phosphorylated CaMKII in *S. mansoni* Life Stages 157
5.3.4 Detection of Total CaMKII 159
5.3.5 Inhibition of *S. mansoni* CaMKII 161
5.3.6 Stimulation of CaMKII in Somules with PMA 165
5.3.7 Action of Praziquantel on Activated CaMKII in Somules and Adult Worms 167
5.3.8 Immunolocalization of Phosphorylated CaMKII in *S. mansoni* 170
5.3.9 RNAi of CaMKII in Adult Worms 186
5.3.10 Effect of CaMKII SiRNAi on Adult Worm Motility 190
5.4 Discussion 194
5.4.1 Detection of Activated CaMKII in schistosomes 195
5.4.2 Immunolocalization of Activated CaMKII in Schistosomes 196
5.4.3 Modulation of Activated CaMKII in *S. mansoni* 199

5.4.4 Effect of Praziquantel on Schistosomes – a link to CaMKII? 200
5.4.5 Reduced CaMKII and its effect on *S. mansoni* 202
6 Conclusion 204

Figures

Figure 1.1. World map depicting the distribution of the different species of human schistosome. 5

Figure 1.2. The *S. mansoni* granuloma. 8

Figure 1.3. The schistosome life cycle.. 16

Figure 1.4. Basic anatomy of the free-swimming cercariae..... 18

Figure 3.1. Analysis of phosphorylated proteins in adult *S. mansoni*. 53

Figure 3.2. Workflow diagram of processes carried out during the PTM Scan done in conjunction with Cell Signalling Technology..... 54

Figure 3.3. Graphical representation of phosphoproteomic data for adult *S. mansoni*.. 58

Figure 3.4 Overlap between IMAC and pS/pT IAP data. 59

Figure 3.5. Pie chart illustrating the proportion of *S. mansoni* adult worm peptides phosphorylated on either serine, threonine, or tyrosine residues. 60

Figure 3.6. The percentage distribution of phosphorylated serine, threonine, and tyrosine residues in the *S. mansoni* proteome. 61

Figure 3.7. Distribution of adult *S. mansoni* phosphorylation motif classes.. 62

Figure 3.8. Tyrosine centred motifs discovered in the *S. mansoni* phosphoproteome.... 63

Figure 3.9. Examples of serine and threonine centred motifs discovered in the *S. mansoni* phosphoproteome. 64

Figure 3.10. Distribution of substrate motifs generated from *S. mansoni* phosphopeptide data assigned to putative upstream protein kinases using Phosida. 67

Figure 3.11. Distribution of substrate motifs generated from *S. mansoni* phosphopeptide data assigned to putative upstream protein kinases using HPRD. 68

Figure 3.12. The distribution of protein kinases identified in the *S. mansoni* adult worm PTM scan across each of the PTM approaches.....69

Figure 3.13. The number of adult *S. mansoni* protein kinases identified possessing one or more phosphorylation sites within each of the 10 kinase groups.. 70

Figure 3.14 Schematics of four kinases; Smp_164930, Smp_008260, Smp_155720 and Smp_128480, d 73

Figure 3.15. Distribution of *S. mansoni* phosphoproteomic Gene Ontology (GO) assignments using Ensembl metazoa. 74

Figure 3.16. Biological Processes for *S. mansoni* adult phosphoproteins. 76

Figure 3.17. Cellular Components for *S. mansoni* adult phosphoproteins.....77

Figure 3.18. Molecular Function for *S. mansoni* adult phosphoproteins.. 78

Figure 3.19. Top 50 results from all GO SLIM hits for *S. mansoni* adult phosphoproteins. 79

Figure 3.20. The *S. mansoni* adult worm phosphoprotein interactome.. 85

Figure 3.21. Cluster 1 from Clusterviz MCODE analysis of the *S. mansoni* adult worm phosphoproteome. 87

Figure 3.22. Cluster 2 from Clusterviz MCODE analysis of the *S. mansoni* adult worm phosphoproteome.. 88

Figure 3.23. Cluster 3 from Clusterviz MCODE analysis of the *S. mansoni* adult worm phosphoproteome. 89

Figure 3.24. Cluster 4 from Clusterviz MCODE analysis of the *S. mansoni* adult worm phosphoproteome. 90

Figure 4.1. Schemaric diagram of generalised peptide array use. Modified from Intavis 103

Figure 4.2 Flow diagram portraying the decisions in choosing peptides for the development of the *S. mansoni* specific array using data obtained from Scansite 112

Figure 4.3. Failed CelluSpots custom *S. mansoni* peptide array..... 118

Figure 4.4. CelluSpots custom array incubated with adult male worm homogenate.... 119

Figure 4.5. Screening the CelluSpots custom array with reduced amounts of protein.. 121

Figure 4.6. CelluSpots custom array incubated with adult male or female homogenates. 123

Figure 4.7. Model representation of each of the four replicates of the custom..... 126

Figure 4.8. Graph illustrating the mean normalised spot intensities for each peptide .. 127

Figure 4.9. Phosphorylation of Src peptide (substrate) by *S. mansoni* adult worm homogenates..... 128

Figure 5.1. Structure of CaMKII.. 139

Figure 5.2. CaMKII domain structure. 141

Figure 5.3. Regulation of CaMKII by autophosphorylation. 142

Figure 5.4. Bioinformatic analysis of *S. mansoni* CaMKII..... 155

Figure 5.5. Detection of phosphorylated CaMKII in *S. mansoni*..... 157

Figure 5.6. Detection of phosphorylated CaMKII in *S. mansoni* life stages. 158

Figure 5.7. Detection of total CaMKII in *S. mansoni* life stages. 160

Figure 5.8. Gene expression of *S. mansoni* CaMKII. 161

Figure 5.9. Pharmacological inhibition of phosphorylated *S. mansoni* CaMKII by KN93.. 162

Figure 5.10. Temporal inhibition of *S. mansoni* CaMKII by KN93. 163

Figure 5.11. Pharmacological inhibition of phosphorylated CaMKII in *S. mansoni* homogenates.....164

Figure 5.12. Effect of PMA on *S. mansoni* CaMKII phosphorylation.. 166

Figure 5.13. The effect of PZQ on CaMKII phosphorylation in 24 h *in vitro* cultured *S. mansoni* somules. 169

Figure 5.14. The effect of praziquantel (PZQ) on CaMKII phosphorylation in mixed adult *S. mansoni* 169

Figure 5.15. *S. mansoni* cercariae negative controls. 171

Figure 5.16. Distribution of activated CaMKII in *S. mansoni* cercariae. 172

Figure 5.17. Distribution of activated CaMKII within the head of a cercaria. 173

Figure 5.18. Distribution of activated CaMKII in the nervous system of cercariae. 174

Figure 5.19. *S. mansoni* somule negative controls. 176

Figure 5.20. Distribution of activated CaMKII in the nervous system of 24 h *in vitro* cultured somules.....177

Figure 5.21. Serial optical z-sections through an *S. mansoni* somule highlighting activated CaMKII.. 178

Figure 5.22. Distribution of activated CaMKII possibly associated with flame cells in 24 h *in vitro* cultured somules.....179

Figure 5.23. *S. mansoni* adult male and female worm negative controls.....181

Figure 5.24. Distribution of activated CaMKII associated with the nervous system of adult male worms 182

Figure 5.25. Activated CaMKII associated with the tegument of adult male and female worms. 183

Figure 5.26. Distribution of activated CaMKII associated with the vitellaria of adult female worms 184

Figure 5.27. Distribution of activated CaMKII associated with the nervous system of adult female worms 185

Figure 5.28. SiRNA-mediated suppression of CaMKII in *S. mansoni*.. 189

Figure 5.29. Motility of adult male *S. mansoni* after CaMKII knockdown.. 191

Figure 5.30. Motility of adult female *S. mansoni* after CaMKII knockdown. 192

Figure 5.31. Global effects of CaMKII siRNA on adult *S. mansoni* movement.. 193

Tables

Table 1.1. Protein kinases identified in *S.mansoni*.....25

Table 3.1. Example of results gained from initial bioinformatics.....51

Table 3.2. Example of Table 1 (pY IAP).....56

Table 3.3 Phosida motif matcher results of upstream motifs.....66

Table 3.4. List of kinases families.....72

Table 3.5 List of proteins from PTM scan which have been identified as tegumental proteins within the literature.....81

Table 3.6. List of top 25 proteins with the highest number of protein – protein interactions.....84

Table 3.7 Top 20 hits from a KEGG analysis performed on the PTM Scan dataset.....92

Table 4.1 List of proteins found to be significantly different between arrays probed with male and female adult worm lysate. 125

Table 5.1 Sequences of siRNAs.....145

Abbreviations

ANOVA- Analysis of Variane
aPK – Atypical Protein Kinase
BLAST – Basic Local Alignment Search Tool
BME – Basal Medium Eagle
BSA – Bovine Serum Albumin
CaM - Calmodulin
CAMK – Ca^{2+}/Calmodulin Kinase
CAMKII - Ca^{2+}/Calmodulin Kinase II
CK1 – Casein Kinase 1
CST – Cell Signalling Technology
DMSO - Dimethyl sulfoxide
DNA - Deoxyribonucleic acid
DTT – Dithiothreitol
ECL – Enhanced Chemiluminescent
EDTA - Ethylenediaminetetraacetic acid
ePK – Eukaryotic Protein Kinase
ERK - Extracellular Signal–Regulated Kinase
EV – Extracellular Vesicle
FBS – Foetal Bovine Serum
FDR – False Discovery Rate
GCPR – G Coupled Protein Receptors
GO – Gene Ontology
GPX - Glutathione S Peroxidase
GST - Glutathione S Transferase
H & E - Haematoxylin and Eosin
HBSS – Hanks Balanced Salt Solution
HEPES - 4-(2-hydroxyethyl)-1-piperazineethanesulfonic acid
HIV - Human Immunodeficiency Virus
HPRD – Human Protein Reference Database
HRP – Horseradish Peroxidase
IAP – Immunoaffinity Purification
IDT – Integrated DNA Technologies
IFN - Interferon

IMAC - Immobilized Metal Ion Affinity Chromatography

KEGG – Kyoto Encyclopaedia of Genes and Genomes

LC-ESI-MS/MS - Liquid Chromatography-Electrospray Ionization-Tandem Mass Spectrometry

LHS – Left Hand Side

LSHTM – London School of Health and Tropical Medicine

MCODE - Molecular Complex Detection

MDA – Mass Drug Administration

min - Minutes

NCBI - National Centre for Biotechnology Information

NIH-NIAID – National Institute of Health - National Institute of Allergy and Infectious Diseases

PBS – Phosphate Buffered Solution

PKA – Protein Kinase A

PKC - Protein Kinase C

PMA - Phorbol 12-myristate 13-acetate

PTK – Protein Tyrosine Kinase

PTM – Post Translational Modificatio

PZQ – Praziquantel

RHS – Right Hand Side

RIPA - Radioimmunoprecipitation Assay Buffer

RPMI - Roswell Park Memorial Institute (culture medium)

s - Seconds

SDS PAGE - Sodium Dodecyl Sulfate Polyacrylamide Electrophoresis

SiRNA – Small Interfering Ribonucleic Acid

Smp – *Schistosoma mansoni* Protein

SOD - Superoxide Dismutase

STRING - Search Tool for the Retrieval of Interacting Genes/Proteins

TDR- Special Programme for Research and Training in Tropical Diseases

TFA - Trifluoracetic Acid

TGF – Tumour Growth Factor

Tris - Tris(hydroxymethyl)aminomethane

TSP – Tetraspanin Protein

TTBS - Tween-Tris-Buffered Saline

WHO – World Health Organisation

1 INTRODUCTION

1.1 Schistosomiasis

Human schistosomiasis is the disease caused by parasitic blood flukes of the genus *Schistosoma*. Current estimates indicates that schistosomiasis affects more than 230 million people, with up to 700 million people at risk of infection, across 78 countries[1] (Chitsulo et al., 2004; Colley et al., 2014; Vos et al., 2012). The disease can cause multiple debilitating symptoms including, abdominal pain, anaemia, growth stunting and diarrhoea, leading to long term and chronic conditions such as increased frequency in urination, haematuria, inflammation and scarring of the urogenital system, and even bladder cancer in the case of urogenital schistosomiasis. However, with hepato-intestinal schistosomiasis chronic symptoms include hepatosplenism, portal hypertension, periportal fibrosis and liver cirrhosis (Colley et al., 2014; Mostafa, et al., 1999). Dependant on the species, symptoms can present themselves when the eggs, laid by the parasitic adult worms become trapped in host tissues leading to obstruction and inflammation in either the urinary or intestinal system. Human schistosomiasis is largely restricted to Africa. However, it can also be found in the Middle East, Central and South America and Asia (Colley et al., 2014). The primary drug used to combat human schistosomiasis is praziquantel (PZQ), and currently its mode of action is not understood. This is one factor, another is the issue found where cases of resistance to PZQ occur, possibly due to its exclusive use in mass drug administration (MDA). This in turn leads to an ever-increasing need for in depth research into the biology of these worms, with the aim to extend our understanding and potentially develop therapeutic tools to control and even eradicate schistosomiasis in the future.

[1] http://www.who.int/mediacentre/factsheets/fs115/en/

1.2 Epidemiology

Schistosomiasis is most rife in tropical and subtropical areas, with poorer communities suffering most from infection, mainly due to poor sanitation, lack of safe drinking water and education (McManus et al., 2018). There are three main species of *Schistosoma* that are infectious to humans, *Schistosoma mansoni, Schistosoma japonicum and Schistosoma haematobium,* whereas *Schistosoma mekongi, Schistosoma guineensis and Schistosoma intercalatum* are of lesser importance and consequently have been less researched. *S. japonicum* is also zoonotic, infecting an array of mammalian reservoir hosts including water buffaloes, cattle, rodents, dogs, sheep and pigs (You & McManus, 2018). These parasites can be split into two broad groups according to the excretory system in which the parasites cause pathology; *S. haematobium* causes urinary schistosomiasis, whereas the remaining five species cause intestinal schistosomiasis. Sub-Saharan Africa, South America, and the Arabian Peninsula are the main geographical areas where *S. mansoni* is endemic, whereas *S. japonicum* is predominantly found in China, the Philippines and Indonesia (Gryseels et al., 2006) (Figure 1.1). The minor species are found in more restricted areas, with *S. mekongi* located in certain districts of Cambodia and Lao People's Democratic Republic (Muth et al., 2010), and *S. guineensis and S. intercalatum* in Lower Guinea and the Democratic Republic of Congo (Webster et al., 2006). Schistosomiasis is principally a disease of rural areas, with water sources such as ponds, lakes and natural streams providing a point of infection to the population (Gryseels et al., 2006). However, the transmission of the disease to non-endemic areas has been aided by development of modern-day water resources such as dams and irrigation systems (Steinmann et al., 2006). Recently, there has been a human schistosomiasis outbreak in Corsica, when a number of cases of urogenital schistosomiasis were diagnosed in patients from Germany and France (Berry et al., 2014; Boissier et al., 2015; Holtfreter et al., 2014). Unusually, whilst taking

the patients' history, it was noted that the individuals had not visited a schistosomiasis endemic region but had all visited southern Corsica in France for their holidays in 2013, and specifically they had all been swimming in the Cavu River in the north of Porto Vecchio (Boissier et al., 2016). This area of Corsica is home to *Bulinus truncatus* which is an intermediate host for schistosomes, providing the setting for a successful infection (Boissier et al., 2016). Interestingly, the patients tested positive not only for *S. haematobium*, but some were also found to be excreting eggs originating from a *S. haematobium–S. bovis* hybrid, which has been commonly found in Senegal (Huyse et al., 2009; Webster et al., 2013). Senegal is a popular holiday destination for the French, most probably due to the free travel between the two countries, stemming from a time when Senegal was a French colony (Blach et al., 2012; Steiner et al., 2013). France is also the most popular destination for the Senegalese, who also travel to Corsica to work during the summer season; this could explain how Corsica became infected with schistosomes (Gerdes, 2007). Worryingly, *B. truncatus* is found across southern Europe and with the mean water temperature set to rise in the coming years (van Vliet et al., 2013) and migration from endemic areas of schistosome infections to Southern Europe continuing, there exists real potential for more infections occurring across Europe in the future (Boissier et al., 2016).

Figure 1.1. World map depicting the distribution of the different species of human schistosome. Adapted from Gryseels et al. 2006**.**

1.3 Pathogenesis of Schistosomiasis

Human schistosomiasis infection begins when the skin of a human host is penetrated by a free-swimming larva (cercaria) of the schistosome (Section 1.5), this can manifest itself as a temporary urticarial rash, potentially lasting up to a few days as maculopapular lesions (Ross et al., 2007). As the parasite migrates through the body, a hypersensitivity reaction known as Katayama syndrome can occur, with symptoms including myalgia, cough, headache, fever, and abdominal tenderness; this syndrome is often associated with travellers rather than communities in endemic regions who may have built up a tolerance to migrating schistosomes (Ross et al., 2007). Once the parasites have developed into sexually mature male or female worms, they pair up and remain *in copula*, with the female worm lying inside the males' gynaecophoric canal. The female is then fertilized and is able to lay eggs; it is the eggs that become trapped in the host's tissues which causes the chronic pathology characteristic of schistosomiasis. With intestinal schistosomiasis (caused by *S. mansoni, S. japonicum, S. intercalatum,* and *S. mekongi*) the worms reside in the portal vasculature, from which the eggs are transmitted to the lumen of either the intestines or to the liver aided by antigenic glycoproteins secreted by the egg which induce an immune reaction (McManus et al., 2018). With *S. haematobium*, the worm pairs are located in the blood vessels of the urinary system, and the eggs become lodged and migrate through the host's bladder wall causing an immune response (Shebel et al., 2012); bladder cancer can also occur (Santos et al., 2014). Furthermore, there are strong links between female genital schistosomiasis caused by *S. haematobium* and HIV (Kjetland et al., 2006). It is the eggs that become embedded in the hosts' tissue that induce a strong Th2 immune response, which leads to a granulomatous reaction around the egg (Fairfax et al., 2012). Initially after infection with schistosomes, the host immune system elicits a

type 1 immune response caused primarily by the antigens on the surface of the worm. The type 1 immune response consists predominantly of Th1 cells and the release of interferon (IFN)-λ and IL-12 (Pearce & MacDonald, 2002). Once the parasites have matured, paired up and have begun to produce eggs, the Th1 immune response begins to slow being replaced by a powerful Th2 immune response. The antigenic egg secretions induce the Th2 response, causing a Th2 cell increase accompanied by the production of IL-4, IL-5, and IL-13 as well as an upregulation in immunoglobulin (Ig) E levels and eosinophils in the circulation. This culminates in a granulomatous inflammation surrounding the egg consisting of a cluster of CD4+ T cells, eosinophils, macrophages, neutrophils and fibroblasts (Figure 1.2); as these granulomas heal they cause considerable fibrosis within the organs they are lodged in, this is the mark of a chronic schistosomiasis infection (Fallon et al., 1998; Herbert et al., 2004; Jankovic et al., 1998). Chronic intestinal schistosomiasis presents itself with fatigue, anorexia, intermittent abdominal pain, rectal bleeding, diarrhoea, portal and pulmonary hypertension, hepatomegaly, and hepatic fibrosis (Colley et al., 2014). Chronic urinary schistosomiasis caused by *S. haematobium* presents with lower abdominal pain, increased (and painful) urination and haematuria. These symptoms are caused by mucosal granulomas in the bladder, seminal vesicles, lower ureters, the vas deferens, prostate, and the female genital system (Barsoum, 2013).

Figure 1.2. The *S. mansoni* granuloma. A) Histology section (stained with H&E) of liver from a normal mouse with a granuloma surrounding an *S. mansoni* egg. B) Graphical representation of the cells involved in the formation of *S. mansoni* egg-induced liver granuloma. LNFPIII = Lacto-N-fucopentaose III, α1 = α1 antigen, ω1 = ω1 antigen, these are all products which are present during the formation of a granuloma. Adapted from Hams et al., 2013.

1.4 Control and Prevention of Schistosomiasis

1.4.1 Praziquantel

In 2016 the World Health Organisation (WHO) estimated there were at least 206.4 million people that needed preventative treatment for schistosomiasis[2] , but it was estimated that by the end of 2018, up to 645 million tablets of PZQ would have been used by up to 235 million people. Preventative treatment aims to control the levels of schistosomiasis infection in endemic areas through the mass treatment of groups at risk of infection,

[2] http://www.who.int/news-room/fact-sheets/detail/schistosomiasis

including children and workers in jobs with a high level of exposure to fresh water (e.g. fishermen). In particular, areas with high disease rates will be treated with more frequency in comparison to areas with a moderate level of infection. If the infection rate can be controlled within the 'at-risk' groups, the hope is that transmission of the disease will be lowered facilitating eradication in endemic areas[2]. The drug of choice for mass administration is PZQ, which was chosen as it is the safest and most effective low-cost option. Thus, despite PZQ not being able to prevent re-infection, it can be accessed for use again easily and it is effective against all significant forms of schistosomiasis (Cioli & Pica-Mattoccia, 2003). However, historically, less than one third of all the people identified to need MDA actually received the treatment (WHO, 2006).

Praziquantel is a pyrazino-isoquinoline derivative, which is classed as an anthelmintic due to its efficacy against many flatworms, including schistosomes against which it has been used for more than 40 years (Cioli & Pica-Mattoccia, 2003). Despite this, very little is understood about PZQ and how it works as an anthelmintic, even after extensive research to discover its mode of action. PZQ was initially discovered in the 1970s by Bayer (Vale et al., 2017) in the form of PZQ1. However, the current day form PZQ is dispensed as an equal mixture of enantiomers of biologically active PZQ2 (*R*-PZQ) and biologically inactive PZQ3 (*S*-PZQ) as a racemate (Olliaro et al., 2014). The drug easily permeates tissues and exhibits a low solubility which defines it as a class II drug as described by the Biopharmaceutics Classification System and the Biopharmaceutics Drug Disposition Classification (Vale et al., 2017). However, one large drawback of the drug is its inability to kill juvenile forms of schistosomes, hence the need for multiple treatments (Vale et al., 2017). Another issue surrounds the metabolism of PZQ. While it is known that PZQ is predominantly metabolized by the hosts CYP3A and CYP2B1

isoforms of cytochrome P450 (an enzyme involved in metabolism of drugs), the full mechanism of PZQ metabolism is not wholly understood and needs further investigation (Godawska-Matysik & Kieć-Kononowicz, 2006). The main mystery, however, concerns the mechanism(s) by which PZQ kills schistosomes. Data also exists which indicates that calcium plays an important role. Initially, there is a large influx of calcium into the parasite following PZQ treatment, followed by contractions of the parasite muscles, as well as changes to the surface tegument, this includes swelling, lesions and blebbing on the surface; furthermore vacuolization and disruption of the subtegumental tissues occurs (Cioli & Pica-Mattoccia, 2003; Cioli et al., 2014; Shaw & Erasmus, 1987; Vale et al., 2017). Early research focused on Ca^{2+} influx into the parasite through voltage-gated calcium channels, potentially causing the muscle contractions and changes in tegumental structure (Harnett & Kusel, 1986; Kohn et al., 2001; Pax et al., 1978). However, more recent research determined that the schistosomicidal effect of PZQ does not solely rely on calcium influx, (Nogi et al., 2009; Pica-Mattoccia et al., 2008) and in 2017 a study discovered that PZQ is a GPCR ligand, this means GPCRs in schistosomes and other flatworms should be a priority in future screening as the could be a key target for future antischistosomal drug development (Chan et al., 2017). Overall, additional research is needed to definitively discover PZQs mode of action.

As mentioned above, PZQ has been used in monotherapy for over 40 years particularly in MDA control programmes aimed at reducing infection rates within groups located in endemic areas. This exclusive long-term reliance on PZQ has raised the question, ‘is resistance to PZQ possible?’ (Vercruysse et al., 2011). As also outlined earlier, not all individuals in an MDA programme receive praziquantel treatment, therefore the population of worm’s calculated after an MDA campaign could include worms from

patients who did not receive MDA treatment (Shuford et al., 2016). Nonetheless, there have been cases of reduced susceptibility to praziquantel in *S. mansoni* reported in Senegal (Stelma et al., 1995) and Egypt (Ismail et al., 1996). For *S. japonicum*, there has been research into possible cases of resistance (Wang et al., 2012; Wu et al., 2011) with the overall conclusion being there was no problem with resistance to PZQ in this species. Again, there appears to be no evidence for resistance in *S. haematobium*, although there have been multiple reports of problems clearing the infection (Alonso et al., 2006; Herwaldt et al., 1995; Silva et al., 2005). Resistance to PZQ has also been generated in the laboratory with *S. mansoni* (Couto et al., 2011; Fallon & Doenhoff, 1994; Ismail et al., 1994) and in *S. japonicum* (H.-J. Li et al., 2011). It could be that due to difficulties in detecting low levels of infection after treatment, there is overestimation in PZQ efficacy, and consequently there is a need to improve sensitive diagnostics for the detection of schistosomiasis (Vale et al., 2017). Nevertheless, the potential for schistosome resistance against PZQ emerging, its inactivity towards juvenile forms of the parasite, and its inability to prevent re-infection highlight the need to develop of new treatments towards schistosomiasis. This would ensure effective approaches are always available in the fight to control, prevent, and eventually eradicate schistosomiasis globally.

1.4.2 Vaccine Development

Whilst PZQ remains the chosen method of treatment for schistosomiasis, there are other options being explored. One treatment option is the development of a vaccine against schistosomes. The parasites have a complex life cycle (Section 1.5), which provides a number of potential windows of opportunity for vaccine design in the prevention of parasite migration and maturation in the definitive host (Tebeje et al., 2016). The list of

potential target molecules for vaccine design currently exceeds 100 candidates, with approximately one quarter of these displaying an ability to protect against schistosomiasis within the murine model (Siddiqui et al., 2011). Out of this list, only three molecules have moved forward to human clinical trials, namely fatty acid binding protein (Sm14) and tetraspanin (Sm-TSP-2) in *S. mansoni* and glutathione transferase in *S. haematobium* (Sh28GST); currently, there are no human trials for a vaccine against *S. japonicum* (Merrifield et al., 2016). However, it is interesting to note that a recent report has controversially suggested that use of a murine model when developing a vaccine against schistosomiasis may be fundamentally wrong due to the difference in strength of the pulmonary capillaries between mice and humans (Wilson et al., 2016). This is due to the capillaries in mice being a smaller and therefore weaker size than the capillaries in humans, this small size could halt the larval schistosomes journey, ultimately hindering the growth of schistosomes. This means when using a murine model, schistosome numbers may be lower than when using a human model (Wilson et al., 2016). With this in mind, some candidates may have been overlooked when tested in murine models, therefore there may be more potential targets than previously thought. Some of the protein vaccine targets within *S. mansoni* include: 1) Sm14, a fatty acid binding protein (Tendler & Simpson, 2008); 2) Sm28GST, a 28kDa glutathione transferase that is involved in fatty acid metabolism as well as prostaglandin D2 synthesis, and potentially has a role in host immune evasion (Capron et al., 2001); 3) Sm-TSP-2, a tetraspanin found in the outer layer of the parasite tegument exposed to the hosts' immune system (Loukas et al., 2007); 4) Smp-80, which is the larger of the subunits of calpain, a protease located in the tegument of the parasite (Ahmad et al., 2010); and 5) Sm29, a membrane-bound glycoprotein that is also located in the parasite tegument that is potentially involved in immunoregulation (Oliveira et al., 2016). In addition to these molecules, there is also research into targeting

antioxidants Cu–Zn superoxide dismutase (SOD) and glutathione S peroxidase (GPX), which when used as a DNA based vaccine have shown promising results (Shalaby et al., 2003). Furthermore, research has been conducted into blocking the uptake of nutrients from the blood ingested from the host, as this is a critical process that is essential to the parasites' survival (Figueiredo et al., 2015). Moving forward, the development of a vaccine employing either these listed candidates or other targets yet to be discovered/validated is a vital move in the fight to cure schistosomiasis, especially with the threat of resistance on the horizon.

1.5 Life Cycle of *S. mansoni*

The schistosome life cycle is complex (Figure 1.3). Intermediate and definitive hosts are used, and elaborate transformations of the parasites morphology and physiology occur within these hosts for development and reproduction, and to permit movement between the hosts in freshwater. Once fully grown, schistosomes can survive in the human host for an average of 3 – 10 years (Colley et al., 2014). However, there have been cases of the parasite living for up to 40 years (Warren et al., 1974). The life cycle begins when a schistosome egg enters freshwater, this signals for the egg to hatch into one free living miracidium. Miracidia are ~150 μm in length (Walker, 2011) and have enough energy to survive for up to 24 h, they are covered in cilia that enable them to swim through the water in search of a suitable host snail (Colley et al., 2014). Each species of schistosome has a preferred species of snail as its intermediate host; *S. mansoni* require snails of the genus *Biomphalaria* (Colley et al., 2014), *Biomphalaria glabrata* is found in the Americas or *Biomphalaria pfeifferi* are located in Africa (Gray et al., 2011) although many other species capable of transmitting *S. mansoni* in these areas do exist. However,

for *S. japonicum* the main snail host genus is *Oncomelania*, and *S. haematobium* are transmitted by species of *Bulinus* (Gryseels et al., 2006). Miracidia locate their snail host by sensing chemical signals, light, currents, and temperature (Samuelson et al., 1984; Walker, 2011). Once an appropriate snail has been located, the miracidium attaches to its epithelium using its apical papillae and penetrates by releasing proteases from the lateral and apical glands, these enzymes degrade the snail tissue and allow the miricidium to bury into the snail (Walker, 2011). Once inside the intermediate host, the miricidium develops into a post-miracidium by losing its ciliated plates, before transforming to a mother sporocyst (Walker, 2011). Mother sporocysts will asexually yield daughter sporocysts, which are created from germinal cells (Meuleman et al., 1980). The daughter sporocysts go through a number of developmental alterations including the change of the tegmental structure to include a surface coat, spines, and a basal membrane, as well as the production of a birth pore (Meuleman et al., 1980). It is through the birth pore that the next free-living (but non-feeding) stage is released, these are the clonally-propagated cercariae which emerge from the snail intermediate host into freshwater approximately 4 – 5 weeks after the initial snail infection (Walker, 2011). Cercariae are often found just below the surface of the water, to increase their chances of coming into contact with their definitive human host (Haas et al., 2008). They are comprised of an anterior head and a posterior bifurcated tail, which is also referred to as the furca; the cercaria is covered in a continuous single tegument with ciliated sensory papillae (Graefe et al., 1967; Krishnamurthy et al., 2017). Internally the anatomy consists of a nervous system, flame cells for osmoregulation, a ventral sucker (a.k.a acetabulum), an oesophagus leading to two gut caeca as well as a variety of glands filled with essential enzymes to help the cercariae adhere to and penetrate the host (Walker, 2011). To locate and penetrate its definitive host the cercariae must remain motile but they have limited glycogen reserves

that last for up to ~12 h; the swimming mechanism cercariae use is a novel gait described as a 'T-swimmer gait' in recent research (Krishnamurthy et al., 2017). Host location is aided by detection of skin chemicals such as arginine, ceramides, and linoleic acid, as well as movement and shadows in the water (Haas et al., 2001; Haeberlein & Haas, 2008). Upon locating the definitive host, the cercaria penetrates the outer dermis, shedding its tail and secreting the contents of the pre-acetabular glands which consist of proteinases capable of skin lysis (Ingram et al., 2012; Salter et al., 2000). Finally, the cercariae lose their osmo-protective glycocalyx and generate a new double bilayer outer membrane, which allows the parasite to present new glycoproteins (Haas et al., 1997; Walker, 2011). Following penetration, the cercariae transform into schistosomules (somules), which are the larval forms of the parasite that reside in the definitive host. These somules (skin somules) remain in the human skin for between 48 to 72 h (depending upon species) before they move to the lung capillaries (lung somules) followed by the liver (liver somules), although it should be noted that this journey from the skin to the liver is not fully understood and further research is needed to discover the intricacies of this journey (Jones et al., 2008). It is believed the somules enter the host circulation through the venule wall, and travel through the capillaries of the pulmonary circulation through the lungs, before passing through the systemic circulation into the hepatic portal system. The expedition from skin to liver takes approximately 7 days (Walker, 2011). Here the worms begin to feed on host blood and they become sexually distinguishable; the male and female adolescent worms mature, and pair-up and remain *in copula* for egg production (Walker, 2011). The pairing of the worms is a vital step in parasite development as only as pairs can fully mature to sexually-reproducing adults. Once maturation is complete the final migration of adult *S. mansoni* occurs *via* the portal veins to the mesenteric venules; here paired worms will dwell for life. Once mature, the paired female adult

worms are able to lay 100-300 eggs per day, these are destined to be released into the environment *via* excretion through the intestinal lumen. However, despite this many eggs become trapped in the sinusoids of the liver as the blood within the portal vasculature flows in the opposite direction from the intestine carrying the eggs away from the intestinal lumen (Colley et al., 2014; Pearce & MacDonald, 2002). It is the trapped eggs that elicit the pathology of schistosomiasis, driven by a harsh Th2 cell mediated response causing the granulomas which are the root cause of the morbidity associated with schistosomiasis (Pearce & MacDonald, 2002).

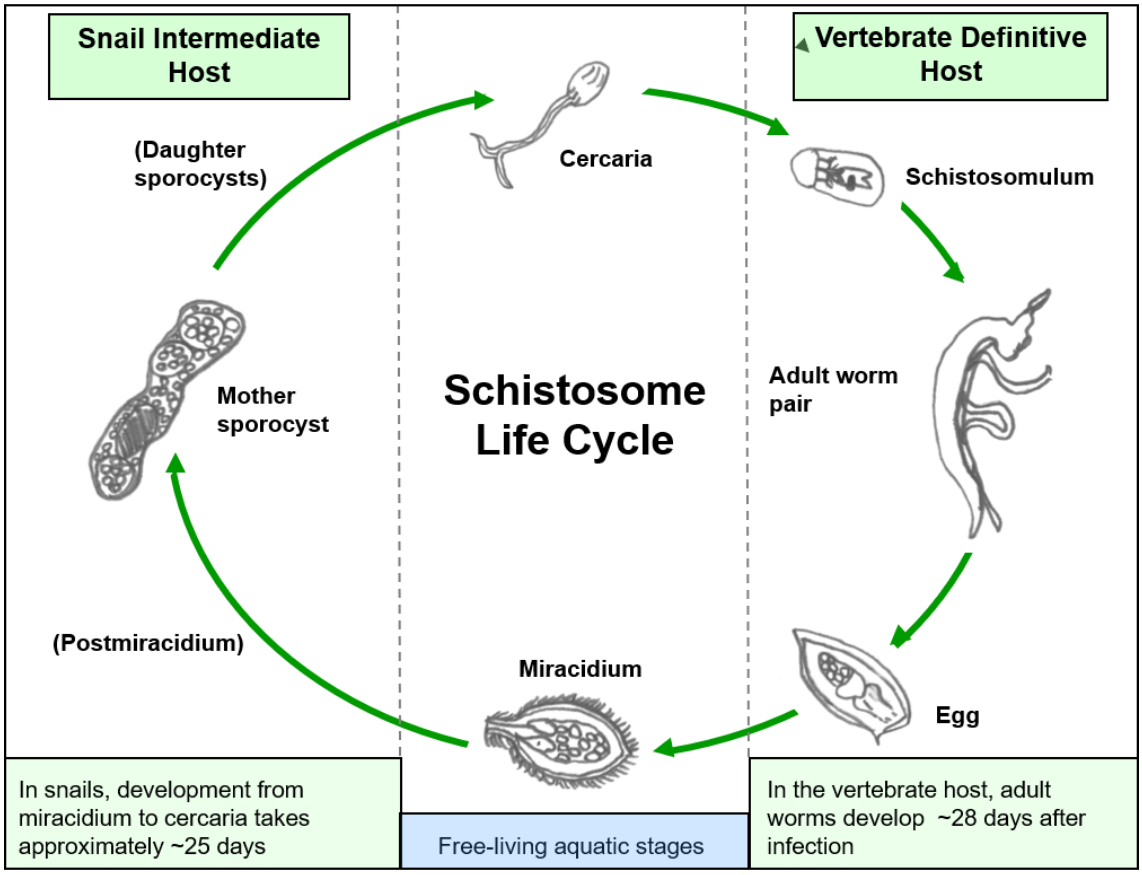

Figure 1.3. The schistosome life cycle. Adapted from McKenzie et al. (2018).

1.6 The Biology of Selected Schistosome Life Stages

1.6.1 The Cercaria

Each cercaria measures approximately 500 μm in length, depending on the elongation/contractile status of the parasite (Dorsey et al., 2002). The cercaria is anatomically split into two main sections (Figure 1.4), the body (head) and the bifurcated tail, and is made up of an estimated 1000 different types of cells which are predominantly muscle cells (Dorsey et al., 2002). This is due to the cercaria's role in host location/penetration, whereby muscle cells are needed to aid swimming towards the host, to attach and creep on the host skin to find a suitable penetration site, and to facilitate penetration of the dermal layers (Dorsey et al., 2002). Within the cercaria head are pre- and post-acetabular glands which contain enzymes capable of skin lysis and adhesion (McKerrow & Salter, 2002). Upon location of a definitive host the contents of these glands are secreted to aid entry to, and movement through, the skin (McKerrow & Salter, 2002). The nervous and osmoregulatory systems extend from the head down into the tail. The osmoregulatory system employs flame cells with cilia which move excess fluid and waste from the interstitial spaces into the protonephridial system (Collins et al., 2011). The whole parasite is encased in a tegument, a syncytium that varies between 0.2 μm and 0.5 μm thick; the surface membrane of the tegument is trilaminate and is covered in a glycocalyx (Dorsey et al., 2002). Spines can also be found within the tegument spanning most areas of the cercariae.

Figure 1.4. Basic anatomy of the free-swimming cercariae. Green highlights the tegument, purple the oesophagus, yellow the ventral sucker, red the nervous system and blue the pre- and post-acetabular glands. The image was adapted from Dorsey et al. (2002).

1.6.2 The Somule

Upon penetration of the skin the tail is shed and the cercaria transforms into a somule; this marks the beginning of a radical change in the parasite's morphology/physiology. As described (Section 1.5), the cercariae will have released enzymes from the pre- and post-acetabular glands to aid entry to the human skin, at this point the larva is named a skin

stage somule and shall remain in the epidermis for around 24 h (He et al., 2002). Once the cercarial membrane has been shed, the development of the somule's heptalaminate surface membrane ensues, providing protection from the host. Thus, the skin stage somule quickly gains resistance to the hosts immune response (El Ridi et al., 2003; Hockley & McLaren, 1973). The journey of the skin somule commences with migration from the epidermis to the dermal vessels over a period of ~72 h (He et al., 2002). Somules also secrete the immunoregulatory prostaglandin D2 during migration through the skin, which suppresses the passage of the Langerhans cells from the epidermis halting their development to dendritic cells that could attack the somule (Angeli et al., 2001). Once they have penetrated the dermal vessels, the somules journey to the pulmonary artery and then into the pulmonary capillaries. This is where they become more slender lung-stage somules, which are still under a significant attack from the host immune system (He et al., 2002). Immune response evasion by the somule is thought to be supported by tegumental remodelling with the addition of membranous vesicles to the apical membrane resulting in a sustained continuous syncytial membrane surround the somule, along with the ability to activate complement and bind to antibodies on the surface of the parasite (Gobert et al., 2007). During transformation to somule from cercaria, the parasite's energy metabolism changes to anaerobiasis; glucose transporters also become expressed at the membrane supplying the somules with glucose to provide energy (McKenzie et al., 2018; Skelly et al., 1998). From the lungs the somules take varying routes through the systemic vasculature to reach their final destination in the mesenteric venules of the host (Walker, 2011).

1.6.3 The Adult Male and Female Worm

Schistosomes are the only truly dioecious species in their otherwise hermaphroditic phylum (Loker & Brant, 2006) and during growth from adolescent to adult worm, development of the sex organs begins. Maturation of the female sex organs only ensues once the male and female adult worms have coupled (they remain *in copula* until death), the worms will remain monogamous for the majority of pairs. However, they do have the ability to change their mate (Colley et al., 2014; Tchuem et al., 1996). If the female does not encounter a male partner, they will remain small in size and their gonads remain under-developed; however, if a male does not encounter a female their growth is not hindered (Kunz, 2001). The pairing of the male and female worms, with the female residing permanently in the males' gynaecophoric canal, induces the maturation of the ovary which produces the oocytes, and the vitelline gland which produces material such as the eggshell proteins (Kunz, 2001). The oocyte, eggshell proteins, and other materials fuse together to form the egg within the female ootype; the egg then travels up the uterus to the birth pore at the ventral tegumental surface of the female worm through which the egg is expelled (Kunz, 2001). Females are able to lay eggs at 4-6 weeks post-infection and are capable of producing hundreds of eggs each day (Kunz, 2001; Walker, 2011). As well as the development of the sex organs, the adult female worm grows to become long and slender, cylindrical in shape, and measuring 7-20 mm in length, whilst the adult males are shorter, and more muscular[3]. Adult males and females are both encased in a complex syncytial tegument, formed at the somule stage (Section 1.6.2) that protects the worms from the host immune system, although how the tegument functions in protection is not

[3] https://www.cdc.gov/parasites/schistosomiasis/biology.html

fully understood. However, we do know that the adult worms possess somatic stem cells which allow the parasite to regenerate its tegument, and also bind antigens from the host (Colley et al., 2014; Hockley & McLaren, 1973; Mclaren & Hockley, 1977; Skelly & Wilson, 2006). There are differences in the tegument between the sexes, the male tegument being more complex, is covered in tubercles, wrinkles, grooves and spines which are also present in the gynaecophoric canal which suggests the spines may play a role in the pairing of the worms (Machado-Silva et al., 1997; Pereira et al., 2011). The tegument also plays a role in many other systems including excretion, signal transduction, osmoregulation, nutrition and crucially host immune evasion (Van Hellemond et al., 2006). Both sexes possess a ventral sucker used for attachment, a digestive tract that divides then then joins at the end of the worm and is closed, an excretory system to expel unwanted materials, and an advanced neural system (Bogitsh & Carter, 1977; Mair et al., 2000). Because of their blind gut, schistosomes vomit undigested blood products back into the host bloodstream (Skelly et al., 2014).

1.7 Cell Signalling in *S. mansoni*

Schistosomes have an intricate life cycle, through which they traverse from water to snail intermediate host, back to water and finally to a mammalian definitive host, across which they develop through six major different life stages (egg, miracidia, sporocyst, cercariae, somule, adult worm (male or female). The cell signalling behind these transformations will be extensive, providing a whole variety of potentially druggable/vaccine-targetable proteins to develop future therapies for schistosomiasis. Schistosomes, uniquely in their phylum, live a dioecious lifestyle, and the dependence on the coupling of a male and

female worm to signal the maturation of the female sex organs, provides a further platform upon which to study schistosome cell signalling. Understanding the cell signalling processes behind not only schistosome development and coupling, but also the worms' basic biology will provide us with valuable insight that may promote the discovery of novel drug targets.

1.7.1 Protein Kinases

Protein kinases are enzymes which add phosphate groups from either ATP or GTP to an amino acid residue on their substrate targets, eliciting a conformational change in the target protein which either activates or deactivates it and sends out a signal(s) dependant on the activation status effecting downstream molecular events (Hanks et al., 1988). Protein kinases can be categorised under two superfamilies, eukaryotic protein kinases (ePKs) which have a conserved catalytic domain in common, or atypical protein kinases (aPKs). Eukaryotic protein kinases can be subdivided into groups that highlight the similarity in the catalytic domain sequences, the way in which the kinases are regulated and the presence/absence of accessory domains (Martin et al., 2010). These groups are AGC (cAMP-dependent protein kinase/protein kinase G/protein kinase C extended), CAMK (Calcium/Calmodulin regulated kinases), CK1 (Cell Kinase I), CMGC (Cyclin-dependent Kinases and other close relatives), RGC (Receptor Guanylyl Cyclase's), STE (MAP Kinase cascade kinases), PTK (Protein Tyrosine Kinase) and TKL (Tyrosine Kinase Like); finally, an additional group named 'Other' exists for additional protein kinases that do not fit into the standard eight ePK groups (Andrade et al., 2011). Protein kinases have become increasingly researched in the medical field as they are considered druggable targets. One case that illustrates success concerns the drug Gleevac® that treats

cancers including chronic myelogenous leukaemia and acute lymphocytic leukaemia; Gleevac® is a protein kinase inhibitor which prevents cellular activation by upstream kinases of the kinase PTK (Eglen & Reisine, 2009). Protein kinases are also being considered as drug targets against parasites such as *Trypanosoma, Leishmania*, and *Plasmodium* causative agents of trypanosomiasis, leishmaniasis and malaria, respectively (Naula et al., 2005; Ward et al., 2004), as well as against schistosomes (Beckmann & Grevelding, 2010; Dissous et al., 2007; Grevelding et al., 2018). This latter work has been aided with the advent of the *S. mansoni* genome and its subsequent updates and through transcriptomics providing an abundance of bioinformatic information to help identify new druggable targets (Andrade et al., 2011; Berriman et al., 2009).

1.7.2 Protein Kinases in *S. mansoni*

Characterisation of the *S. mansoni* kinome identified 252 ePKs, which equates to 1.9% of the predicted proteome (Andrade et al., 2011); when alternative splicing is considered the number of protein kinases could be considerably larger (Walker et al., 2014). Despite this large number of protein kinases only a small number have been explored in further detail (Table 1.1). One of the more comprehensively researched cell signalling pathways in *S. mansoni* is the transforming growth factor-β (TGF-β) pathway, which plays a role in the regulation of cell division and cell survival in humans (Clark & Coker, 1998). A number of TGF-β signalling elements have been discovered in *S. mansoni*, these are TβRI/TβRII homologues SmTβR1 (SmRK1) and SmTβRII (SmRKII), and four Smad proteins (SmSmad1, SmSmad1b, SmSmad2, SmSmad4) (Beall et al., 2000; Carlo et al., 2007; Osman et al., 2001; You et al., 2011). Research into SmTβRII found it plays a role in host parasite signalling when it was discovered that SmTβRII is able to activate

SmTβR1 in the presence of human TGF-β (Loverde et al., 2007); SmTβRII may also play a vital role in schistosome reproduction as it has been located in both vitelline and gut epithelium in females and the sub-tegument in males (Beckmann & Grevelding, 2010; Loverde et al., 2007). The PTKs are involved in communication and regulation in *S. mansoni*, and out of the 252 ePKs, 90 of these are classified as PTKs and around 43 as TKLs (Andrade et al., 2011). The PTKs that have so far been investigated in *S. mansoni* are tyrosine kinase 3/4/5/6 (SmTK3), SmTK4, SmTK5, SmTK6 and cytoplasmic protein-tyrosine kinase SmFes (Bahia et al., 2006; Bahia et al., 2007), which were found to play a role in reproduction, mitogenic activity, female egg production and larval transformation, implicating them as possible drug targets against egg production to supress disease pathology (You et al., 2011). Another important kinase group actively researched in schistosomes is the AGC group, the first kinase discovered in the group was protein kinase C1 (PKC1) (Bahia, Andrade, et al., 2006). PKCs are involved in a wide array of cellular processes such as cell differentiation, cellular motility, survival, apoptosis gene expression, the cell cycle, growth, and development (Newton, 1995). In particular, our laboratory has found a role for PKC and extracellular signal-regulated kinases (ERKs) in the regulation of movement, attachment, pairing and egg release within *S. mansoni*, again indicating kinases that could be a potentially attractive drug targets (Ressurreição et al., 2014). Another AGC member that has been researched, including within our laboratory is protein kinase A (PKA); this kinase is one of the most comprehensively researched kinases in schistosomes, since the discovery of smPKA-C, the catalytic subunit in adult worms, which was found to be essential for the worm's survival (Swierczewski & Davies, 2009). Research at Kingston University investigated the role PKA plays in movement of adult worms (de Saram et al., 2013) and its signalling pathway in cercariae and somules (Hirst et al., 2016). Other important kinases have been

investigated in *S. mansoni* (Table 1.1), but the function(s) of many of the 252 ePKs remain unknown.

Protein Kinases Studied in *S.mansoni*	**Reference**
S. mansoni epidermal growth factor receptor (SER)	Ramachandran et al., 1996
S. mansoni mitogen-activated protein kinase (MAP kinase)	Schüssler et al., 1997
S. mansoni GTPase activating protein (GAP)	Schüssler et al., 1997
S. mansoni receptor kinase (SmRK1)	Davies et al., 1998
S. mansoni tyrosine kinase 5 (SmTK5)	Kapp et al., 2001
S. mansoni tyrosine kinase 4 (SmTK4)	Knobloch et al., 2002
S. mansoni receptor tyrosine kinase 1 (SmRTK1/SmVKR1)	Vicogne et al., 2003
S. mansoni receptor kinase 2 (SmRK2)	Forrester et al., 2004
S. mansoni tyrosine kinase 3 (SmTK3)	Kapp et al., 2004
S. mansoni protein kinase C (SmPKC1)	Bahia et al., 2006
S. mansoni cytoplasmic protein-tyrosine kinase (SmFes)	Bahia et al., 2007
S. mansoni insulin receptor 1 and 2 (SmIR1, SmIR2)	Khayath et al., 2007
S. mansoni Ste20-like kinase (SmSLK)	Yan et al., 2007
S. mansoni cAMP-dependant protein kinase (SmPKA-C)	Swierczewski & Davies, 2009
S. mansoni protein kinase C β (PKCβ)	Ludtmann et al., 2009
S. mansoni tyrosine kinase 6 (SmTK6)	Beckmann et al., 2011
S. mansoni p38 mitogen-activated protein kinase (p38MAPK)	Ressurreição et al., 2011
S. mansoni venus kinase receptor 1 (SmVKR1)	Gouignard, 2011
S. mansoni venus kinase receptor 2 (SmVKR2)	Gouignard, 2011
S. mansoni polo-like kinase 2 (SmSak)	Long et al., 2012
S. mansoni cAMP-dependant protein kinase (PKA)	de Saram et al., 2013
S. mansoni fibroblast growth factor receptor (Smfgfr)	Collins et al., 2013
S. mansoni extracellular signal regulated Kinase (ERK)	Ressurreição et al., 2014
S. mansoni nucleotide kinases – deoxyriboside, uridine, cytidine	Naguib & el Kouni, 2014
S. mansoni protein kinase B/AKT (SmAKT)	Morel et al., 2014

Table 1.1. Protein kinases studied in *S. mansoni* listed in chronological order. Adapted from McKenzie (2018).

1.7.3 Aims

1. To perform a post translational modification can on mixed adult worms of *S. mansoni* enabling characterisation of the phosphoproteome.

2. To design, develop and test a schistosome specific kinome array for use in conjunction with *S. mansoni*.

3. To explore the Ca^{2+}/Calmodulin Kinase II signalling pathway within differing life stages of *S. mansoni.*

4. To bring all the knowledge gained in these steps together to further the understanding of the cell signalling within *S. mansoni*.

2 General Materials and Methods

2.1 Reagents

2.1.1 Antibodies

The following antibodies were obtained from Cell Signalling Technology (New England Biolabs, Hitchin, UK): 1) rabbit polyclonals - IgG horse radish peroxidase (HRP)-linked (#7074), Phospho-(Ser) PKC Substrate (#2261); 2) Rabbit monoclonals - Phospho-PKA Substrate (RRXS*/T*) (#9624), p-AKT Substrate (RXXS*/T*) (#9614), Phospho-CaMKII (T286) (#12716), and CaMKII (pan) (#3362). The HRP-conjugated actin antibody (i-19) (#sc1616) was from Santa Cruz Biotechnology (Heidelberg, Germany), whereas the Alexa Fluor 488 goat anti-rabbit IgG (#A11008), was obtained from Life Technologies (Thermo Fisher Scientific, Loughborough, UK).

2.1.2 Immunohistochemistry Reagents

Normal goat serum (10%; #50062Z), was obtained from Life Technologies and the 18 x 18 and 20 x 20 mm cover slips were from Menzel-Gläser (Braunschweig, Germany). Rhodamine phalloidin (#P1951) and silane-prep slides (#S4651) were purchased from Sigma Aldrich (Poole, UK). The formaldehyde solution (#28906), Triton X-100 and glass microscope slides were obtained from Thermo Fisher. Finally, the Vectashield mounting medium was purchased from Vector Laboratories (Peterborough, UK).

2.1.3 Western Blotting Reagents

Nitrocellulose blotting membrane (0.45 μm) (#10600002), Amersham ECL Prime Western blotting detection reagent (#RPN2232) and gel blotting paper (#10426981) was purchased from GE Healthcare (Chalfont St. Giles, UK). The 10- and 15-well Bolt 4-12% Bis-Tris Plus electrophoresis gels (#NW04120BOX/#NW04125BOX), Bolt MES Running Buffer (20X) (#B000202), Bolt sample reducing agent (10X) (#B0009) and Bolt LDS sample buffer (4X) (#B0008) were all bought from Life Technologies. The Ponceau S solution (#P7170) was purchased from Sigma Aldrich whereas the Restore Western blotting stripper buffer (#21059) and SuperSignal molecular weight protein ladder (#84785) were bought from Thermo Fisher.

2.1.4 Other Consumables and Reagents

The inhibitor KN93 (#422771) was purchased from Calbiochem (Merck, Feltham, UK). The Falcon 15 ml high-clarity polypropylene conical tubes were obtained from BD Biosciences, (#8362523) (Wokingham, UK). The yellow pipette tips 2-200 µl were from Elkay Laboratories (#01B) (Basingstoke, UK) whereas the radio immunoprecipitation assay (RIPA) buffer 10X, (#9806) and kinase buffer 10X, (#9802) were from Cell Signalling Technology. Microcentrifuge conical tubes, (#11558232), blue pipette tips 200-1000 µl, (#FB34611), and crystal pipette tips 0.1-10 µl, (#FB34521) were purchased from Thermo Fisher Scientific together with 3 ml transfer pipettes, (#1343-9108), phosphate buffered saline (PBS) tablets (#10388739). Basal Medium Eagle (1X, BME) (#41010-026), RPMI-1640 (#11875-101) and HEPES buffer (#15630080) were from Gibco (Thermo Fisher Scientific). Parafilm (#P7543-1EA), tris(hydroxymethyl)amino-methane (Tris) (#252859),

Hanks balanced salt solution (HBSS) (#H9269), bovine serum albumin (BSA) (#A3059-10G), dimethyl sulfoxide (DMSO) (D8418), λ-phosphatase (P9614), and antibiotic-antimycotic (100X) (A5955) were all bought from Sigma Aldrich. Halt protease and phosphatase inhibitor cocktail (100X) (#78440), Pierce™ detergent-compatible Bradford assay kit (#23246), Pierce™ sequenal grade urea (#29700), TBS Tween-20 buffered saline (TTBS) (#28360), single use Sterilin (universal) tubes (#3308), 48-well tissue culture plates (#3308), glycine (#G/P460/53), SuperSignal West Pico chemiluminescent substrate #(34080) and foetal bovine serum (FBS) (A38401) were all obtained from Thermo Scientific.

2.2 General Methods

2.2.1 Ethics

The parasites were obtained from BioGlab Ltd (courtesy of Professor Mike Doenhoff, the University of Nottingham, UK). Laboratory animal use was within a designated facility regulated under the terms of the UK Animals (Scientific Procedures) Act 1986, complying with all requirements. The University of Nottingham Ethical Review Committee approved work involving mice and work was carried out under Home Office licence 40/3595.

2.2.2 SDS-Page and Western Blotting

To prepare parasite samples for electrophoresis, the parasites were placed into 1.5 ml microfuge tubes on ice for 5 minutes (min) to stop any signalling within the parasite. The

parasites were then centrifuged at 13,400 rpm in an Eppendorf mini centrifuge for 45 seconds (s), and the supernatant was removed from the microfuge and discarded leaving pelleted parasites in the microfuge tube. An appropriate volume of Bolt LDS sample buffer (4X) and Bolt sample reducing agent (10X) was added to the sample, which was then heated at 95°C for 5 min. Finally, the sample was sonicated for 1 min, before a final pulse in the centrifuge to ensure all sample was collected in the base of the tube. If storing at -20°C before running on a gel, protease, and phosphatase inhibitors were added to the sample.

Sodium dodecyl sulfate polyacrylamide gel electrophoresis (SDS-PAGE) was performed using the prepared protein samples. Samples were electrophoresed on either 10- or 15-well Bolt 4-12% Bis-Tris Plus precast polyacrylamide gels. The gels were clamped into a Bolt mini gel tank, and MES SDS running buffer was added to the gel tank. The samples were loaded into the wells, alongside a SuperSignal molecular weight protein ladder. The gel was run at 165 V, and ~180 mA – 90 mA, until the sample has reached the bottom of the gel cassette. After the run completed, the gel was removed from the cassette and placed into blotting buffer (192 mM glycine, 25 mM tris(hydroxymethyl)aminomethane, in 20% (v/v) methanol made up to 1 L with distilled H_2O). Using a semi-dry electro transfer unit set to 15 V and 280 mA (Thermo Fisher Scientific), proteins were transferred to the 0.45 μm nitrocellulose membrane. To ensure proteins had successfully transferred, the membrane was briefly washed in distilled water and stained with Ponceau S. The stain was removed by washing with a solution of tris-buffered saline containing 0.1% (v/v) tween-20 (TTBS) 3 times for 5 min each. To block the membrane ensuring no non-specific antibody binding the membrane was incubated in 1% (w/v) BSA in TTBS for 1 h before incubation with the primary antibody (typically at 1:1000 dilution in 1% BSA TTBS) overnight at 4°C. The

following day, blots were washed 3 times for 5 min each in TTBS before incubation with secondary antibody (typically 1:3000 dilution in 1% BSA TTBS) for 2 h at room temperature. After a final washing (TTBS 3 times for 5 min each), the blot was ready for visualisation. This was carried out by covering the membrane with SuperSignal West Pico chemiluminescence substrate (Thermo Fisher) or Amersham ECL Prime Western Blotting Detection Reagent and exposing to a cooled CCD GeneGnome chemiluminescence imaging system (Syngene, Cambridge, UK). Finally, to ensure that the protein samples loaded into each lane of the gel had similar amounts of total protein, the membrane was stripped using Restore Western Blot Stripping Buffer, before extensive washing in TTBS. The membrane was then incubated in HRP-conjugated anti-actin antibody (1:3000 dilution in TTBS). The resulting actin signal was used to normalise the immunoreactive band intensities for the other target proteins, this analysis was carried out using Gene Tools Software (Syngene, Cambridge UK). The analysis was performed by using the Gene Tools Software to quantify the level of protein in the actin and the level of protein in the band identified by the chosen antibody. Using these results the amount of protein in the either the actin or antibody could be divided by the control (which was normalised to 1) to get the relative result. Finally, to get the actin corrected result the relative result from antibody band was divided by the relative result from the actin band.

2.2.3 Snail Husbandry

Infected *B. glabrata* (M-line), which serve as intermediate host for *S. mansoni* (PR-1 strain) were provided by the Biomedical Research Institute (BRI; Maryland, USA) *via* the National Institute of Health – National Institute of Allergy and Infectious Disease (NIH-NIAID)

Schistosomiasis Resource Center under NIH-NIAID Contract No. HHSN272201000005I. When required, extra M-line snails infected with an identical strain of *S. mansoni* were kindly provided by Nuha Mansour/Quintin Bickle from the London School of Hygiene and Tropical Medicine (LSHTM, UK). Snails were maintained in 1.5 L transparent plastic containers (Really Useful Box Company) until they reached patency (approximately 35 days post-infection). Snails from the BRI were kept ~50/box with ~1 L of tap water filtered through a Brimark carbon filtration unit (Silverline UK; Devon, UK). Snails from LSHTM were kept in approximately 1 L distilled water with 1 ml added salts (100 g calcium carbonate, 10 g magnesium carbonate, 10 g sodium chloride, 2 g potassium chloride dissolved in 3 L distilled water; this salt formula was also kindly provided to us by Nuha Mansour at the LSHTM). All snails were fed dried round lettuce twice a week and occasional fish food.

Each snail box was cleaned once a week with the water changed twice weekly. Discarded water was carefully decanted into buckets containing 2% Virkon (Thermo Fisher Scientific) and left for ~5 days before disposing the mixture. Dead snails were removed daily in order to reduce overall mortality of the group. The boxes containing snails were housed in an LMS or Sanyo incubator at 26°C under a 12 h/12 h light dark cycle. During patency, snails were maintained at the same temperature but in continued darkness.

2.2.4 Isolation of *S. mansoni* for experiments

2.2.4.1 Isolation of cercariae

To shed the cercariae the patent snails were transferred into a glass beaker filled with 50 ml of filtered water placed under a light source for 2 h to encourage shedding of the cercariae from the snails. The cercariae were then carefully removed from the beaker using a glass

pipette, and either fixed in ice-cold absolute acetone for immunohistochemistry or transformed to somules.

2.2.4.2 Transformation of Cercariae to Somules

The collected cercariae were transferred carefully to sterile 15 ml Falcon tubes using a sterile pipette; the tubes were then placed on ice for 30 min, followed by centrifugation for 8-10 min at 0.5 rcf. The supernatant was removed and discarded using a pipette, leaving approximately 3 ml water and the pellet in the tube. Next, 5 ml pre-warmed (37˚C) BME was added; antibiotics/antimycotic solution was added to the BME before use to restrict bacterial growth. The tubes were vortexed for 5-7 min; 3 ml of HBSS, was added to the solution, and the tube was placed on ice for a further 7 min before centrifuging for 2 min at 0.5 rcf. The supernatant was then removed and discarded leaving ~3 ml in the tube, which was poured into a high-walled glass Petri dish. BME, pre-warmed in the incubator, was added to the dish, and the dish was swirled by hand under a dissecting microscope to concentrate the cercariae 'heads' into the centre of the dish. To enumerate somules, the heads were first collected into a 15 ml falcon tube, and 1 µl was taken three times from the centre of tube, vortexing in between each, then placed onto a flat glass plate. The 'heads' were then removed using a pipette and were plated into individual wells of a 24 well culture plate (Nunc) in BME and were placed in a CO_2/37˚C incubator for experiments. Each drop could then be visualised under a light microscope and the number of heads counted per 1 µl and averaged between the 3 samples, then this number could be used to calculate the number of heads in the final BME sample. Typically, 1000 somules (i.e. transformed cercariae 'heads') were plated per well in 1 ml of BME.

2.2.5 Statistical Analysis

Analysis of variance (ANOVA) and Fisher's post-hoc multiple comparison test was performed to analyse the effects of the individual treatments at specific time points using Minitab 18.

3 PHOSPHOPROTEOMICS OF ADULT *SCHISTOSOMA MANSONI*

3.1 Introduction to Phosphoproteomics

Proteomics is the large-scale study of the proteins within a cell, tissue or organism and often focuses of the structure and the function of the proteins. Proteomics can be sub-divided into more specific studies of proteins, for example investigating post-translational modifications (PTM's), which are often integral to the function of the protein (Deracinois et al., 2013). Post-translational modifications can include methylation, acetylation, oxidation, ubiquitination, and, for the purpose of this study, phosphorylation. The study of the proteins affected by a phosphorylation PTM is known as phosphoproteomics (Kosako & Nagano, 2011). Phosphoproteomics is a rapidly developing area of research, however, there are some issues with the techniques involved, for example not all phosphoproteins are easily identifiable by one method and complex mixtures containing non-phosphorylated proteins can be a problem (Reinders & Sickmann, 2005). Typical phosphoproteomic analysis begins with the preparation of samples in suitable buffer systems that limit the loss of phosphorylation, followed by the detection of phosphoproteins using Western blotting techniques with phospho-specific antibodies. Next phosphopeptides are enriched to ensure the analysis is not hindered significantly by the presence of non-phosphorylated proteins. Enrichment techniques include immunoprecipitation with phospho-specific antibodies, or immobilized metal-ion affinity chromatography (IMAC) (Zhao & Jensen, 2009).

Immunoprecipitation uses phospho-specific antibodies to bind to targeted phosphoproteins, enabling these chosen protein-antibody complexes to be concentrated through centrifugation and washing the sample. IMAC works by binding phosphorylated peptides and proteins to the stationary phase through electrostatic interactions with positively charged metal-ions that are bound to the column material, leaving the non-phosphorylated proteins to be washed through (Zhao & Jensen, 2009). The following step in a phosphoproteomic analysis would be the identification of the phosphorylated amino acid residues, which is most commonly done by mass spectroscopy identification (Kosako & Nagano, 2011; Reinders & Sickmann, 2005). Mass spectroscopy results are then analysed in a number of different ways to answer the specific questions of the study.

3.1.1 Phosphoproteomics in Parasites

Phosphorylation has a huge impact on the biological performance of proteins, altering everything from cellular activity, signalling and localization to complex formation, providing the basis for the formation of intricate signalling pathways regulated by kinases and phosphatases. Therefore, a complete and detailed study that would lead to information on the structure and dynamics of these signalling pathways is essential to elucidate fundamental mechanisms of cellular processes and diseases. Phosphoproteomics has not been used extensively to explore kinase-mediated PTM in parasites, however, some noteworthy studies exist. For example, with *Plasmodium falciparum* there have been several studies, including a phosphoproteomics investigation of the intraerythrocytic developmental stages (Pease et al., 2013), and of the phosphoproteome of the *P. falciparum* schizont (Lasonder et al., 2012). In *Leishmania*, phosphoproteomics was used to investigate signalling in *L. donovani* axenic amastigotes using LC-ESI-MS/MS analysis of IMAC-

enriched phosphoprotein extracts (Hem et al., 2010) and another investigation identified a novel regulatory phospho-serine residue in the C-terminal auto-inhibitory domain within this parasite that could be involved in the regulation of kinases (Cayla et al., 2014). In *Trypanosoma brucei* a global quantitative phosphoproteomic study was performed on both the bloodstream and procyclic forms to identify the protein groups and phosphorylation sites, and then a comparison was carried out between the results gained from the two life stages (Urbaniak et al., 2013). Also, in *Trypanosoma cruzi*, an elegant analysis on the sub-proteome of the parasite's plasma membrane was performed (Queiroz et al., 2013).

3.1.2 Proteomics and Phosphoproteomics in Schistosomes

For schistosomes, several general proteomic studies have been carried out including a study characterizing the protein expression profiles of different developmental stages and tissues at the host-parasite interface (eggshell and tegument) for *S. japonicum* (Liu et al., 2006). For *S. mansoni*, adult worm proteomic studies have also identified important proteins in parts of the tegument (e.g. Braschi et al., 2006; Braschi & Wilson, 2006). More recently, in *S. japonicum* a proteomic analysis of the exposed tegumental proteins was carried out identifying a total of 179 proteins in females and 300 in males (Zhang et al., 2013). Furthermore, a proteomic analysis of the tegument of *S. mansoni* schistosomules was recently performed identifying more than 450 proteins including signalling proteins such as protein kinase A (PKA) (Sotillo et al., 2015). A proteomic analysis centring on the identification of extracellular vesicles in *S. mansoni* identified 109 proteins, including homologs to eukaryotic EVs as well as hypothetical proteins found in high abundance (Nowacki et al., 2015). In terms of phosphoproteomics there have only been two studies in

schistosomes which have collectively characterized *in vivo* phosphorylation of proteins within *S. japonicum* schistosomules and adult worms using an IMAC and TiO_2 based phosphoproteomic approaches (Cheng et al., 2013; Luo et al., 2012). With the huge advances in proteomic techniques and lack of exploration utilising these techniques in *S. mansoni* this project aims to characterise the phosphoproteome of mixed adult worms and unravel the proteins and signalling systems associated with it.

3.1.3 Aims

5. To perform a PTM scan on mixed adult worms of *S. mansoni* enabling characterisation of the phosphoproteome.
6. To discover overrepresented and novel phosphorylation site motifs as well as putative upstream protein kinases,
7. To explore the molecular function, and interactions between phosphoproteins.
8. To determine which kinases are identified in the dataset.

3.2 Methods

3.2.1 Preparation of material for PTM Scan analysis

Urea lysis buffer was prepared containing 20 mM HEPES (pH 8.0), 9.0 M urea (Pierce Sequanal grade), 1 mM sodium orthovanadate (activated), 2.5mM sodium pyrophosphate and 1 mM β-glycerol-phosphate. 50 mL of Milli-Q purified water was added to these reagents and left on a magnetic stirrer until dissolved. All glassware used to prepare the buffer was new and cleaned with Milli-Q purified water to ensure no detergents were present as these could interfere with the LC-MS/MS analysis. Sodium orthovanadate was dissolved in Milli-Q purified water and the pH adjusted to 10 using NaOH whilst stirring. The solution was then boiled until colourless and left to cool to room temperature. The pH was readjusted again using NaOH and boiling until colourless and returned to room temperature, this step was repeated until the solution remained colourless and the pH stable at 10. The final volume was adjusted with water and stored in 0.5 mL aliquots at -20°C until use.

Mixed adult male and female worms in groups of 10 from multiple infections that had been passaged through different snails (~400 worms in total) were added to 100 µl of urea lysis buffer and homogenized at 4°C using a motorized microfuge pestle (Kimble-Chase). Samples were centrifuged at 20,000 *x g* for 10 min at 4°C, and the supernatants removed and pooled together. Aliquots of homogenate from each processed batch were removed for protein estimation (20 µl; Bradford assay) using BSA as the protein standard and Western blot analysis (30 µl). Samples were then stored at -80°C until shipment to Cell Signalling Technology (CST) for phosphoproteomic analysis after immunoaffinity purification (IAP)

with anti-phospho antibodies or isolation of peptides using IMAC. The batches were pooled and yielded a total of 12.8 mg protein (2.09 mg/ml).

3.2.2 Phosphoproteomic Analysis

Phosphoproteomic analysis was done under contract by CST; antibody-based IAP (via PTMScan Discovery - PhosphoScan) and IMAC were performed to isolate phosphopeptides. Prepared supernatants were reduced with 4.5 mM DTT for 30 min at 55°C followed by alkylation with 10 mM iodoacetamide for 15 min in the dark at room temperature. After four-fold dilution in 20 mM HEPES (pH 8.0) samples were digested overnight with 10 μg/ml trypsin-TPCK (Worthington). Resultant peptides were acidified with trifluoroacetic acid (TFA; 1%) and desalted by solid-phase extraction with Sep Pak C18 cartridges (Waters); eluted peptides were next dried under vacuum and stored at -80°C.

Either pY or pS/pT antibody mixes were used for immunoprecipitations. Saturating amounts of the antibodies were bound to 40 μl packed protein A agarose beads (Roche) overnight at 4°C. Total peptides were resuspended in MOPS IAP buffer (50 mM MOPS, pH 7.2, 10 mM KH_2PO_4, 50 mM NaCl) and centrifuged (5 min, 10,000 *x g*). Phosphopeptides were then enriched by mixing the sample with the antibody bead slurries (2 h at 4°C) and pulse centrifuging (30 s, 2,000 *x g*, 4°C) and washing (two washes with 1 ml MOPS IAP buffer and four washes with 1 ml MQ-H_20 (Burdick and Jackson). Isolated peptides were then sequentially eluted with TFA (0.15%; 65 μl then 55 μl, 10 min each) at room temperature, and desalted/concentrated over spin tips packed with Empore C18 (Sigma) and eluted with

40% acetonitrile in 0.1% Trifluoracetic acid (TFA). Eluted peptides were dried under vacuum.

For enrichment of phosphopeptides (pS/pT) by IMAC, nickel-agarose beads (Invitrogen) were first ethylenediaminetetraacetic acid (EDTA)-treated to displace nickel, washed thrice with H_2O, loaded with $FeCl_2$ (aqueous) for 30 min, and rewashed. To enrich phosphopeptides, 10 µl Fe^{3+}-agarose slurry was mixed with 0.5 mg peptide in 1 ml 0.1% TFA/80% acetonitrile for 30 min at room temperature. The beads were then washed thrice with 0.1% TFA/80% MeCN to remove unbound peptides and bound peptides were eluted twice sequentially using 50 µl of 2.5% ammonia/50% acetonitrile for 5 min each and dried under vacuum. The samples were then resuspended in TFA (100 µl 0.15% + 2 µl 20%), desalted/concentrated and dried as previously. Finally, the peptides were resuspended in formic acid (0.125%) for LC-MS/MS.

The enriched phosphopeptides were analysed on an LTQ-Orbitrap ELITE mass spectrometer running XCallibur 2.0.7 SP1 (Thermo Scientific), with technical replicate analytical injections of each sample run to increase the number of identifications. The peptides were loaded directly onto a PicoFrit capillary column (10 cm x 75 µm; New Objective) packed with Magic C_{18} AQ reverse-phase resin. The peptides were eluted with a 150 min linear gradient of acetonitrile in 0.125% formic acid delivered at constant flow rate of 280 nl/min. Tandem mass spectra were collected in a data-dependent manner using a top 20 MS/MS method, with the following parameters: normalized collision energy, 35%; activation Q, 0.25; and activation time, 20 ms; repeat duration, 35 s; dynamic repeat count, 1. Real time

recalibration of mass error was performed using lock mass with a singly charged polysiloxane ion (m/z = 371.101237).

The MS/MS spectra were evaluated using SEQUEST, and CORE (Harvard University) as previously detailed for PTMScan (Gnad et al., 2013; Stokes et al., 2015). Briefly, searches were done against the *S. mansoni* genomic database using Ensembl Metazoa[4] (version 98.5); with a mass accuracy of +/- 5 ppm for precursor ions and 1Da for product ions. Enzymes specificity was limited to trypsin, cysteine carboxamidomethylation was specified a fixed modification; oxidation of methionine and the appropriate phosphorylation PTM were permitted as variable modifications. Reverse decoy databases were included to estimate FDR, and initially filtered at 2.5% FDR using ProteinSieve within CORE.

3.2.3 Bioinformatics – Primary Peptide Scan

An initial bioinformatic screen was undertaken for potential phosphorylated peptides in *S, mansoni* employing the results of identified phosphorylated peptides from studies using *S. japonicum* (Cheng et al., 2013; Luo et al., 2012). A protein BLAST against the *S. mansoni* genome was performed for each *S. japonicum* phosphorylated peptide using NCBI (Altschul et al., 1990) and GeneDB (Logan-Klumpler et al., 2012). The 'hit' with the highest peptide identity to the search peptide was selected (above percentage identity of 60%) and the phosphosite in the query peptide was then searched within the *S. mansoni* protein, to determine if this was conserved in *S. mansoni*. If conserved, the +7/-7 amino acids

[4] www.metazoa.ensembl.org

surrounding the putative *S. mansoni* phosphorylated site were noted, along with accession number and Smp identifier. The resulting *S. mansoni* peptide was entered into the Scansite3 online tool[5] to search for motifs likely to be phosphorylated by a protein kinase (Obenauer, Cantley, & Yaffe, 2003). Scan by input sequence was used, and the peptide scanned at both high and medium stringencies and the output recorded.

3.2.4 PTM Scan Bioinformatics – Motif Analysis

To sort peptides into classes according to their chemical properties (acidic, basic, proline, tyrosine, or other) the list of phosphorylated peptides from results Tables 1, 2 and 3 from CST were first re-processed to remove duplicates and ensuring that isoforms were considered as individual entries. A programme was then developed in collaboration with Dr Jean-Christophe Nebel using the following decision tree rules (Villén et al., 2007):

1. The 6 neighbouring amino acids before and after the phosphorylation site were obtained.
2. pY at position 0 then classify as “tyrosine”.
3. P at +1 then classify as “proline-directed”.
4. Positions +1 to +6 contain five or more D and E residues then classify as “acidic”.
5. K or R at position −3 then classify as “basic”.
6. D or E at +1, +2, or +3 then classify as “acidic”.

[5] https://scansite4.mit.edu/4.0/#home

7. Between −6 and −1, 2 or more K or R residues then classify as “basic”.

8. Remaining peptides are classified as “other”.

A degenerate set of peptides was also produced using the following: A = AG, D = DE, F = FY, K = KR, I = ILVM, Q = QN, S = ST, C = C, H = H, P = P, W = W to allow for the possibility of amino acid substitutions. This set of peptides was also processed to classify the peptides according to their chemical properties. Due to peptides often being classified in more than one category, for example basic and proline-directed, another category was developed and named ‘mixed’.

Following this, motif analysis using the normal and degenerate peptide lists was carried out to test for motif overrepresentation. This was done with the online tool MotifX (Chou & Schwartz, 2011) using the following default parameters: 1) Phosphorylation motif window = 13 amino acids; 2) P-value threshold: 1×10^{-6} for S, T & Y residues; 3) Occurrence threshold: 20; and 4) Using a background of all 11,723 *S. mansoni* proteins (Proteome ID: UP000008854).

3.2.5 Upstream Kinase Motif Analysis

The overrepresented motifs identified by MotifX were subjected to a further analysis to identify potential upstream kinases. This was performed using the PhosphoMotif finder tool[6] on the Human Protein Reference Database (HPRD), by entering each identified motif and selecting either serine/threonine or tyrosine depending on which phosphorylation site was

[6] http://www.hprd.org/PhosphoMotif_finder

relevant for the motif. A second analysis using Phosida[7] was performed, linking known upstream kinases to identified motifs. All output was recorded in a table and a graphical representation of the data was formed using Excel.

3.2.6 Gene Ontology

Gene ontology (GO) analysis was carried out using the online programme Ensembl Metazoa (Kersey et al., 2014). A full list of GO terms was obtained using the biomart tool, selecting the metazoa mart under the database option followed by the *S. mansoni* genes dataset. Under 'filters', the gene option was expanded and a full list of the gene ID's (Smp identifiers, *S. mansoni* proteins) for each of the phosphorylated proteins was input. The gene filter was minimized, the GO filter was expanded, and all 3 options selected; GO term accession, GO term name, and GO evidence code. Results were exported into .XML form and saved (carried out on the 05/11/15) for analysis.

3.2.7 GO SLIM

GO Slim was performed using the Blast2Go PRO tool (Conesa et al., 2005). A full list of Smp identifiers representing all of the phosphorylated proteins from *S. mansoni* were imported to the programme, the list was mapped using the mapping tool, and then annotated using the annotation tool. This process annotated each protein with full GO terms. Using the

[7] http://www.phosida.de/

Blast2Go analysis option, the proteins were then annotated using GO SLIM, then using the graph tool a combined graph was constructed, one using the total set of results and one for each of the biological processes, molecular function and cellular component, which resulted in a flow chart combined graph for each. For each of these combined graphs a separate pie and bar chart was constructed for each level depicted on the flow chart using the relevant options.

3.2.8 Analysis of Protein Kinases

Using the *S. mansoni* kinome (Andrade et al., 2011) as a knowledgebase, protein kinases possessing identified phosphorylation sites were tabulated. Identification of the predicted activation loop for each protein kinase was achieved by manually searching for the conserved DFG motif (Nolen et al., 2004) within each sequence and/or extracting the relevant sequence from the conserved protein domain tool within NCBI BLASTp and InterPro. Phosphorylation site(s) within each loop were next manually annotated with reference to each identified phosphopeptide.

3.2.9 STRING Analysis

The full protein–protein interaction data for *S. mansoni* was downloaded from the STRING website[8]. The proteins in the phosphoproteomic dataset were the extracted from the total

[8] http://string-db.org/newstring_cgi/show_download_page.pl.

interaction dataset using interactions with a confidence score of 0.7 or higher to enable interactions between only the phosphorylated proteins to be visualised. The phosphorylated proteins with the highest number of interactions were noted and each of these were re-entered into the STRING database to extract networks for the top 25 most highly interacting proteins.

3.2.10 Phosphorylated Protein Interaction Network Analysis

The *S. mansoni* phosphoproteome interaction network was constructed from all *S. mansoni* protein−protein interaction data with a confidence level of 0.7 that were matched with the phosphorylated *S. mansoni* proteins identified in this study using Cytoscape for visualization and the plugin application StringApp. The phosphointeractome was analysed for highly connected nodes within the network using the molecular complex detection (MCODE) clustering algorithm that was available as a Cytoscape plug-in using default parameters, set to maximum 100 interactors and >0.7 confidence.

3.2.11 KEGG Analysis

A Kyoto Encyclopaedia of Genes and Genomes (KEGG) analysis was performed using the basic version of BLAST2GO. All the Smp identifiers for the phosphorylated proteins were submitted to BLAST2GO, the analysis drop down menu was selected and pathway maps from the KEGG database were accessed and linked through to the proteins through the online KEGG resource. Results were presented in a table documenting the pathway, number of proteins involved, and number of enzymes involved.

3.3 Results

3.3.1 Initial Bioinformatics

Investigation into the integral mechanism of protein regulation through phosphorylation within *S. mansoni* began with a literature search to find studies that had examined phosphorylated proteins within schistosomes using phosphoproteomics. A research group from the Shanghai Veterinary Research Institute had isolated and characterized phosphorylated proteins within schistosomula and adult male and female worms of *S. japonicum* (Cheng et al., 2013; Luo et al., 2012). This group used two phosphoproteomic approaches, firstly, immobilized metal-ion affinity chromatography (IMAC) (Luo et al., 2012) and, secondly, a TiO_2 based method (Cheng et al., 2013). These two studies identified 127 phosphorylation sites in 92 proteins, and 180 phosphopeptides in 148 proteins, respectively (Cheng et al., 2013; Luo et al., 2012). The results from these studies provided a useful resource to begin a phosphoproteomic investigation within *S. mansoni*. A full list of *S. japonicum* phosphoproteins were generated and a BLAST search was performed against each of these phosphopeptides against the *S. mansoni* genome using GeneDB[9] (Logan-Klumpler et al., 2012); the percentage identity for each phosphopeptide was noted, and any 'hits' with identity less than 60% were considered as being poorly conserved and no further analysis was carried out. The phosphorylated residue in the *S. japonicum* peptide was then manually checked for conservation against the *S. mansoni* 'hit' sequence, and if the phosphorylation site was conserved then the 6 amino acids either side of the central residue were recorded providing an *S. mansoni* phosphopeptide with the phosphorylation site

[9] https://www.genedb.org/

highlighted, this resulted in identification of 185 *S. mansoni* proteins . Finally, the putative *S. mansoni* phosphopeptides were uploaded to Scansite to search for motifs that are likely to be phosphorylated by specific protein kinases (Obenauer et al., 2003). Using this tool (at high and medium stringencies) a list of 75 potential upstream protein kinases capable of phosphorylating the peptides was generated (Table 3.1, Appendix File 1).

S. japonicum peptide	*S. japonicum* protein	Phosphosite in search peptide	*S. mansoni* Peptide	Phosphosite in *S. mansoni* peptide	Peptide identity to search (%)	*S. mansoni* protein	Potential upstream kinase	References
K.WDHIEVsDDEDDTHPNIDTPSLFR.W	CDC37 cell division cycle 37 homolog	Ser15	KWDHIEVSDDEDDTH	Ser15	100	Hsp90 co chaperone Cdc37	Casein Kinase 2	Cheng et al 2012
K.EVsDDEAEKEETKNESEEAEDKPK.V	heat shock protein 90	Ser225	KERTKEVSDDESEKV	Ser225	73	heat shock protein	Casein Kinase 2	Cheng et al 2012
R.FIsETDSVYR.T	programmed cell death-involved	Ser521	KPRKRFISETDSIYR	Ser504	92	programmed cell death involved protein	Akt Kinase/ 14-3-3 Mode 1	Cheng et al 2012
K.NSREsEEsGGEDEFQVEK.I	heterochromatin protein 1	Ser9	PSKNSPQSEESAGED	Ser9	85	chromobox protein		Cheng et al 2012
R.RHsVAAESFNPATVNDLEPVVHPK.S	cAMP-dependent protein kinase R2	Ser57	YIGARRQSVAAESFN	Ser58	85	cAMP dependent protein kinase R2	Aurora B (AuroB)/ Protein Kinase A (PKC epsilon on M)	Cheng et al 2012
R.LTTDsGSAATAFLSGAK.G	alkaline phosphatase	Ser123	SDRLTTDSGSAATAF	Ser123	89	alkaline phosphatase	Casein Kinase 1	Cheng et al 2012

Table 3.1. Predicting phosphorylation sites in *S. mansoni* proteins. Example of results gained from an initial bioinformatics investigation where phosphorylated peptides from *S. japonicum* (Cheng et al., 2013) were BLAST searched against the *S. mansoni* genome at GeneDB. Potential upstream kinases for the phosphorylated peptides were predicted using Scansite (Obenauer et al., 2003).

3.3.2 Phosphoproteomics of adult *S. mansoni*

To gain a deeper understanding of phosphorylated proteins within adult worms and provide an underlying dataset for further exploration of the *S. mansoni* phosphoproteome, mixed male and female adult worms were processed for phosphoproteomic analysis under contract with Cell Signalling Technology (CST). This analysis was made possible through a specific investment from Kingston University, as the analysis was costly; cost also precluded analysis

of separate sexes. Approximately 400 adult worms from a mixed male and female population (derived from several batches of worms from separate snail and mouse infections over a period of three months) were homogenised in a urea lysis buffer made to specific CST instructions (Section 3.2.1); protein extracts were then clarified. The relative quality of the samples after preparation and storage at -80˚C was assessed by performing a Western blot with aliquots and probing with anti-phospho-PKA, -PKC and -AKT substrate-motif antibodies (Figure 3.1) to globally assess the phosphorylation state of substrates of these kinases. A large number of phosphorylated proteins were detected with each of these antibodies, demonstrating that the individual samples had been successfully prepared, did not degrade over time in storage, and were suitable for phosphoproteomic analysis. The samples were then pooled to provide sufficient material for phosphoproteomics (final yield 12.8 mg protein at 2.09 mg/ml) and were shipped to CST, where three technical replicates were performed using this sample.

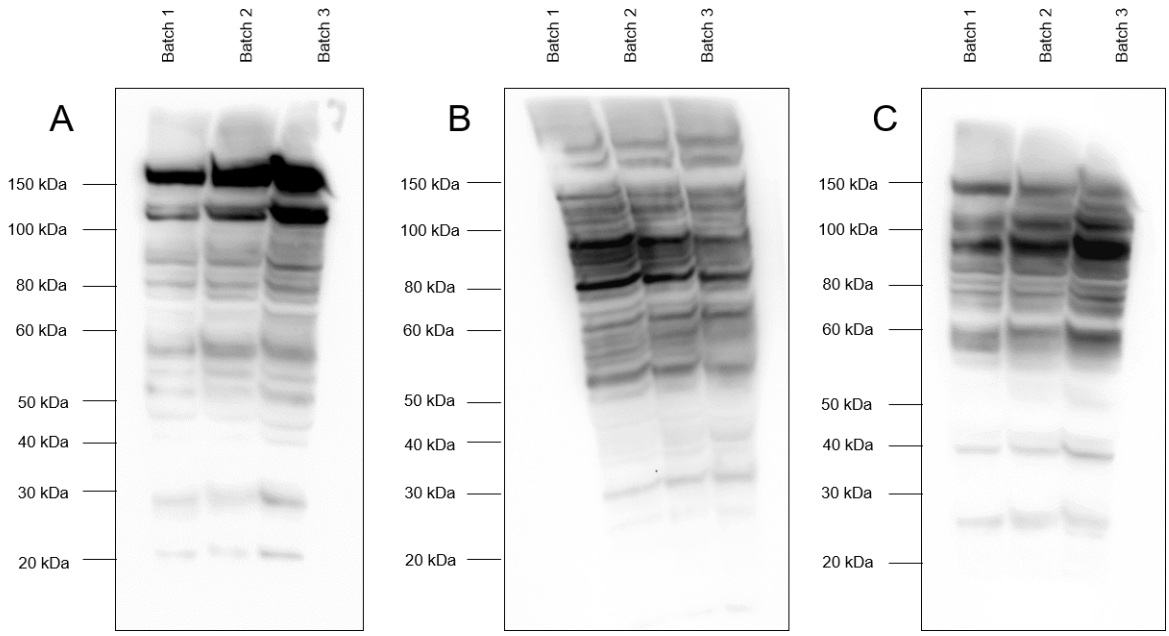

Figure 3.1. Analysis of phosphorylated proteins in adult *S. mansoni*. Western blots of protein extracts from mixed male and female populations were probed with anti-phospho kinase substrate antibodies: (A) anti-phospho-PKA substrate antibody; (B) anti-phospho-PKC substrate antibody; and (C) anti-phospho-AKT substrate antibody. Each lane represents a sample from different batches of adult worms which were processed over a three month period, with one shipment per month (labelled as batch 1, batch 2 and batch 3).

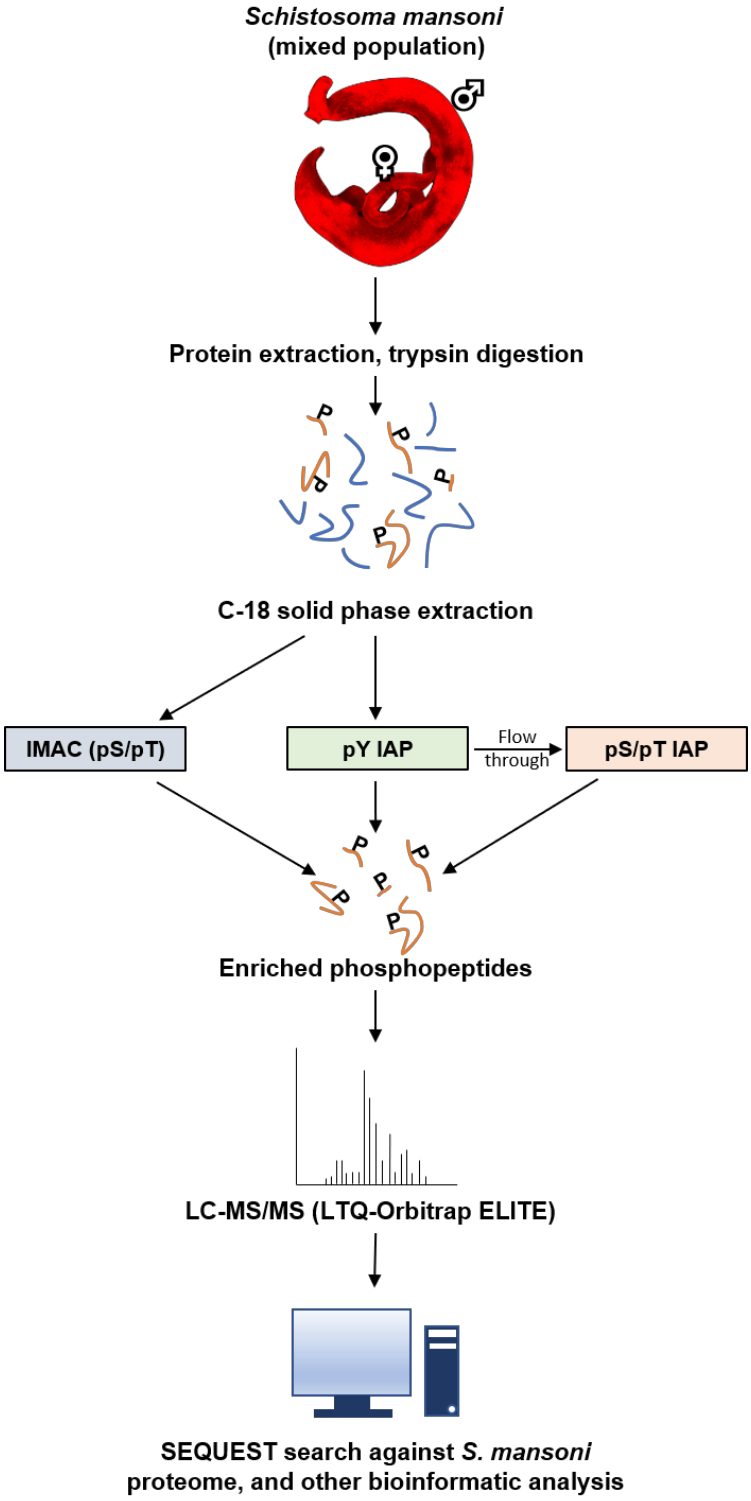

Figure 3.2. Workflow diagram of processes carried out during the PTM Scan done in conjunction with Cell Signalling Technology.

Once analysis was complete (Figure 3.2), CST provided the results in three separate tables. Tables 1, 2 and 3 listed the phosphoproteins detected following enrichment with phospho-

tyrosine immunoaffinity purification (IAP) (pY IAP), IMAC, and phosphoserine/threonine (IAP pS/pT IAP), respectively. The pS/pT IAP is a motif antibody mix used for profiling substrates of kinases, including substrates such as: AKT, AMPK, MAPK, CDK, PKA, PKC, CKII and others. The pS/pT IAP was performed using the pY IAP flow through. The table layout is summarised in Table 3.2 and the complete tables are contained within additional files 2-4.

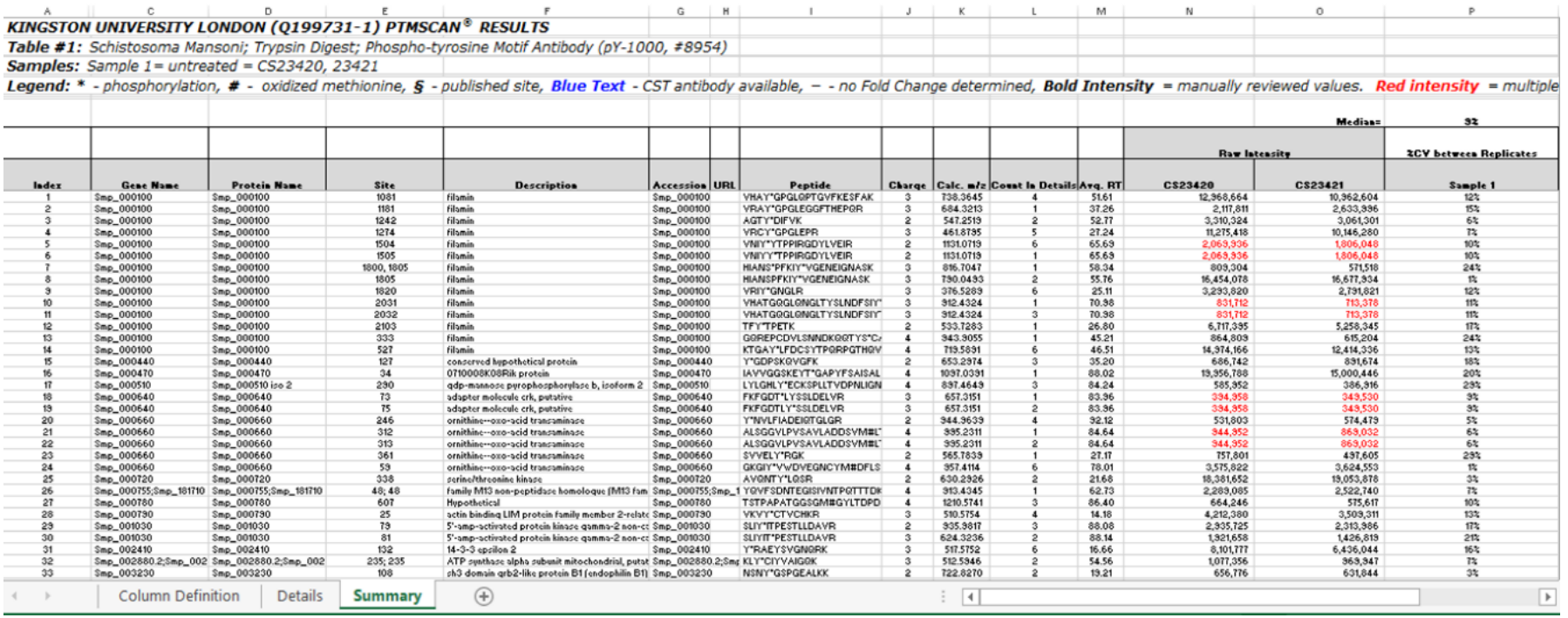

KINGSTON UNIVERSITY LONDON (Q199731-1) PTMSCAN® RESULTS

Table #1: *Schistosoma Mansoni; Trypsin Digest; Phospho-tyrosine Motif Antibody (pY-1000, #8954)*

Samples: *Sample 1 = untreated = CS23420, 23421*

Legend: * - phosphorylation, # - oxidized methionine, § - published site, **Blue Text** - CST antibody available, – - no Fold Change determined, **Bold Intensity** = manually reviewed values. **Red intensity** = multiple

												Median=	32
												Raw Intensity	%CV between Replicates
Index	Gene Name	Protein Name	Site	Description	Accession	URL	Peptide	Charge	Calc. m/z	Count in Details	Avg. RT	CS23420	CS23421	Sample 1
1	Smp_000100	Smp_000100	1081	filamin	Smp_000100		VHAY*GPGLGPTGVFKESFAK	3	738.3645	4	51.61	12,368,664	10,362,604	12%
2	Smp_000100	Smp_000100	1181	filamin	Smp_000100		VRAY*GPGLEGGFTHEPQR	3	684.3213	1	37.26	2,117,811	2,633,386	15%
3	Smp_000100	Smp_000100	1242	filamin	Smp_000100		AGTY*DIFVK	2	547.2519	2	52.77	3,310,324	3,061,301	6%
4	Smp_000100	Smp_000100	1274	filamin	Smp_000100		VRCY*GPGLEPR	3	461.8795	5	27.24	11,275,418	10,146,280	7%
5	Smp_000100	Smp_000100	1504	filamin	Smp_000100		VNIY*YTPPIRGDYLVEIR	2	1131.0719	6	65.69	2,063,936	1,806,048	10%
6	Smp_000100	Smp_000100	1505	filamin	Smp_000100		VNIYY*TPPIRGDYLVEIR	2	1131.0719	1	65.69	2,063,936	1,806,048	10%
7	Smp_000100	Smp_000100	1800, 1805	filamin	Smp_000100		HIANS*PFKIY*VGENEIGNASK	3	816.7047	1	58.34	803,304	571,516	24%
8	Smp_000100	Smp_000100	1805	filamin	Smp_000100		HIANSPFKIY*VGENEIGNASK	3	790.0493	2	55.76	16,454,078	16,677,934	1%
9	Smp_000100	Smp_000100	1820	filamin	Smp_000100		VRIY*GNGLR	3	376.5289	6	25.11	3,293,820	2,791,821	12%
10	Smp_000100	Smp_000100	2031	filamin	Smp_000100		VHATGQGLGNGLTYSLNDFSIY*	3	912.4324	1	70.38	831,712	713,378	11%
11	Smp_000100	Smp_000100	2032	filamin	Smp_000100		VHATGQGLGNGLTYSLNDFSIY*	3	912.4324	3	70.38	831,712	713,378	11%
12	Smp_000100	Smp_000100	2103	filamin	Smp_000100		TFY*TPETK	2	533.7283	1	26.80	6,717,395	5,258,345	17%
13	Smp_000100	Smp_000100	333	filamin	Smp_000100		GGREPCDVLSNNDKGGTYS*C#	4	943.3055	1	45.21	864,803	615,204	24%
14	Smp_000100	Smp_000100	527	filamin	Smp_000100		KTGAY*LFDCSYTPGRPGTHGV	4	719.5891	6	46.51	14,374,166	12,414,336	13%
15	Smp_000440	Smp_000440	127	conserved hypothetical protein	Smp_000440		Y*GDPSKGVGFK	2	653.2974	3	35.20	686,742	891,674	18%
16	Smp_000470	Smp_000470	34	0710008K08Rik protein	Smp_000470		IAVVGQSKEYT*GAPYFSAISAL	4	1097.0391	1	88.02	19,356,788	15,000,446	20%
17	Smp_000510	Smp_000510 iso 2	290	gdp-mannose pyrophosphorylase b, isoform 2	Smp_000510		LYLGHLY*ECKSPLLTVDPNLIGN	4	897.4649	3	84.24	585,952	386,916	23%
18	Smp_000640	Smp_000640	73	adaptor molecule crk, putative	Smp_000640		FKFGDT*LYSSLDELVR	3	657.3151	1	83.36	334,958	349,530	3%
19	Smp_000640	Smp_000640	75	adaptor molecule crk, putative	Smp_000640		FKFGDTLY*SSLDELVR	3	657.3151	2	83.36	334,958	349,530	3%
20	Smp_000660	Smp_000660	246	ornithine--oxo-acid transaminase	Smp_000660		Y*NVLFIADEIGTGLGR	2	944.9639	4	92.12	531,803	574,479	5%
21	Smp_000660	Smp_000660	312	ornithine--oxo-acid transaminase	Smp_000660		ALSGGVLPVSAVLADDSVM#L*	4	995.2311	1	84.64	944,952	863,032	6%
22	Smp_000660	Smp_000660	313	ornithine--oxo-acid transaminase	Smp_000660		ALSGGVLPVSAVLADDSVM#L*	4	995.2311	2	84.64	944,952	863,032	6%
23	Smp_000660	Smp_000660	361	ornithine--oxo-acid transaminase	Smp_000660		SVVELY*RGK	2	565.7839	1	27.17	757,801	497,605	23%
24	Smp_000660	Smp_000660	59	ornithine--oxo-acid transaminase	Smp_000660		GKGIY*VWDVEGNCYM#DFLS	4	957.4114	6	78.01	3,575,822	3,624,553	1%
25	Smp_000720	Smp_000720	338	serine/threonine kinase	Smp_000720		AVGNTY*LGSR	2	630.2926	2	21.68	18,381,652	19,053,878	3%
26	Smp_000755;Smp_181710	Smp_000755;Smp_181710	48; 48	family M13 non-peptidase homologue (M13 fam	Smp_000755;Smp_1		YGVFSDNTEGISIVNTPGTTTDK	4	913.4345	1	62.73	2,289,085	2,522,740	7%
27	Smp_000780	Smp_000780	607	Hypothetical	Smp_000780		TSTPAPATGGSGM#GYLTDPD	4	1210.5741	3	86.40	664,246	575,617	10%
28	Smp_000790	Smp_000790	25	actin binding LIM protein family member 2-relate	Smp_000790		VKVY*CTVCHKR	3	510.5754	4	14.18	4,212,380	3,509,311	13%
29	Smp_001030	Smp_001030	79	5'-amp-activated protein kinase gamma-2 non-c	Smp_001030		SLIY*ITPESTLLDAVR	2	935.9817	3	88.08	2,935,725	2,313,986	17%
30	Smp_001030	Smp_001030	81	5'-amp-activated protein kinase gamma-2 non-c	Smp_001030		SLIYIT*PESTLLDAVR	3	624.3236	2	88.14	1,321,658	1,426,819	21%
31	Smp_002410	Smp_002410	132	14-3-3 epsilon 2	Smp_002410		Y*RAEYSVGNGRK	3	517.5752	6	16.66	8,101,777	6,436,044	16%
32	Smp_002880.2;Smp_002	Smp_002880.2;Smp_002	235; 235	ATP synthase alpha subunit mitochondrial, putat	Smp_002880.2;Sm		KLY*CIYVAIGQK	3	512.5946	2	54.56	1,077,356	969,947	7%
33	Smp_003230	Smp_003230	108	sh3 domain grb2-like protein B1 (endophilin B1)	Smp_003230		NSNY*GSPGEALKK	2	722.8270	2	19.21	656,776	631,844	3%

Column Definition | Details | Summary

Table 3.2. Example of the phosphoproteomic spreadsheet provided by CST for adult *S. mansoni* phosphoproteins. A snapshot of the start of Table 1 (pY IAP) - PTM scan 'Summary' results tab; 'Column Definition' and 'Details' tabs are also provided on each spreadsheet. The full results tables can be seen in additional files 2-4.

3.3.3 Depth and Character of the *S. mansoni* phosphoproteome

Analysis of the PTM Scan data began with determining how many proteins, phosphorylation sites, and redundant/non-redundant phosphopeptides had been detected. For pY IAP a total of 3954 redundant phosphopeptides (multiple unique peptides assigned to the same protein), and 2015 non-redundant phosphopeptides were identified for 681 proteins, in which 1508 phosphorylation sites were detected (Figure 3.3). The pS/pT IMAC identified 28,912 redundant and 12,575 non-redundant phosphopeptides from 2686 proteins, in which there were 10,528 phosphorylation sites (Figure 3.3). Finally, the pS/pT IAP, performed on the pY IAP flow through, identified 4432 redundant and 1918 non-redundant phosphopeptides from a total of 757 proteins with 1550 phosphorylation sites (Figure 3.3). Combining and filtering these results to remove duplicates produced a final list of 15,844 phosphopeptides, which consisted of 3176 proteins which had 12,936 phosphorylation sites (Figure 3.3). Justification for performing the additional pS/pT IAP step using the residual sample from pY IAP came with the discovery of approximately 10% more unique pS/pT sites than were discovered using IMAC enrichment alone (Figure 3.4).

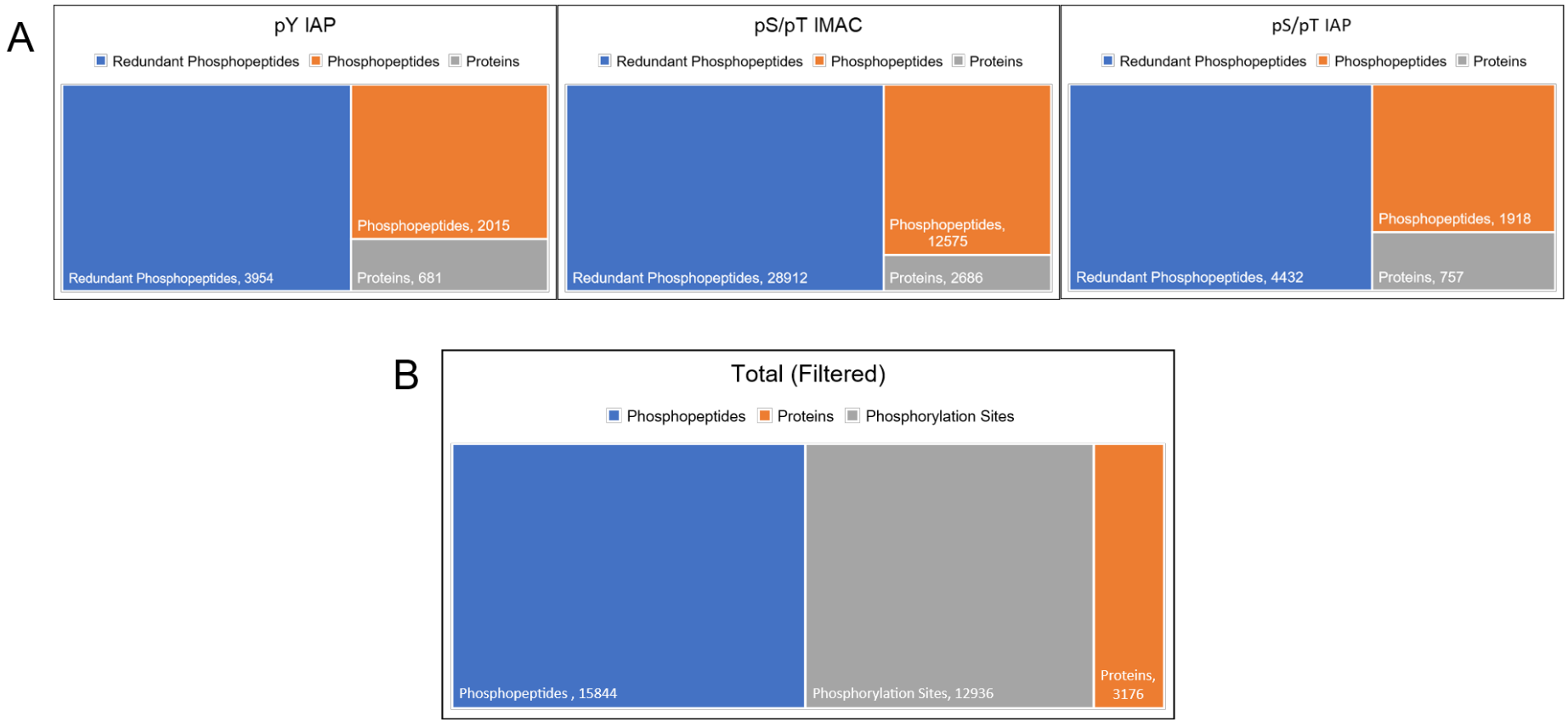

Figure 3.3. Graphical representation of phosphoproteomic data for adult *S. mansoni*. The number of redundant phosphopeptides, non-redundant phosphopeptides, and proteins from the PTM Scan analysis. (A) pY IAP, pS/pT IMAC pS/pT IAP data are derived from data tables 1-3 (Additional files 2-4), respectively. (B) Total count of phosphopeptides, proteins and phosphorylation sites after filtering data from pY IAP, pS/pT IMAC pS/pT IAP.

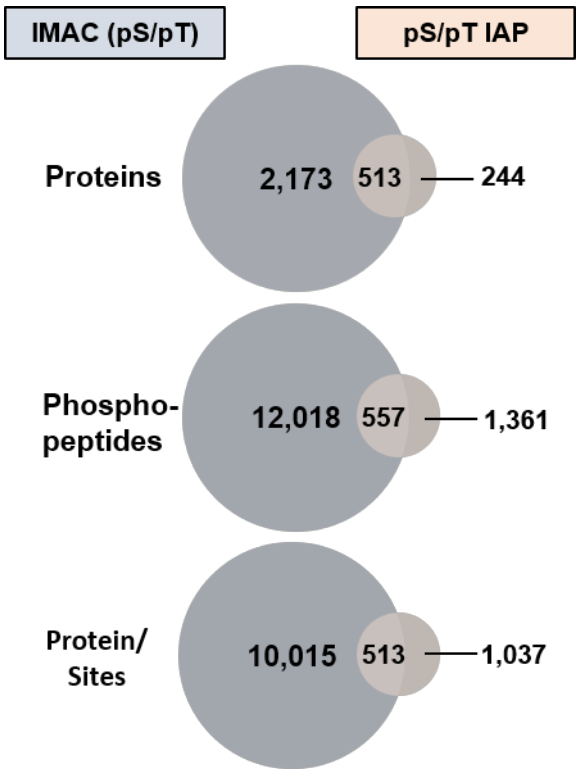

Figure 3.4 Overlap between IMAC and pS/pT IAP data. Data obtained from IMAC or pS/pT IAP were compared to establish the number of additional proteins, phosphopeptides, and protein/site identifications achieved with the additional pS/pT IAP step.

Next, the distribution of phosphorylation sites across the *S. mansoni* proteome was investigated which found 67.8% of the phosphopeptides are phosphorylated on serine, 20.1% on threonine and 12.1% on tyrosine (Figure 3.5).

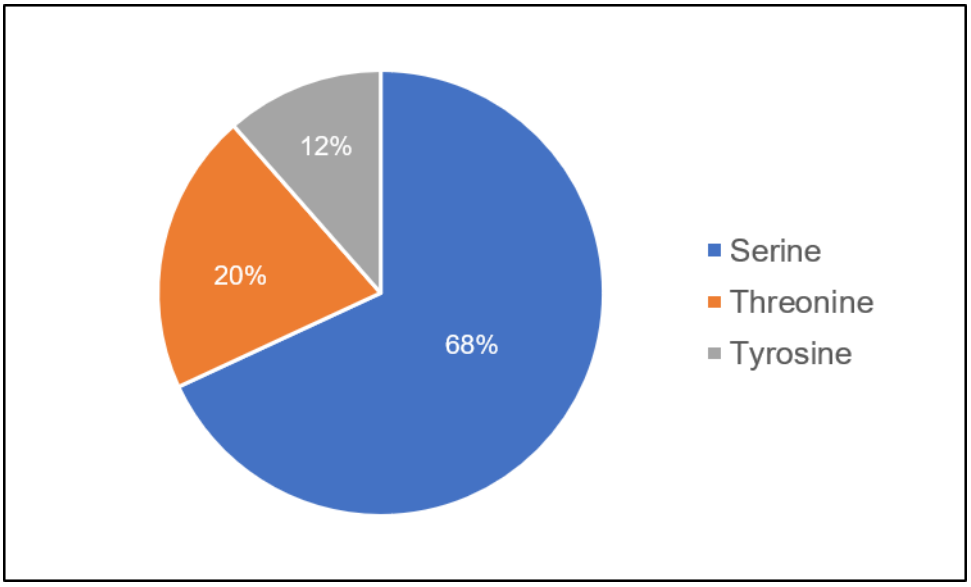

Figure 3.5. Pie chart illustrating the proportion of *S. mansoni* adult worm peptides phosphorylated on either serine, threonine, or tyrosine residues**.**

When the distribution of phosphoserine, phosphothreonine and phosphotyrosine sites was compared to that of *Plasmodium falciparum*, *Trypanosoma brucei*, *Homo sapiens*, and *Mus musculus* (Huttlin et al., 2010; Lasonder et al., 2012; Nett et al., 2009; Sharma et al., 2014) a similar distribution was evident throughout the species, although *S. mansoni* appeared to have a higher than usual percentage of phosphorylated tyrosine's in comparison to the other species, and less phosphorylated serine residues (Figure 3.6). (Andrade et al., 2011; Robinson et al., 2000).

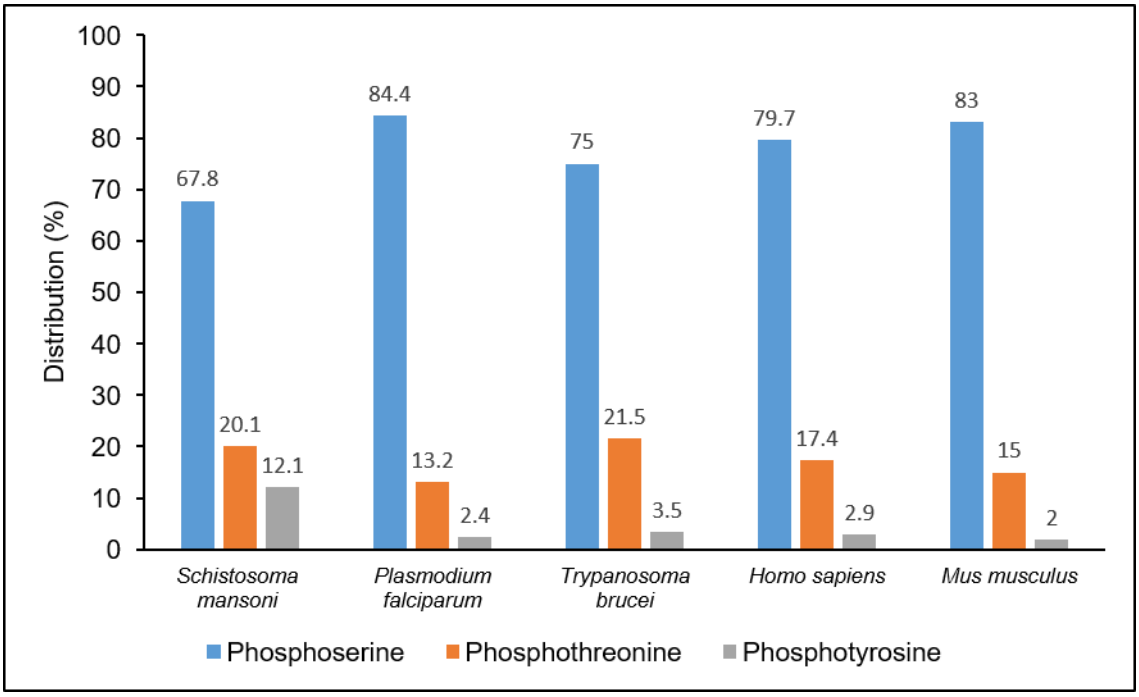

Figure 3.6. The percentage distribution of phosphorylated serine, threonine, and tyrosine residues in the *S. mansoni* proteome. Results compared to that within *P. falciparum*, *T. brucei H. sapiens* and *M. musculus*.

3.3.4 Peptide Classification and Motif Analysis

Previously, researchers have employed a technique whereby phosphorylated peptides in a dataset were characterised by the chemical properties associated with the phosphopeptide sequence (-6 to +6, surrounding the phosphorylation site; e.g. Huttlin et al., 2010) enabling categorisation as acidic, basic, proline-directed, tyrosine, or 'other' using a decision tree (Section 3.2.4). Of the total phosphopeptides, 12% were categorised as tyrosine – the least represented – followed by 17% basic, 20% proline-directed, 22% acidic and 29% where classified as 'other' (Figure 3.7).

The peptides were then subjected to motif analysis using MotifX, a *de novo* motif searching algorithm that is designed to extract overrepresented patterns to identify any common motifs

that may be present. Analysis was performed with default parameters using a normal and a degenerate set of phosphopeptides (using the potential amino acid substitutions A = AG, D = DE, F = FY, K = KR, I = ILVM, Q = QN, S = ST, C = C, H = H, P = P, W = W).

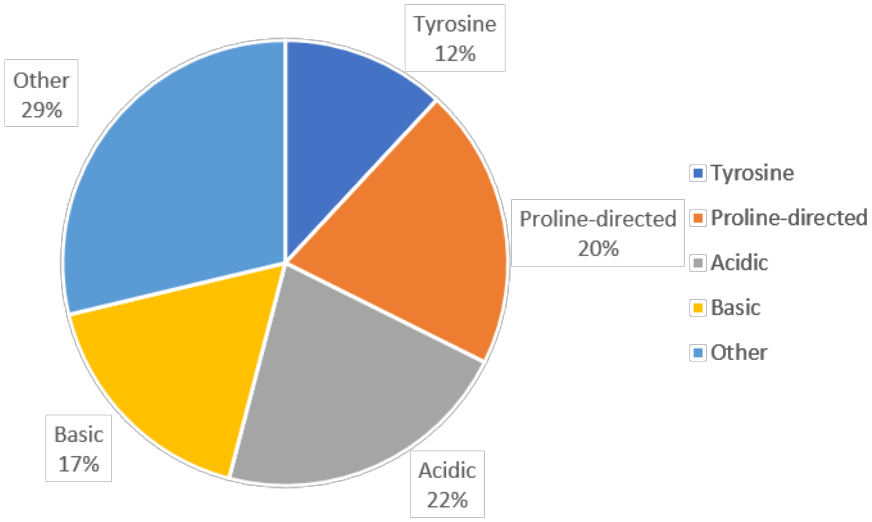

Figure 3.7. Distribution of adult *S. mansoni* phosphorylation motif classes. Classes were defined by the chemical properties of the sequence window peptide (13 amino acids) as acidic, basic, proline-directed, tyrosine or 'other' by a decision tree method.

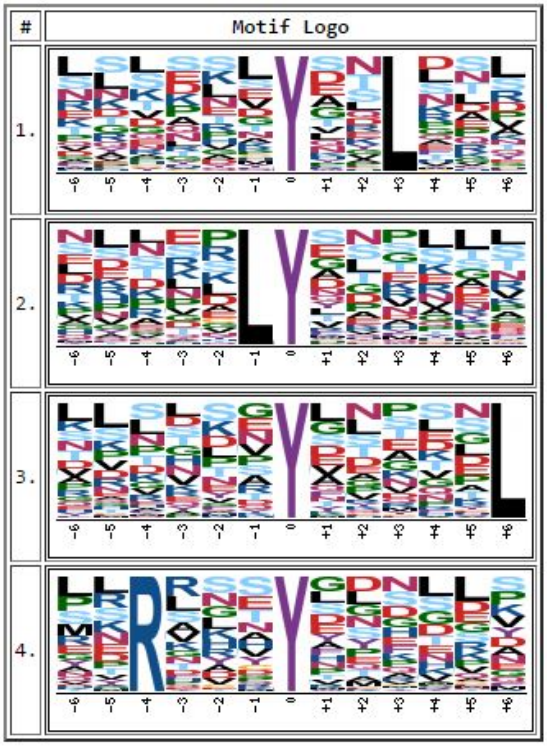

Figure 3.8. Tyrosine centred motifs discovered in the *S. mansoni* phosphoproteome. Results were generated from MotifX (http://motif-x.med.harvard.edu/) when the tyrosine phosphorylated peptides were submitted to the programme; the *S. mansoni* full proteome was used as the background.

Using the normal phosphopeptide set (not the degenerate set) and adjusting the programme parameters to set the central residue to tyrosine in MotifX, four motifs were significantly enriched at high confidence (Figure 3.8). The same search repeated for threonine generated 24 enriched motifs whereas 65 enriched motifs were identified with serine as the central residue (Figure 3.9). Sixty serine/threonine centred motifs were identified using the degenerate amino acid set. The full lists of enriched motifs can be found in Appendix File 5.

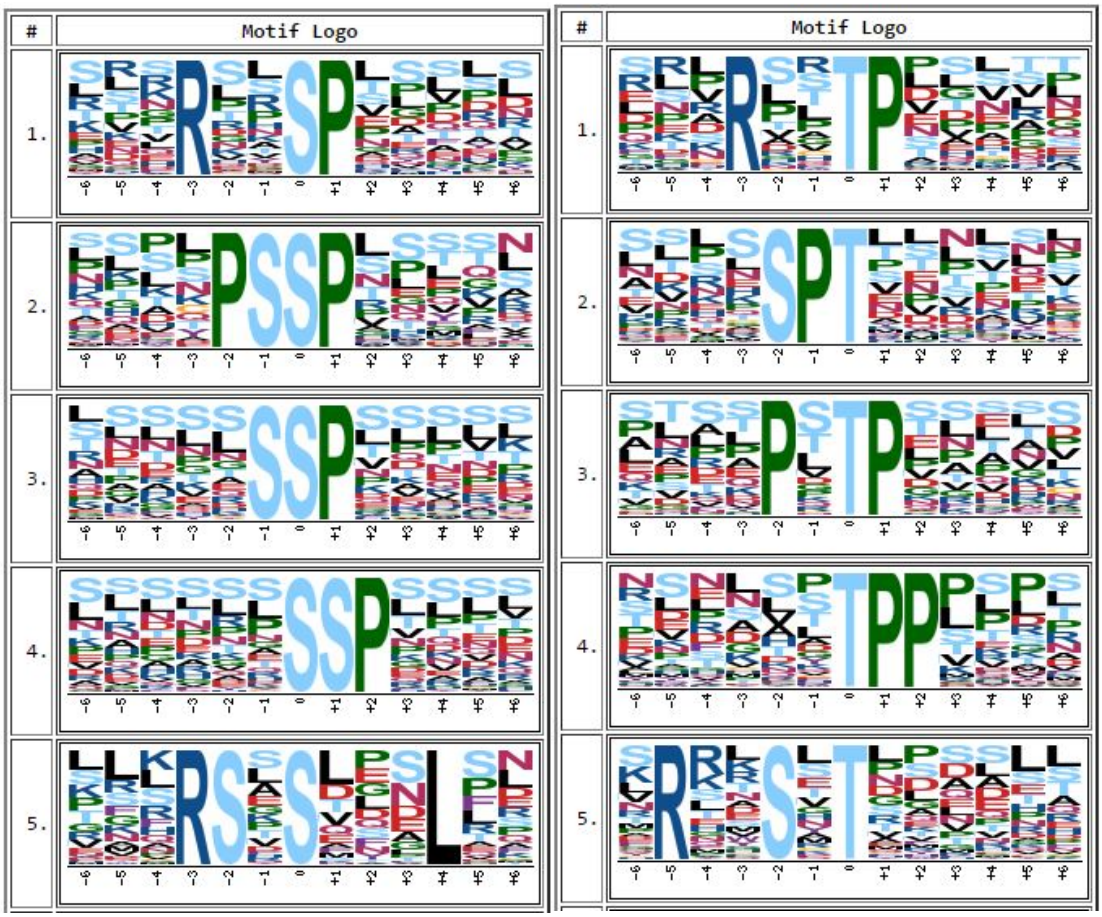

Figure 3.9. Examples of serine and threonine centred motifs discovered in the *S. mansoni* phosphoproteome. Results were generated from from MotifX (http://motif-x.med.harvard.edu/); left hand column shows the top five identified motifs with serine set as the central residue and the right hand column shows top five identified motifs with threonine set as the central residue; the *S. mansoni* full proteome was used as the background .

The identified motifs were subsequently classified according to their chemical properties as acidic, basic, proline-directed, tyrosine or 'other' by the decision tree method. This, however, did not result in many classifications. The tyrosine centred motifs were all classified as 'other', whereas 9 out of the 65 serine centred motifs were classified as proline-directed and 13 basic, with the remaining 43 classified as 'other'. Finally, 8 out of 24 threonine centred motifs were classified as proline directed, and 16 categorised as other. None were found to be in the either the acidic, tyrosine or other classes. The full data can be found in Appendix File 6.

3.3.5 Upstream Kinase Analysis

Analyses were next performed to determine if the significantly overrepresented *S. mansoni* peptide motifs detected by MotifX could be matched to any known motifs that were associated with upstream protein kinases (i.e. the motifs would represent protein kinase substrates). This could highlight protein kinases of interest for further investigation. A number of online tools can perform such analysis, but for the purposes of this investigation Phosida Motif Matcher and HPRD PhosphoMotif Finder (Amanchy et al., 2007; Gnad et al., 2011) were used. Both of these platforms use published literature to support their output and so were deemed to provide more robust results. However, as Phosida was found to be more stringent when assigning an upstream kinase to a motif, Phosida results were used primarily to support HPRD findings. The list of motifs obtained from MotifX (65 serine centred, 24 threonine centred, and 4 tyrosine centred – normal amino acid set) were submitted to the Phosida motif matcher and the output can be seen in Table 3.3. The most striking result was that out of the 93 motifs generated by MotifX, the greatest proportion (13) were putative substrates for calmodulin-dependent protein kinase II (CaMKII) (Figure 3.10). It should be noted that none of the tyrosine centred motifs were linked to any upstream kinase motifs and therefore only serine and threonine centred motifs are shown (Table 3.3).

Upstream KInase	Motif (Serine) Phosida	Motif (Threonine) Phosida	Total
CaMKII	xxxRxxSPxxxxx xLxRxxSxxxLxx xxxRxxSSxxxxx xxxRxxSLxxxxx xxxRxxSxxxLxx xxxRxxSxxxxxL xRxRxxSxxxxxx xxxRxxSxxxxxx xxRxxSSxxxxxx xRxxSxSxxxxxx RxxSxxSxxxxxx	xxxRxxTPxxxxx xRxxSxTxxxxxx	13
PKA	xxxRRxSLxxxxx xxxRRxSxxxxxx xxxRKxSxxxxxx	None	3
ERK/MAPK	xxxxPxSPxxxxx	xxxSPxTxxxxxx	2
PKD	xLxRxxSxxxLxx	None	1
CHK1	xLxRxxSxxxLxx	None	1
CHK2	xLxRxxSxxxLxx	None	1
Aurora	xxxRRxSLxxxxx	None	1
Aurora-A	xxxRRxSLxxxxx	None	1
AKT	xRxRxxSxxxxxx	None	1
CK1	xxSPxxSxxxxxx xxxxxxSxxxSPx	xxxxxxTxxxSxx	3
CK2	xxSPxxSxxxxxx	None	1
GSK-3	xxxxxxSxxxSPx	None	1

Table 3.3 Putative protein kinases matched to substrate motifs generated from *S. mansoni* phosphopeptide data. Phosida motif matcher (http://www.phosida.de/) was used to identify possible upstream protein kinases for overrepresented phosphorylated motifs generated using the list of phosphorylated peptides and the Motif X tool.

The Human Protein Resource Database (HPRD) includes a PhosphoMotif finder tool (http://www.hprd.org/PhosphoMotif_finder) that was used in other studies (e.g. Lasonder et al., 2012) and so was chosen to support Phosida findings. HPRD groups a number of substrate motifs together, for example, those for GSK-3, ERK1, ERK2, CDK5 substrate motif and ERK1, ERK2 kinase substrate motif, which provides less confident results, although consequently more putative upstream kinases were identified (Figure 3.11)

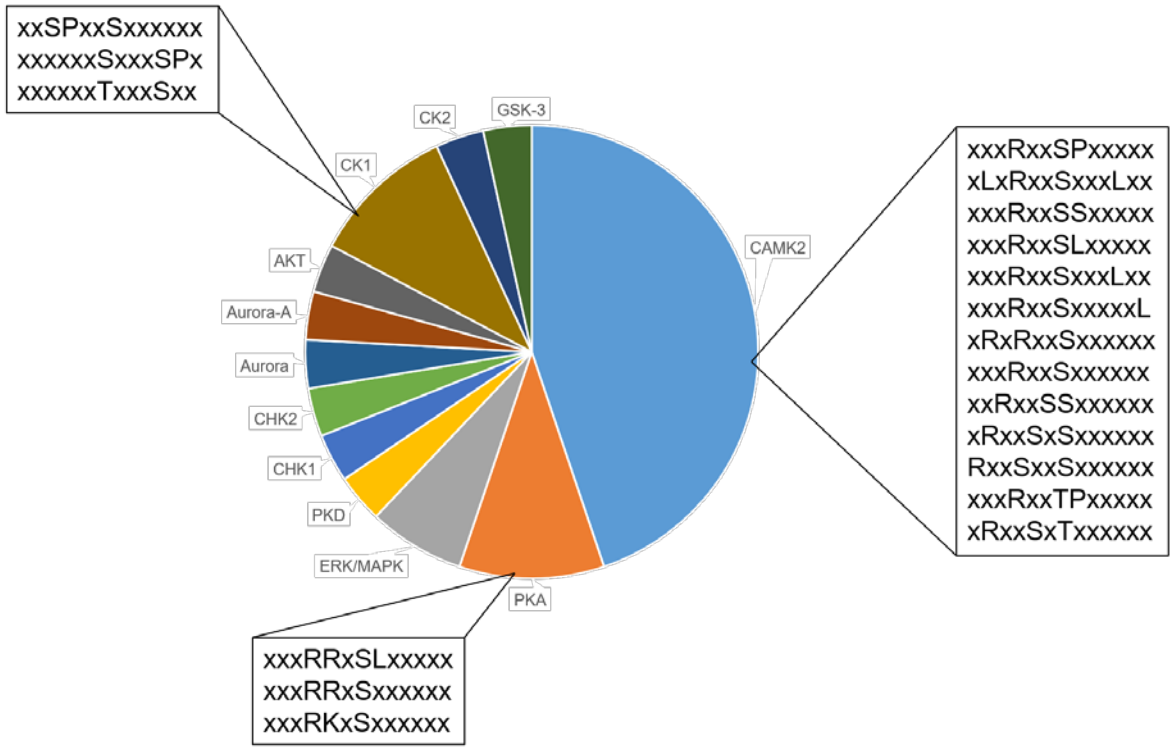

Figure 3.10. Distribution of substrate motifs generated from *S. mansoni* phosphopeptide data assigned to putative upstream protein kinases using Phosida. Upstream protein kinase assignment was generated using Phosida, and examples of motifs acquired from Motif X that matched to the upstream kinase motifs CaMKII, CK1 and PKA from Phosida Motif Matcher are shown.

CaMKII was also identified as a prominent putative upstream kinase when using HPRD, with a total of 20 motifs matched. However, the GSK-3, ERK1, ERK2, CDK5 substrate motif group had the highest number (30) of motif matches. This may be due to the 'group'

covering four different protein kinases, rather than one. Unlike Phosida, HPRD highlighted the presence of putative PKC substrate motifs, with 20 discovered overall. A number of other possible upstream kinases for the generated substrate motifs were highlighted by HPRD such as ATM kinase, PAK2 kinase and G-protein coupled receptor kinase. Putative assignment of upstream kinases to motifs will help support the development of work into *S. mansoni* kinase substrates including those used in the schistosome-specific kinase array in Chapter X and may aid future analyses of kinase mediated events in these worms.

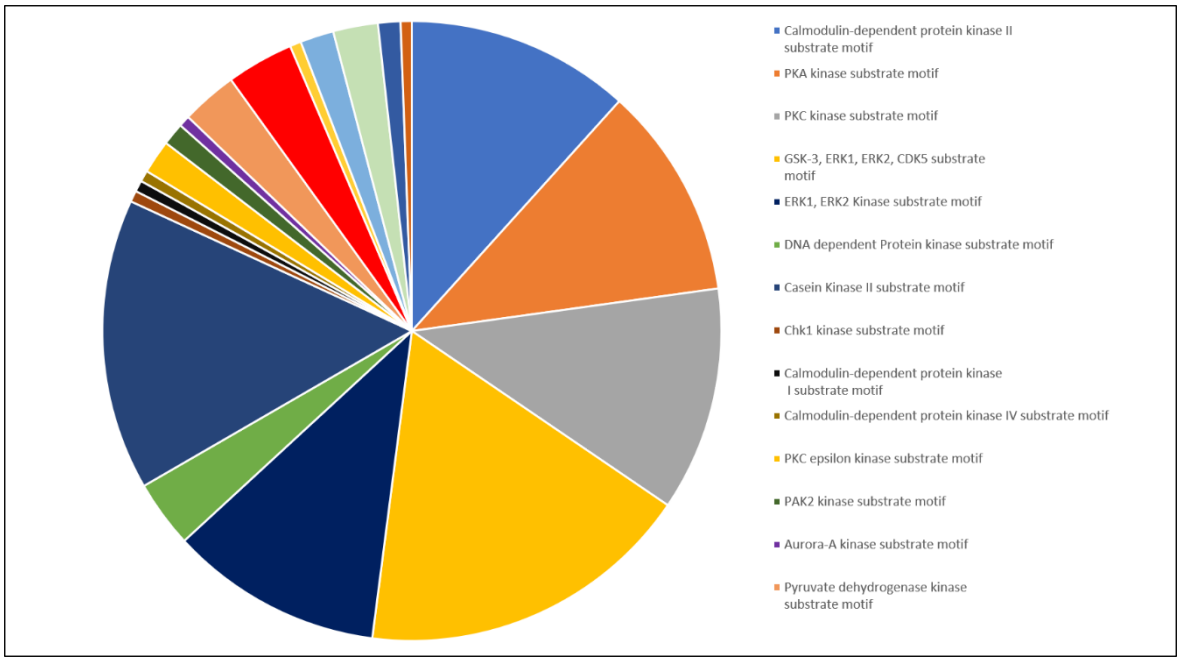

Figure 3.11. Distribution of substrate motifs generated from *S. mansoni* phosphopeptide data assigned to putative upstream protein kinases using HPRD.

3.3.6 Phosphorylation of Eukaryotic Protein Kinases in *S. mansoni*

In 2011, Andrade and team determined there were 252 ePKs in the predicted proteome of *S. mansoni,* they noted that this kinome comprised ~1.9% of the predicted proteome (Andrade et al., 2011). In an attempt to annotate the kinome with identified phosphorylation sites, the

list of *S. mansoni* protein (Smp) identifiers corresponding to the 252 ePKs was obtained (Andrade et al., 2011). Each Smp identifier was then manually searched for within each of the three results tables for the pY IAP, IMAC and pS/pT IAP enrichments to identify 'hits'. A total of 136 hits contained one or more phosphorylation sites out of a possible 252 kinases This included removal of all the isoforms in the list, this was to ensure all results were accurate when it came to scrutinising the phosphosites associated with the isoforms, as it cannot be determined if a phosphosite would be found in each of the isoforms. A total of 808 phosphorylation sites (S=531, T=171, Y=105) were identified within the 136 hits (Figure 3.12), full detail can be found in Appendix File 7.

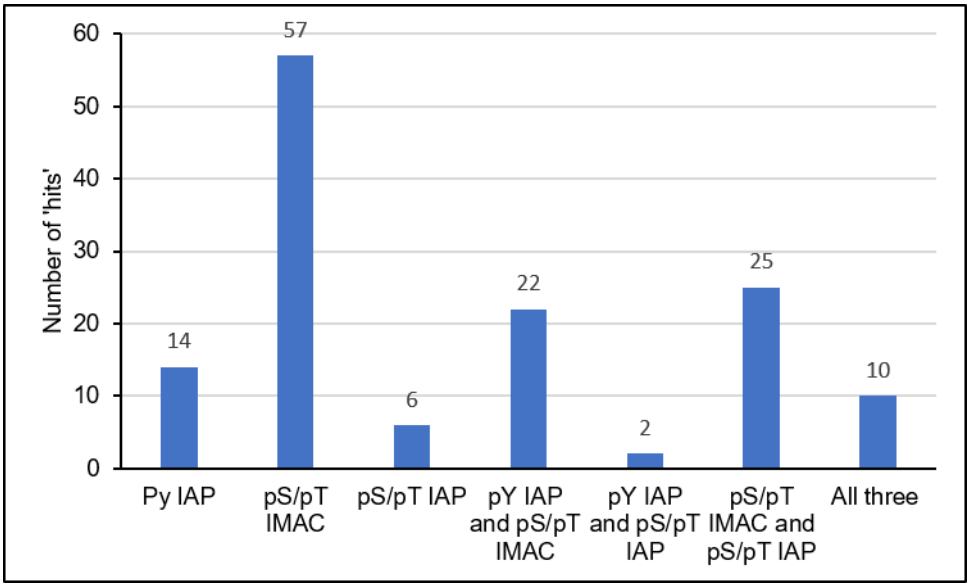

Figure 3.12. The distribution of protein kinases identified in the *S. mansoni* adult worm PTM scan across each of the PTM approaches.

Further analysis of the 136 phosphorylated kinases identified revealed they belonged to all ten kinase groups: AGC, CAMK, CK1, CMGC, Other, RGC, STE, TK, TKL and unknown (Figure 3.13). These were split into 59 protein kinase families (Table 3.4).

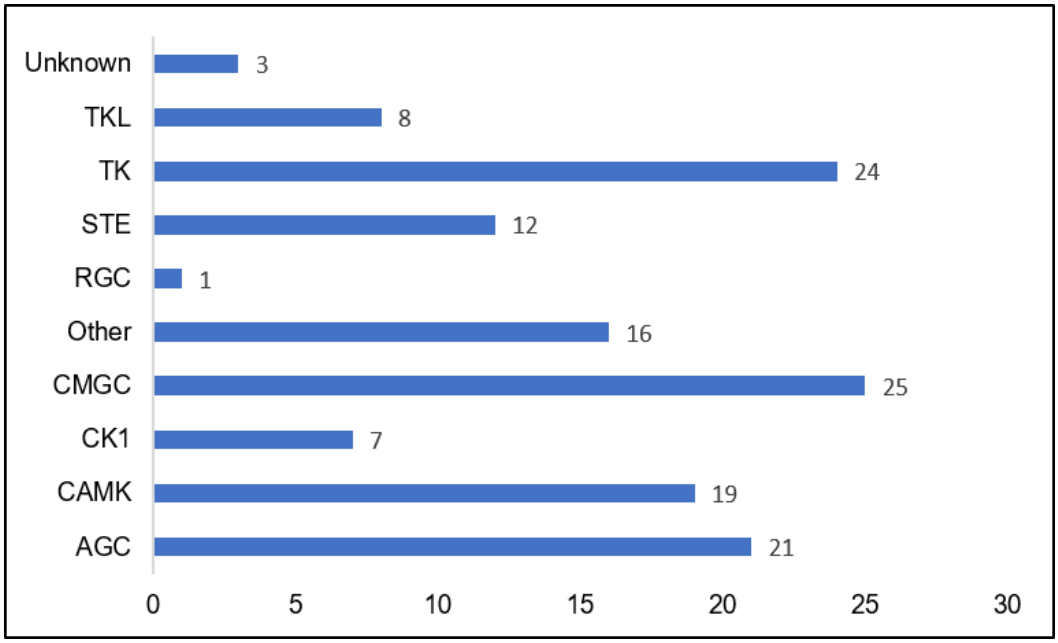

Figure 3.13. The number of adult *S. mansoni* protein kinases identified possessing one or more phosphorylation sites within each of the 10 kinase groups. Assignment to group was based on the classification of Andrade et al. (2011).

The group with the largest number of *S. mansoni* protein kinases with identified phosphorylated residue(s) retrieved from the PTM scan was the CMGC group, closely followed by the TK group (Figure 3.13). A number of protein kinases were next selected to explore the positions of their phosphosite(s), because it was observed that some could be found within the protein kinase domains. Within this domain there is an activation loop, in which a key residue can be found that once phosphorylated a conformational change of the kinase occurs (Beenstock et al., 2016). Kinases are thus activated through phosphorylation of certain residues in the activation loop, which promotes an open and extended (active) conformation to facilitate substrate binding (Beenstock et al., 2016). Examples of where this occurred included in the β-type protein kinase C isoform (Smp_128480), which had three close Thr residues which were phosphorylated, including the Thr residue which is also

phosphorylated in human PKCβI within the activation loop; this result correlates with previous findings using 'smart' anti-phospho-PKC antibodies to detect activated PKC in *S. mansoni* (Ressurreição et al., 2014). Several phosphorylation sites were found in the two *S. mansoni* glycogen synthase kinase 3 (GSK3)-like proteins (Smp_008260 and Smp_155720). Multiple sites are located within the activation loop of these proteins. There were also a number of phosphorylation sites identified in the tyrosine kinase activated CDC42 kinase-1-like, this included Tyr^{377} in the protein tyrosine kinase domain which in humans (Tyr^{287}) is the primary autophosphorylation site integral to the kinases activity (Mahajan et al., 2005) (Figure 3.14). The full list of phosphorylated sites and the presence of these within the protein kinase domain can be found in Appendix File 7.

Kinase Family	Count	Kinase Family	Count	Kinase Family	Count
Abl	2	LISK	2	RSK	2
Ack	2	LRRK	1	SCY1	3
CAMK1	1	MAPK	5	Sev	1
CaMKII	1	MLCK	2	Src	4
CAMKL	9	MLK	1	SRPK	1
CDK	7	Musk	1	STE11	1
CK1	5	NAK	2	STE20	8
CK2	1	NDR	2	STE7	3
CLK	2	NRBP	1	STKR	3
Csk	1	PEK	2	SYK	2
DAPK	1	PHK	1	Tec	1
DMPK	4	PIM	1	TLK	1
DYRK	7	PKA	4	TTBK	1
EGFR	2	PKC	3	ULK	4
Eph	1	PKG	3	VKR	2
Fak	1	PKN	1	VPS15	1
Fer	1	PLK	1	VRK	1
GRK	4	RAF	1	WNK	1
InsR	1	RGC	1	Unknown	7
		Ror	1		

Table 3.4. List of protein kinase families associated with the phosphorylated protein kinases identified in the PTM scan.

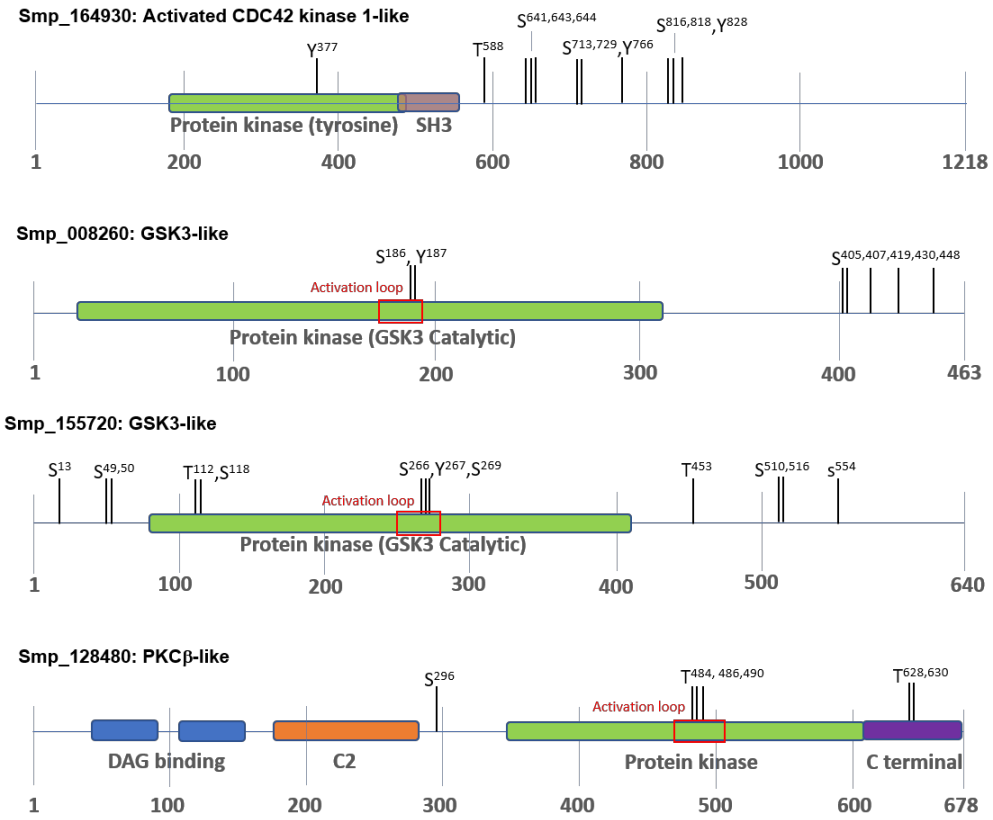

Figure 3.14 Schematics of four kinases; Smp_164930, Smp_008260, Smp_155720 and Smp_128480, found to have phosphosites in the integral activation loop displaying identified phosphorylation sites both within and outside of their protein kinase catalytic domains; phosphorylated residues discovered within the activation loops are highlighted

3.3.7 Gene Ontology

Gene ontology (GO) is a method of describing gene products with regards to their biological processes, cellular components, and molecular functions regardless of the species, in an attempt to provide controlled and consistent descriptions for all gene products across all species within databases. Gene ontology terms were applied to all of the phosphorylated proteins identified in this investigation, firstly to provide generalised descriptions for each protein, and secondly to identify any overrepresented protein groups.

The full list of Smp identifiers were uploaded into the Ensembl Metazoa online tool (Kersey et al., 2014), and filters applied against the *S. mansoni* database to provide the GO term accession, GO term name, and GO evidence code. This provided a table comprising corresponding GO term name, description, accession number and domain The GO domain gives a general overview of proteins, classifying in either a biological process, molecular function, or a cellular component category. Figure 3.15 illustrates the GO distribution of the phosphoproteomic data; just over half of the proteins were classified as having a molecular function, followed by just over a quarter with biological process and 14% with cellular component. Finally, only 9% of the phosphorylated proteins were not classified under any GO domain and therefore there were no annotations available to these proteins at the time of analysis and so were assigned an unknown GO classification.

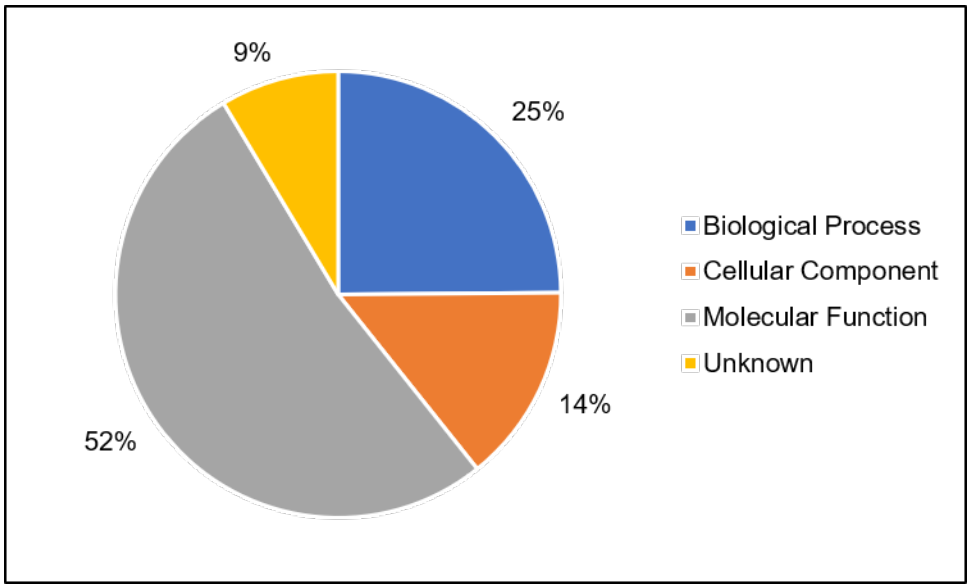

Figure 3.15. Distribution of *S. mansoni* phosphoproteomic Gene Ontology (GO) assignments using Ensembl metazoa.

GO SLIMs are condensed versions of GO and they contain a subset of the terms available at the GO resource, providing and easy and more concise way to perform GO analysis on large datasets. To perform GO SLIM the Blast2GO tool was used (Conesa et al., 2005) with the phosphoprotein Smp identifiers as input. This analysis predicted that the *S. mansoni* adult worm phosphoproteins were involved in a wide variety of processes. Under 'biological process', the top categories were the metabolic processes: cellular, primary, organic substance, nitrogen compound, and single-organism; as well as biosynthetic and catabolic processes, and organizational/localization processes (Figure 3.16). The largest categories under cellular component were: cell part, membrane-bounded organelle and protein complex, non-membrane-bounded organelle, and vesicle (Figure 3.17) highlighting the broad distribution of *S. mansoni* phosphoproteins across the cell compartments. Finally, molecular function generated the most assignments, as predicted by the Ensembl Metazoa GO analysis (Figure 3.18), with the predominant annotations involving binding, which included ion binding, bridging, heterocyclic compound binding, protein binding, organic cyclic compound binding and lipid binding. Hydrolase activity and transferase activity were also found to be highly represented. The GO SLIM output was next amalgamated to provide an overview of the top 50 GO SLIM terms giving an insight into the main functions/roles the phosphoproteins in adult *S. mansoni* (Figure 3.19). This illustrated that the most 'hits' (annotations) were for cell part, followed by a large number of annotations for cellular metabolic process and ion binding. The overarching results from the GO SLIM analysis was that the phosphoproteins are involved in a wide variety of processes and functions which are integral to schistosome viability.

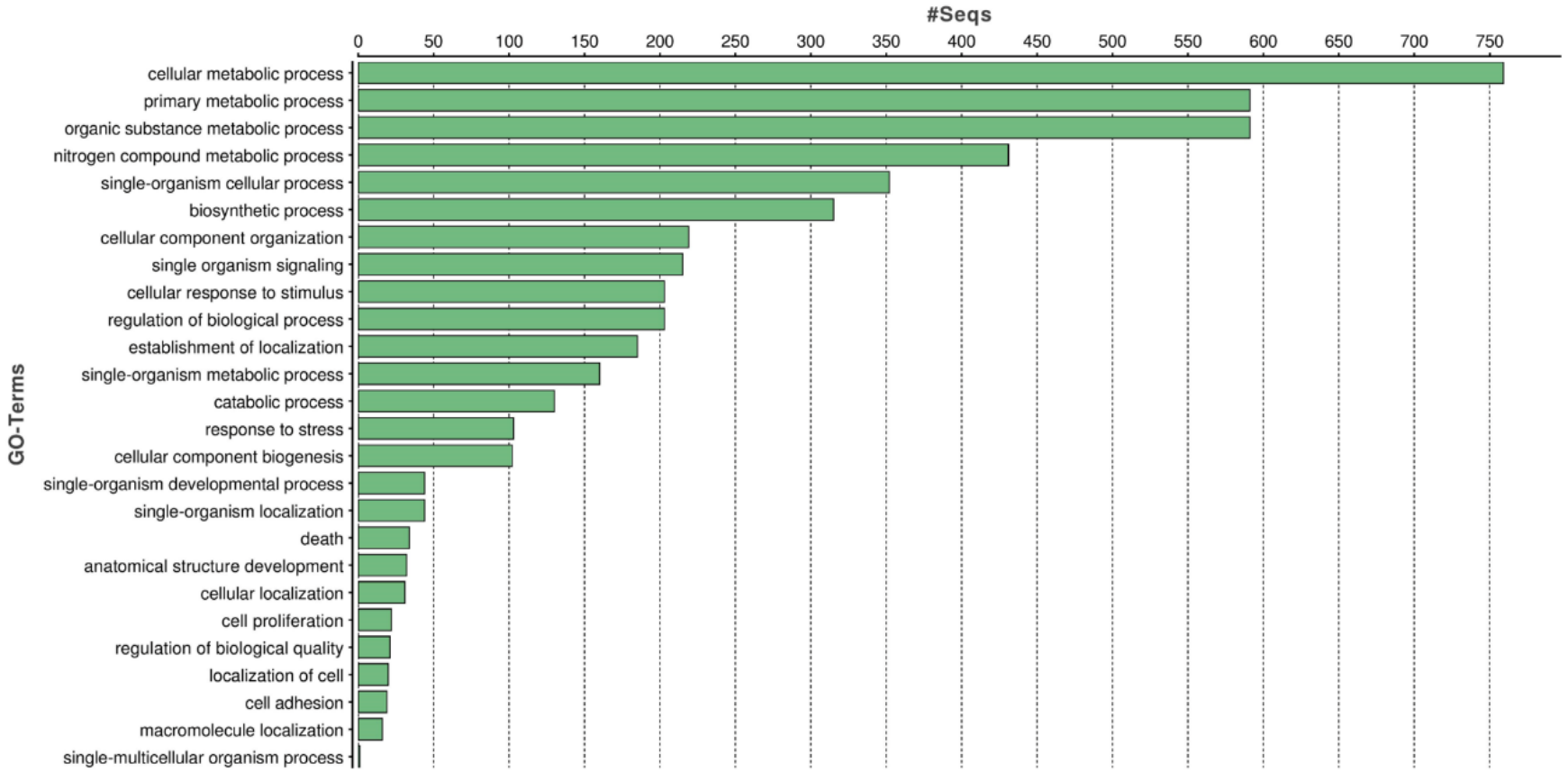

Figure 3.16. Biological Processes for *S. mansoni* adult phosphoproteins. GO Slim analysis of was performed using Blast2GO with the Smp identifiers from the phoshoproteomic dataset used as input.

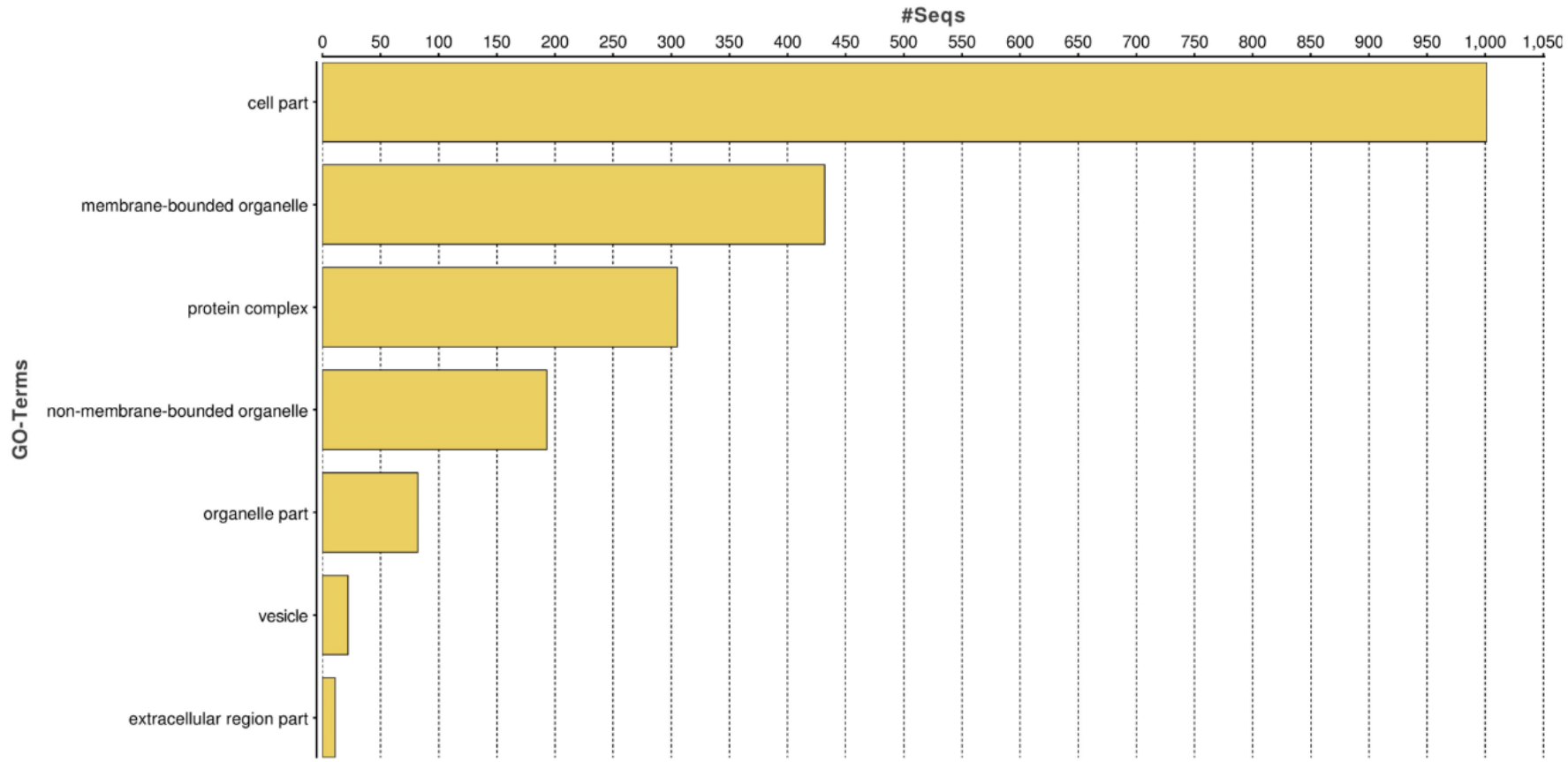

Figure 3.17. Cellular Components for *S. mansoni* adult phosphoproteins. GO Slim analysis of was performed using Blast2GO with the Smp identifiers from the phoshoproteomic dataset used as input.

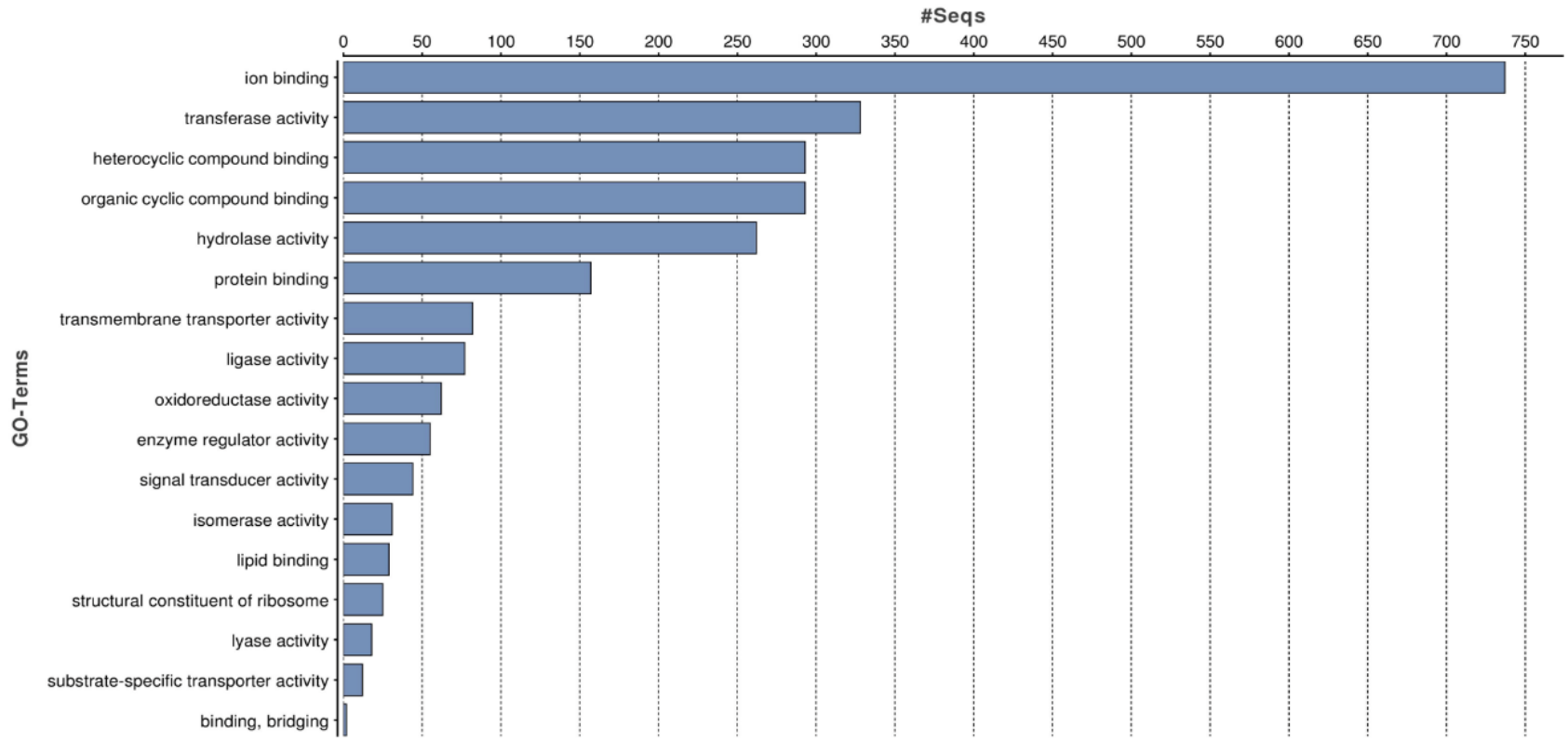

Figure 3.18. Molecular Function for *S. mansoni* adult phosphoproteins. GO Slim analysis of was performed using Blast2GO with the Smp identifiers from the phoshoproteomic dataset used as input.

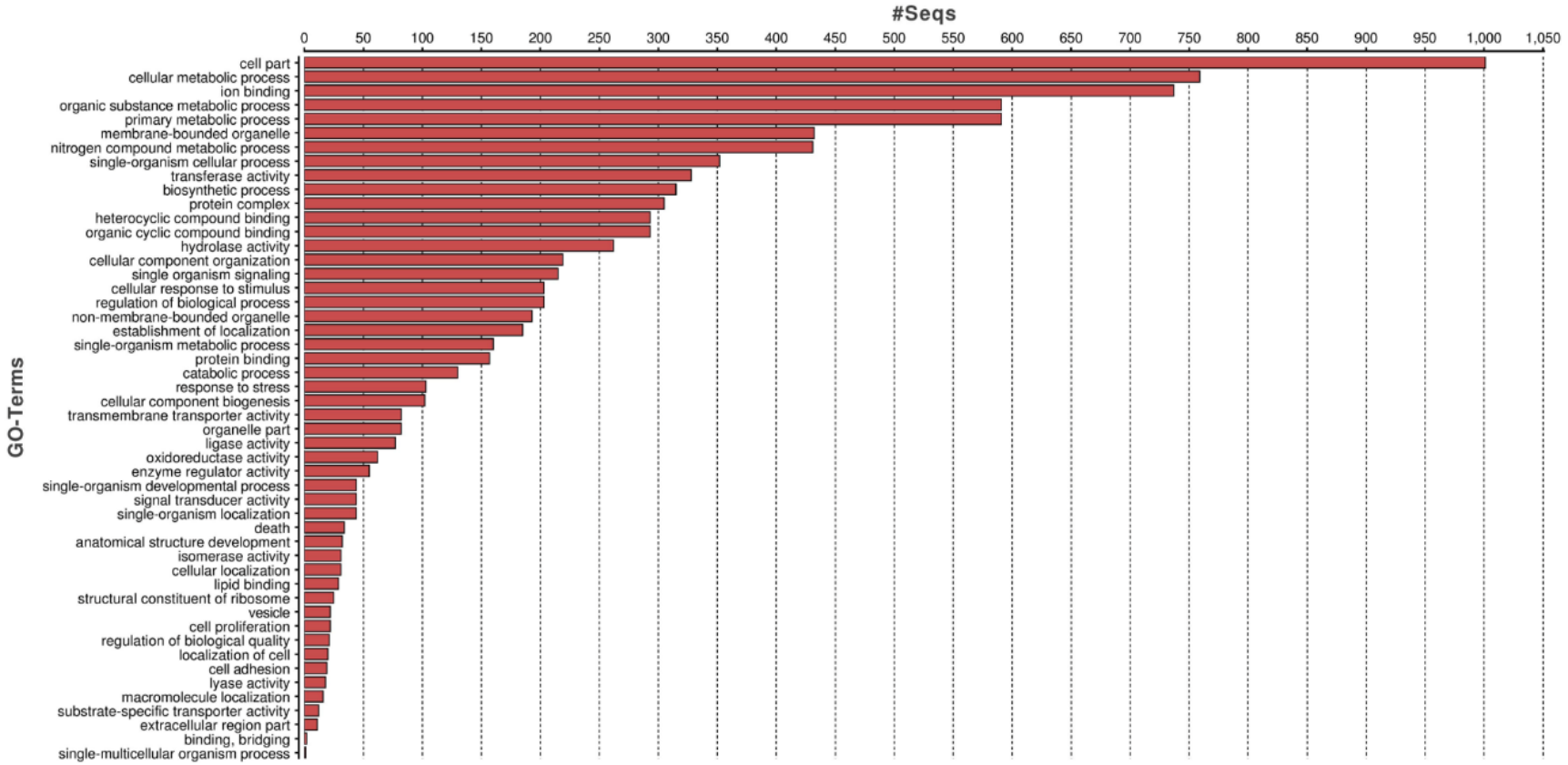

Figure 3.19. Top 50 results from all GO SLIM hits for *S. mansoni* adult phosphoproteins. GO Slim analysis of was performed using Blast2GO with the Smp identifiers from the phoshoproteomic dataset used as input**.**

3.3.8 Phosphoproteins in the Tegument

The tegument has undergone much research in adult *S. mansoni* as well as in other species of schistosomes due to its integral role in host-parasite interactions. It is one of the main structures that is in constant contact with the human host and yet it manages to help the parasite evade the host immune responses, enabling them to survive for an average of 3 – 5 years with the potential of living up to 30 years in some cases (Gryseels et al., 2006). Recently, proteomic studies focusing on the tegument of the schistosomule have been published, highlighting potential therapeutic targets within the tegument of the developing parasite (Sotillo et al., 2015). With the aim of linking previously identified tegumental proteins in *S. mansoni* with the phosphoproteins identified here, the literature was interrogated to find proteomic studies that specifically studied the adult worm tegument and a corresponding list of identified proteins in the *S. mansoni* tegument was compiled (Braschi et al., 2006; Braschi & Wilson, 2006; Castro-Borges et al., 2011a; Castro-Borges et al., 2011b; van Balkom et al., 2005) and compared to the PTM scan data. This list consisted of 68 proteins, of which 48 were found to be phosphorylated (Table 3.5). The list should not be considered comprehensive as it is somewhat constrained by the limited number of proteomic 'hits' found within proteomic studies of the tegument. Also, presence of a match does not definitively signify that the tegumental protein is phosphorylated as the phosphorylated proteins identified here were extracted from the entire worm.

Smp Identifier	Protein Description	Smp Identifier	Protein Description
Smp_003230	Endophilin (BAR domain)	Smp_074150	Annexin type V
Smp_003990	Triose Phosphate Isomerase (TPI)	Smp_075420	Unknown
Smp_005740	Aquaporin-3	Smp_077720	Annexin 2
Smp_008660	Gelsolin	Smp_086480	Sm21.7
Smp_012440	Glucose transport protein type 1 — GluTP1	Smp_086530	Dynein light chain
Smp_015020	Na+/K + ATPase alpha subunit	Smp_091240	Voltage-dependent anion-selective channel (VDAC)
Smp_016780	α- tubulin	Smp_091710	Actin
Smp_017730	200 kDa GPI-anchored surface protein - Sm200_a	Smp_094420	Rab GDP dissociation inhibitor
Smp_020550	Proteoglycan-like	Smp_095360	Fatty acid-binding protein (Sm14)
Smp_024110	Enolase	Smp_095520	Dynein light chain
Smp_030730	β- tubulin	Smp_096760	Phosphoglycerate mutase
Smp_037230	Fimbrin	Smp_102070	Glutathione S-transferase 26 kDa
Smp_038950	Lactate dehydrogenase	Smp_106930	HSP 70
Smp_042020	ATP-diphosphohydrolase 1	Smp_106930	Heat shock protein 70 (Hsp70)
Smp_042160	Frutose Biphosphate Aldolase	Smp_127820	Unknown
Smp_045200	EF-hand calcium binding protein - Sm22.6	Smp_130280	unknown (EGF-like domain protein)
Smp_048230	High-affinity copper uptake protein (HACUP)	Smp_137410	Calpain
Smp_049250	Major egg antigen (P40)	Smp_141010	Dysferlin
Smp_054160	Glutathione S Transferase 28 kDa (GST)	Smp_146950	unknown (Ig-like domain)
Smp_056970	Glyceraldehyde 3P dehydrogenase	Smp_155890	Alkaline Phosphatase
Smp_059660	unknown	Smp_157500	Calpain
Smp_065610	Pyruvate kinase	Smp_161030	Unknown
Smp_072330	Hsp90	Smp_163720	Endophilin (BAR domain)
Smp_074140	Annexin type IV	Smp_176200	Superoxide Dismutase (SOD)

Table 3.5 Phosphorylated *S. mansoni* proteins that have been identified as tegumental proteins within the literature. Smp identifiers for the phosphorylated proteins were matched to those identified in proteomic research (Braschi et al., 2006; Braschi & Wilson, 2006; Castro-Borges et al., 2011a; Castro-Borges, et al., 2011b; van Balkom et al., 2005)

3.3.9 Protein – Protein Interactions

Next, potential interactions between the phosphorylated proteins were explored. The study of protein-protein interactions can be investigated using the online tool STRINGdb[10] (Search Tool for Retrieval of Interacting Genes), which predicts protein–protein interactions to help determine what is functionally occurring during cellular processing (Szklarczyk et al., 2015). STRING works using known experimental interactions, knowledge from manually curated databases, automated text-mining a number of algorithms to determine a functional relationship between two proteins (Szklarczyk et al., 2015). Because the online interface of STRINGdb can only process <3000 proteins at a time the STRINGdb developers advised downloading the complete set of predicted *S. mansoni* protein-protein interactions and manually mapping the phosphorylated proteins to this set. Dr Jean-Christophe Nebel kindly performed the mapping (at <0.7 confidence) resulting in a table of 25 proteins with the highest number of interactions (Table 3.6). An alternative way to evaluate the protein-protein interactions between the adult worm phosphorylated proteins was using Cytoscape 3.7.1[11]. Cytoscape is a software platform which is open source, it can be used for visualising molecular interaction networks as well as biological pathways; these networks can then be annotated further with GO annotations, gene expression profiles and other important data. Key to interaction analysis using Cytoscape is the String application[12] (StringApp) which links Cytoscape to STRINGbd enabling interactions between input proteins to be visualised. The complete list of *S. mansoni* phosphoproteins was uploaded to StringApp running within

[10] https://string-db.org/

[11] https://cytoscape.org/download.html

[12] http://apps.cytoscape.org/apps/stringapp

Cytoscape. The resulting network or “phosphoprotein interactome” comprised 1,586 nodes and 12,733 edges at high confidence >0.7 (Figure 3.20).

SMP Number	Name	Interactions	Position
SMP_009580	ubiquitin	882	1
SMP_046690	polyubiquitin C	882	2
SMP_072330.2	heat shock protein	458	3
SMP_147210 (Discontinued May 2014)	ubiquitin (ribosomal protein L40)	424	4
SMP_065840 (Now known as SMP_210730)	DNA topoisomerase 2 alpha	310	5
SMP_130310	prolyl oligopeptidase (S09 family)	264	6
SMP_089430	ubiquitin (ribosomal protein L40)	252	7
SMP_128380.2	glutamate synthase	248	8
SMP_123710	acetyl-CoA carboxylase	232	9
SMP_063830	GMP synthase (glutamine hydrolyzing)	230	10
SMP_106150	carbamoyl-phosphate synthase large chain, putative	204	11
SMP_072140	Rho2 GTPase	186	12
SMP_173390	DnaJ protein subfamily C	182	13
SMP_102040.1	receptor for activated PKC	178	14
SMP_156670	DNA directed RNA polymerase II subunit RPB1	176	15
SMP_157740	DNA directed RNA polymerase III subunit RPC1	176	16
SMP_046600	actin	160	17
SMP_143150	elongation factor 2	160	18
SMP_161920	actin	160	19
SMP_030300.4	endoplasmin	158	20
SMP_122910	Serine:threonine protein kinase mTOR	158	21
SMP_136750 (Now known as SMP_213390)	ribosomal protein s6 kinase beta 1	158	22
SMP_012930	inosine 5' monophosphate dehydrogenase 2	154	23
SMP_133020	p38 MAP kinase MPK2 protein	154	24
SMP_140690	DNA directed RNA polymerase I subunit RPA2	152	25

Table 3.6. The top 25 phosphorylated *S. mansoni* proteins with the highest number of protein–protein interactions.

Figure 3.20. The *S. mansoni* adult worm phosphoprotein interactome. Predicted interactions between the phosphoproteins (at high, 0.7, confidence) were visualised in Cytoscape using StringApp. A maximum of 100 interactions were set for each node.

This phosphoproteome interaction network, however, was too dense and overpopulated to draw any valuable insights, therefore the next step was to extract useful data from the interactome. Analysis of the literature (Dashatan et al., 2018; Kwon et al., 2017; Yang et al., 2016) revealed a useful Cytoscape application named Clusterviz[13] (Wang et al., 2015), which discovers 'clusters' of highly interconnected nodes within a network; these clusters can often be protein complexes and parts of pathways. Clusterviz, run using default settings and the MCODE algorithm, extracted 55 clusters of highly interconnected nodes. The majority of these clusters (49/55) were allocated an MCODE score of 10 or less, so clusters scoring >10 were evaluated further using KEGG within Cytoscape. This highlighted a several clusters of interest (Figures 3.21-3.24). The highest scoring cluster (MCODE score 31.16), had 32 nodes and 483 edges and was dominated by ribosomal proteins (Figure 3.21). Further clusters were found to be associated with ribosomal biogenesis, proteasomes, phagosomes, and spliceosomes (Figures 3.22-3.24).

[13] http://apps.cytoscape.org/apps/clusterviz

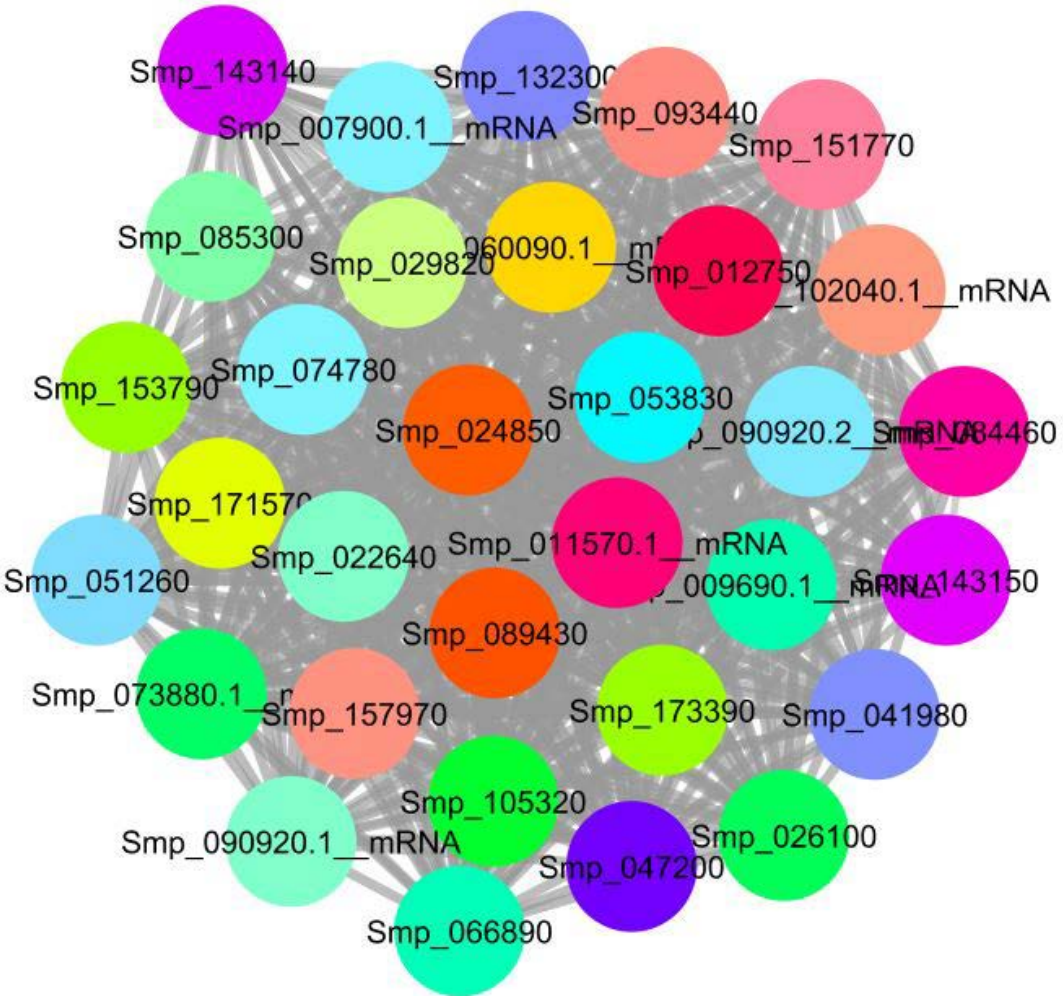

Figure 3.21. Cluster 1 from Clusterviz MCODE analysis of the *S. mansoni* adult worm phosphoproteome. Interactions between phosphorylated proteins reveal a ribosomal cluster with nodes 32 and edges, 483; MCODE score ~31.161, KEGG: Ribosome (24/32 phosphorylated proteins).

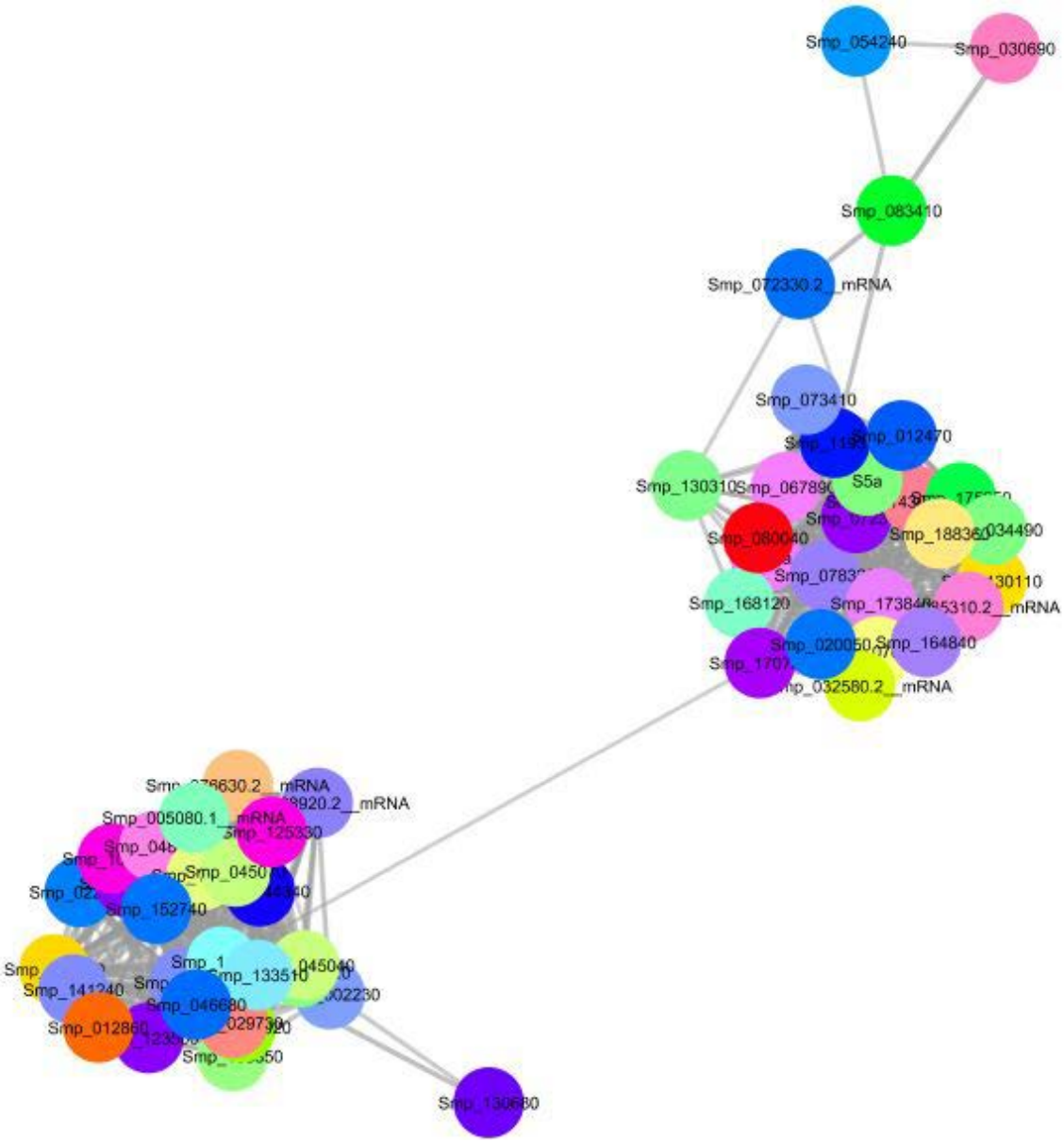

Figure 3.22. Cluster 2 from Clusterviz MCODE analysis of the *S. mansoni* adult worm phosphoproteome. Interactions between phosphorylated proteins reveal a ribosomal biogenesis and proteasome cluster with nodes: 54; edges: 551; MCODE score 20.792, KEGG: Proteosome (14/54); Ribosome biogenesis (9/54 phosphorylated proteins).

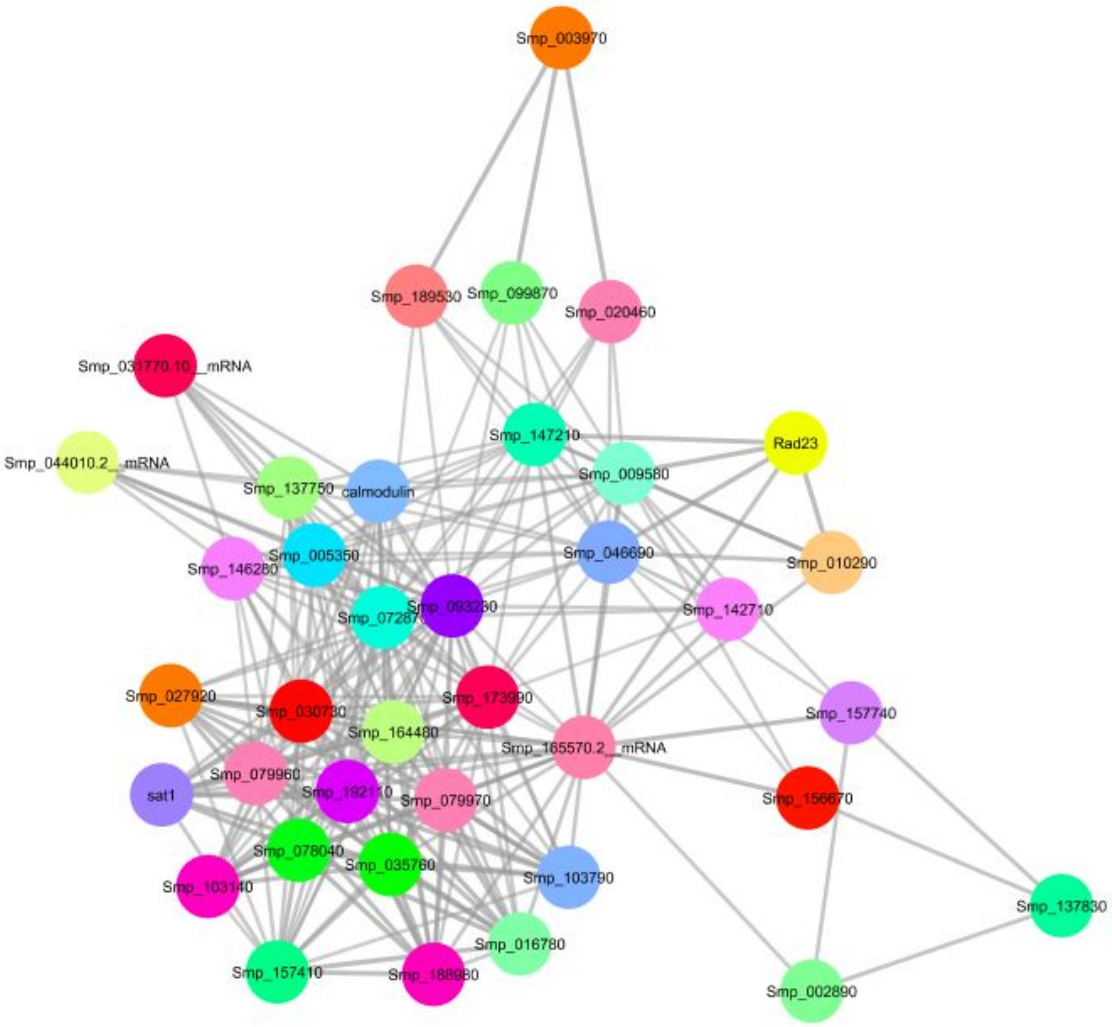

Figure 3.23. Cluster 3 from Clusterviz MCODE analysis of the *S. mansoni* adult worm phosphoproteome. Interactions between phosphorylated proteins reveal a phagosome cluster with nodes: 38; edges: 241; MCODE score 13.027, KEGG: Phagosome (5/38 phosphorylated proteins).

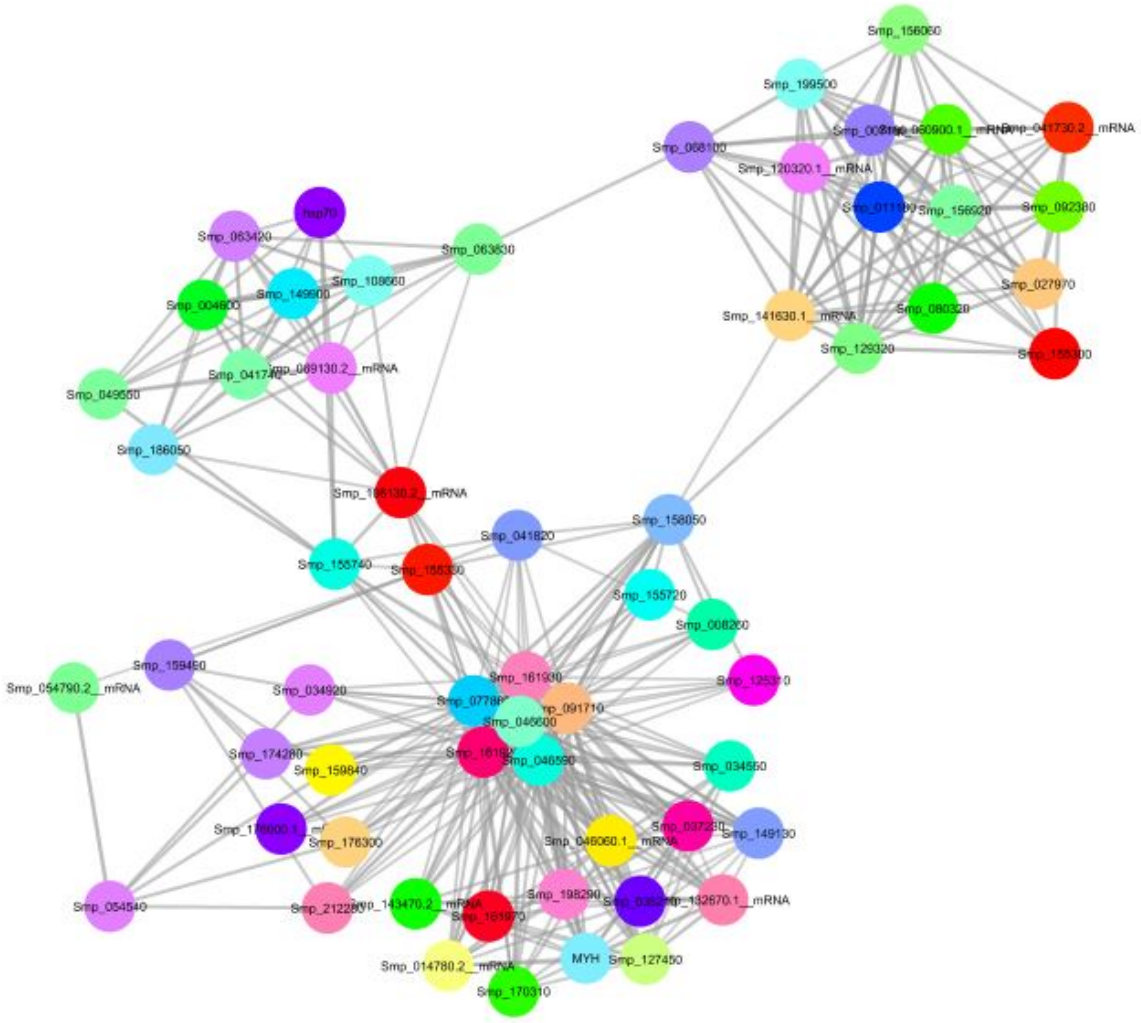

Figure 3.24. Cluster 4 from Clusterviz MCODE analysis of the *S. mansoni* adult worm phosphoproteome. Interactions between phosphorylated proteins reveal a spliceosome cluster with nodes: 61; edges: 365; MCODE score ~12.167, KEGG: Spliceosome (9/61 phosphorylated proteins).

3.3.10 KEGG Analysis

Kyoto Encyclopaedia of Genes and Genomes (KEGG) aims to provide information collated from a number of resources to identify a representation of the biological systems through a variety of pathways, including genomic, chemical, and health information. A KEGG analysis of the phosphoproteins was performed using BLAST2GO. The analysis identified 84

pathways with the top 20 displayed in Table 3.7. The top ‘hit’ was for the biosynthesis of antibiotics pathway, with 59 sequences and 39 enzymes found, this was closely followed by purine metabolism with 57 sequences and 21 enzymes involved, the full table of KEGG results can be found in Appendix File 8. Overall, a large variety of pathways were found to be associated with the *S. mansoni* adult worm phosphoproteome, spanning a variety of metabolic, signalling, biosynthesis, and degradation pathways; metabolic pathways featured the most.

Number	Pathways	Proteins	Enzymes
1	Biosynthesis of antibiotics	59	39
2	Purine metabolism	57	21
3	Aminoacyl-tRNA biosynthesis	22	18
4	T cell receptor signalling pathway	21	2
5	Pentose phosphate pathway	19	10
6	Pyrimidine metabolism	18	14
7	Glycerolphospholipid metabolism	17	13
8	Pyruvate metabolism	17	12
9	Carbon fixation in photosynthetic organisms	15	8
10	Phosphatidylinositol signalling system	14	8
11	Starch and sucrose metabolism	13	7
12	Amino sugar and nucleotide sugar metabolism	12	7
13	Galactose metabolism	10	4
14	Methane metabolism	10	6
15	Cysteine and methionine metabolism	10	8
16	Propanoate metabolism	9	7
17	Glycerolipid metabolism	9	6
18	Inositol phosphate metabolism	9	6
19	Glutathione metabolism	9	6
20	Carbon fixation pathways in prokaryotes	9	6

Table 3.7. Top 20 hits from a KEGG analysis performed on the *S. mansoni* adult worm phosphoproteome.

3.4 Discussion

This investigation set out to explore the depth of the phosphoproteome of adult *S. mansoni* worms by generating data using a PTM Scan to identify peptides and thus proteins which had been phosphorylated on tyrosine, threonine and/or serine residues *in vivo*. This led to the identification of 15,844 phosphopeptides within 3,176 proteins which contained 12,936 phosphorylation sites for further analysis. These results represent the largest known phosphoproteomic dataset for any schistosome. With published phosphoproteomes for the parasites *T. brucei*, *P. falciparum*, *M. musculus* and *H. sapiens* containing 852, 2541, ~36,000 and ~700,000, phosphorylation sites respectively (Lasonder et al., 2012; Nett et al., 2009; Pease et al., 2013; Sharma et al., 2014) these data are also possibly are the largest for any parasite to date. Alternative proteomic (rather than phosphoproteomic) investigations using the *Schistosoma* model have involved a more targeted approach. For instance, in *S. haematobium*, extracts representing differing tissues involved in host-parasite interaction, i.e. excretory/secretory, tegumental and egg proteins, were characterised by LC-MS/MS, leading to the discovery of 558 unique proteins across each of these extracts (Sotillo et al., 2019). The same researchers also investigated the proteome of the tegument of *S. mansoni* (Sotillo et al., 2015). While focusing on discrete regions of the parasite is useful in terms of determining specific diagnostic markers and target proteins for vaccine studies, for example, it does not give the whole overview of the parasite's proteome. Phosphoproteomes, in particular, are valuable because they provide a signature of kinase mediated signalling events, which underpin the regulatory biology of an organism (Mayya & Han, 2009), and protein phosphorylation has proved crucial to the expansion of knowledge in health and disease warranting further exploration employing phosphoproteomics (Ardito et al., 2017; Cohen, 2001; Hunter, 2002).

3.4.1 Protein Kinases and Substrate Motif Analysis

Protein kinases (which phosphorylate target motifs in substrate proteins) often present as ideal drug targets due to their central involvement in the signalling pathways of essential regulatory and developmental processes, as well as their tendency to contain conserved structures (Hanks, 2003; Manning et al, 2002). After the publication of the *S. mansoni* genome (Berriman et al., 2009), the predicted *S. mansoni* kinome containing 252 ePKs was annotated and published (Andrade et al., 2011). The current investigation found 136 of these ePKs to be phosphorylated in regions including the catalytic domain, the activation loop and others (e.g. regulatory domains). Protein kinases often represent a small number of the total number of proteins in a species and in *S. mansoni* the 252 ePKs is estimated to represent 1.9% of the predicted proteome (Andrade et al., 2011). As 3,176 phosphorylated proteins were identified here, these protein kinases are responsible for phosphorylating at least ~22% of the *S. mansoni* adult proteome (based on 14,528 transcripts recorded on WormBase Parasite). Clearly the number of phosphorylated proteins actually present in the worm will be greater as low concentration phosphopeptides will have gone undetected in the current study. Interestingly, the percentage distribution of phosphorylated residues indicated that although *S. mansoni* had the highest percentage of residues phosphorylated on serine (68%), it was proportionately lower than in other species such as *P. falciparum* (84.4%) and *M. musculus* (83%) (Huttlin et al., 2010; Lasonder et al., 2012). This is particularly interesting as the number of protein tyrosine kinases (a total of 34, comprising 15 receptor tyrosine kinases and 19 cytosolic tyrosine kinases) in *S. mansoni* (represents 13.5% of the kinome) is lower when compared to that for human (90 tyrosine kinases representing ~17% of the kinome) (Andrade et al., 2011; Robinson et al., 2000). Research into *P. falciparum* showed that the distribution of serine, threonine and tyrosine phosphorylation's fluctuated greatly between the different parasite life stages (Pease

et al., 2013) highlighting the importance of analysing more *S. mansoni* life stages in future research. As well as being distinguished by the residue(s) they are phosphorylated on, proteins can be split into classes according to the amino acid motifs surrounding the phosphorylation residue acting as a recognition motif for a kinase, this was first done using a decision tree created during the analysis of the mouse phosphoproteome (Huttlin et al., 2010). In both the mouse and *P. falciparum* schizont phosphoproteomes, proline-directed sites were the most common (Huttlin et al., 2010; Lasonder et al., 2012). Using the same decision tree approach and excluding sites allocated as 'other', this was not the case within adult *S. mansoni* worms as acidic-directed motifs represented 22% of the total, although proline directed constituted 20%. Tyrosine-directed motifs were also poorly represented as in other organisms. Overall, there was no particular motif category which dominated as was the case when exploring different tissues in *M. musculus* where higher proportions of proline-directed motifs had been discovered in the spleen, testis and pancreas (Huttlin et al., 2010). Once again this highlights a case for future phosphoproteomic studies across the life stages of *S. mansoni* to determine any significant differences. Given the small size of schistosomes, phosphoproteomic analysis of specific tissue types would be exceptionally challenging using existing technologies.

An alternative way to interpret phosphorylation motifs is to look at those which are over-represented; this analysis was performed using MotifX which identified four over-represented tyrosine-, 25 threonine- and 65 serine-centred motifs. The aim was to further classify these motifs as with the entire dataset (above) according to Huttlin et al. (2010), however this was less successful with only 22 of the 65 serine-centred motifs classified (9 proline-directed and 12 basic-directed), 8 of the 24 threonine-centred motifs (8 proline-directed) and none of the tyrosine centred motifs classified.

Lastly, the over-represented motifs generated by MotifX were subjected to further analysis to determine if these motifs were linked to potential upstream protein kinases. This was carried out using two tools, HPRD and Phosida. The highest number of 'hits' (i.e. motifs with putative upstream kinases assigned) were for integral signalling pathway kinases such as CK1 and PKA, the second of which has been extensively explored in our laboratory (de Saram et al., 2013; Hirst et al., 2016) and others (Swierczewski & Davies, 2009, 2010b, 2010a). However, CaMKII was the most assigned putative upstream kinase, demonstrating its likely importance in the regulation of multiple processes in schistosomes. This kinase was therefore selected for further study in Chapter 5. Research into CK1 within the bloodstream form of *T. brucei* found the kinase to be integral to the parasites viability with RNAi of casein kinase 1 isoform 2 resulting in rapid cessation of growth, gross morphological changes, multinucleation and cell death (Urbaniak, 2009). Whereas investigation within *Leishmania major* found a CK1 isoform 2 is the primary target of selective trisubstituted pyrrole and imidazopyridine compounds which have been found to inhibit the proliferation of *L. major* promastigotes and *T. brucei* bloodstream parasites (Allocco et al., 2006) representing a potential for development of a therapeutic agent against these parasites. CK1 could represent an interesting kinase for future research within *S. mansoni* considering its crucial role within other parasites. It is worth noting that not all of the over-represented motifs were assigned to a potential upstream kinase, this could mean they represent novel motifs and may be specific to schistosome protein kinases, and again therapeutic agents targeting these novel motifs could potentially be developed.

3.4.2 Functional Annotation of *S. mansoni* Phosphoproteins

The *S. mansoni* phosphoproteome was functionally annotated using both GO and GO Slim. With GO, the dominant gene ontology category in the adult worm phosphoproteome was molecular function with 52% of the phosphoproteins classified under this category, followed by 25% biological process and 14% cellular component. Thus over half of the identified phosphoproteins are involved in activities which occur at a molecular level such as catalytic and binding activities; this correlates with the idea that phosphorylation is a switch turning a protein activity on or off or providing a docking site for other proteins (e.g. phosphotyrosine acting as a Src homology 2 (SH2) domain binding site) and hence phosphoproteins are often involved in signalling pathways at the molecular level. GO Slim analysis provided a further subset of categories for the phosphoproteins and top classification was 'cell part', closely followed by cellular 'metabolic process' and 'ion binding'. Again, this cements the understanding that the majority of the phosphoproteins in *S. mansoni* adult worms are involved in molecular processes vital to the parasite's viability. A KEGG analysis was also performed to further annotate the dataset through providing a representation of the biological systems associated in the data, the primary classification was 'biosynthesis of antibiotics pathway', followed next by 'purine metabolism'. These results support the findings from the GO analysis finding the phosphoproteins in the dataset to be involved in integral signalling pathways in the parasite.

One of the key structures that is functionally involved in the interaction between mammalian host and parasite is the tegument, the layer that envelopes the entire worm and is thus in constant contact with the host blood. The identified phosphoproteins were therefore matched

to those listed in studies that had previously been identified as being tegumental proteins; these could potentially be involved in the host-parasite signalling pathways proving to be potential targets for drug development. A previous study had carried out a proteomic analysis of the somule tegument (Sotillo et al., 2015), identifying a number of current vaccine targets including calpain (Ahmad et al., 2010), Sm-TSP-2 (Cheng et al., 2013) and Sm29 (Alves et al., 2015). A total of 48 of 68 (71%) identified tegumental proteins were found to be phosphorylated, this represents a large number of potential drug or vaccine targets for which further investigation is needed. One of these identified tegumental proteins was Sm14, a cytoplasmic fatty acid binding protein that has been developed into a vaccine which is currently undergoing Phase II clinical trials (Tendler et al., 2018). Fatty acids are of great importance to schistosomes as they are essential for membrane formation, functioning as lipid anchors for proteins, sexual maturation, and regulation of egg production (Furlong, 1991). In particular, Sm14's role in the uptake, transport, and compartmentalization of fatty acids is vital as schistosomes are unable to synthesise sterols and fatty acids and thus must obtain these from their human host (Esteves et al., 1997). Another identified tegumental phosphoprotein was Hsp90 an evolutionarily conserved molecular chaperone that aids maturation and regulation of proteins involved in cell cycle control as well as signal transduction (Schopf et al., 2017). Hsp90 has several phosphorylation sites identified, and phosphorylation on these sites has been linked to its ability to chaperone various client proteins, although the protein kinases which target these phosphorylation sites are not all known as yet (Mollapour & Neckers, 2012). Within *S. japonicum* a phosphoproteomic approach was taken to identify phosphorylation sites *in vivo* within this parasite, one of these sites was on HSP90 and this investigation found it to be phosphorylated in an evolutionarily conserved manner as well as maintaining the same phosphosite between somule and adult worms (Luo et al., 2012). One final phosphoprotein of interest identified as a tegumental protein was SGTP4, a glucose transporter protein located in

the apical membrane of the mammalian forms of the parasite (McKenzie et al., 2018; Skelly & Shoemaker, 1996) that facilitates the transport of glucose from the hosts bloodstream into the parasite (Krautz-Peterson et al., 2010). Research within our laboratory has identified the activation of the kinase AKT as essential for expression and transport of SGTP4 to the membrane (McKenzie et al., 2018). This investigation has found SGTP4 has be phosphorylated, which as past research has suggested may have been carried out by AKT kinase, solidifying the hypothesis that phosphorylation of SGTP4 by AKT plays an integral role in the transport of glucose from the human host into the parasite.

3.4.3 The *S. mansoni* Phosphointeractome

Phosphorylation of a protein involves, and can further promote, the physical interactions between proteins (de Oliveira et al., 2016). Data on such interactions for certain species is readily accessible, and for others is predicted within databases; so phosphoproteins identified by the PTM scan were mapped onto the protein-protein interaction data to identify phosphoprotein interactions. The STRING database, which was accessed through Cytoscape holds predicted protein-protein interaction data for *S. mansoni*, the programme works using known experimental interactions, knowledge from manually curated databases, automated text-mining a number of algorithms to determine a functional relationship between two proteins (Szklarczyk et al., 2015). A phosphointeractome was created consisting of 1,586 nodes and 12,733 edges; it was a dense network with a large number of connections demonstrating that the adult *S. mansoni* interactome was highly interconnected. The interactome was then analysed using a Clusterviz, a Cytoscape App which searches for highly interconnected regions using the MCODE clustering algorithm; this identified a large number of clusters (55), with 6

clusters having an MCODE score <10. These clusters contained proteins vital to various cellular processes, for example, the cluster with the highest MCODE score was the ribosomal cluster, closely followed by a cluster which contained both ribosomal biogenesis and proteasomal proteins, providing evidence for the hypothesis of the involvement of the ubiquitin-proteasome system in ribosome biogenesis (Stavreva et al., 2006). Ribosomal proteins which are overproduced in *Saccharomyces cerevisiae* are degraded by the ubiquitin-proteasome system (Sung et al., 2016); the cluster analysis could indicate that ribosomal biogenesis is also controlled *via* the ubiquitin-proteasome system in *S. mansoni*. Current research into the *S. mansoni* ubiquitin-proteasome system also indicates it may be important in the cellular stress response in this parasite (de Paula et al., 2015). However research has also highlighted a role for the proteasome as an molecular target in the design of antihelmitics against schistosomiasis with the discovery of the proteasome inhibitor MG-132 affecting *S. mansoni's* development.(Morais et al., 2017). Investigation into *S. mansoni* ribosomal biogenesis has identified a pre-ribosomal precursor SmMAK16 which appears to be involved in the production of 60s free subunits, however this requires further investigation into the elucidation of the full ribosomal biogenesis process (Capowski & Tracy, 2003).Another cluster of interest was the phagosome cluster. Phagosomes are an integral part of the exosome and vesicle system (Mulcahy et al., 2014) which is of particular interest in current schistosome research as vesicles represent an alternative target for the development of diagnostic and therapeutic methods (Coakley et al., 2019; Samoil et al., 2018; Sotillo et al., 2016). .

4 SCHISTOSOME SPECIFIC PEPTIDE ARRAY DEVELOPMENT

4.1 Introduction

Protein–protein interactions, such as those between protein kinases and substrates, drive the majority of the processes within the cell (Nishi et al., 2011). For schistosomes, understanding their biology and protein interactions at a molecular level is key to developing knowledge of the parasite as a whole, and to facilitate the discovery of schistosome-specific drug targets. There are a variety of approaches that have been developed to study protein–protein interactions and high-throughput phosphoproteomics studies have resulted in the generation of phosphopeptide datasets for many model organisms (Boekhorst et al., 2008).Our laboratory studies the interactions of protein kinases within *S. mansoni* as kinase-mediated protein phosphorylation is pivotal in the regulation of cellular responses and phenotypes (de Saram et al., 2013; Hirst et al., 2016; McKenzie, Kirk, & Walker, 2018; Ressurreição et al., 2014; Ressurreição et al., 2011b). To help increase our understanding of protein kinase-mediated signalling events within schistosomes it was decided to develop a schistosome-specific array, on which peptides serve as phosphorylatable targets (substrates) for ‘upstream’ protein kinases.

4.1.1 SPOT Technology

In general, a custom peptide array is developed by designing an array consisting of a number of peptides of interest; these peptides (representing targets) are synthesized and ‘spotted’ in duplicate in arrays on glass slides. Proteins (often enzymes), either

purified or in homogenates, are incubated on top of the slide and then an antibody (or other detection tool) allows for the visualisation of results (Figure 4.1).

Figure 4.1. Schematic diagram of generalised peptide array use. ECL – Enhanced Chemiluminescent Modified from Intavis[14]

[14] https://intavis.com/products/custom-peptide-services/celluspot-custom-peptide-arrays/

In the early 1990's, Ronald Frank developed a new method for performing multiple individual coupling reactions of amino acids in parallel on a membrane sheet, which became known as SPOT synthesis technology (Frank, 1992). Subsequent developments involved placing oligonucleotides onto planar glass surfaces (Maskos & Southern, 1992). Simultaneously, peptide libraries were created including phage display to discover potential drug targets and antibody specificity, and the yeast-two-hybrid systems to uncover protein-protein interaction networks (Fields & Song, 1989; Scott & Smith, 1990). From 1990 when the SPOT technique was presented to 2009, in excess of 400 peer reviewed papers using SPOT technology were published (Volkmer, 2009).

4.1.2 Array Use in Parasitology

There are three leading types of array for high throughput screening, microarrays that detect the expression of genes, peptide arrays which can determine protein-protein interactions, and protein arrays which enable the study of activation and interactions of proteins. These approaches have been used in investigations across parasite species, often with the goal of identifying a target(s) that can be used in the development of a drugs against the parasite (Macarron et al., 2011). For example, experiments using peptide arrays have been carried out on *Plasmodium falciparum*, causative agent of malaria. *P. falciparum* peptide arrays were probed with sera from individuals who had either been infected with the parasite or had been immunized identifying 72 highly immunoreactive proteins which could potentially be targets for vaccine development (Doolan et al., 2008). Following this, a similar study developed a protein array which covered 23% of the *P. falciparum* proteome; when arrays were probed with either plasma from subjects with sterile protection or no protection after

immunization, 19 pre-erythrocytic stage antigens were identified which could be involved in protection against malaria (Trieu et al., 2011). Others created arrays which contained approximately 23% of the *P. falciparum* proteome; plasma was acquired from subjects of a variety of ages before and after the malaria season in Mali to determine how antibody responses in these two situations differed in the hope to identify useful vaccine targets (Crompton et al., 2010).

Peptide arrays have also been used in research on *Toxoplasma gondii* and *Trypanosoma cruzi*, causative agents of toxoplasmosis and Chagas disease, respectively. A peptide array generated using antigenic epitopes of *T. gondii* proteins that had either been identified in previous publications or using *in silico* bioinformatic approaches was screened against a variety of seropositive human plasma samples. This approach positively identified 69% of these samples and highlighted epitopes that could be candidates for alternative serological diagnosis of *T. gondii* (Maksimov et al., 2012). In *Trypanosoma cruzi* high density peptide arrays were incubated with samples of blood from patients who had Chagas disease, again highlighting antigens of interest as well as mapping the specificities of B-cell responses against this human pathogen (Carmona et al., 2015).

4.1.3 Array Use in Schistosomes

In schistosomes, a protein array was developed comprising 232 schistosome proteins (McWilliam et al., 2014). This was incubated with samples from lymph nodes of previously infected rats which were subsequently challenged with 350 cercariae, followed by removal of skin and lung lymph nodes at 5 and 9 days after challenge respectively. As rats show

antibody-mediated immunity against larvae during secondary infections, the lymph node cell suspensions were cultured *in vitro* for 5 days to allow secretion of antibodies, finally the supernatant was collected and used as the antibody probe on the protein array. Results from this assay found novel antibodies from the somule stage that would be ideal targets for vaccine development; specifically the researchers identified Sj-L6L-1 as a good candidate for vaccine development due to its antigenicity in the somule stage but not the adult worm stage (McWilliam et al., 2014). Arrays have also been used to study the tegumental protein Sm21.7, a cytoskeletal antigen which presents as a good target for vaccine development (Rezende et al., 2018). First, Sm21.7's structure was determined then a prediction of the B-cell epitope to Sm21.7 was made, enabling 16 peptides which corresponded to the B-cell epitope to be synthesised and spotted onto an array. The array was probed with either sera from mice immunized with recombinant Sm21.7 or sera from human patients with *S. mansoni* infections; peptides associated with the dynein light chain domain located at the C-terminal region of Sm21.7 reacted most strongly with the mouse sera, advancing knowledge in epitope recognition relevant to the goal of creating an antigen-specific vaccine towards schistosomiasis (Rezende et al., 2018).

4.1.4 Kinomics using Peptide Arrays

Advances in our understanding of the transcriptome (Protasio et al., 2012) and tissue-specific proteomes of *S. mansoni* (Braschi et al., 2006; Castro-Borges, Dowle, et al., 2011; Curwen et al., 2004; Guillou et al., 2007; Van Hellemond et al., 2006) have provided a wealth of background knowledge on the biology of this parasite. Such work supports our understanding of the mechanisms controlling the cellular physiology of *S. mansoni*, but

much remains to be understood concerning cell signalling in these parasites. Protein kinases are integral to the signalling pathways which control cell cycle entry, survival, and differentiation (Manning et al., 2002), and understanding the biology of these enzymes can lead to development of treatment options in diseases, particularly those which occur through kinase dysregulation, for example the dysregulation of Abl kinase in humans causes chronic myelogenous leukaemia. However, a protein kinase inhibitor drug, Gleevec, has been developed as a successful treatment for this disease (Lin et al., 2013). The study of protein kinase signalling usually involves focusing on one kinase at a time and therefore high throughput techniques such as those involving peptide arrays can be useful in the screening of cell signalling processes.

This study aimed to create an array containing peptides that are kinase substrates to profile the kinase activities of *S. mansoni,* with the aim of being able to look at the differences in kinase phosphorylation between life stages and sexes so we may highlight potential kinases of interest, which could be developed later down the line as a therapeutic agent against *S. mansoni*. Peptides represent the primary structure of a protein and, for a given kinase, there is high conservation of specificity regarding the -4/+4 residues surrounding the phosphosite (Kreegipuu et al., 1998) and that higher order secondary or tertiary structures are unimportant. Such arrays have been employed successfully in several biological systems. For example, Pepscan[15] created one of the first human kinase arrays which consisted of 1,176 substrate peptides that were almost all derived from human kinase consensus sequences; this array proved to be an extremely useful tool when studying kinase signal transduction (Löwenberg et al., 2006a; Löwenberg et al., 2006b; Parikh et al., 2009). Not only was this

[15] https://www.pepscan.com/

1,176 substrate peptide array successful in screening human samples, its use with *Arabidopsis thaliana* helped demonstrate that the LKB1/SNRK1/MAP kinase pathway played a major role in sugar sensing within plants (van Veelen et al., 2011). Kinome profiling within plants has also been achieved (Ritsema & Peppelenbosch, 2009). For example, the *A. thaliana* kinome was explored using PepChip Kinase arrays probed with *A. thaliana* lysate following the production of phytohormones in response to biotic attack; certain phytohormones were found to control cross-talk between signalling for defence mechanisms as well as response to light (Ritsema et al., 2010). Returning to kinomics in mammals, the PepChip Kinase array helped determine the effects of the arenavirus 'Pichinde' on the immune response of guinea pigs (Bowick et al., 2007). Several key signalling 'nodes' were identified highlighting differences between phosphorylation events in mild and lethal infections; the nodes might represent potential targets for antiviral drugs (Bowick et al., 2007).

Each of the aforementioned studies used commercially available peptide arrays however, some researchers have developed their own custom array for more definitive characterisation of protein kinase activities in a particular species. An example being Robertson et al. (2014), who created a honeybee-specific peptide array using knowledge of the honeybee proteome and phosphosite prediction software. Experiments were then performed using extracts from honeybees that were either resistant or susceptible to the Varroa mite, highlighting differences in kinomic profiles between the two and indicating markers that could be used in the development of a future breeding programme to increase the number of honeybees resistant to Varroa mite infection (Robertson et al., 2014). Research such as this demonstrates the benefit of developing species-specific kinase arrays.

4.1.5 Aims

The research in this chapter aimed to develop a signalling-biased peptide array for screening *S. mansoni* protein kinase activities in homogenates of *S. mansoni*.

Specific objectives were to:

1. Use knowledge obtained from the PTM scan alongside other research to build a low-density 96 spot schistosome-specific peptide array for kinomic profiling;
2. Determine a working protocol for the use with the schistosome specific array;
3. Test the developed array using *S. mansoni* proteins from differing life stages.
4. Determine if the peptide arrays can be used to identify any significant similarities or differences between *S. mansoni* sexes.

4.2 Methods

4.2.1 Array Protocol

4.2.1.1 Peptide Array Development

The phosphopeptide data set was submitted to ScanSite[16] to identify potential upstream protein kinases responsible for the identified phosphorylation events, this revealed a total of 595 motifs ascribed to kinases. The Scansite-predicted phosphorylation site within each peptide was then screened against the original phosphopeptide data to ensure correct phosphosite match; peptides with mismatched sites were excluded. Results were then filtered for interesting protein kinases to be represented on the array, a spreadsheet of results was curated to help with the filtering of protein kinases, this included the kinase name and group, the surface access value, whether the scan had been performed at high or medium stringency, and the peptide used in the scan. Cross referencing with the PTM scan results allowed annotation of the substrate name, the phosphorylation site number, substrate function, Smp identifier; gene expression data was also collated from GeneDB. Each 15 mer peptide selected for the array was then resubmitted to Scansite, interrogating for mammalian and/or yeast upstream kinases. Sometimes this revealed a possible additional upstream protein kinase for a particular peptide. If more than one phosphorylation site was predicted by Scansite, then the resulting additional site(s) were only listed if they were also found to be phosphorylated in the experimental PTM scan data. This processed resulted in 60 selected peptides.

[16] www.scansite4.mit.edu

To identify further peptides for inclusion on the array (Figure 4.2), the experimental data tables were manually screened to identify additional peptides within signalling-related proteins. The full protein sequence for each candidate was retrieved and submitted to Phospho.ELM via PhosphoBLAST[17], and also to Scansite, to identify putative upstream kinases. In some cases, no upstream kinase for a phosphosite was predicted; nevertheless, if the protein was deemed interesting in terms of schistosome biology, the relevant phosphopeptide was flagged for inclusion on the array. Finally, additional peptide substrates were included based on existing knowledge of schistosome protein kinase substrate preferences (de Saram et al., 2013; McKenzie et al., 2018; Ressurreição et al., 2014; Ressurreição et al., 2011b, 2011a; Walker, Ressurreição, & Rothermel, 2014). All protein kinase names on the array were checked/updated according to the terminology used in the *S. mansoni* kinome paper (Andrade et al., 2011). Finally, gene expression data for each protein represented on the array was obtained from GeneDB[18]. The final *S. mansoni* custom 'CelluSpot' 96-spot peptide array was printed under contract by Intavis Bioanalytical Instruments AG. Each slide comprises two sub-arrays, each with identical peptides(See Appendix File 10).

[17] http://phospho.elm.eu.org/pELMBlastSearch.html

[18] www.genedb.org

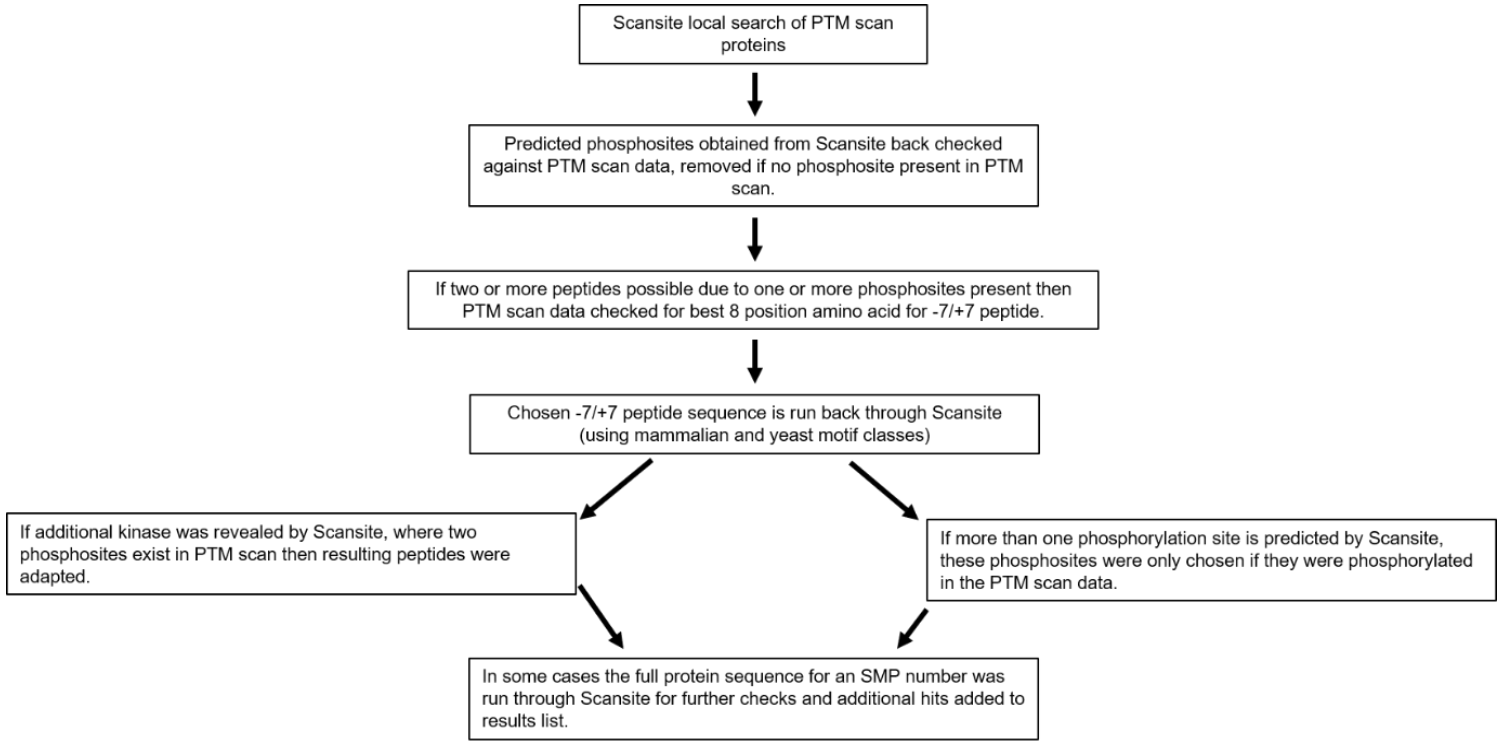

Figure 4.2 Flow diagram portraying the decisions in choosing peptides for the development of the *S. mansoni* specific array using data obtained from Scansite

4.2.1.2 Preparation of Somule and Adult worm Samples

In vitro cultured 24 h somules were transferred into a microfuge tube and left on ice for 5 min. The microfuge tube was centrifuged at 13,400 rpm for 1 min using a MiniSpin Centrifuge (Eppendorf) and the supernatant was removed and discarded. Cell lysis buffer. 10 µl per 1000 somules (Cell Signalling Technologies, #9803S) and an appropriate volume of Halt^{TM} Protease Inhibitor Cocktail less the EDTA component (100 X; Thermo Scientific, #87786) were added and the sample left on ice for 30 min. The sample was then homogenised on ice using a motorized pestle mixer (VWR) for 10 min, followed by sonicating for 1 min in an ultrasonic bath and was re-centrifuged for 3 min at 13,400 rpm and the supernatant removed and retained, whilst the pellet went through one final homogenisation using a motorized pestle mixer (VWR) for 5 min, before centrifuging for one final time for 3 min at 13,400 rpm. The supernatant was pooled and placed into a fresh microfuge tube and stored at -80°C until use. The adult worms were prepared in an identical fashion expect that they were cut up into small pieces with micro scissors in the cell lysis buffer (50 µl per 5 worms) before incubation on ice.

4.2.1.3 Preparation of Phos-Tag Biotin Complex Solution

The following reagents were added to a microfuge tube and left for 30 min at room temperature: 469 µl TTBS (Thermo Scientific, #28360), 10 µl 1.0mM Phos-tag Biotin (BTL-III) (Wako Chemicals GmbH, #308-97201), 20 µl 1.0mM $ZnCl_2$ (Sigma, #39059-11ML-F), 1 µl HRP-Streptavidin complex (AmershamTM GE Healthcare, #RPM1231-100 µl). The solution was transferred to a centrifugal filter device cup (Nanosep 30K Omega, Pall

Corporation, #OD030C33) and centrifuged at 14,000 x g for 20 min at room temperature. The excess solution was removed and diluted into 15 ml of washing buffer (TTBS, 1.0M $NaOC_2$, and 1% BSA), then stored at 4ºC for up to 30 days. If not used in the 30 days, the washing buffer was discarded and remade.

4.2.1.4 Array Protocol

Blocking solution (10 ml of 10% BSA (Sigma, #A3059-10g) in TTBS) was made, and the array slide (Intavis) was immersed in the blocking solution and agitated on the rocker overnight at 4°C. The arrays were washed with washing buffer (TTBS, 1.0M $NaOC_2$, and 1% BSA) two times for 5 min each. Whilst the array washed, the *S. mansoni* extract was prepared. The appropriate amount of parasite sample was determined by protein estimation and was removed from the -80°C. A total of 200 µl of incubation solution was prepared; this comprised of 100 µg of homogenate, 2 µl of 10 mM ATP (Cell Signalling Technologies, #9804S) and the volume made up to 200 µl with 10 X kinase buffer (Cell Signalling Technologies #9802). The solution was then pipetted onto the labelled array, and a Lifter Slips Slide (Electron Microscopy Sciences, #72183-75) floated on top of the sample upon the array. The array was placed into a humid Tupperware box at 37°C on an orbital shaker for 3 h. The array was then washed using washing buffer two times for 5 min each before. Being incubated in Phos-tag Biotin complex solution (Section 4.2.1.3) for 1 h at room temperature on a rocker. The array was washed once more using washing buffer twice for 5 min. Phosphorylated peptides were then detected as spots using G-Box (Syngene) chemiluminescence imaging station using an ECL detection kit (AmershamTM GE Healthcare, #RPN2232), images were typically gathered every 30 s for 5 mins.

4.2.1.5 Bradford Protein Assay

Six standard dilutions of BSA, 0 - 1.5 µg/ml, (Sigma Aldrich, A3059) were made using cell lysis buffer . Next, 5 µl of each of these protein standards were added to a clear bottomed 96-well plate in duplicate. Homogenate samples (5 µl each) was pipetted into an adjacent well. Next, 300 µl of Pierce™ detergent compatible Bradford assay reagent (Thermo Fisher, #23246S) was added to each well and mixed using a pipette and left for 10 min at room temperature, before placing in the microplate reader (FluoStar Optima, BMG Labtech). The absorbance of each protein standard and 'unknown' sample were read at 620 nm. Using Microsoft Excel, the absorbance data for the standards was used to create a graph with line of best fit, allowed protein concentrations in the samples to be determined.

4.2.1.6 Protein Array Analyser for ImageJ

The plugin for Protein Array Analyser for Image J was downloaded[19] into the plugins folder for ImageJ2 (Rueden et al., 2017). This software has been used in numerous studies to evaluate spot intensities on arrays (Dionne et al., 2018; Dukic et al., 2018; Fujita-Yamaguchi et al., 2018). An image of each array was opened using the protein array analyser tool, a grid of dots was then placed onto to the array image and analysed producing intensity data; each of the two sub arrays on the slide was analysed independently. The data from the grid measurements table was captured and a model created using these measurements to give a

[19] http://image.bio.methods.free.fr/ImageJ/?Protein-Array-Analyzer-for-ImageJ.html

visual representation of the array. The spot with the highest intensity for each array was located and was used to normalise the array to enable comparison between the arrays before further analysis was carried out.

4.3 Results

4.3.1 Schistosome Specific Peptides

There were 93 schistosome specific peptides chosen to be included on the array of which 68 (73 %) have been assigned a putative upstream protein kinase based on bioinformatic predictions and knowledge from the literature/other studies in our laboratory. The remainder (25 peptides) still contain bona-fide phosphorylation sites but lack upstream kinase annotation; these peptides were included because they represent proteins that were considered important to schistosome biology for example SGTP4 and SmTK4. A full list of peptides included on the array can be found in Appendix File 9 , and their placement on the array can be found in Appendix File 10.

4.3.2 Preliminary Array Testing

Upon receipt of the arrays a protocol needed to be established and optimised for schistosome kinomics. The method created by Eiji Kinoshita at the Department of Functional Molecular Science at Hiroshima University (Kinoshita et al., 2012) which employs the highly sensitive phos-tag biotin (BTL-111)-streptavidin system was used as a template on which to develop a protocol for *S. mansoni* homogenates; however, a number of technical issues presented during the development phase. Arrays were blocked with a 10% BSA solution overnight as recommended by Dr Kinoshita's protocol. Following blocking, the slides were washed and incubated with the test homogenate. However, because worm extracts are small in volume, the arrays cannot be flooded with

homogenate and a method to incubate homogenate solely on top of the array was needed. To try to overcome this a hydrophobic pen was used to draw a zone around the outside of the array, and the homogenate was pipetted within and placed on an orbital shaker at low speed at 37ºC for 3 h. Unfortunately, this approach resulted in insufficient phosphorylation of peptide spots (Figure 4.3), possibly because the hydrophobic ink may have inhibited the phosphorylation reaction. LifterSlip cover slips were next trialled, which prevent the coverslip and the array from touching; the homogenate solution sits on top of the array slide but under the coverslip during the incubation period without running off the slide.

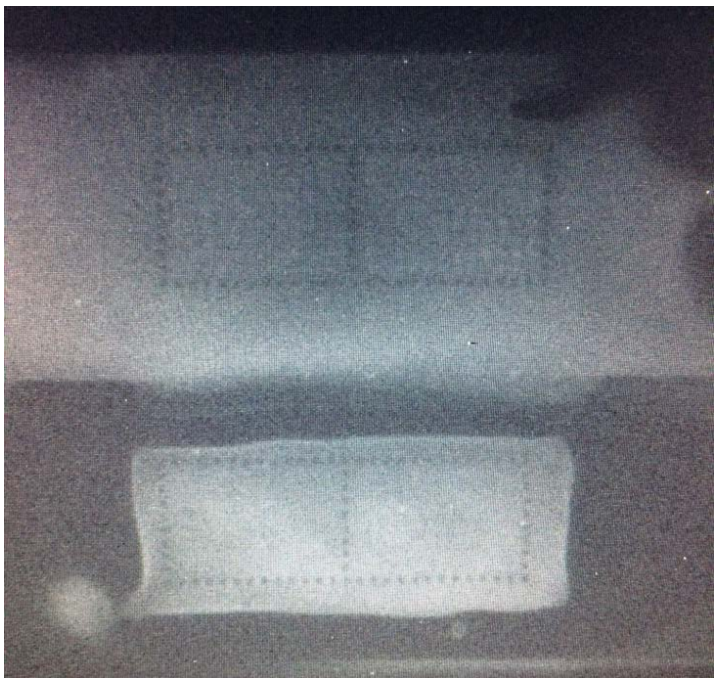

Figure 4.3. Failed CelluSpots custom *S. mansoni* peptide array. A hydrophobic pen was used to draw a border around the peptide arrays to allow incubation of homogenate in a small area. However, no spot phosphorylation was seen. Note the darker perimeter spots which are not peptide spots; phosphorylated spots should appear within these zones.

Although the homogenate was incubated with the array at 37ºC for 3 h, the team at Hiroshima University suggest an incubation time of 1 h at room temperature (Kinoshita et al., 2012); this alternative incubation regimen was tested but it did not lead to peptide phosphorylation. The incubation was adjusted back to 3 h at 37ºC and peptide spot phosphorylation was observed; therefore, all subsequent assays were incubated for 3 h at 37ºC.

4.3.3 Array Results

Now that a working protocol had been established, the arrays could be used to detect peptide phosphorylation by *S. mansoni* homogenate. The first tests were performed with adult male worm extract, because more males were often supplied, and they are larger than female worms. The initial test employed 50 µl adult male worm lysate (plus 148 µl of kinase buffer and 2 µl 10 mM ATP); using the Bradford Protein Assay it was calculated that this sample contained ~125 µg of protein (Figure 4.4).

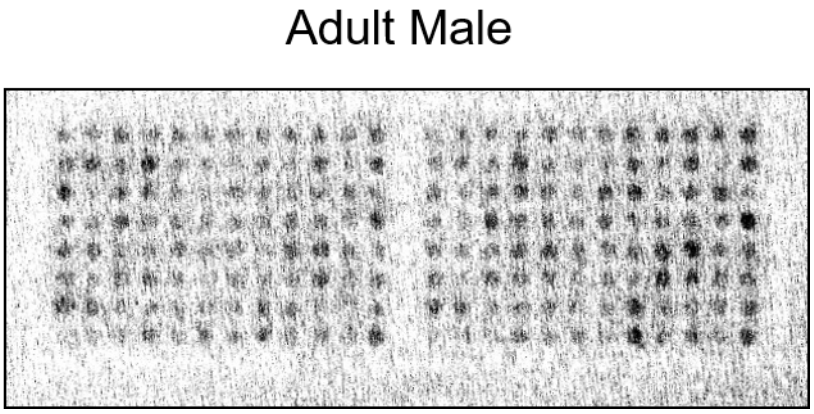

Figure 4.4. CelluSpots custom array incubated with 125 µg adult male worm homogenate. Sub-arrays on the left hand side (LHS) and right hand side (RHS) are identical with each containing 96 spots.

This first image captured was quite ‘grainy’ demonstrating the need to perfect techniques when using the GBOX system and ECL to image the phosphorylated peptides (spots). However, importantly, this array showed a number of peptides spots of high signal intensity, as well as an assortment of other lower intensity spots indicating that protein kinases in the adult male lysate were phosphorylating peptides on the array and that the schistosome specific arrays were designed appropriately.

Due to the small size and limited supply of schistosomes, maximising the use of schistosome material for arraying is an important parameter. Furthermore, diluting samples by 50% can improve the signal to noise ratio of kinomic chips (Ritsema et al., 2007). Therefore, in the next experiment 62.5 µg (rather than 125 µg) of adult male protein was tested to ascertain if it was possible to detect peptide phosphorylation and reduce signal to noise. Somule lysate was also prepared for testing.

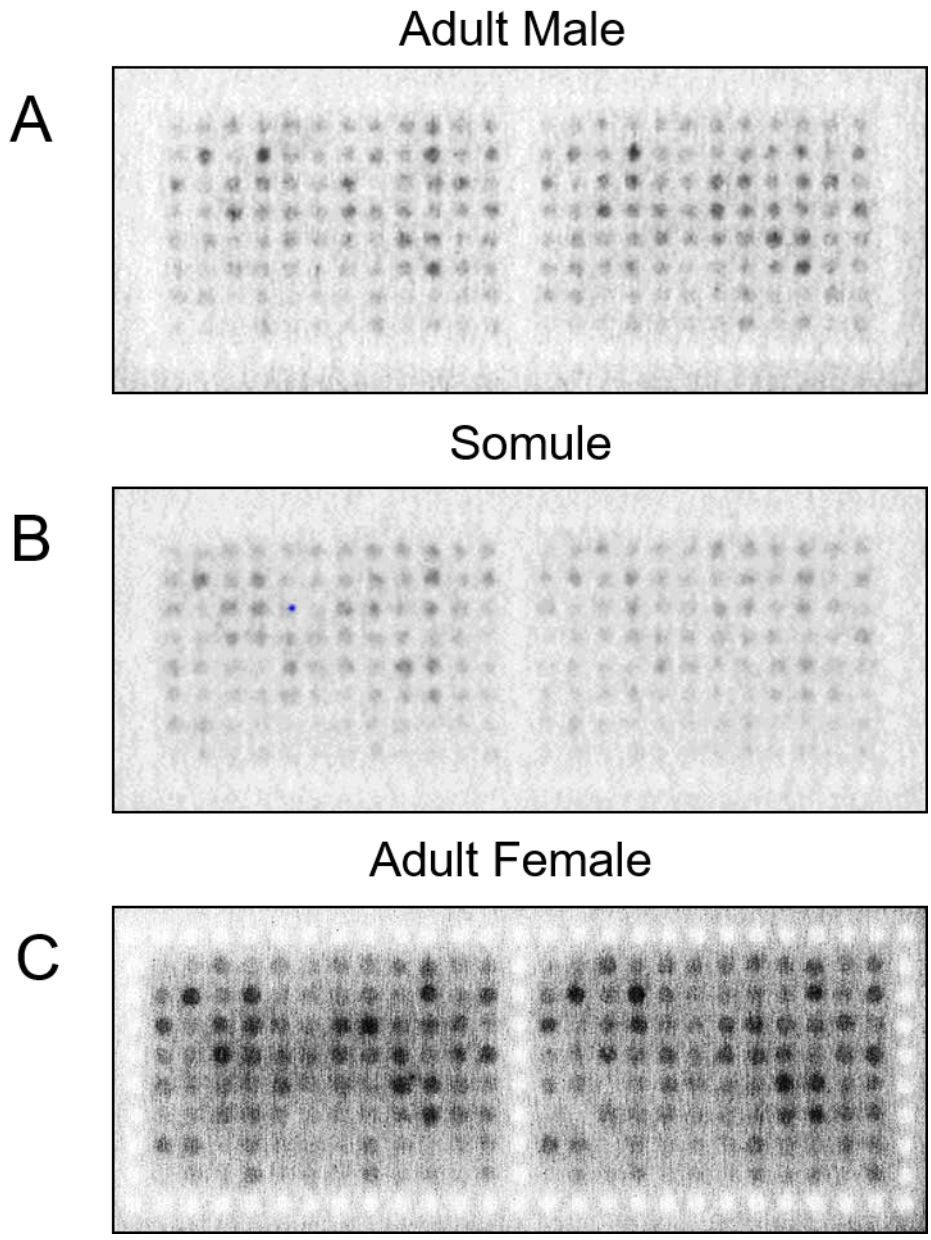

Figure 4.5. Screening the CelluSpots custom array with reduced amounts of protein. Array probed with A) 62.5 µg adult male lysate (half the amount of protein previously tested); B) 62.5 µg of somule lysate; C) 46.7 µg of female lysate. Sub-arrays on the LHS and RHS are identical with each containing 96 spots.

Whilst it was possible to detect phosphorylation of peptides with the lower amount of *S. mansoni* protein, the overall results were not robust enough and the less intense, harder to visualise, spots on the array may become problematic when using analysis software to quantify the results (Figure 4.5A, B). Nevertheless, an attempt was also made using a low

amount of female protein (46.7 µg), to determine whether female extracts can phosphorylate the peptides on the array. This was found to be successful with high intensity spots observed (Figure 4.5C), which seemed to have better definition than the male and somule arrays (Figures 4.5A, B). However, because the arrays were performed on different days, these results could not be directly compared to one another to establish if differences in phosphorylation patterns between life stages were evident. Accordingly, an experiment of two peptide arrays, one with male lysate and one with female with the same amount of protein (98.9 µg) was performed on the same day.

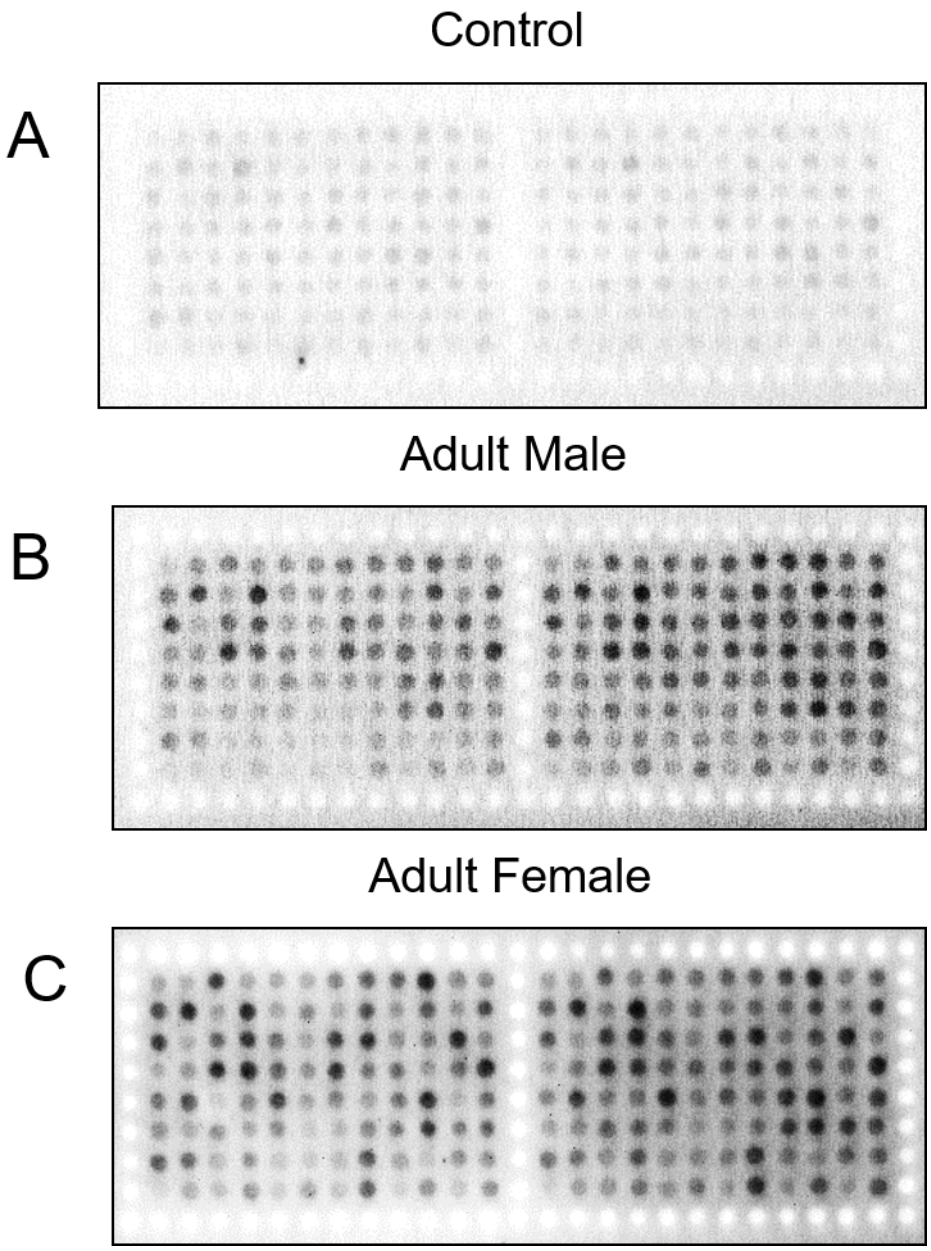

Figure 4.6. CelluSpots custom array incubated with adult male or female homogenates. A) Control slide incubated in buffer without homogenate. B) and C) Arrays probed with adult male and female homogenates, respectively (98.9 µg of each). All arraying was performed concurrently. Sub-arrays on the LHS and RHS are identical with each containing 96 spots.

In comparison to the control there was considerable phosphorylation in both the male and female peptide arrays (Figure 4.6). Visually, both arrays had some spots with

similar levels of phosphorylation and others with apparently different phosphorylation although quantification was needed to assess differences. A common theme across all of the slides tested was the somewhat stronger phosphorylation pattern to the right hand side of the array in comparison to the left hand sub-array, this was potentially down to the technical process, as when preparing the slides the samples was pipetted into the centre of the slide, however, the LifterSlip was placed onto of the slide/sample from right to left (to try and minimise bubbles in the sample). It was anticipated that normalisation of each sub-array to a spot during quantification of the arrays would 'smooth' out the disparity.

4.3.4 Quantification of Array Results

To elucidate the similarities and differences in peptide phosphorylation mediated by the protein extracts from the two sexes of adult worm quantification was performed. This was done using a plugin named Protein Array Analyzer for ImageJ[20]. As each of the arrays comprise two duplicate sub-arrays, for analysis they were considered as two individual (technical) replicates, left-hand and right-hand sides, giving a total of 4 assays per sex (from two biological replicates). Each 'spot' could then be assigned a number and model based on the intensity of the spots was generated to provide a global visual representation (Figure 4.7). Array data was normalised and mean intensities for spots phosphorylated by male and female extracts calculated together with standard deviations; a t-test was performed to resolve significant differences (Figure 4.8). The analysis identified 14 differentially phosphorylated peptides ($P \leq 0.10$), with eight

[20] http://image.bio.methods.free.fr/ImageJ/?Protein-Array-Analyzer-for-ImageJ.html

being different at P≤0.05 (Table 4.1). These peptides were from the substrate proteins (with putative upstream kinases listed in brackets where known), Rho2 GTPase putative, Insulin receptor, SmTK4, AMPKL/CAMK (AMPKK), protein phosphatase 2c gamma putative (cdc2/cdk5), Vacuolar protein sorting 26 - VPS26 putative, AKT (Src), high voltage-activated calcium channel beta subunit 1 putative (PLK1), pak-interacting exchange factor beta-pix/cool-1, putative (EGFR), p38MAPK (MAP2K), Heat shock protein putative (CK2), Multivalent antigen sj97 GAPDH (PKC epsilon), TGF-beta signal transducer Smad2 putative and CDK/PITSLRE (AKT) which was found to be the most significantly different (P=0.00173) (Figure 4.8). The phosphorylation pattern for the peptide AMPKL/CAMK observed across all arrays is provided in Figure 4.9 to illustrate the variability between spots (P=0.019).

Male Average	Female Average	TTest	Protein
0.66934	0.921646	0.001726	Serine/Threonine protein kinase - CDK/PITSLRE (AKT)
0.441682	0.585251	0.011831	Rho2 GTPase, putative (-)
0.19381	0.304541	0.015038	Tyrosine Kinase - Insulin receptor (-)
0.286364	0.507192	0.016201	Tyrosine kinase - SmTK4 (-)
0.540172	0.86564	0.018997	Serine/threonine protein kinase - AMPKL/CAMK (AMPKK)
0.530888	0.772165	0.0298	protein phosphatase 2c gamma, putative (cdc2/cdk5)
0.436185	0.641216	0.036387	Vacuolar protein sorting 26, VPS26, putative (-)
0.559172	0.856597	0.048962	Serine/Thereonine kinase - AKT (Src)
0.371103	0.489524	0.054913	high voltage-activated calcium channel beta subunit 1, putative (PLK1)
0.382792	0.605079	0.064053	pak-interacting exchange factor, beta-pix/cool-1, putative (EGFR)
0.611816	0.79257	0.065629	Serine/Threonine protein kinase - p38MAPK (MAP2K)
0.65652	0.840271	0.069545	Heat shock protein, putative (CK2)
0.478223	0.641381	0.07101	Multivalent antigen sj97 GAPDH (PKC epsilon)
0.258008	0.377455	0.075132	TGF-beta signal transducer Smad2, putative (-)

Table 4.1 Proteins (peptides) found to be significantly differentially phosphorylated between custom CelluSpots arrays probed with male and female adult worm homogenates. The protein listed in brackets is the putative upstream kinase (where known). The average values are normalised value. Data for all spots can be seen in Figure 4.8.

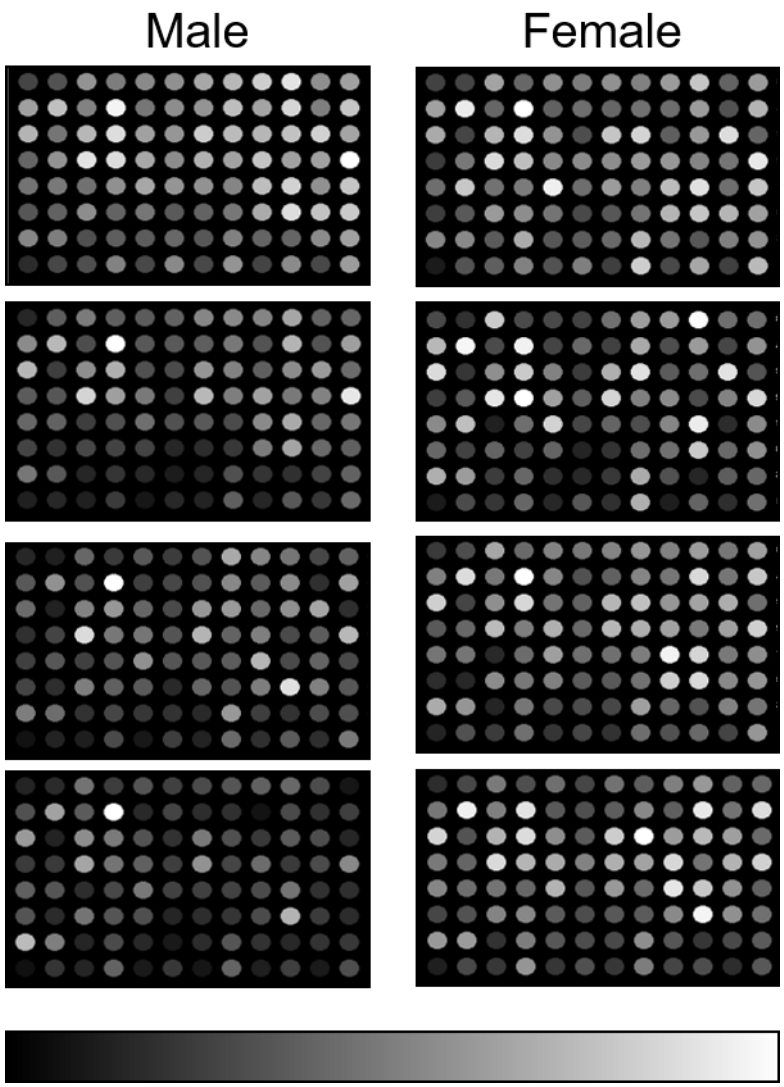

Figure 4.7. Model representation of each of the four replicates of the custom CelluSpots peptide arrays probed with either *S. mansoni* male (left) or female (right) adult worm homogenates. The intensity scale for the dots is presented below the arrays with black being the least intense and white the most intense.

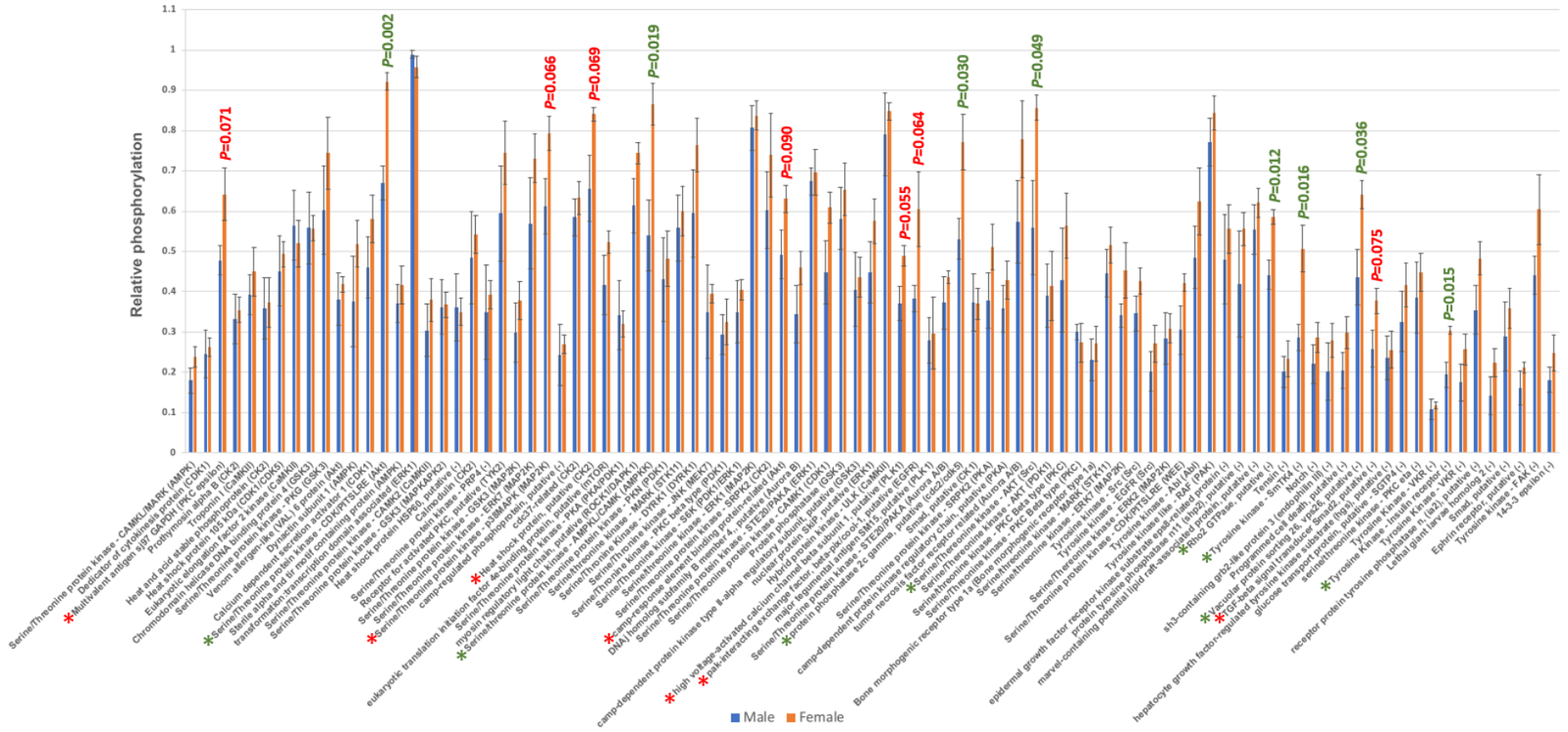

Figure 4.8. Graph illustrating the mean normalised spot intensities for each peptide (n=4 ± S.E.M.) using the ImageJ plugin 'Protein Array Analyzer', representing the differences between mean phosphorylation by male (blue) and female (orange) homogenates. Results were evaluated using Student's t-test (P≤0.1 green, and P≤0.05 red). For each substrate peptide the putative upstream kinase (where known) is annotated within brackets.

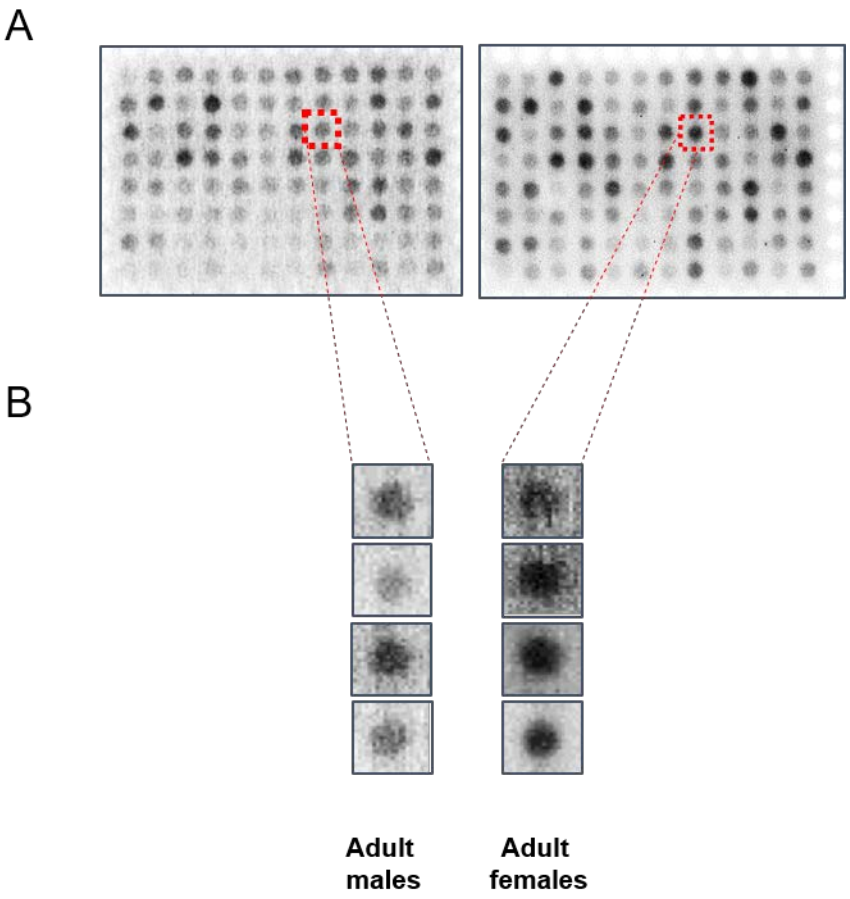

Figure 4.9. Phosphorylation of AMPKL/CAMK peptide (substrate) by *S. mansoni* adult worm homogenates. (A) Example of the CelluSpots custom array incubated with male (left) and female (right) homogenates. with the spot corresponding to Src highlighted in red. (B) A zoomed image of each of the arrays on the AMPKL/CAMK spot, plus also three from other replicates, for both adult male and female arrays; note the difference in intensity between AMPKL/CAMK phosphorylation by adult females extracts compared to those of adult males. The mean relative values for AMPKL/CAMK were 0.54 and 0.87 in males and females respectively (P=0.019; Table 4.1).

4.4 Discussion

4.4.1 Development of the Array

In recent years there has been an emerging trend to explore signalling patterns in humans more globally using high-throughput methods such as peptide kinomics arrays (Hayashi et al., 2005; Sikkema et al., 2012; Strehl et al., 2011). This approach can provide a wealth of knowledge to further understanding of the biological complexities of cell signalling, and ultimately identify potential proteins that may represent good therapeutic targets. The overarching aim of the current investigation was to develop a schistosome-specific kinase array for the use in future research into protein kinase signalling in schistosomes. In particular, it could be used for exploring signalling across all life stages of the parasite, as well as in response to growth factors from the host and to drugs such as PZQ. To be able to build a meaningful peptide array, which is not built upon bioinformatic prediction alone, knowledge of phosphorylation sites within the proteome is ideally needed. Thus, drawing upon data revealed in the PTM Scan (Chapter 3) and its analysis, a list of phosphopeptides of interest was selected for inclusion on the array, supported by existing knowledge of current kinases of interest and previous investigations into the kinase signalling pathways carried out within our laboratory (de Saram et al., 2013; Hirst et al., 2016; McKenzie et al., 2018; Ressurreição et al., 2014, 2016, 2011b). This led to the inclusion of 96 peptides on interest on the array (including control spots), many of which have putative upstream protein kinases assigned that were predicted using Scansite and other approaches. Other peptides lacking the predicted upstream kinase annotation were included as they are interesting proteins in the context of their importance to schistosome biology, examples being 1) SGTP4, which was recently found to be regulated by AKT in *S.*

mansoni (McKenzie et al., 2018); 2) smad proteins which are known to be involved in TGFβ signalling within the parasite (Loverde et al., 2007); 3) insulin receptor which can be activated in worms by host insulin (Khayath et al., 2007); and 4) two venus kinase receptors (VKRs) which are known to play a role in schistosome reproduction (Vanderstraete et al., 2014).

4.4.2 Preliminary Array Trials

Many researchers detect phosphorylated peptides on arrays using γ-32p ATP; however, non-radioactive methods are becoming more popular as they are gaining in sensitivity and are safer to use. Kinoshita et al. (2012) developed a protocol for Intavis CelluSpots peptide arrays in conjunction with their own detection method employing Zn^{2+}-Phos-tag-bound HRP-Streptavidin (Phos-tag BTL-111); this system could be detected simply with ECL chemiluminescence, and had been used successfully in their subsequent studies (e.g. Kinoshita-Kikuta et al., 2016; Kinoshita et al., 2013). This method was therefore trialled with the custom schistosome-specific peptide array. The protocol from Intavis advised using 5% BSA for blocking, however Kinoshita et al. identified issues with false-positive ECL signals which they believed were caused by the Phos-tag-bound HRP-Streptavidin interacting with the cellulose support on the array, therefore they used a higher concentration (10% BSA) for blocking (Kinoshita et al., 2012). In the current study, 10% BSA also resulted in low background. Unlike when working with human cells (which can be grown in large numbers), schistosome material is limited in quantity and is constrained by maintaining the lifecycle and the need for mice. Kinoshita et al. 2012 used human cell lysates and could incubate the

arrays in large volumes of lysate, with protein amounts varying from 60-125 µg. For schistosomes, arrays were initially tested with 60 µg of protein mixed with kinase buffer in a final volume of 200 µl, and to ensure the homogenate remained on the slide the homogenate was pipetted within a circle drawn with a hydrophobic pen. However, this approach failed (Figure 4.3), presumably due to the hydrophobic pen interfering with the phosphorylation reaction and/or detection method, so an alternative approach needed to be found. LifterSlip coverslips used by other researchers (Haider et al., 2016; Zhang & Zeng, 2011), were tested; this allowed for the sample to be pipetted on the array, with the LifterSlip™ carefully placed on top permitting uniform dispersal of the sample across the array. Arrays were also placed on a rocker in a humid box at 37ºC during incubation as done by other researchers using LifterSlips (Haider et al., 2016; Zhang & Zeng, 2011). Kinoshita's protocol (and that of Intavis) recommends that arrays are incubated in the lysate for 1 h at room temperature, however this resulted in a failed assay. The success achieved after 3 h incubation at 37 ºC may have been due to the prolonged interaction time between the homogenate and the peptide spots, and the increase in temperature that would have favoured the kinetics of the kinase reactions. Overall, these preliminary tests utilised knowledge from a number of research groups who had developed their own peptide chip assays, along with the guidance from the manufacturer to create our own working protocol for testing *S. mansoni* extracts with the novel custom peptide chip. Although, 3 h was used for subsequent assays, future projects should evaluate the performance of the arrays after longer incubation times (e.g. 5 h) with schistosome extract as they may permit the use of lower protein amounts.

4.4.3 Employment of the Developed Array

Further tests revealed that the best detection with low signal to noise ratio came when using ~100 µg of *S. mansoni* protein. As this larger quantity of protein was easier to obtain from adult worms rather than cercariae or somules it was decided to concentrate experiments on the adult worm stage. Logically, the aim was to try to determine differences in array spot phosphorylation between adult male and adult female worm extracts. Interestingly, the majority of the 93 *S. mansoni* peptides were similarly phosphorylated by the two sexes, however eight peptides that were identified as being significantly differentially phosphorylated ($P \leq 0.05$) between males and females, with the greater phosphorylation generated by female extracts. These peptides (with putative upstream kinases in brackets if known) were from CDK/PITSLRE (Akt), AMPK (AMPKK), Akt (Src); SmTK4 (not known), insulin receptor (not known); protein phosphatase 2c gamma (cdc2/cdk5), Rho2 GTPase (not known), and vacuolar protein sorting 26 (not known). A further seven peptides; multivalent antigen sj97 GAPDH, p38 MAPK, heat shock protein, camp-response element binding protein-related, high voltage-activated calcium channel beta subunit 1, pak-interacting exchange factor beta-pix/cool-1, and Smad2, were found to be differentially phosphorylated at a lower significance level ($P \leq 0.10$) and should therefore be considered as being possibly differentially phosphorylated and worthy of future investigation. The peptides displaying the greatest phosphorylation included transformation:transcription domain associated protein in male and female worms, and the serine/threonine protein kinases CDK/PITSLRE and AMPK with putative upstream protein kinases being ERK1, AKT, and AMPKK, respectively; others included ERK1, Raf, AKT, and hybrid protein kinase ULK, with putative upstream

kinases identified as MAP2K, PAK, Src, and CaMKII. AKT has been researched in our laboratory, specifically its interactions with SGTP4 and how they work together to regulate the uptake of glucose in schistosomes (McKenzie et al., 2018). The results here, indicate that female worms may have enhanced AKT activity which is known to generate higher VAL6 phosphorylation, this substrate has been linked to the oral and ventral suckers of *S. mansoni* adult males (Rofatto et al., 2012) and tissue expression levels localising SmVAL6 to the oral and ventral suckers were subsequently found to be higher in males than females.(Fernandes et al., 2017).These studies contrast with this result, showing that whilst tissue expression levels are higher in males, phosphorylation of VAL6 is higher in females suggesting its biological significance in females as well as males. ERK1, also characterized in our laboratory, has differing phosphorylation levels on the array between male and female extracts; our research group explored ERK signalling in early developmental stages of *S. mansoni* and determined the link between lipid rafts and ERK signalling, and also discovered that the attenuation of ERK signalling reduces the release of acetabular gland contents in cercariae, proving ERKs key role in host penetration (Ressurreição et al., 2014, 2015); ERK has also been found to play a role in egg laying and movement of the adult worms (Ressurreição et al., 2014). Src belongs to the Src family, a type of Cytosolic Tyrosine Kinase (CTK) (Avelar et al., 2011), also belonging to this group is SmTK3 which plays a significant role in the proliferation of vitelline cells (Knobloch et al., 2007).Treatment of paired adult worms with a Src inhibitors combined with TbRI serine/threonine kinase inhibitor reduced mitosis and egg production (Knobloch et al., 2007). The Src/Abl hybrid kinase SmTK6, Syk kinase SmTK4 are also thought to act alongside SmTK3 to transduce signals integral to gametogenesis in parasite gonads (Svenja Beckmann et al., 2011, 2012). Each of these phosphoproteins represent

potential targets for drug development and highlights the need for further research into the remaining phosphoproteins to discover their role in the parasite and their potential to also be targeted in the goal of eliminating schistosomiasis.

Whilst peptide arrays provide a cost effective and accurate insight into cell signalling events, offering information on up to thousands of peptides on just one array, there are limitations to this procedure. Interpretation of the data gained from these high-throughput assays, often relying on data that has been previously confirmed in past research, followed by the selection of a few phosphorylation events deemed to be of interest and providing further in-depth analysis into these through the use of Western blotting etc. Techniques into applying reliable data mining of the large amount of knowledge an array can provide need to be developed to ensure a peptide array becomes a significant tool rather than creating hypotheses for future work (Arsenault et al., 2011). Moreover, there are drawbacks to the use of peptides instead of the whole protein, whilst the use of a peptide ensures a simple linear way to determine whether or not a sample phosphorylates the peptide, the specificity and efficiency of the kinase carrying out the phosphorylation cannot be guaranteed. Furthermore, the use of lysates releases kinases from their compartmentalisation in their intracellular location, potentially displacing them and allowing the phosphorylation of a peptide which may not occur *in vivo* (Arsenault et al., 2011). There are various other techniques available for scrutinising phosphorylation events, these include kinase assay kits which monitor the kinases activity and any substances which may interfere with its functioning, this includes assays which have been developed to quantify the activation status of a many kinases in the same cell lysate (Yu et al., 2009). Alternatively there is KESTREL

(kinase substrate tracking and elucidation) which identifies specific sequences which have been phosphorylated *in vivo* (Bonetta, 2005). Alternatively, there are techniques such as those used in Chapter 3, where phosphoproteins are purified by either IMAC or phospho-antibodies and subsequently identified through LC-MS/MS. To discover phosphorylation sites *in vivo* there is the option to generate a screening peptide library, or a novel approach has been developed using crosslinkers between substrates to identify a kinase (Bonetta, 2005). These represent a powerful set of tools available to researchers to expand the knowledge on kinase signalling.

This analysis has been limited to only male and female adult worms and more studies to expand knowledge of cell signalling in schistosomes could be performed, including testing all larval life stages of the parasite, as well as the parasites' response to relevant substances such as glucose, linoleic acid, praziquantel, and host growth factors. While it is difficult to predict whether the sensitivity of the array would permit subtle changes/differences to be detected without large numbers of replicates we anticipate they would provide significant insight to signalling with relative ease, as has been the case here with CDK and other proteins such as AKT and SmTK4. The current array is low-density and there is the argument that other peptides could be considered for inclusion on future arrays. The peptides were chosen using guidance from the PTM Scan data and prior knowledge of cell signalling in schistosomes; although this is not an exhaustive list of proteins of interest, now this novel array has been created, it would be easy to modify through the inclusion/exclusion of proteins on the array to tailor it to the research needs of others. Design of the current array was global in its approach to inclusion of peptides; however, it could also be modified to include more

tissue specific peptides i.e. those from tegumental proteins, or life-stage specific proteins. The current proteomic knowledge of *S. mansoni* (Braschi et al., 2006; Braschi & Wilson, 2006; Sotillo et al., 2015) would provide the foundation upon which the peptide chip could be modified to further such investigations. In other systems peptide chips have been developed to determine the differences between resistance, for example a species-specific peptide chip was developed to analyse the differences between the honeybee's resistance to Varroa mite infestation (Robertson et al., 2014). This idea could be translated to emerging resistance to PZQ in schistosomes, with the development of not just an *S. mansoni* array, but one for each of the important *Schistosoma* species with the inclusion of resistance relevant proteins; indeed, given the conservation of many proteins across schistosome species (Berriman et al., 2009; Young et al., 2012; Zhou et al., 2009), peptides may be similar and a single array may be sufficient. In this context, it would be interesting to compare responses of the existing array to homogenates of *S. mansoni*, *S. haematobium*, and *S. japonicum*.

5 Investigation of Ca2+/Calmodulin dependent protein kinase II (CaMKII) signalling in *Schistosoma mansoni*

5.1 Introduction to CaMKII

5.1.1 Ca^{2+}/Calmodulin Dependant Protein Kinase II

Ca^{2+}/calmodulin dependant protein kinase II (CaMKII) is a crucial transducer of the divalent cation Ca^{2+}, one of the most widely utilized second messengers in cellular signalling that instructs CaMKII to phosphorylate a wide range of substrates. The majority of the intracellular effects of Ca^{2+} are mediated through the ubiquitous Ca^{2+} sensing protein, calmodulin (CaM), a 17 kDa Ca^{2+}-binding molecule that is highly conserved (Swulius & Waxham, 2008). CaMKII is also highly conserved across animal species (Hudmon & Schulman, 2002). CaMKII is a unique Ser/Thr protein kinase due to its dodecameric assembly comprised of two joined hexameric rings (Figure 5.1). The holoenzyme is inactive until exposed to Ca^{2+}/CaM and yet can attain Ca^{2+}/CaM-independent activity following activation and autophosphorylation of a certain threonine residue (Swulius & Waxham, 2008). Humans express four main CaMKII isoforms, CaMKIIα/β/γ/δ, however when splice variants are considered there are closer to 30 variants (Erondu & Kennedy, 1985). Due to differences in the isoforms' primary structure and alternative splicing, the four kinases vary in size ranging between 50–68 kDa. CaMKII is predominantly expressed in the brain (Erondu & Kennedy, 1985), however at least one CaMKII isoform has been identified in every cell type examined in humans (Bayer et al., 1999; Tombes et al., 2003).

Figure 5.1. Structure of CaMKII. (A) Model illustrating the two hexameric rings stacked on top of each other to form a dodecameric structure joined by the association domain. (B) The crystal structure of the autoinhibited kinase domain of CaMKII shown in two views, 90º rotated from each other. The Thr286 phosphorylation site is also highlighted. Adapted from Rosenberg et al., 2005.

5.1.2 CaMKII Signalling

Signal transduction by the CaMKII holoenzyme involves a complex mix of protein localization, heterooligomerization, the concentrations of Ca^{2+}/CaM, CaMKII autophosphorylation, and dephosphorylation of CaMKII by phosphatases (Griffith, 2004). Without Ca^{2+}, CaMKII remains in its inactive form due to the autoinhibitory domain interacting with the catalytic (kinase) domain. Upon signalling, an influx of positively charged Ca^{2+} is attracted to calmodulin due to its negatively charged EF-hand motif's (Lewit-Bentley & Réty, 2000) (Figure 5.2). Once Calmodulin has bound Ca^{2+}, it undergoes a conformational change, allowing it to bind to the autoinhibitory regulatory segment of CaMKII located C-terminal to the catalytic domain. This

removes the autoinhibitory domain and exposes the Thr286 residue on the regulatory domain (Lewit-Bentley & Réty, 2000; Rosenberg et al., 2005). To activate the kinase, Thr286 is autophosphorylated by the catalytic domain (Figure 5.2) (Lai et al., 1986). CaMKII will then remain activated even in the absence of Ca^{2+}/CaM as such phosphorylation prevents the regulatory domain from rebinding to the catalytic domain (Lai et al., 1986); this also increases the enzymes' affinity for CaM by ~10,000-fold, a mechanism known as CaM trapping (Meyer et al., 1992). The association domains (Figure 5.1) hold the CaMKII dodecameric holoenzyme together as two stacked hexameric rings (Gaertner et al., 2004). Once one kinase subunit has been activated it can phosphorylate only the adjacent subunits in the hexameric ring that are also bound to Ca^{2+}/CaM, eventually leading to an enzyme that is activated even without bound Ca^{2+}/CaM (Soderling et al., 2001). This feature of Ca^{2+}/CaM-independent activity is an important mechanism as it is involved in long-term potentiation which plays a significant role in learning and memory within humans (Lisman et al., 2012).

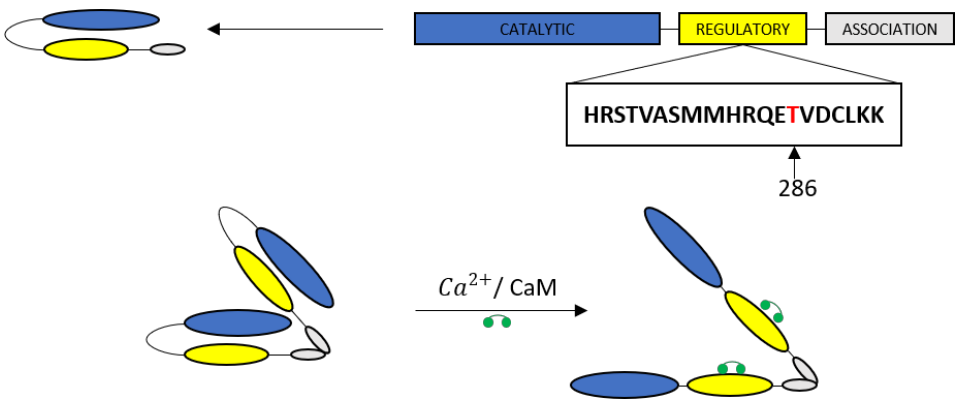

Figure 5.2. CaMKII domain structure and activation. CaMKII is comprised of a catalytic kinase domain (blue), a regulatory domain (yellow), and an association domain (grey). Ca2+/CaM (green) binds to the regulatory domain causing disassociation which leads to activation of the catalytic domain through autophosphorylation of Thr286.

After some time the intracellular Ca^{2+}/CaM levels will drop sufficiently to cause the dissociation of Ca^{2+}/CaM from the kinase, which in turn reveals a further autophosphorylation site in the regulatory domain (Thr305/306 depending on the CaMKII isoform) which can be autophosphorylated if the kinase is still in its active (Thr286 phosphorylated) state (Figure 5.3) (Hanson et al., 1994). Once Thr305/306 has been phosphorylated, rebinding of Ca^{2+}/CaM is restricted and the kinase activity becomes autonomous (Ca^{2+} independent) (Griffith, 2004). CaMKII is integral to a wide variety of signalling cascades and plays roles in neuronal processes such as synaptic plasticity, long-term potentiation and memory (Lisman et al., 2012; Shioda & Fukunaga, 2017), CaMKII is also heavily involved in cardiac signalling (Erickson, 2014), regulation of the human chloride channels within the epithelium (Ho et al., 2001), as well as signalling within T Cells (Bui et al., 2000). To return the kinase to its basal activation state Thr286 must be dephosphorylated by phosphatases including PP1 and PP2A (Strack et al., 1997). Stimulation by Ca^{2+}/CaM is necessary to restart the signalling cycle (Griffith, 2004).

Figure 5.3. Regulation of CaMKII by autophosphorylation. Inactive CaMKII (top left) binds Ca^{2+}/CaM activating it (CaM Bound). Binding of Ca^{2+}/CaM to a subunit causes adjacent subunits to be autophosphorylated on Thr286. The active CaM Trapped kinase remains active even as calcium levels fall. After Ca^{2+}/CaM dissociates, the enzyme remains active (Ca^{2+} Independent). When Ca^{2+}/CaM dissociates an additional site in the regulatory domain is revealed (Thr305/Thr306), which becomes autophosphorylated. The pThr286/pThr305/pThr306 CaMKII remains active but is incapable of binding Ca^{2+}/CaM (Capped). Phosphatases will then return the kinase to its inactive form. Adapted from Griffith (2004).

5.1.3 CaMKII in Schistosomes

There has been minimal research into CaMKII within schistosomes. The most notable work focused on adult *S. japonicum* which were exposed to sub-lethal doses of PZQ and then analysed for gene expression by microarray which highlighted CaMKII as being overexpressed (You et al., 2013). Next, the authors performed RNAi to supress CaMKII in the worms which were then exposed to PZQ and their motility analysed. Reduced expression of CaMKII in PZQ-exposed worms lead to a reduction in worm movement. This indicated that CaMKII may play an integral role in PZQ's mode of action, which is currently unknown, highlighting CaMKII as a potential drug target (You et al., 2013). With this in mind, there is scope to greatly expand our knowledge on CaMKII signalling within schistosomes, particularly given that CaMKII was identified as one of the most common upstream kinases in the phosphoproteomic work (Chapter 3) highlighting its likely importance to schistosome biology in general.

5.1.4 CaMKII Inhibitors

There are several commercially available inhibitors of CaMKII, these include peptide inhibitors such as CaMKIIN and CaMKIINtide which bind to CaMKII only when it is in its activated form. This interaction blocks the exposed kinase portion of the protein once activated, consequently inhibiting autophosphorylation of CaMKII when bound to Ca^{2+}/CaM (Pellicena & Schulman, 2014). Other inhibitors, such as the substrate-based inhibitors autocamtide-2 and autocamtide-3 (Hanson et al., 1989), AC3-I (Braun & Schulman, 1995) and AIP (Ishida et al., 1995), target the autoinhibitory portion of CaMKII.

By far the most commonly used inhibitor of CaMKII is KN93 (Sumi et al., 1991). KN93 inhibits CaMKII by competing with Ca^{2+}/CaM binding (Pellicena & Schulman, 2014). Thus, the inhibitor prevents autophosphorylation of CaMKII at Thr286 because the site remains unavailable to the neighbouring segment in the CaMKII holoenzyme, (Rich & Schulman, 1998).

5.1.5 Aims

This Chapter aims to investigate CaMKII in *S. mansoni* cercariae, somules and adult worms. Specific objectives are to:

1. Validate an antibody capable of detecting CaMKII phosphorylation (activation) in *S. mansoni*.
2. Determine CaMKII activation processes in *S. mansoni* and localise the active kinase within intact parasites.
3. Identify a suitable inhibitor to suppress CaMKII activation in *S. mansoni*.
4. Determine how integral CaMKII is to schistosome viability.

5.2 Methods

5.2.1 RNAi Reagents

The OPTI-MEM® was obtained from Gibco (Thermo Fisher Scientific) and the 4 mm gap electroporation cuvettes were from VWR (#732-1137) (Lutterworth, UK). The RNase-free duplex buffer (#11-04-02-01), double stranded scrambled negative control sequence (#51-01-14-04) and siRNAs (labelled CD.Ri.52244.13.18, CD.Ri.52244.13.2, CD.Ri.52244.13.18) were purchased from Integrated DNA Technology (IDT, Iowa, USA).

siRNA Name	Sequences
CD.Ri.52795.13.1	Sequence rCrCrC rCrUrG rArArG rCrUrA rArGrA rArUrU rUrArA rUrCA A Sequence 2 rUrUrG rArUrU rArArA rUrUrC rUrUrA rGrCrU rUrCrA rGrGrG rGrUrA
CD.Ri.52795.13.2	Sequence rArGrA rCrUrU rArCrU rCrArG rUrUrU rCrUrA rGrArU rArAA T Sequence 2 rArUrU rUrArU rCrUrA rGrArA rArCrU rGrArG rUrArA rGrUrC rUrUrG
CD.Ri.52795.13.18	Sequence rGrArA rUrUrA rCrUrG rUrCrA rGrArA rUrArA rUrAT T Sequence 2 rArArU rArUrU rCrUrG rArUrG rArCrA rGrUrA rArUrU rCrArC

Table 5.1 Sequences of siRNAs chosen from the Custom Dicer-Substrate siRNA tool[21] at Integrated DNA Technologies.

To select the siRNAs the Custom Dicer-Substrate siRNA tool at IDT (Integrated DNA Technologies) was used. The coding DNA sequence for Smp_011660 was pasted into the FASTA sequence box, and setting the input format to sequence, and selecting 'Other (Manual BLAST) under BLAST species. Searching using these parameters gave several potential siRNAs. To ensure coverage across the whole sequence, three siRNAs that spanned

[21] https://www.idtdna.com/site/order/designtool/index/DSIRNA_CUSTOM

the protein were chosen, these were CD.Ri.52244.13.18, CD.Ri.52244.13.2, CD.Ri.52244.13.18 (See Table 5.1).

5.2.2 Primary Antibodies

The main antibody used was anti-phospho-CaMKII (Thr286; Cell Signalling Technology #12716 (CST)) rabbit monoclonal antibody. The anti-phospho-CaMKII antibody was created by immunizing animals with a synthetic phosphopeptide corresponding to residues surrounding Thr287 of human CaMKII-β protein, which also have a high similarity in sequence to that of SmCaMKII (Figure 5.4). A rabbit monoclonal 'total' CaMKII antibody (CST; #4436) that detects the protein irrespective of its phosphorylation state was also used.

5.2.3 Lambda Phosphatase Assay

Duplicate samples of 24 h somules were processed for SDS-PAGE and Western blotting (Section 2.2.2). Once the proteins had been transferred to the nitrocellulose membrane, the membrane was washed and blocked for 1 h at room temperature with constant agitation using TTBS containing 1% BSA and 0.1% Triton X-100. After blocking, the two lanes were separated by cutting the membrane, and the control sample was placed in blocking buffer containing 2 mM $MnCl_2$, whilst the sample to be dephosphorylated was placed in an identical solution but also containing 400 U/ml of λ-phosphatase (Sigma-Aldrich). The blots were incubated overnight at 4ºC on a rocker. Following this the membranes were washed in PBS with 0.1% Tween 20 for 3-5 min, before being washed in 4-5 changes of distilled water. The blots were then incubated in primary and secondary antibodies and visualised as detailed in

the Western blotting protocol (Section 2.2.2). To demonstrate that similar amounts of protein had been loaded into each lane of the gel, each membrane was stripped using Restore Western blot stripping buffer (Thermo Scientific) before washing blots in TTBS and incubating blots with HRP-conjugated anti-actin antibodies (1:3000 dilution in TTBS, Santa Cruz Biotechnology #SC-47778HRP).

5.2.4 KN93 Inhibition Assays

Inhibition assays with live somules were either done as dose-response using different concentrations of KN93 (Calbiochem #422711), or time response assays using 10 μM KN93 for increasing durations. KN93 was water soluble and was initially prepared as a 5 mM stock solution for dilution into assays. Groups of approximately 1,000 (24 h) somules cultured *in vitro* overnight in 1 ml BME at 37ºC/5% CO_2 in individual wells of a 48-well culture plate (Thermo Scientific) were exposed to either 1, 10, 25 or 50 μM KN93 for 2 h, or to 10 μM KN93 for 30, 60, 90 and 120 min with water (vehicle; no treatment) controls also included;. all KN93 incubations were performed at 37ºC/5% CO_2. The samples were then heated to 95ºC on a hot block (Eppendorf Thermomixer) for 5 min and sonicated for 1 min before being processed for Western blotting (Section 2.2.2) with anti-phospho-CaMKII (Thr286) antibodies. Membranes were stripped using Restore Western blot stripping buffer before washing in TTBS and incubating with HRP-conjugated anti-actin antibodies (1:3000 dilution in TTBS). The immunoreactive signal analysed using GeneTools (Syngene) for phosphorylated CaMKII was then adjusted to normalized actin results to compensate for any differences in total protein loading between lanes.

KN93 inhibition assays were also performed with homogenates of 24 h *in vitro* cultured somules. To do this, approximately 5,000 somules were placed into microfuge tubes and centrifuged at 13,400 rpm for 5 min using a MiniSpin Centrifuge (Eppendorf). Then 400 µl of 1 x kinase buffer (CST), and 4 µl of HALT protease and phosphatase inhibitor cocktail (Thermo Fisher Scientific) were added. The sample was then homogenized on ice for 5 min using a glass homogeniser. The homogenate was equally divided between five tubes and 10 µM KN93 added for increasing durations. The samples were then heated to 95ºC on a hot block (Eppendorf Thermomixer) for 5 min and sonicated for 1 min before the samples were then prepared for Western blotting (Section 2.2.2) with anti-phospho-CaMKII Thr286 antibodies and anti-actin antibodies after stripping. Normalization and adjustment for actin was performed as detailed above.

5.2.5 Praziquantel Assays

PZQ (Sigma-Aldrich) was received in powder form, this was prepared into a stock solution by dissolving 0.2 mg PZQ in 1 ml of DMSO. Approximately 1,000 24 h *in vitro* cultured somules, or 1 male and 1 female adult worm in RPMI at 37ºC were prepared in individual wells of a 48 well issue culture plate. Parasites were then exposed to PZQ (final concentration 0.2 µg/ml) or DMSO (control, 0.01%) for 15, 30, 60 and 120 min before placing on ice. The samples were then heated to 95ºC on a hot block (Eppendorf Thermomixer) for 5 min and sonicated for 1 min before preparation for Western blotting (Section 2.2.2) with anti-phospho-CaMKII (Thr286) antibodies. Blots were stripped and probed with anti-actin antibodies and band intensities normalised as detailed above.

5.2.6 Immunohistochemistry

Whole parasites were fixed in 3.7% paraformaldehyde and stored at 4ºC until use. For processing, samples were washed in PBS before transferring to well of a 48-well tissue culture plate (if working with cercariae and somules) or screw-capped 1.5 ml microcentrifuge tubes (for adult worms). Samples were then blocked in 1% glycine solution for 10-15 min before being permeabilized for 1 h with 1% Triton-X100. Parasites were then washed in PBS twice for 15 min. Excess PBS was removed, before blocking the parasites with 10% normal goat serum (Thermo Fisher Scientific) for 2 h; after this the parasites were washed 3 times for 10 min each in PBS. The parasites were then incubated with anti-phospho-CaMKII (Thr286) antibodies at 1/50 in 1% BSA for 3 days at 4ºC on a platform rocker. Next the parasites were washed in PBS three times for 30 min each before adding the Alexafluor 488 secondary antibody (Thermo Fisher Scientific) at 1/500 and 1 µl of rhodamine phalloidin (5 µg/ml, Sigma-Aldrich). The parasites were then incubated at 4ºC on a rocker for a further 24 h, after which they were washed 3 times each for 30 min in PBS. The parasites were then placed onto silane prepared slides (Sigma-Aldrich, #S4651) if using cercariae and somules, or glass slides (Thermo Fisher Scientific) if using adult worms and fixed to the slide by warming on a hot plate at ~60ºC. Vectorshield (Vector Laboratories) antifade mounting medium was added to the samples before carefully placing a cover slip on top and fixing in place using clear nail varnish. Slides were also prepared with just the secondary antibody, and not the primary, as controls. Slides were stored in the dark at 4ºC. The parasites were visualised using a Leica TCS SP2 AOBS confocal laser scanning microscope using a 40 or 60 X oil immersion objective and images collected using associated Leica software. The levels of autofluorescence/background on the control slides were

determined, and the autofluorescence was reduced by reducing the power of the photomultiplier tube. The same settings were then used to visualise the test slides.

5.2.7 RNAi

All worm manipulations were performed in a laminar flow hood to ensure sterility. Worms received from the Sanger Institute were placed in the incubator at 37ºC/5% CO_2 for 1 h. They were then transferred with fine forceps to individual wells (3 worms per well) of a 48-well tissue culture plate each containing 1 ml pre-warmed Opti-MEM, 20 µl of antibiotic antimycotic solution and 40 µl foetal bovine serum (FBS). Worms were then placed in the incubator at 37ºC5% CO_2 overnight.

The following day, the worms were removed from the wells and placed into sterile electroporation cuvettes which had a gap size of 4 mm (VWR). The cuvettes had been filled with 100 µl pre-warmed Opti-MEM for the media control, 100 µl pre-warmed Opti-MEM plus 7.5 µl of scrambled siRNA for the scrambled control, and 100 µl pre-warmed Opti-MEM plus 2.5 µl of each of the three chosen siRNAs (Section 5.2.1). The siRNAs were made up to a concentration of 1 µg/µl. Each treatment was done in triplicate. Worms in each cuvette were electroporated using a Gene Pulser Xcell^{TM} (BioRad) set to 120 V for 20 ms. Following electroporation, the worms were placed in wells of a new 48-well tissue culture plate, with each well containing 1 ml pre-warmed Opti-MEM, 20 µl antibiotic/antimycotic solution and 40 µl FBS; plates with worms were then transferred to the incubator at 37ºC and 5% CO_2.

On each sampling day, worms for each treatment (control, scrambled control, and siRNA) were removed from the 48-well plate and pooled in a 1.5 ml microfuge tube placed on ice containing 15 µl RIPA buffer and HALT phosphatase and protease inhibitor cocktail; the worms were cut into small pieces using micro scissors and left on ice for approximately 10 min. The worms were then homogenised on ice using a motorized pestle mixer (VWR), and homogenates clarified using an Eppendorf MiniSpin centrifuge at 13,400 rpm for 1 min. The supernatant was transferred to a 1.5 ml microfuge tube, before an appropriate volume of Bolt LDS sample buffer 4X and Bolt sample reducing agent 10X was added to each sample. The samples were then heated to 95ºC on a hot block (Eppendorf Thermomixer) for 5 min and sonicated for 1 min before either electrophoresing immediately for Western blotting (Section 2.2.2) with anti-phospho-CaMKII (Thr286) antibodies or stored at -80ºC until use. Blots were stripped and re-probed for actin as detailed above (Section 2.2.2).

5.2.8 Worm Motility Analysis

Using a Motic SMZ-171 microscope with Moticam 1080 Digital Camera system, movies of 30 s duration were captured in triplicate of adult male and adult females which had been treated with either the scrambled control or the pooled CaMKII siRNAs. Each movie was viewed and worm motility analysed and assigned a score according to the WHO-TDR scoring system: 4 = normally active; 3 = slowed activity; 2 = minimal activity, occasional movement of head and tail; 1 = absence of motility apart from gut movements; 0 = total absence of mobility (Ramirez et al., 2007).

5.2.9 Statistics

To determine if mean values were statistically significant for the KN93 inhibition assays, a one-way ANOVA with a Tukey post-hoc test was employed using SPSS (IBM). A standard paired two tailed t-test was performed using Excel 2010 to analyse of the effect of siRNA on adult worm movement.

5.2.10 Bioinformatics

FASTA protein sequences were obtained from Uniprot for each of the four human isoforms of CaMKII α, β, γ and δ (CaMKIIα accession number = Q9UQM7, CaMKIIβ accession number = Q13554, CaMKIIγ accession number = Q13555 and CaMKIIδ accession number = Q13557). A basic local alignment search tool (BLAST) was performed using the protein-protein BLAST tool from NCBI (https://blast.ncbi.nlm.nih.gov/Blast.cgi?PAGE=Proteins) and entering in each human CaMKII isoform FASTA sequence and performing a alignment search against the organism Schistosoma (taxid:6181).

5.3 Results

5.3.1 Bioinformatics

During investigation of the phosphoproteome of adult *S. mansoni*, CaMKII was highlighted as a potentially important upstream kinase that was involved in the phosphorylation of several overrepresented motifs (Section 3.2.5). An investigation into CAMKII signalling was therefore deemed valuable particularly given that CaMKII has not been studied in detail in this species. Initially, the FASTA protein sequence for each of the four human isoforms of CaMKII (α, β, γ and δ) were obtained (Gaertner et al., 2004), and a BLASTp performed against *Schistosoma* (Taxid:6181) using NCBI to determine the protein(s) with closest identity to human CaMKII's. Comparing to human CaMKII-α, an *S. mansoni* 'protein kinase' with 68% identity (accession number CCD81917.1) was found. One other 'hit' with a greater identity score (70%), was found, however, this was from *S. haematobium* rather than *S. mansoni*. The best BLASTp 'hits' against human CaMKII-δ and human CaMKII-γ were for the same protein kinase (accession number CCD81917.1), with identities of 72% and 63%, respectively. Human CaMKII-β however had the highest identity (77%) with protein kinase CCD81917.1, indicating that the human β isoform is most similar to the CaMKII of *S. mansoni*. When the protein sequence for CCD81917.1 was BLASTed against *S. mansoni* on GeneDB[22] there was 100% identity with protein kinase 'Smp_011660.2'. Currently (23/04/19) when searching for the terms 'CaMKII' or 'Calcium/Calmodulin dependent protein kinase II' within the *S. mansoni* genome there is no match, indicating that

[22] http://www.genedb.org/blast/submitblast/GeneDB_Smansoni

CaMKII is not yet annotated fully. Within the *S. mansoni* kinome, 32 of the protein kinases were identified as members of the CaMK group, 18 of which belong to the CaMKL family (Calcium/Calmodulin Regulated Kinase) (Andrade et al., 2011).

A

```
SmCaMKII      1    MATVLP--KFSDLYSLKEEVGRGAFSIVRKCIQLSTGLEFAAKIINTKRLSTRDMQKLER  58
                   MAT +   +F+D Y L E++G+GAFS+VR+C++L TG E+AAKIINTK+LS RD QKLER
Human CaMKII  1    MATTVTCTRFTDEYQLYEDIGKGAFSVVRRCVKLCTGHEYAAKIINTKKLSARDHQKLER  60
SmCaMKII      59   EARICRLLKHPNIVRLYDDIQDEGFHYLVFDLVTGGELFEDIVAREFYSEADASNCMQQI  118
                   EARICRLLKH NIVRL+D I +EGFHYLVFDLVTGGELFEDIVARE+YSEADAS+C+QQI
Human CaMKII  61   EARICRLLKHSNIVRLHDSISEEGFHYLVFDLVTGGELFEDIVAREYYSEADASHCIQQI  120
SmCaMKII      119  IESVNYCHQNNIVHRDLKPENLLLASKSKGAAVKLADFGLAIEVQGDQPAWFGFAGTPGY  178
                   +E+V +CHQ  +VHRDLKPENLLLASK KGAAVKLADFGLAIEVQGDQ AWFGFAGTPGY
Human CaMKII  121  LEAVLHCHQMGVVHRDLKPENLLLASKCKGAAVKLADFGLAIEVQGDQQAWFGFAGTPGY  180
SmCaMKII      179  LSPEVLRKEPYGKAVDVWACGVILYILLVGYPPFWDEDQNRLYSQIKSGAYDYPSPEWDT  238
                   LSPEVLRKE YGK VD+WACGVILYILLVGYPPFWDEDQ++LY QIK+GAYD+PSPEWDT
Human CaMKII  181  LSPEVLRKEAYGKPVDIWACGVILYILLVGYPPFWDEDQHKLYQQIKAGAYDFPSPEWDT  240
SmCaMKII      239  VTPEAKNLINLMLTVSPARRITAAEALKHPWICQRERVASLVHRQETVECLKKFNARRKL  298
                   VTPEAKNLIN MLT++PA+RITA EALKHPW+CQR  VAS++HRQETVECLKKFNARRKL
Human CaMKII  241  VTPEAKNLINQMLTINPAKRITAHEALKHPWVCQRSTVASMMHRQETVECLKKFNARRKL  300
SmCaMKII      299  KGAILTTMLATRNFSTGR-GTVPGSHTSVTKKSNDGIKESSDS 340
                   KGAILTTMLATRNFS GR  T P + ++    +  G+ E + S
Human CaMKII  301  KGAILTTMLATRNFSVGRQTTAPATMSTAASGTTMGLVEQAKS 343
```

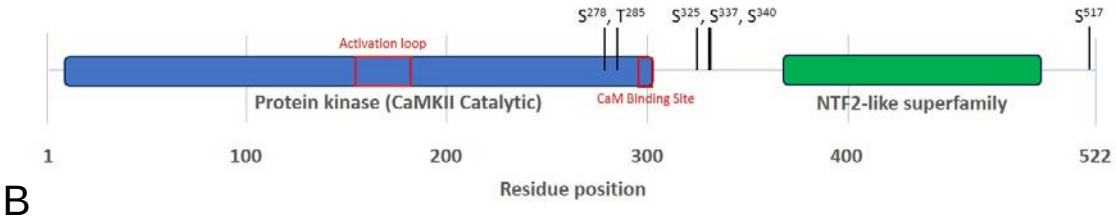

B

Figure 5.4. Bioinformatic analysis of *S. mansoni* CaMKII. (A) Pairwise alignment of the putative *S. mansoni* CaMKII (SmCaMKII) Smp_011660.2, and human CaMKII-β. Alignment revealed 77% homology with human CaMKII-β. The anti-phospho-CaMKII (Thr286) antibody recognition site is highlighted in blue and the respective *S. mansoni* sequence is highlighted red. The conserved Thr residue is in green. (B) Schematic of Smp_011660 depicting the integral domains, binding sites, and phosphorylation sites identified in the phosphoproteomics screen. Note the NTF2 superfamily includes the calcium/calmodulin dependent kinase II association domain.

5.3.2 Antibody Validation

To study CaMKII signalling in *S. mansoni* an antibody was required for use in investigations involving Western blotting and immunohistochemistry, and one that targets the kinase specifically when phosphorylated (activated) would be useful. Using Phosphosite[23] a phospho-specific antibody, phospho-CaMKII (Thr286), was identified and purchased for testing. Typically, such antibodies are designed to recognize only the phosphorylated residue and the amino acid sequence (+7/-7) immediately around the phosphosite. The homology in this region and conservation of the critical Thr residue (Thr285, Thr286 in human CaMKII; Figure 5.4A) between the two proteins suggested that this antibody might be valuable for profiling the phosphorylation (activation) state of *S. mansoni* CaMKII.

To ensure that the antibody targeted the *S. mansoni* kinase only its phosphorylated form, a lambda phosphatase assay was performed to dephosphorylate the protein. Protein extracts from 24 h somules were electrophoresed and transferred to nitrocellulose membrane. One lane was then treated with lambda phosphatase, and the other (control) lane was not. When both lanes were incubated with the phospho-CaMKII and secondary antibodies, the antibody reacted strongly only with the phosphorylated sample and only very weakly with the dephosphorylated sample (Figure 5.5). The specificity of the antibody was high, with one strong immunoreactive band revealed and a very weak band visible in the dephosphorylated lane.

[23] http://www.phosphosite.org

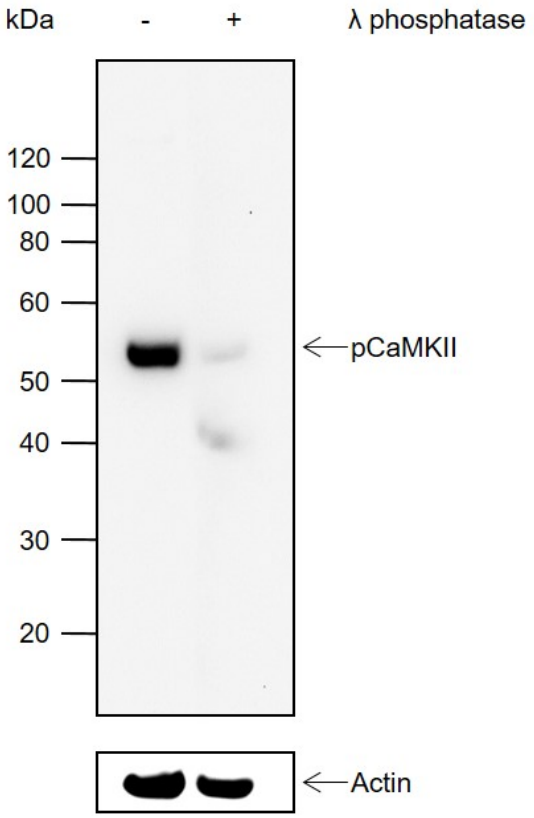

Figure 5.5. Detection of phosphorylated CaMKII in *S. mansoni*. Western blot analysis demonstrating presence or absence of phosphorylated (activated) CaMKII in 24 h somule (~1000 somules per lane) protein extracts treated with (+) or without (-) lambda phosphatase. Please note the second lower mark in + λ phosphatase lane is likely to be a contaminant rather than a second band. The Western blot was processed and probed with anti-phospho-CaMKII (Thr286) antibodies as described in Section 2.2.2; anti-actin antibodies were used to demonstrate the presence of protein in both lanes.

5.3.3 Detection of phosphorylated CaMKII in *S. mansoni* Life Stages

To identify whether CaMKII was expressed and activated in various life stages of *S. mansoni*, cercariae, 24 h somules, and adult worm protein extracts were prepared for Western blotting with anti-phospho-CaMKII antibodies. Western blotting revealed a single strong immunoreactive band in cercariae and somules, with an apparent molecular weight of ~57 kDa (Figure 5.6A). A single immunoreactive band was also observed in the adult

worms (Figure 5.6B). The female worms are smaller than males, reflecting the reduced immunoreactivity in this sex. Currently (26/06/2019) Smp_011660 is annotated as having three variants, Smp_011660.1-3 with MWs of 57, 45, and 58 kDa, respectively, close to the MW of the detected band. In contrast, TDR targets lists the respective MWs at ~59, ~58 and ~54 kDa.

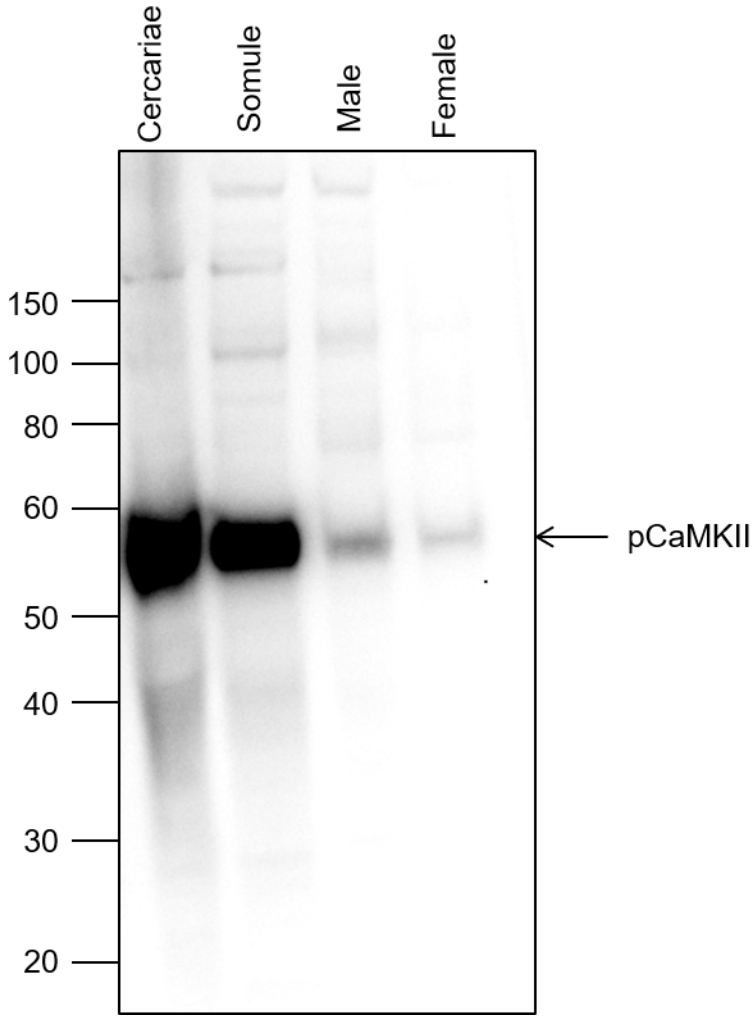

Figure 5.6. Detection of phosphorylated CaMKII in ***S.*** *mansoni* life stages. Western blot analysis demonstrating phosphorylated (activated) CaMKII in cercariae and 24 h somules (~1000 per lane) adult male and female worms (1 worm per lane). Protein extracts were prepared for Western blotting and probed with anti-phospho-CaMKII primary antibodies as described in Section 2.2.2.

5.3.4 Detection of Total CaMKII

For assays such as those involving protein knockdown using RNAi it was necessary to source an antibody that detects the total amount of CaMKII present, including phosphorylated and non-phosphorylated forms. An antibody available from CST, produced by immunizing rabbits with a synthetic peptide surrounding VAL184 of human CaMKIIα, was tested because *S. mansoni* CaMKII (Smp_011660) displayed high conservation with human CaMKIIα in this region. Western blotting with this antibody revealed a single immunoreactive band with an apparent MW of ~57 kDa in cercariae and 24 h somules as well as in adult male and female worms (Figure 5.7). Good immunoreactivity was seen across all life stages with greater immunoreactivity in the cercariae and somules than the adult worms; however, without knowledge of the protein amounts in each sample relative expression levels cannot be compared. Expression data available on Meta Schisto (Figure 5.8), shows that Smp_011660 (CaMKII in *S. mansoni*) is expressed at all life stages (with exception of the egg) and is greater in the cercariae and somules when compared with the adult worms.

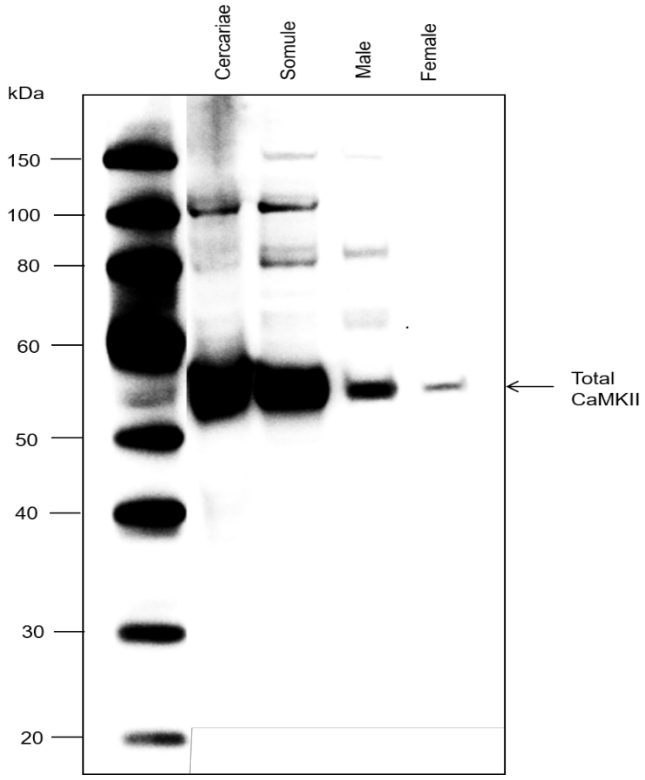

Figure 5.7. Detection of total CaMKII in *S. mansoni* life stages. Western blot demonstrating presence of CaMKII in different life stages of *S. mansoni* (~1000 freshly hatched cercariae, ~1000 24 h *in vitro* cultured somules, 1 adult male and 1 adult female worm). Samples were prepared for Western blotting and probed with total CaMKII primary antibodies as described in Section 2.2.2.

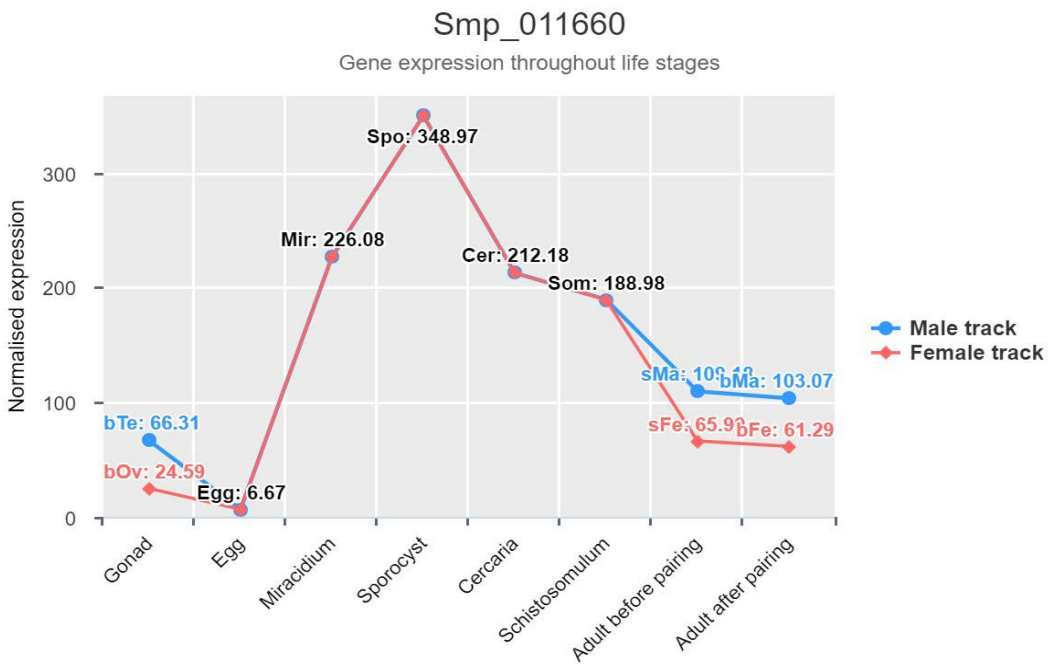

Figure 5.8. Gene expression of *S. mansoni* CaMKII. Graph adapted from Meta Schisto[24] (23/04/19), showing transcript expression levels across all life stages of *S. mansoni* for SMP_011660, CaMKII in *S. mansoni.*

5.3.5 Inhibition of *S. mansoni* CaMKII

As the CaMKII inhibitor KN93 has been used widely in other research, its effects on CaMKII within live *S. mansoni* were evaluated. Recently, KN93 has been discovered to bind to Ca^{2+}/CaM, rather than to the actual CaMKII protein as was previously believed. When KN93 binds to Ca^{2+}/CaM, this stops Ca^{2+}/CaM binding to CaMKII, causing inhibition of CaMKII activation (Wong et al., 2019). To determine if KN93 could inhibit *S. mansoni* CaMKII activation, a dose response assay using 24 h *in vitro* cultured somules was performed. Live somules were exposed to 1, 10, 25 or 50 µM KN93 for 2 h and proteins extracted for Western

[24] https://meta.schisto.xyz/smansoni/smp_011660/

blotting. Each of the four concentrations of KN93 significantly inhibited CaMKII phosphorylation (activation) in the parasite (1 µM at P≤0.05: 10, 25 and 50 µM at P≤0.001; Figure 5.9), with the greatest reduction of immunoreactivity (65%) seen at 50 µM. Therefore, 10 µM was considered a viable concentration of KN93 to use in future experiments, as this dose resulted in good inhibition (62% reduction in phosphorylation) and was not excessively high.

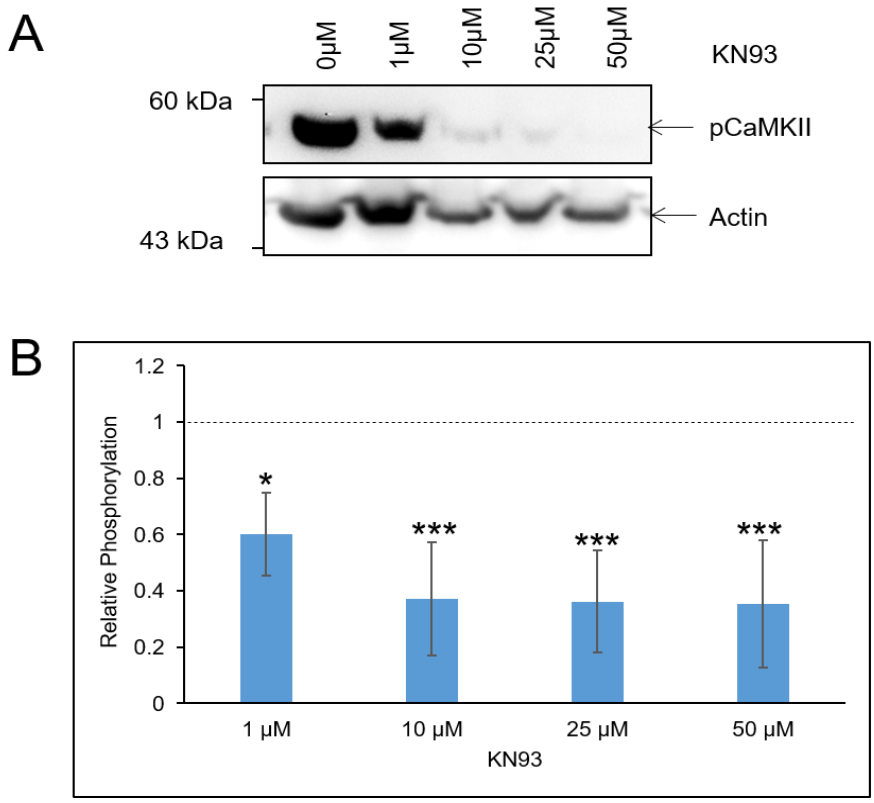

Figure 5.9. Pharmacological inhibition of phosphorylated *S. mansoni* CaMKII by KN93. (A) 24 h *in vitro* cultured somules (1,000 per lane) were treated with 0, 1, 10, 25 or 50 µM KN93 for 2 h and protein extracts processed for Western blotting. The Western blot was processed and probed with anti-phospho-CaMKII (Thr286) antibody as described in Section 2.2.2 and anti-actin antibodies were used to assess any differences in protein loading between samples. (B) Quantification of mean (n=4±SD) phosphorylated CaMKII levels after inhibition for 2 h with KN93, presented with reference to the controls not exposed to the inhibitor (1.00, shown as the dotted line) (*P≤0.05, ***P≤0.001).

Given that KN93 inhibited activation of CaMKII at varying doses in 24 h *in vitro* cultured somules, a time response assay was performed to determine how rapidly inhibition can take place. Somules were exposed to 10 µM KN93 for 30, 60, 90 and 120 min. Results of this assay showed that mean immunoreactivity significantly decreased over time (Figure 5.10), demonstrating that activation of CaMKII is attenuated in somules in a temporal fashion; the strongest effect was seen at 90 min when mean phosphorylation levels were reduced by 68% (P≤0.001).

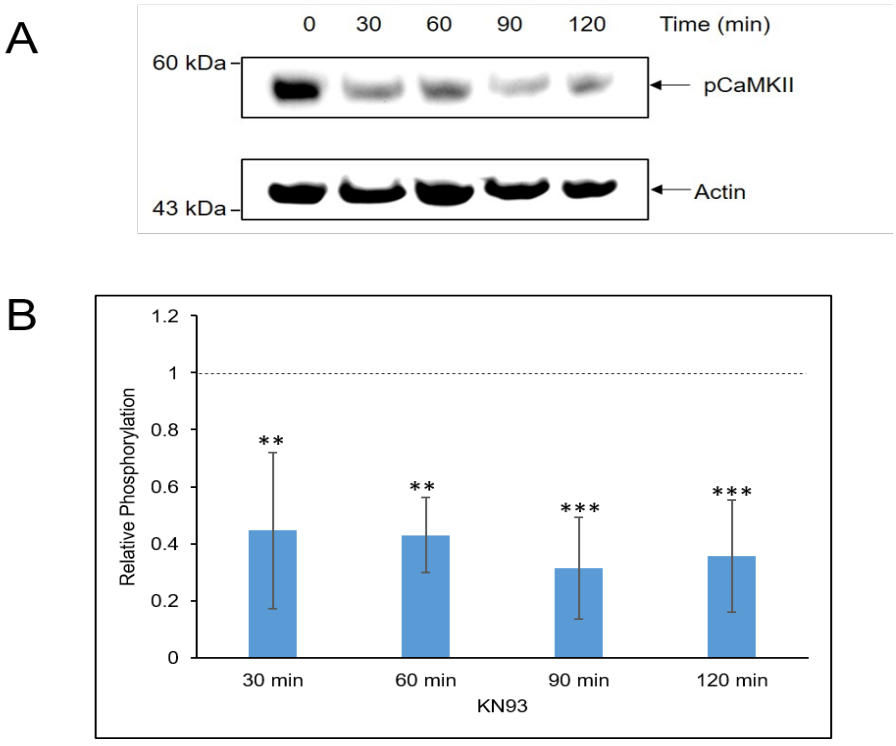

Figure 5.10. Temporal inhibition of *S. mansoni* CaMKII by KN93. (A) 24 h *in vitro* cultured somules (~1,000 per lane) were treated with 10 µM KN93 for 0, 10, 60, 90 and 120 min, and protein extracts processed for Western blotting. The Western blot was processed and probed with anti-phospho-CaMKII (Thr286) antibodies as described in Section 2.2.2 and anti-actin antibodies were used to assess any differences in protein loading between samples. (B) Quantification of mean (n=4±SD) phosphorylated CaMKII levels in whole somules after treatment with KN93 for increasing durations, presented with reference to the controls not exposed to the inhibitor (1.00, shown as the dotted line) (**P≤0.01, ***P≤0.001).

As KN93 appeared to inhibit phosphorylation (activation) of CaMKII after only 30 min, it was hypothesised that this inhibition could potentially occur quicker (or more robustly) if the parasites tissues were disrupted. Parasites were therefore homogenized in a kinase buffer and 10 µM KN93 was added to each of the samples, except the control, and left for either 30, 60, 90 or 120 min (Figure 5.11). Immunoreactivity significantly decreased over time, with the strongest effect seen at 120 min when mean phosphorylation levels were reduced by 85% (P≤0.001).

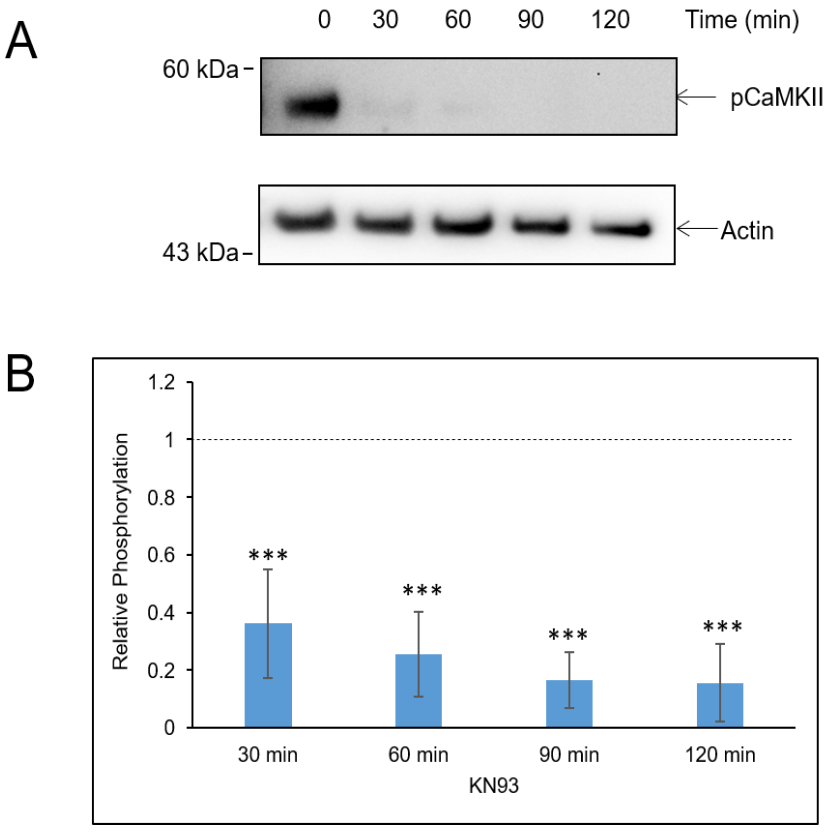

Figure 5.11. Pharmacological inhibition of phosphorylated CaMKII in *S. mansoni* homogenates. (A) 24 h *in vitro* cultured somules were treated with 10 µM KN93 for up to 2 h after homogenization and protein extracts processed for Western blotting. The Western blots were processed and probed with anti-phospho-CaMKII (Thr286) antibodies as described in Section 2.2.2 and anti-actin antibodies were used to assess any differences in protein loading between samples. (B) Quantification of mean (n=4±SD) phosphorylated CaMKII levels after inhibition with KN93, presented with reference to the controls not exposed to the inhibitor (1.00, shown as the dotted line) (***P≤0.001).

5.3.6 Stimulation of CaMKII in Somules with PMA

An attempt was made to stimulate basal CaMKII phosphorylation levels in intact somules. A literature search revealed phorbol 12-myristate 13-acetate (PMA) to be a potential stimulant as it has been shown to generate an increase cytoplasmic Ca^{2+} for short durations in rats (Luo et al., 2012). Assays were performed using 24 h live somules that were exposed to 1μM PMA for 5, 15, and 30 min before processing for Western blotting. However, after three biological replicates the findings were inconclusive, with treated samples showing an immunoreactivity similar to controls (data not shown). As CaMKII in somules seems to possess high basal levels of phosphorylation, it was decided to first inhibit somules with KN93 for 3h before exposing to then to PMA (1 μM) for 5, 15, and 30 min (Figure 5.12). This was repeated six times, however as with the previous assay, and with the exception of a single experiment whereby stimulation of CaMKII phosphorylation was seen as time progressed, the remaining five assays did not show a significant stimulation. It was concluded that PMA did not have a significant effect on CaMKII phosphorylation in live *S. mansoni* somules, at least under the conditions of this assay.

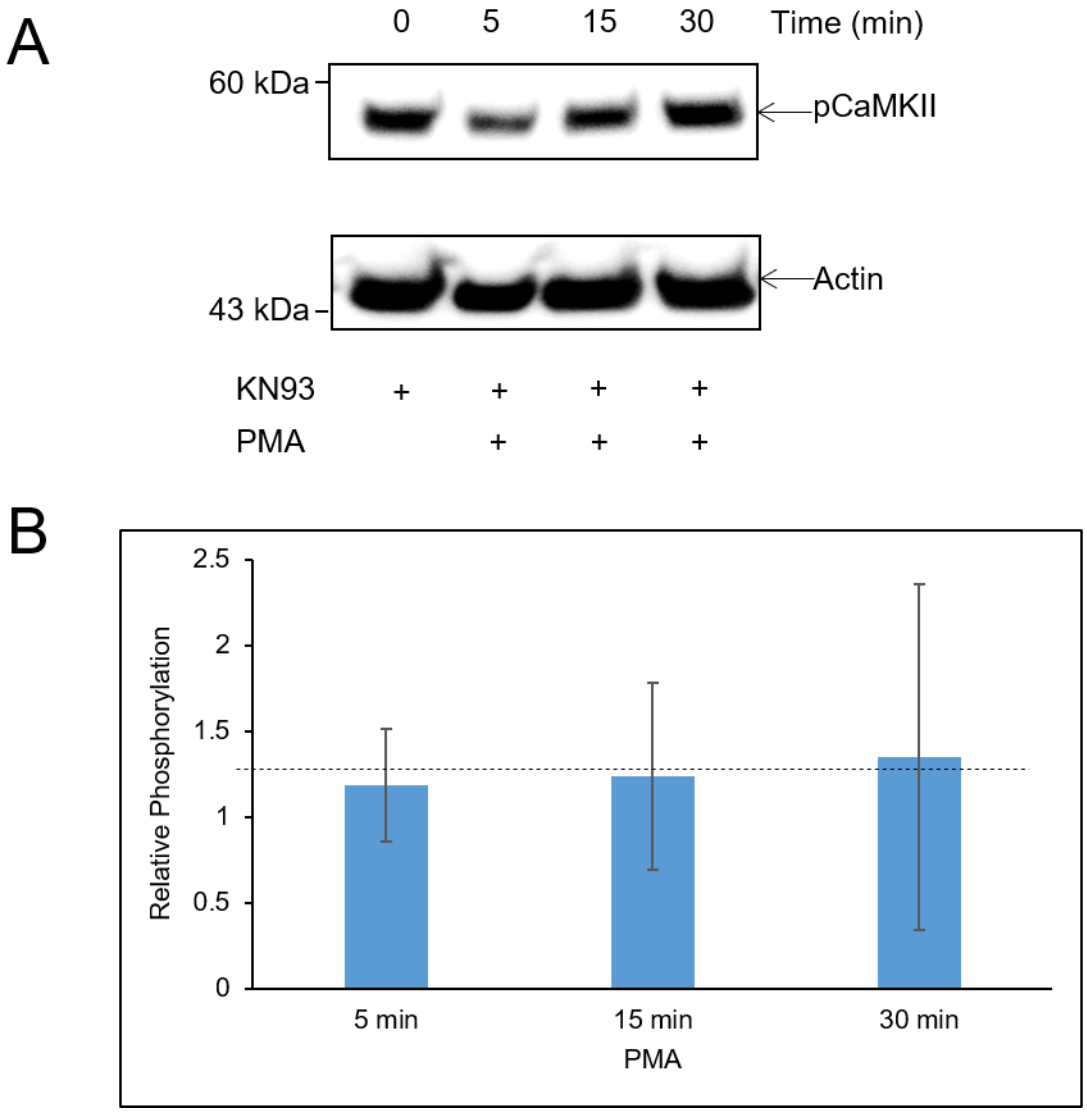

Figure 5.12. Effect of PMA on *S. mansoni* CaMKII phosphorylation. (A) 24 h *in vitro* cultured somules were treated with 10 µM KN93 for 3 h before exposure to 1 µM PMA for 5, 15, and 30 min before proteins were extracted for Western blotting. The Western blot was processed and probed with anti-phospho-CaMKII (Thr286) antibodies as described in Section 2.2.2 anti-actin antibodies were used to assess any differences in protein loading between samples. (B) Quantification of mean (n=6±SD) phosphorylated CaMKII levels in whole somules after treatment with PMA. Presented with reference to the KN93 control (1.00, shown as the dotted line).

5.3.7 Action of Praziquantel on Activated CaMKII in Somules and Adult Worms

PZQ is the main drug used to combat schistosomiasis (Gryseels, 2012). However, while PZQ's mode of action is not well understood, research shows that calcium ion channels play a role in PZQ generated worm death (Doenhoff et al., 2008; Greenberg, 2005; Jeziorski & Greenberg, 2006); Ca^{2+} fluxes in the worm also occur. The binding of calcium to calmodulin enables it to interact with kinases such as CaMKII (Evans & Shea, 2009), therefore the effect of PZQ on CaMKII phosphorylation (activation) within the intact parasite was investigated.

PZQ is regularly used at 0.2 μg/ml in assays involving live schistosomes and is the lowest concentration used that showed a reduction in worm motility (Meister et al., 2014; Xiao et al., 2012), therefore this concentration was chosen. It must be noted that at this concentration only motility has been identified to be affected and this is not indicative of worm death. Furthermore, these studies were performed on adult worms and is has been noted that PZQ could be less effective on 7- and 14-day-old juvenile schistosomes (You et al., 1986), however the 24h somules used in this study have been shown to be susceptible to minimal concentrations of PZQ (Xiao et. al. 1985) . Somules cultured for 24 h in BME were exposed to DMSO (vehicle control) or PZQ for 15 min, 30 min or 60 min and prepared for Western blotting with anti-phospho-CaMKII (Thr286) antibodies. Preliminary experiments showed high levels of immunoreactivity after 15 and 30 min exposure; however, phosphorylation at 60 min was often lower (data not shown). Variability was evident, however, so eight repeats were performed at these earlier time points. Overall, PZQ stimulated CaMKII phosphorylation significantly by 37% at 30 min (Figure 5.13). Although at 15 min mean phosphorylation was similar to that at 30 min, variability between samples was greater resulting in a lack of significant effect.

Next, assays were done on mixed male and female adult worms. The levels of phosphorylated (activated) CaMKII appeared to drop below basal after 15 min exposure before increasing at 60 min. Across multiple experiments, only 60 min exposure to PZQ induced a statistically significant ($P \leq 0.05$) effect with a mean increase in phosphorylation of 56% seen (Figure 5.14). Overall results show the varying levels of activated CaMKII across different time points and life stages in schistosomes, and there appears to be a general trend of activation of CaMKII with PZQ. However further research is needed to unravel why this occurring and what this could mean overall for signalling in the parasite when it comes into contact with PZQ.

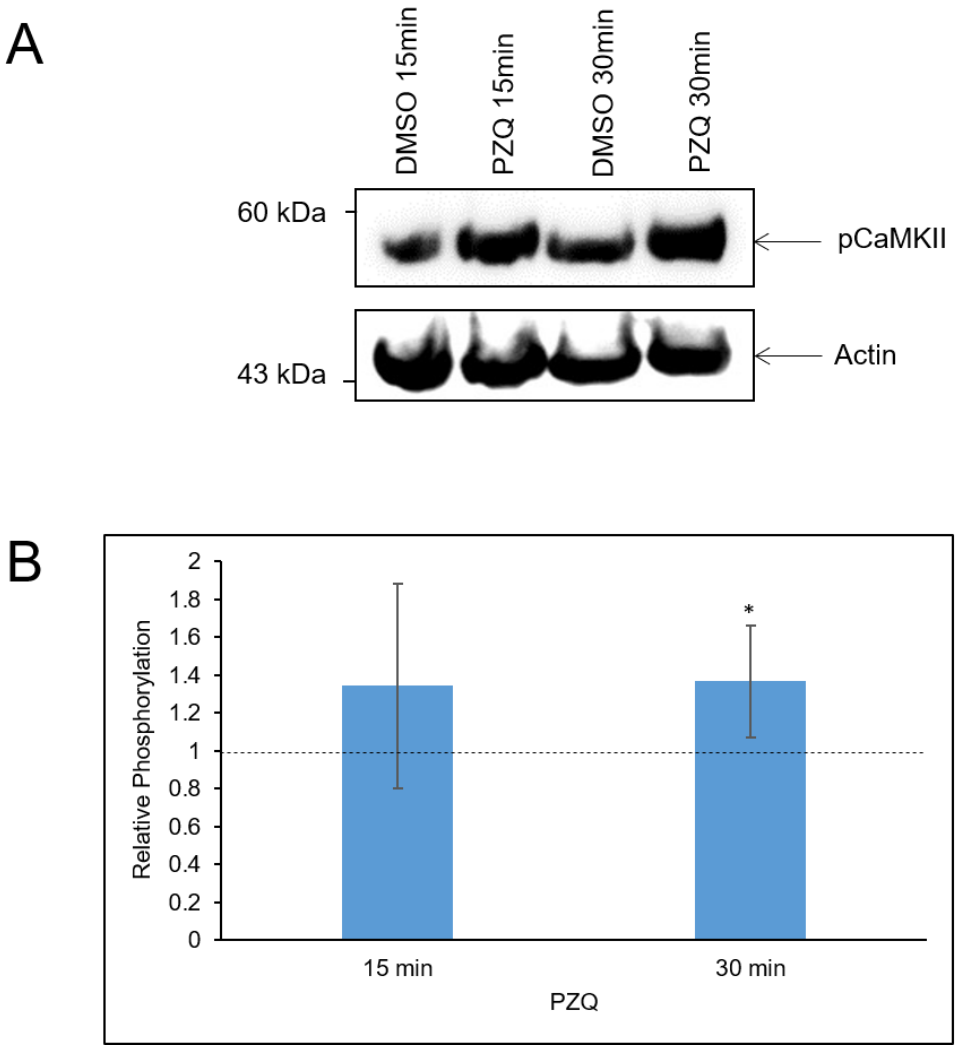

Figure 5.13. The effect of PZQ on CaMKII phosphorylation in 24 h *in vitro* cultured *S. mansoni* somules. (A) Parasites were exposed to PZQ (0.2 µg/ml) or DMSO (control) for 15 or 30 min. Proteins were extracted and processed for Western blotting with anti-phospho-CaMKII (Thr286) antibody as described in Section 2.2.2 and anti-actin antibodies were used to assess any differences in protein loading between lanes. (B) Quantification of mean (n=8±SD) phosphorylated CaMKII levels in somules after stimulation with PZQ, presented with reference to the DMSO control (value = 1.00, shown as the dotted line) (*P≤0.05).

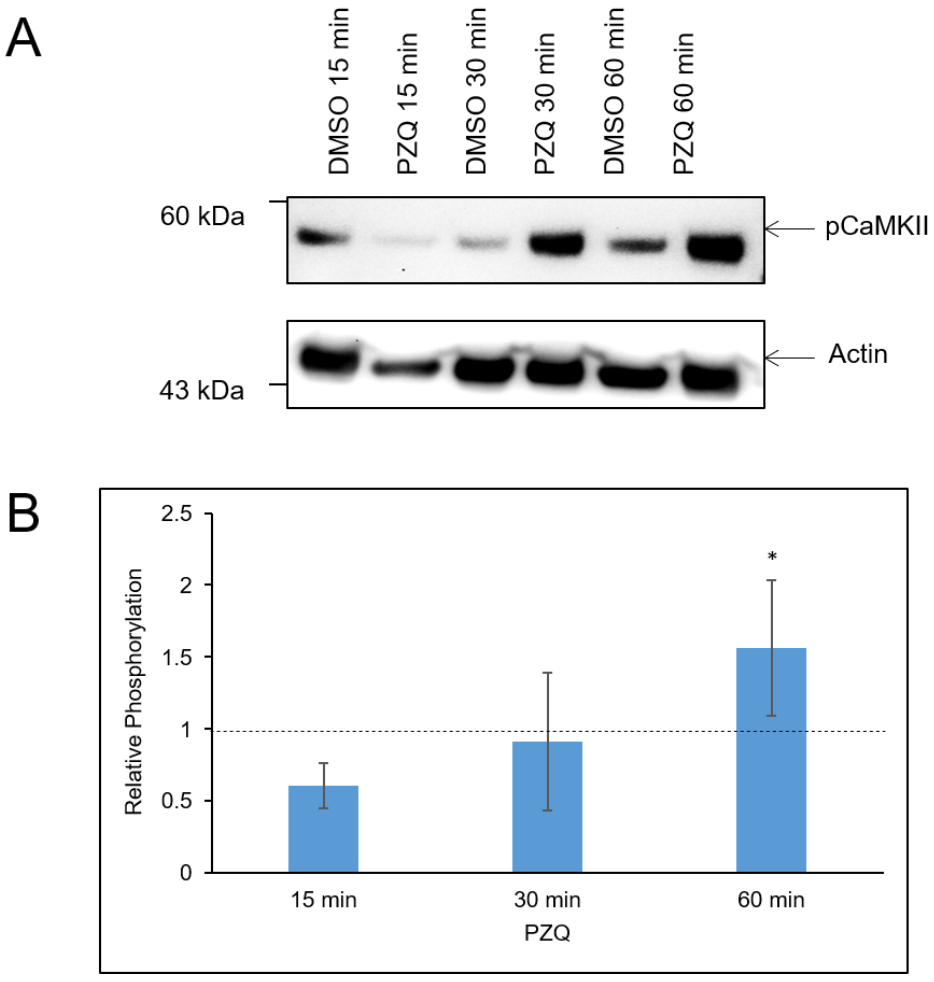

Figure 5.14. The effect of praziquantel (PZQ) on CaMKII phosphorylation in mixed adult *S. mansoni* (A) Parasites were exposed to PZQ (0.2 µg/ml) or DMSO (control) for 15, 30 or 60 min. Proteins were extracted and processed for Western blotting with anti-phospho-CaMKII (Thr286) antibody as described in Section 2.2.2 and anti-actin antibodies were used to assess any differences in protein loading between lanes. (B)

Quantification of mean (n=4±SD) phosphorylated CaMKII levels in adult worms after stimulation with PZQ, presented with reference to the DMSO control used at each time point indicating no stimulation of 1.00 shown as the dotted line (*P≤0.05).

5.3.8 Immunolocalization of Phosphorylated CaMKII in *S. mansoni*

Exploration of the CaMKII signalling pathway within *S. mansoni* was continued with confocal laser scanning microscopy using the smart anti-phospho-CaMKII (Thr286) antibodies to permit visualisation of the activated CaMKII pathway in the parasite. Activated CaMKII was visualised in definitive host-relevant life stages including cercariae, somules and male and female adult worms. In all cases the negative controls displayed negligible fluorescence (Figures 5.15, 5.19, and 5.23).

5.3.8.1 Cercariae

Incubation with anti-phospho-CaMKII (Thr286) primary and Alexa fluor 488 secondary antibodies showed that phosphorylated (activated) CaMKII could be localized successfully within cercariae. Activated CaMKII could be seen prominently and consistently at the tip of the head as a cluster of six regional dots (Figure 5.16A, B); these structures might be associated with the sensory system, leading to the possibility that activated CaMKII may be involved in the cercariae neurosensory processes, including those involved in host location. Small immunoreactive regions were also seen at regular points in pairs across the head of the cercariae; these may either represent sensory structures again, or possibly these are localized to flame cells associated with the osmoregulatory and excretory systems (Figure 5.17). Cercariae usually have 10 flame cells, an anterior dorsal pair, a mid-head ventral pair,

a posterior head dorsal and ventral pairs, and a pair at the anterior end of the tail (Collins et al., 2011). Also, in the head, activated CaMKII localized to the nervous system, in particular the cephalic ganglion (Figure 5.18), but also with nerve net of the ventral sucker (Figure 5.18). In comparison to the head, the tails of the cercariae displayed numerous punctate spots of activated CaMKII (Figure 5.16C/D), these could be seen across the surface, in the nervous system, and at the head tail junction. Here, activated CaMKII may be in the muscle cells of the tail as this enzyme is often associated with muscle (the tail is rich in muscle due to its role in movement) (Witczak et al., 2010), or they could associate with neuronal structures such as nerve endings.

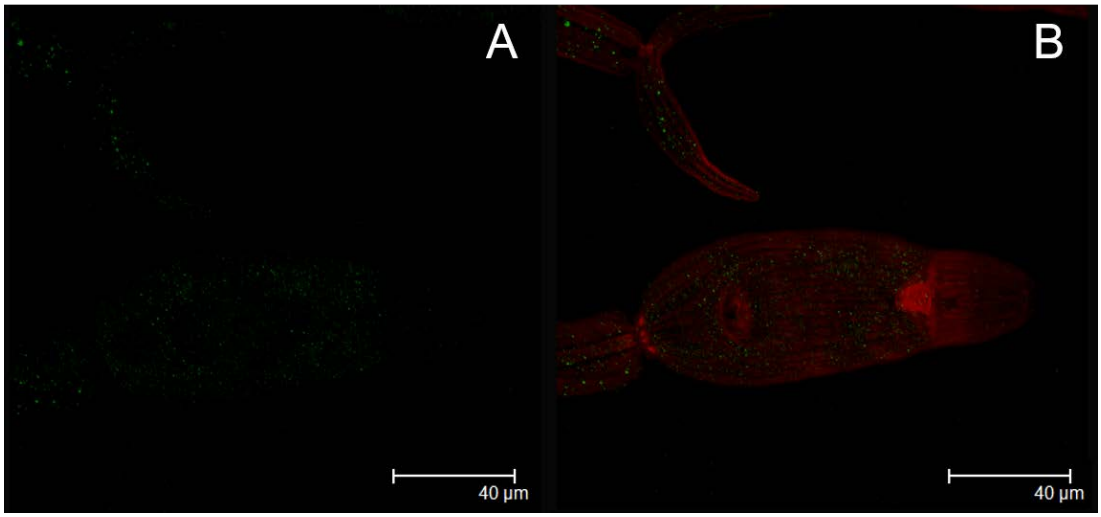

Figure 5.15. *S. mansoni* cercariae negative controls. Cercariae were fixed and stained as detailed in Section 5.2.6 (A) Cercariae stained with only Alexa Fluor 488 secondary antibody (green). (B) Overlay of the Alexa Fluor 488 and F-actin stained with rhodamine phalloidin. Images shown are maximum z-stack projections**.**

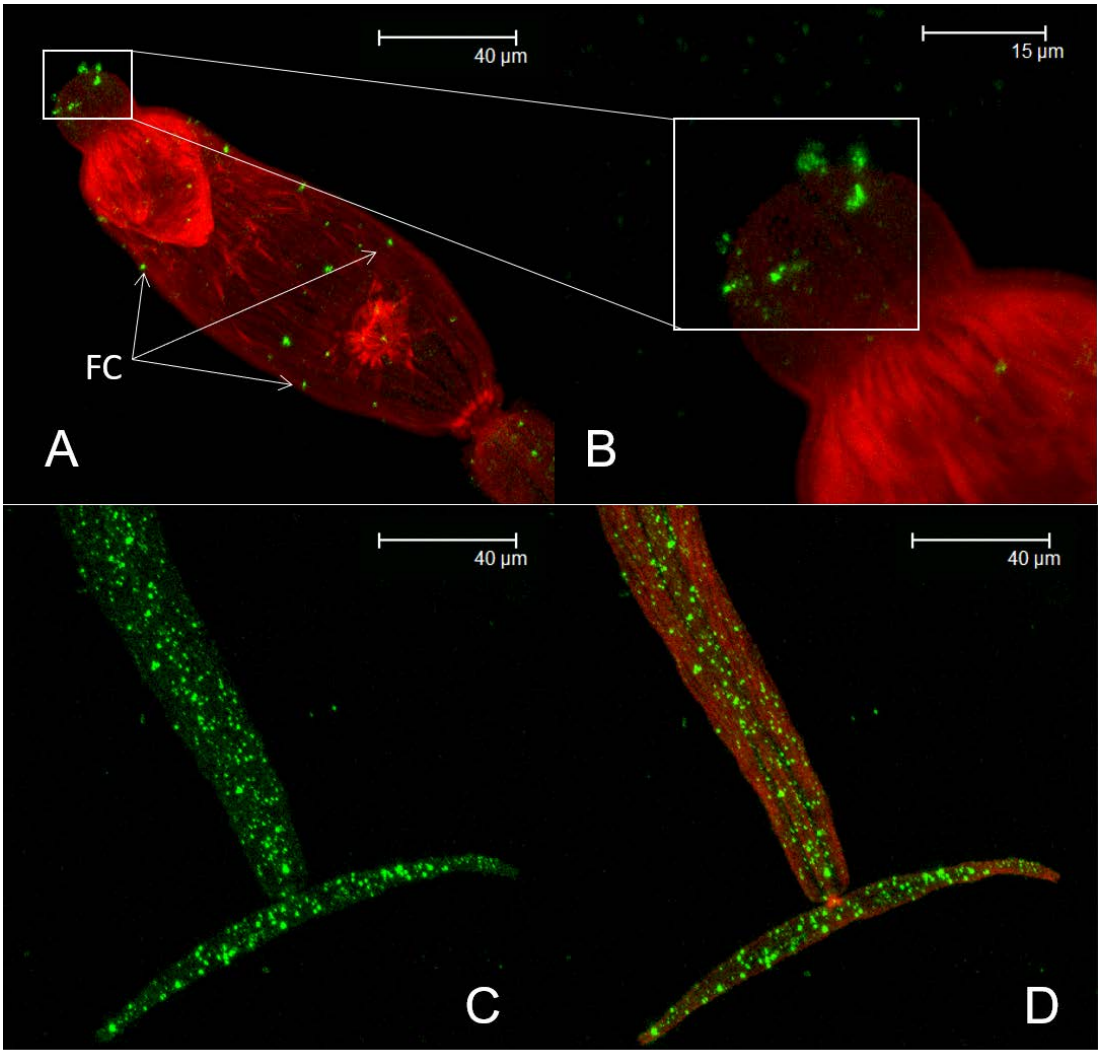

Figure 5.16. Distribution of activated CaMKII in *S. mansoni* cercariae revealed using anti-phospho-CaMKII (Thr286) antibodies (green), and F-actin with rhodamine phalloidin (red). (A) Maximum projection image of a cercaria head showing distribution of sensory structures and potential flame cells (FC). (B) Magnified region of tip of cercariae head (from A) with the white box highlighting the six evenly-distributed sensory-like structures at the tip. (C) Distribution of activated CaMKII across the cercaria tail, shown in (D) as an overlay with F-actin. All z-stacks are shown in maximum projection mode.

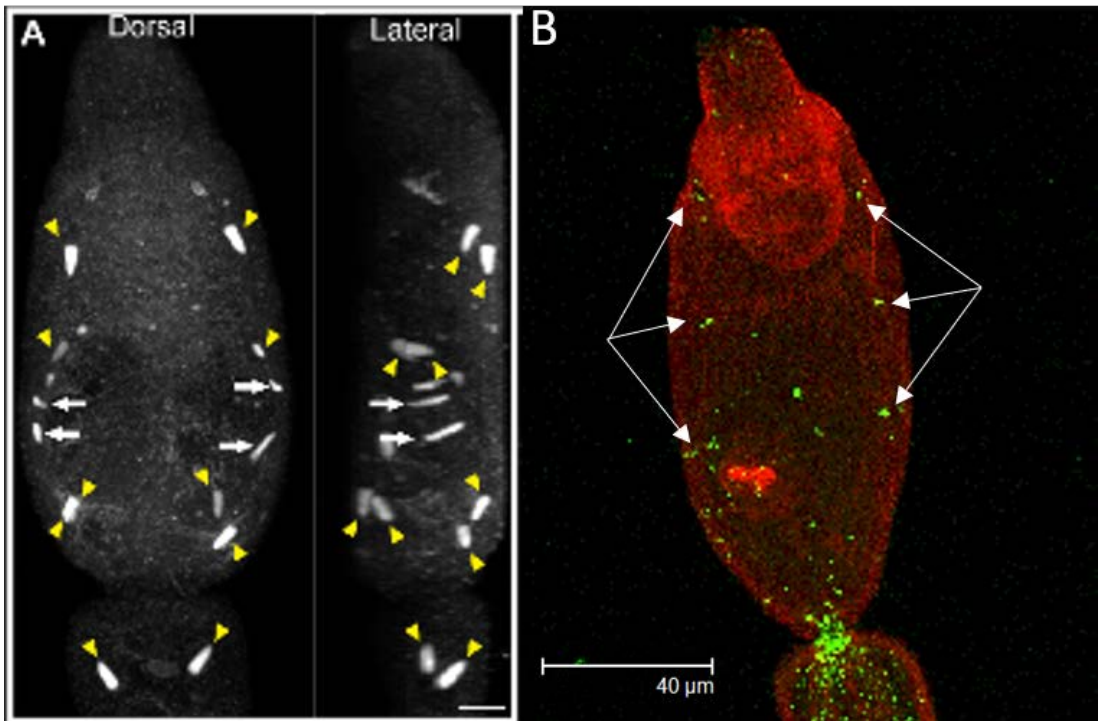

Figure 5.17. Distribution of activated CaMKII within the head of a cercaria. (A) Immunofluorescence with an anti-β-tubulin antibody to label the ciliated tufts of the flame cells (yellow arrowheads) and ciliated regions of the protonephridial tubules (white arrows) within the head and tail, adapted from Collins et al. (2011). (B) Maximum projection image of a cercaria head stained with anti-phospho-CaMKII (Thr286) antibodies (green), and F-actin with rhodamine phalloidin (red); the putative flame cells associated with activated CaMKII are highlighted by the white arrows. All z-stacks are shown in maximum projection mode.

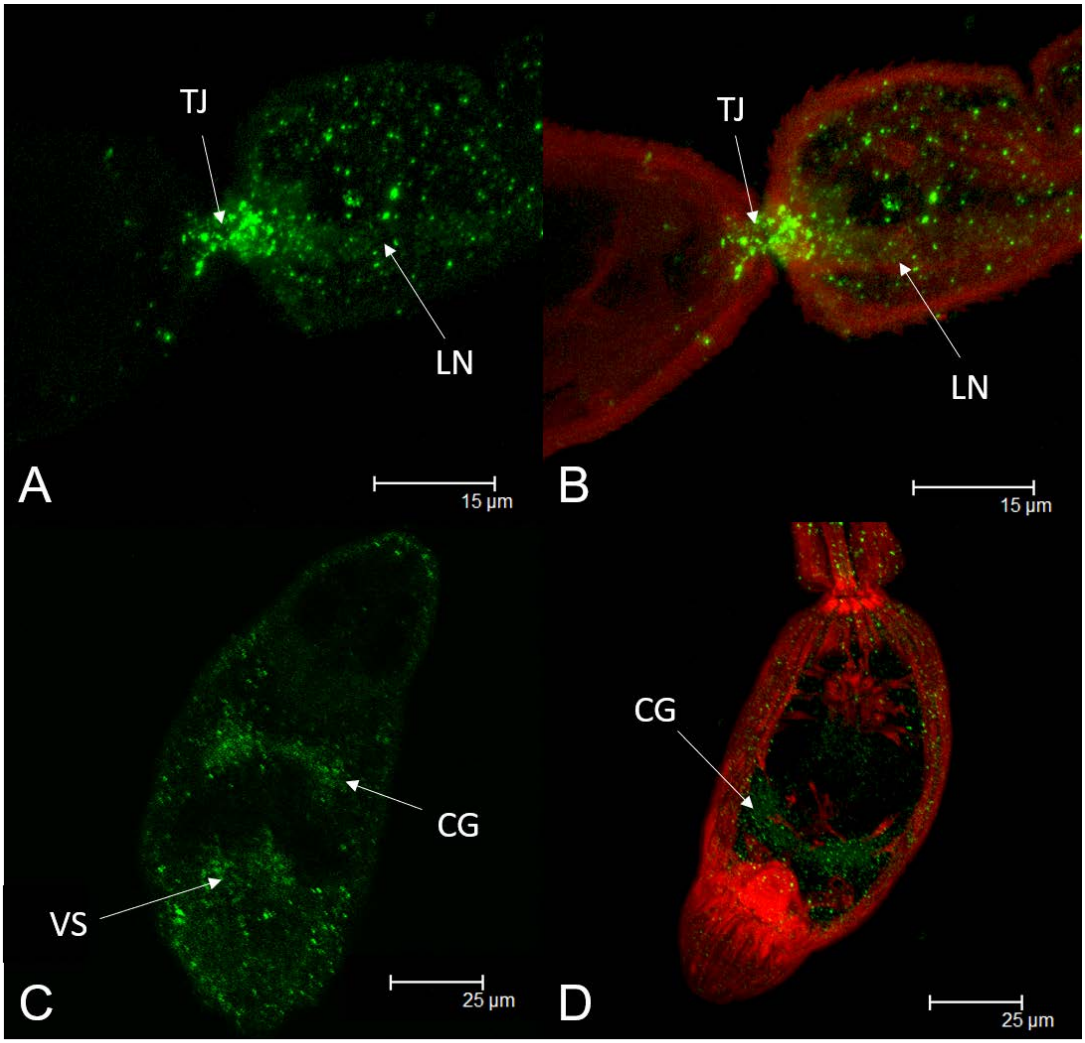

Figure 5.18. Distribution of activated CaMKII in the nervous system of cercariae revealed using anti-phospho-CaMKII (Thr286) antibodies (green), and F-actin with rhodamine phalloidin (red). (A) Maximum projection image of a deep serial scan through the cercaria head-tail junction (TJ) showing strong staining across the junction and the beginning of the longitudinal nerve (LN) of the tail. (B) Overlay of the activated CaMKII and F-actin. (C) Single z-section showing activated CaMKII in the head region, staining can be seen associated with the cephalic ganglion (CG) and the nerve net of the ventral sucker (VS). (D) Maximum projection of deep scan series with overlay of the activated CaMKII staining and the F-actin highlighting the cephalic ganglion. All z-stacks are shown in maximum projection mode.

5.3.8.2 Somules

Incubation of 24 h *in vitro* cultured somules with anti-phospho-CaMKII (Thr286) primary and Alexa fluor 488 secondary antibodies showed that phosphorylated (activated) CaMKII could be also localized successfully within 24 h somules. In particular CaMKII was phosphorylated in the nervous system which could be seen clearly, with the cephalic ganglion a prominent structure (Figure 5.20). The longitudinal nerves protruding from the cephalic ganglion were also discernible, becoming most clear when scrolling through the individual z-sections from a maximum projection of the somule head, where each of the six longitudinal nerves come into view across the images (Figure 5.21). Notably, the activated CaMKII in the nerves was so conspicuous that the nerve connections from the longitudinal nerves to the ventral sucker nerve net could be seen (Figure 5.20C). There appears to be less association of activated CaMKII in the putative sensory structures than seen in the cercariae, although the structures possibly resembling flame cells can be discerned (Figure 5.22). Overall, activated CaMKII appears to be highly linked to the nervous system during the somule larval stage of the parasite.

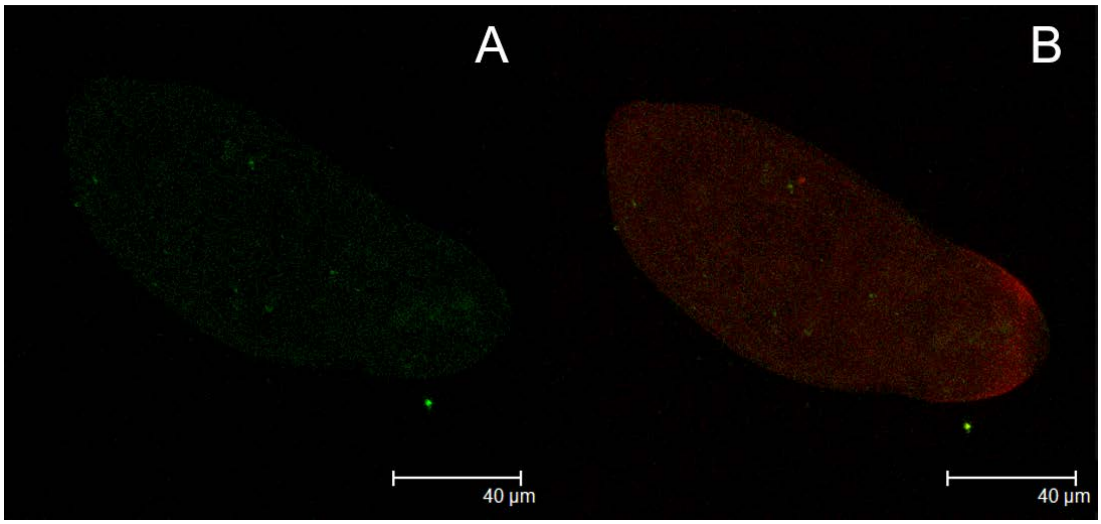

Figure 5.19. *S. mansoni* somule negative controls. Somules were fixed and stained as detailed in Section 5.2.6 (A) Somules stained with only Alexa Fluor 488 secondary antibody (green). (B) Overlay of the Alexa Fluor 488 and F-actin revealed using rhodamine phalloidin. Images shown are maximum z-stack projections**.**

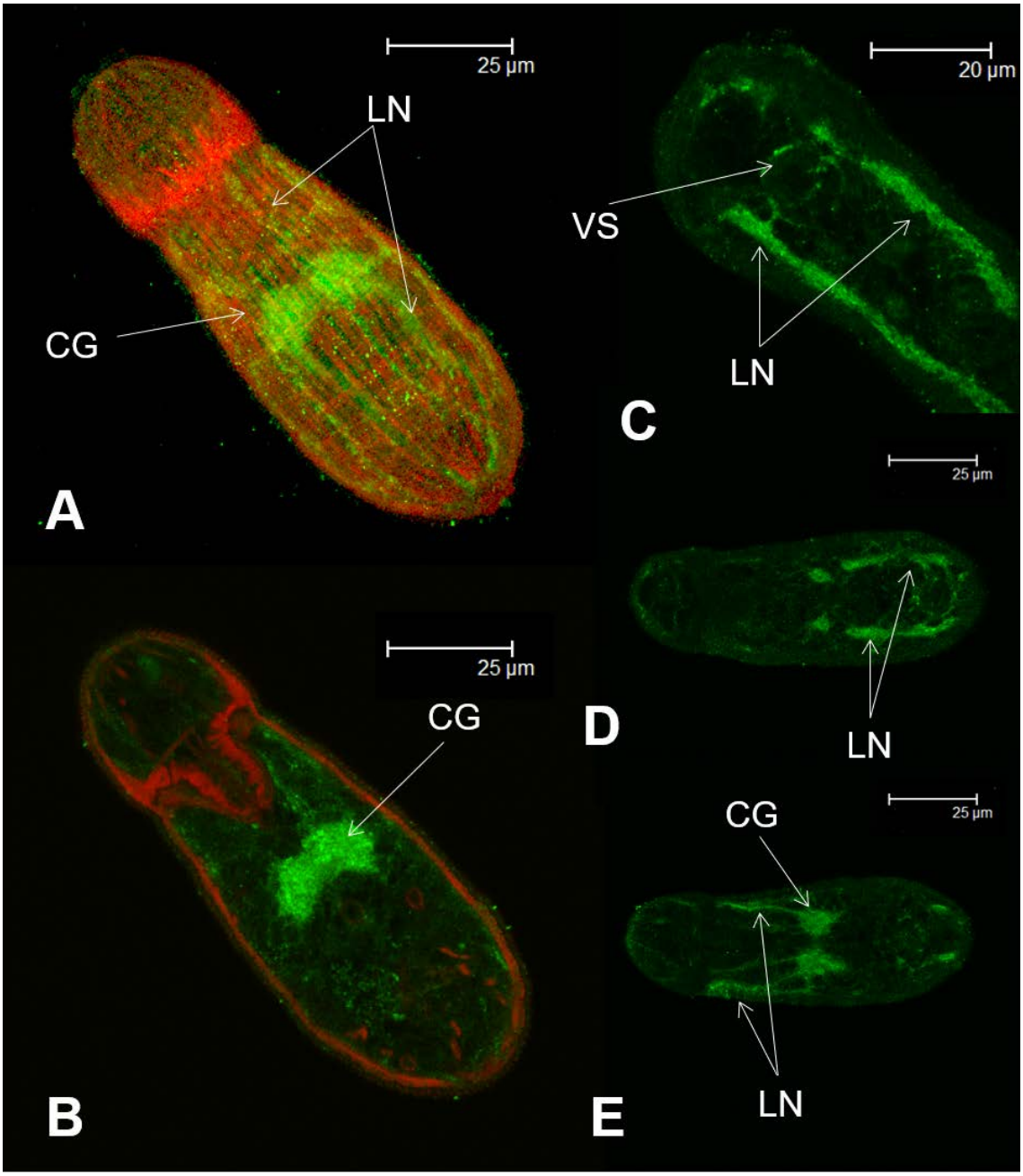

Figure 5.20. Distribution of activated CaMKII in the nervous system of 24 h *in vitro* cultured somules revealed using anti-phospho-CaMKII antibodies (green) and F-actin with rhodamine phalloidin (red). (A) Maximum projection image of a somule with strong staining at the cephalic ganglion (CG) and the longitudinal nerves (LN) in green, overlaid with the F actin. (B) Maximum projection of a deep scan within the somule highlighting the activated CaMKII in the cephalic ganglion (CG). (C) Single z-section showing activated CaMKII associated with the connections from the longitudinal nerves (LN) to the ventral sucker (VS) nerve net. (D) z-section of a somule, with the posterior end showing activated CaMKII in the longitudinal nerves and in addition (E) the cephalic ganglion. All z-stacks are shown in maximum projection mode.

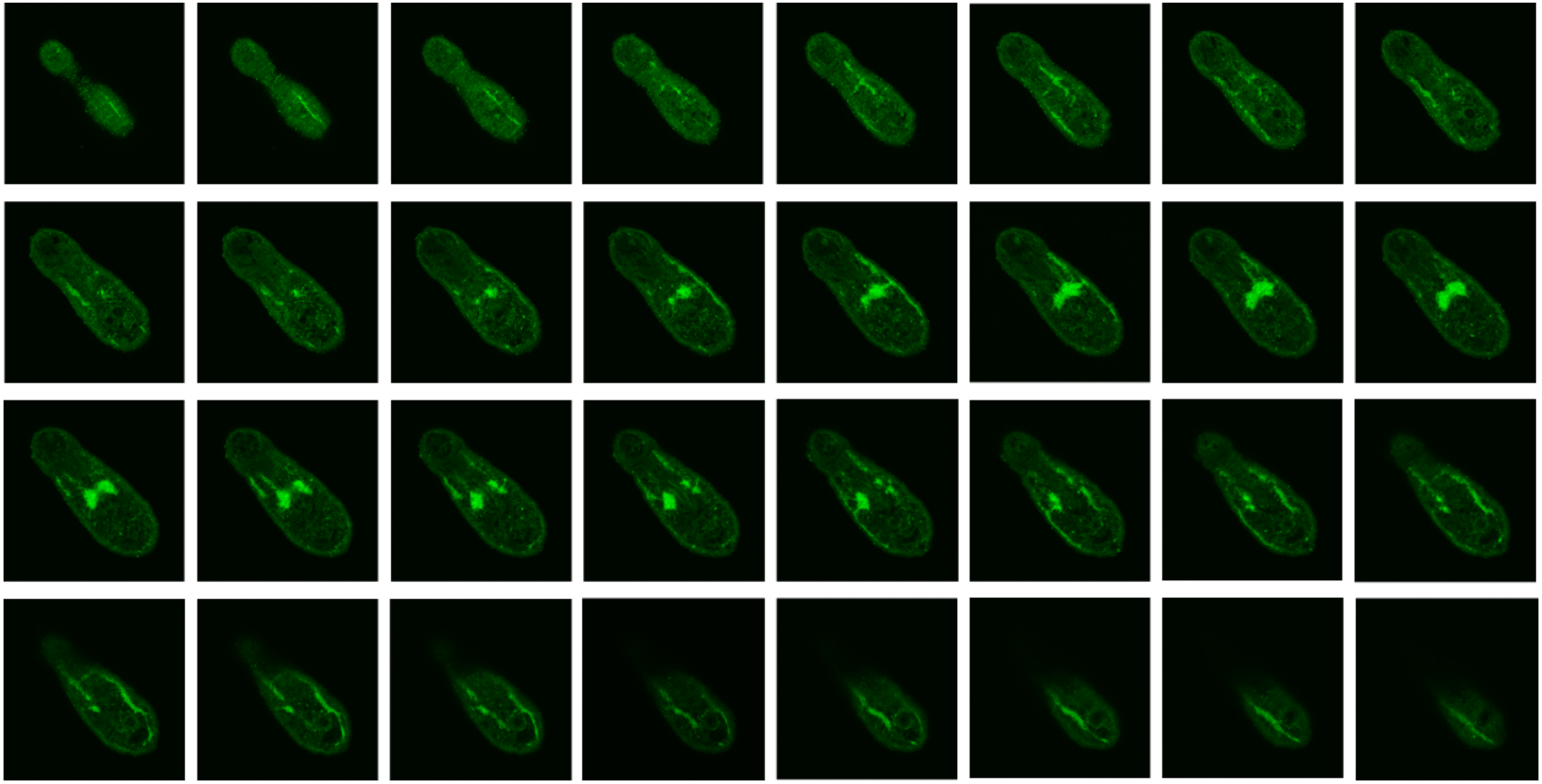

Figure 5.21. Serial optical z-sections through an *S. mansoni* somule highlighting activated CaMKII. The association of activated CaMKII in the nervous system of a 24 h *in vitro* cultured somule is illustrated using anti-phospho-CaMKII (Thr286) antibodies (green).

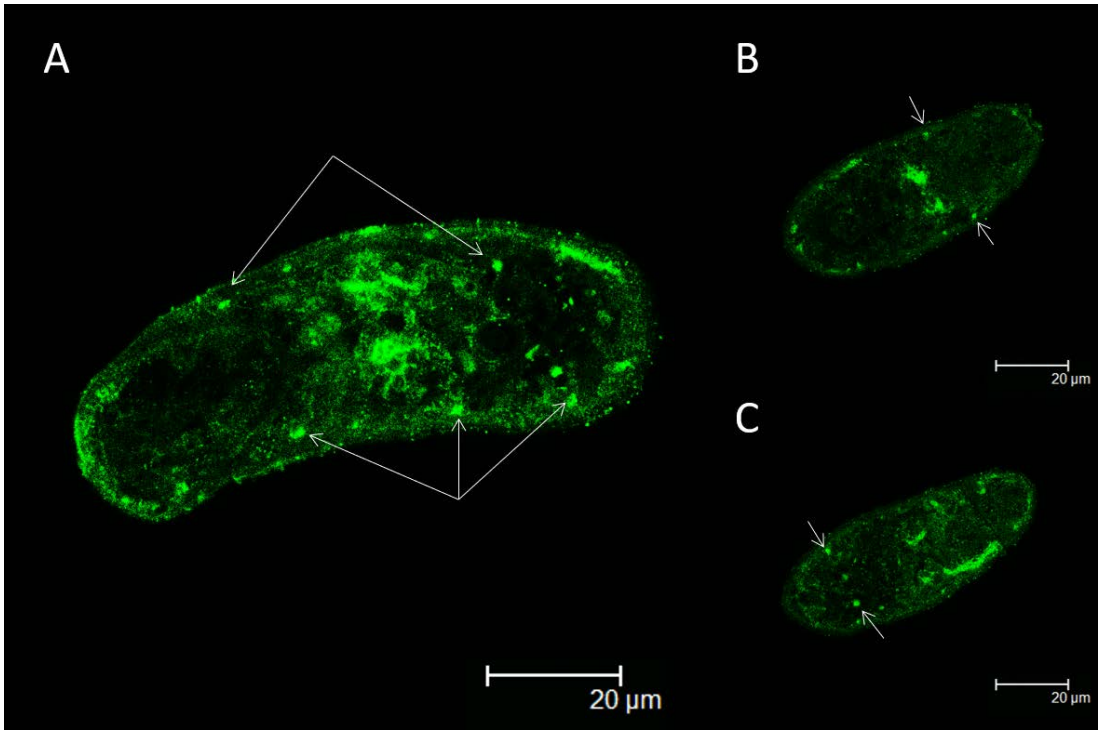

Figure 5.22. Distribution of activated CaMKII likely associated with flame cells in 24 h *in vitro* cultured somules revealed using anti-phospho-CaMKII antibodies (green). (A) Single z-section of a somule with white arrows highlighting the activated CaMKII associated with possible flame cells. (B and C) Single z-section of a somule with white arrows highlighting the activated CaMKII associated with the flame cells in (B) the anterior portion of the head and (C) the posterior portion of a 24 h somule. All z-stacks are shown in maximum projection mode.

5.3.8.3 Adult Worms

Imaging entire adult worms at maximum projection proved to be difficult due to their size, especially for adult males which were often beyond the z limits of the microscope. The association of activated CaMKII with the adult worm tegument also meant internal staining of activated CaMKII was obscured by the staining on the tegument when projected. Thus, CaMKII activation in intact worms was evaluated using mainly individual z-sections, or internal deep-scan z-stacks rather than maximum projections of the whole worms. This

technique enabled the localization of activated CaMKII within the nervous system (Figure 5.24), as seen in both the cercariae and somules. Within males, activated CaMKII could be seen along the full length of the longitudinal nerve, and in the more delicate nerve nets branching off the longitudinal nerve; furthermore, strong staining was seen in the cephalic ganglion and reaching into the nerve nets of the oral and ventral suckers (Figure 5.24). Activated CaMKII could also be seen associated with the tip of the head of the adult males, which could either be the ends of nerves or other sensory structures. There was also a strong association of activated CaMKII with the tegument of both the adult males and females (Figure 5.25); activated CaMKII could be seen particularly in the tubercles of the adult male protruding out above the thick under layers of muscle beneath the tegument (Figure 5.25). Activated CaMKII was also evident in the tegument of the male gynaecophoric canal (Figure 5.25C). Although the female worms do not possess tubercules, activated CaMKII was seen associated with the tegument.

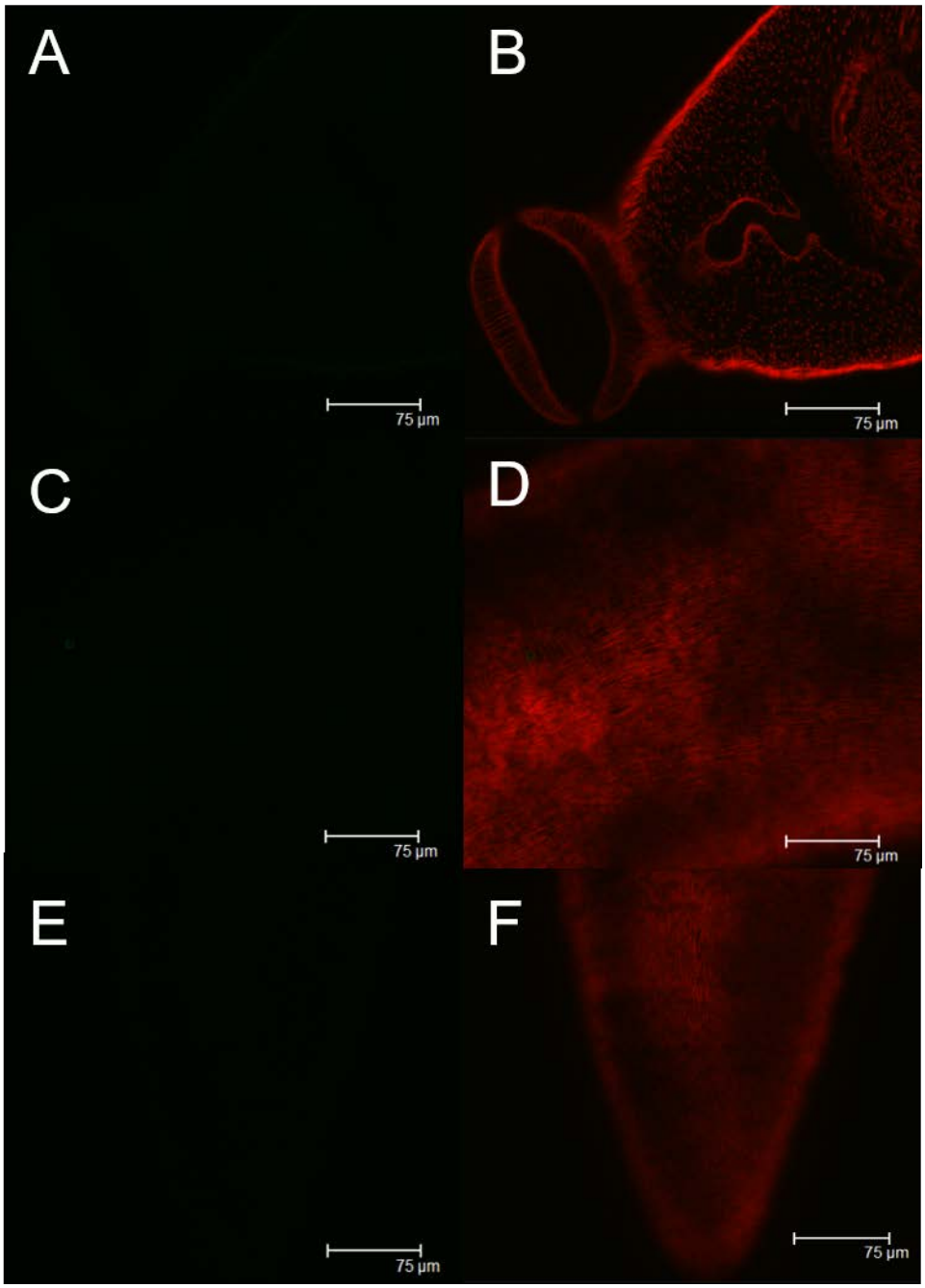

Figure 5.23. *S. mansoni* adult male and female worm negative controls. Adult worms were fixed and stained as detailed in Section 5.2.6 (A) Adult worms stained with only Alexa Fluor 488 secondary antibody (green). (B) Overlay of the Alexa Fluor 488 and the F-actin. Images shown are maximum z-stack projections.

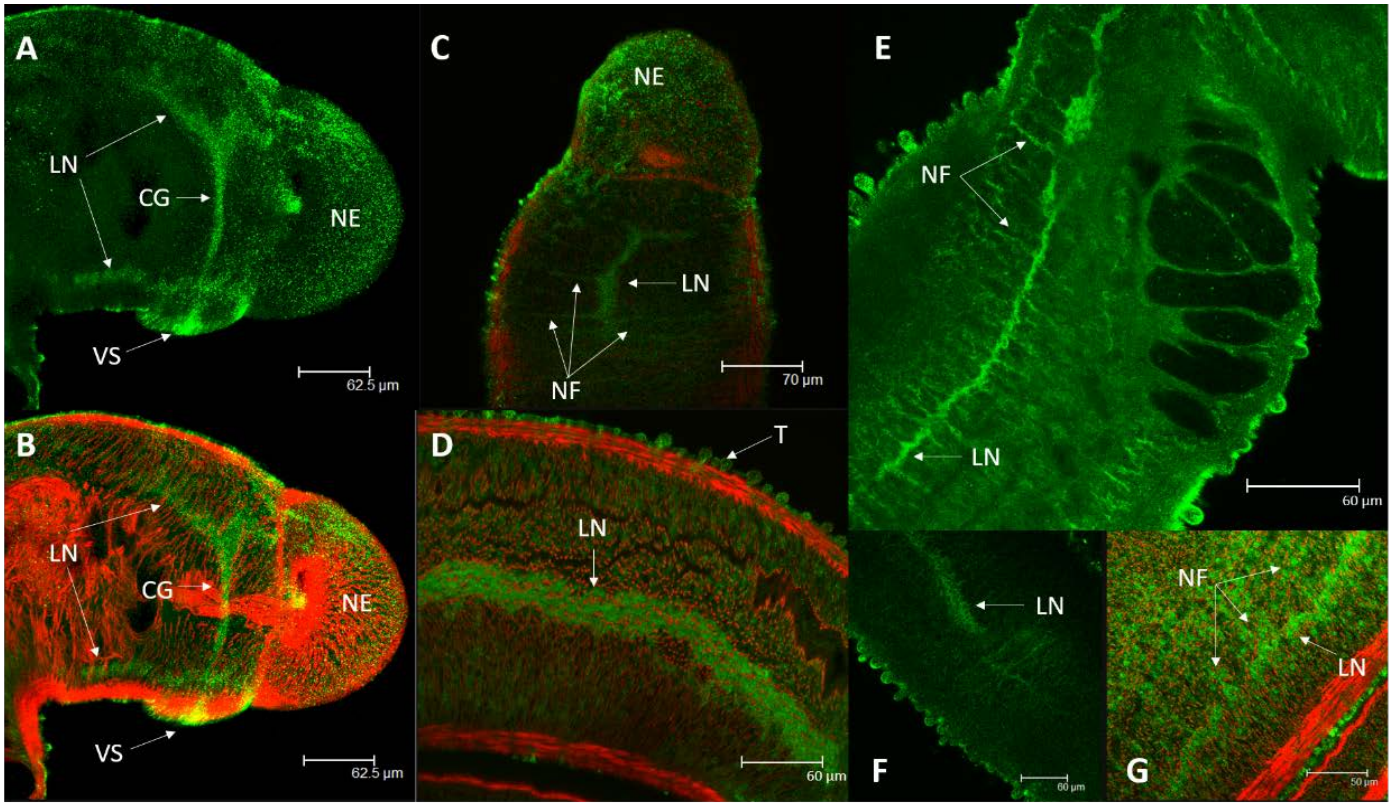

Figure 5.24. Distribution of activated CaMKII associated with the nervous system of adult male worms revealed using anti-phospho-CaMKII antibodies (green), and F-actin with rhodamine phalloidin (red). (A) Z-stack of adult male head region showing activated CaMKII in two of the longitudinal nerves (LN) joining at the cephalic ganglion (CG), nerve endings at the tip of the head (NE), and in ventral sucker (VS) edge. (B) Overlay of F-actin with (A). (C) Overlay of F-actin and activated CaMKII in Z stacks of another male head; activated CaMKII can be seen in the nerve endings at the tip of the head, as well as the longitudinal nerve and the nerve fibres (NF) projecting from it. (E) Maximum z-stack projection of male anterior testes region highlighting the longitudinal nerve and nerve fibres protruding off and lack of staining in the testes. (F) Z-stack projections of adult male highlighting thick trunk of activated CaMKII in the longitudinal nerve. (G) Z stack overlay of activated CaMKII and F-actin showing a longitudinal nerve and nerve fibres in close proximity to the gynaecophoric canal. All z-stacks are shown in maximum projection mode

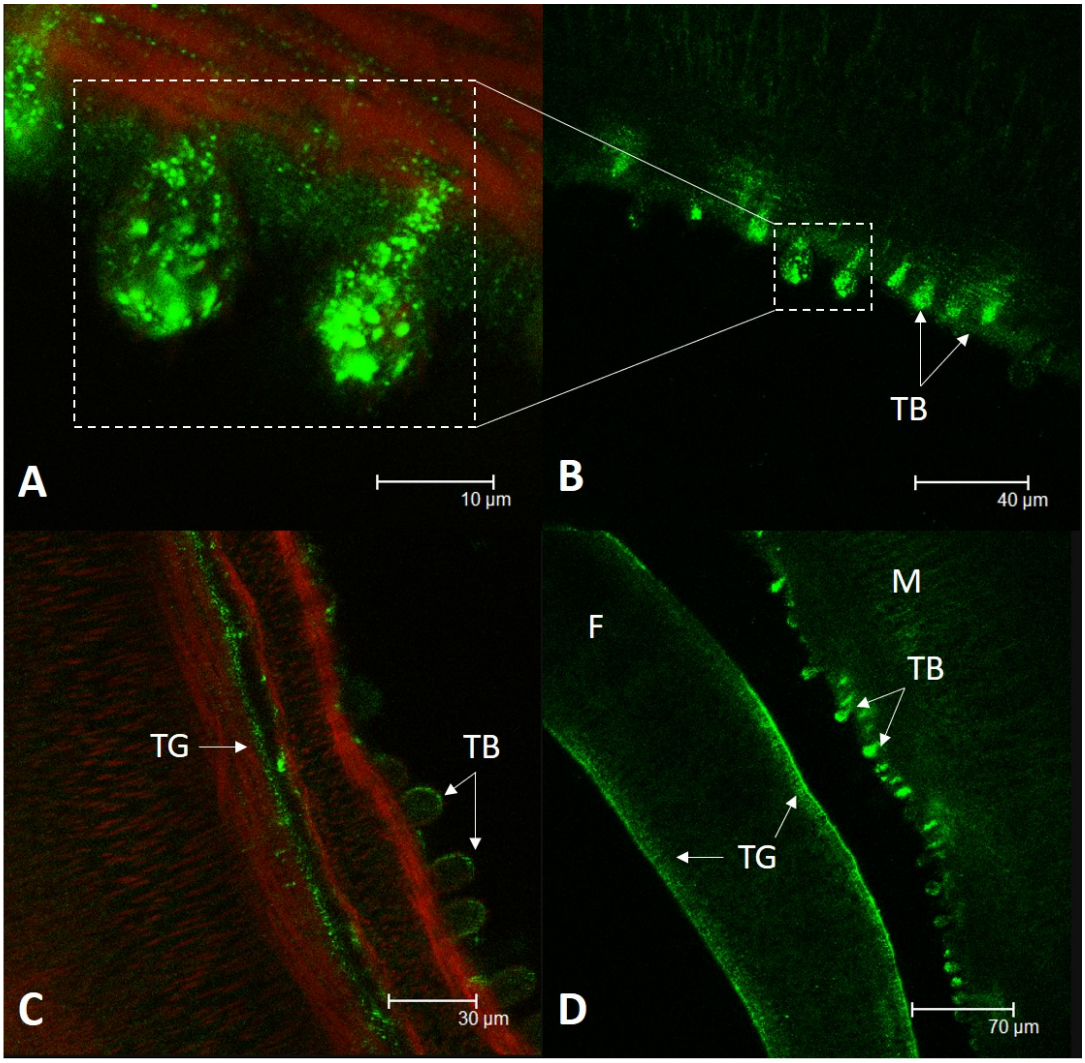

Figure 5.25. Activated CaMKII associated with the tegument of adult male and female worms revealed using anti-phospho-CaMKII antibodies (green) and F-actin with rhodamine phalloidin (red). (A) Magnified region of (B) showing a high concentration of activated CaMKII in punctate regions within the tubercules (TB) of an adult male tegument, F-actin highlights thick band of muscle beneath the tegument. (B) Single Z section of adult male showing activated CaMKII in the tubercules protruding from the tegument. (C) Single Z section overlay of F-actin and activated CaMKII showing the tegument of the gynaecophoric canal of an adult male (TG) and tubercules associated with activated CaMKII. (D) Z section of an adult female and male *in copula*, the activated CaMKII can be seen along the tegument on both sides of the female (F) and in the tubercules of the male (M). All z-stacks are shown in maximum projection mode.

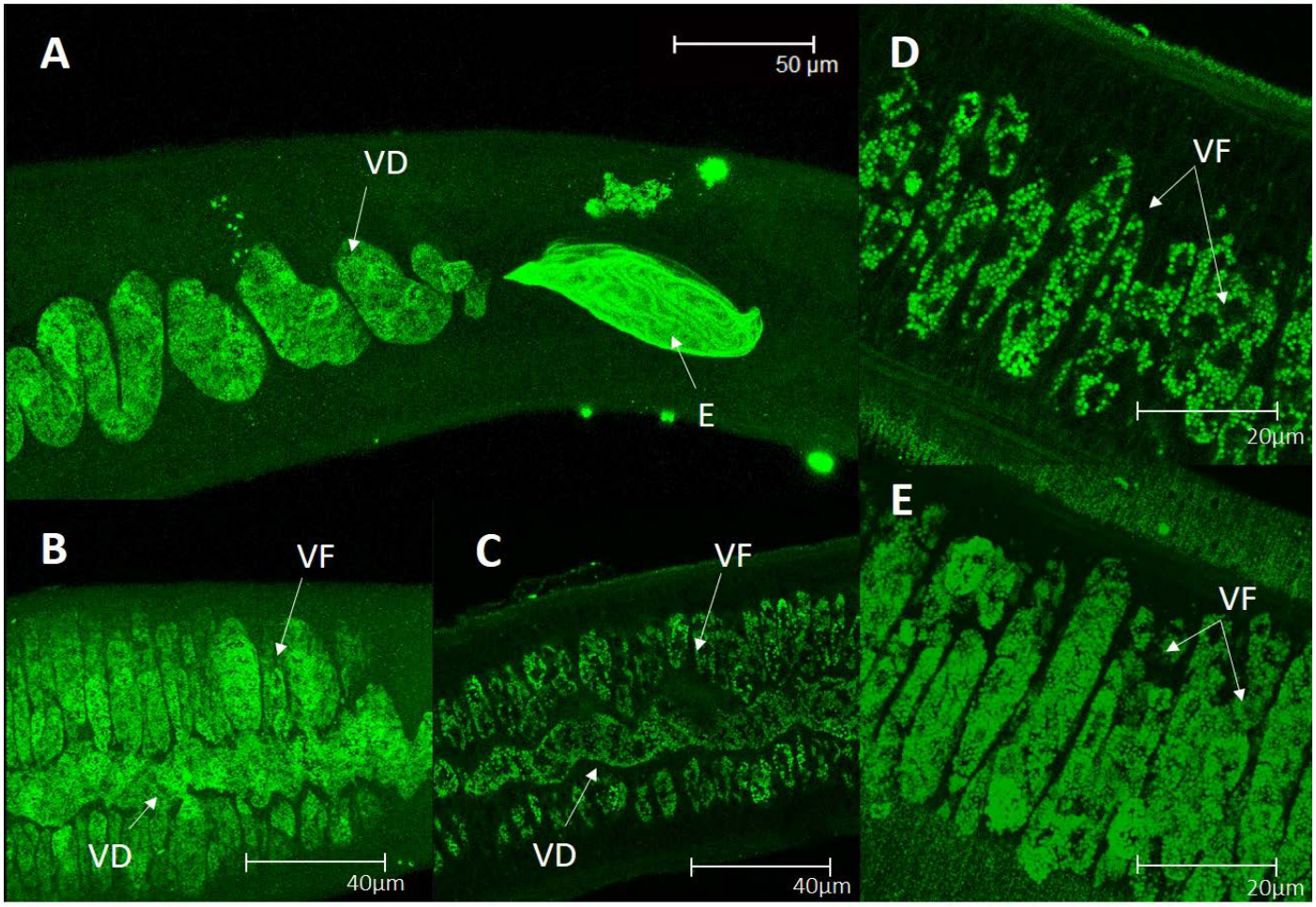

Figure 5.26. Distribution of activated CaMKII associated with the vitellaria of adult female worms revealed using anti-phospho-CaMKII antibodies (green). (A) Deep scan z-stack projection showing activated CaMKII in the vitelline duct leading up to the ootype wherein the egg (E) is formed. (B) Z stack and (C) single z-section of the vitelline follicles (VF) leading to the vitelline duct (VD). (D) z-section and (E) z-stack zoomed in on the vitelline follicles full of individual vitelline cells. All z-stacks are shown in maximum projection mode.

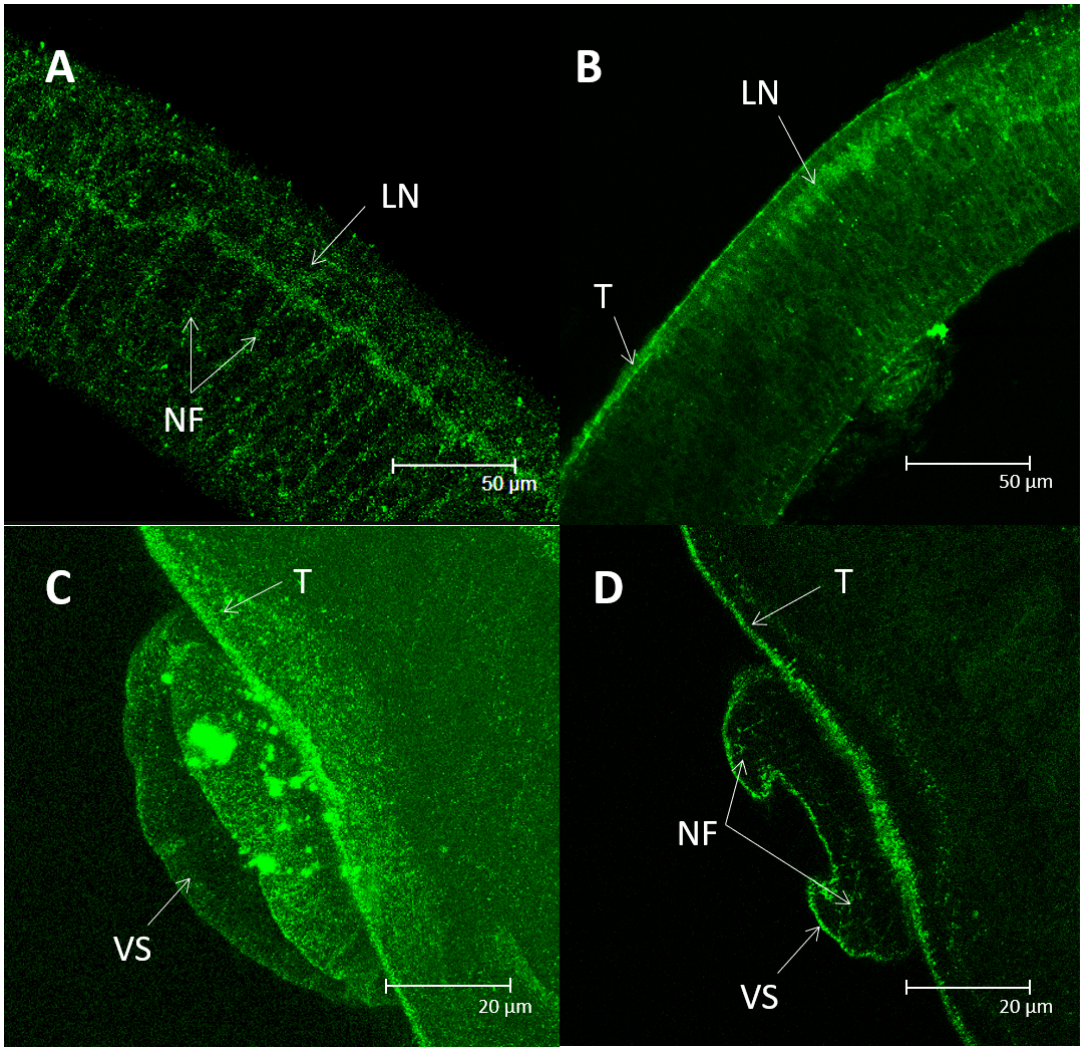

Figure 5.27. Distribution of activated CaMKII associated with the nervous system of adult female worms revealed using anti-phospho-CaMKII antibodies (green). (A) Z-stack showing activated CaMKII in the longitudinal nerve and the nerve fibres projecting from it. (B) Z-stack showing activated CaMKII in the longitudinal nerve, as well as the tegument of the female. (C) maximum projection of activated CaMKII in the ventral sucker (VS) region. (D) The fine nerve fibres projecting into the ventral sucker, as well as the activated CaMKII within the tegument. All z-stacks are shown in maximum projection mode.

Activated CaMKII was also found associated with the nervous system of the females and, although the strength of the signal appeared to be weaker in comparison to the males, it was still clearly found in the longitudinal nerves, and the nerve fibres/nets projecting from them (Figure 5.27); very fine nerve projections could also be determined in the nerve net of the female ventral sucker (Figure 5.27D) illustrating CaMKII activation in these regions. Overall the ventral sucker displayed a strong activated CaMKII signal, this is probably due to both the signal from the CaMKII in the nervous system and the surrounding tegument. Interestingly, activated CaMKII was clearly associated with the vitellaria of the adult females, it could particularly be found in the vitelline follicles, in which individual specialised stem cells could be visualized (Figure 5.26). Activated CaMKII could also be seen in the vitelline ducts into which the vitelline cells enter on their journey towards to vitello-oviduct where they are used in the formation of the egg. Even so, activated CaMKII was not localised in the male and female sexual organs, it could not be found in the ovaries, ootype and Mehlis' gland complex of the females or in the testes and seminal receptacle complex of the males. Overall activated CaMKII could be localised significantly across adult male and females, in the nervous system, tegument and vitellaria emphasizing the key role CaMKII must play within these parasites.

5.3.9 RNAi of CaMKII in Adult Worms

RNA interference (RNAi) has become a vital to help unravel our understanding of the basic biology of schistosomes and evaluate potential drug targets. For example, research using RNAi has identified the key role that cathepsins B and D play in the growth of schistosomes (Correnti et al., 2005; Morales et al., 2008), and how *S. mansoni* leucine

aminopeptidase is integral to the hatching of the miracidium from an egg (Rinaldi et al., 2009). RNAi has also been used to explore roles for protein kinases in schistosomes; for example, RNAi-mediated knockdown of SmTK4 in *S. mansoni* demonstrated a crucial role for SmTK4 in gametogenesis (Beckmann et al., 2010). Therefore, to help determine what role(s) CaMKII might play in schistosomes and in their survival, RNAi was performed to supress CaMKII protein expression in adult worms and their phenotypes evaluated. To attenuate CaMKII expression, custom made small interfering RNAs (siRNAs) were designed. Such siRNAs bind to and promote the degradation of the target messenger RNA (mRNA) (Fire et al., 1998). To enhance chances of success, siRNAs were designed using the online tool Custom Dicer-Substrate siRNA (DsiRNA)[25]. The mRNA FASTA sequence for smCaMKII (Smp_011660.1) was submitted and three resulting siRNAs which spanned the sequence were chosen. A scrambled control siRNA was also used; thus, three samples were compared, a control sample with nothing added, a scrambled control with a scrambled siRNA, and a pooled sample using all three siRNAs which aim to target SmCaMKII. A preliminary experiment was performed to determine the duration required for protein suppression after electroporation, therefore male worms were prepared and processed for Western blotting at 4 and 6 days post-electroporation with siRNAs. This experiment revealed a decrease in total CaMKII immunoreactivity at day 4, however at day 6 results were unclear (data not shown). Visually the day 6 worms did not look healthy, indicating that CaMKII may be important to the survival of the parasite. Therefore, further analyses were performed at day 4. Expression of CaMKII did not appear to differ between control and scrambled control worms, so only the scrambled control was used in subsequent assays. Next, RNAi was performed on females as well as

[25] https://eu.idtdna.com/site/order/designtool/index/DSIRNA_CUSTOM

on males. Again, at day 4, the siRNA-treated males and females looked unhealthy; visual inspection revealed there was decreased motility and some death suggesting a pivotal role for CaMKII. Of the 15 males and 15 females treated with siRNA, 3 males and 3 females had died by day 4, whilst none had died in the control treatments. A Western blot was then performed on protein extracts of the living worms and probed with antibodies that recognize total CaMKII and phosphorylated (activated) CaMKII. Compared to the scrambled control, immunoreactivity was significantly decreased. In male worms total CaMKII expression levels decreased by 66%, with a concomitant 70% reduction in CaMKII phosphorylation (Figure 5.28). These findings were significant at $P \leq 0.05$ and $P \leq 0.01$ (n=3) respectively. For females, total CaMKII expression was supressed by 52%, with CaMKII phosphorylation levels reduced by 45% ($P \leq 0.05$ and $P \leq 0.01$ (n=3) respectively). Thus, suppression of CaMKII was successful in both males and female worms, with males showing a larger mean reduction in both total and activated CaMKII levels 4 days post RNAi.

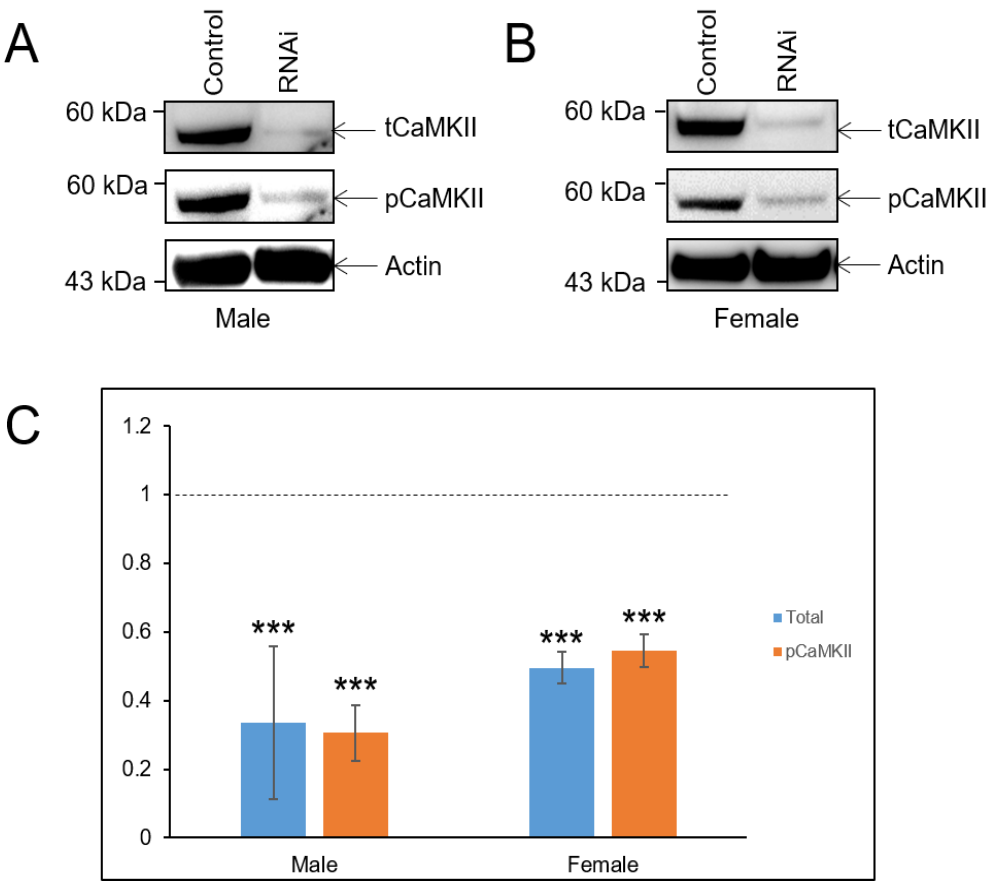

Figure 5.28. SiRNA-mediated suppression of CaMKII in *S. mansoni*. (A) Adult male and (B) Adult female worms were electroporated with siRNA or scrambled siRNA and processed for Western blotting at 4 days post electroporation. The Western blots were processed and probed with total CaMKII antibody (tCaMKII), and stripped and re-probed with anti-phospho-CaMKII (Thr286) antibody (pCaMKII) as described in Section 2.2.2; anti-actin antibodies were used to assess any differences in protein loading between lanes. (C) Quantification of mean (n=3±SD) phosphorylated CaMKII levels in adult worms after suppression of CaMKII in male and females probed with total CaMKII antibody (blue bars) and anti-phospho-CaMKII (Thr286) antibody (orange), presented with reference to the DMSO control used at each time point indicating no stimulation of 1.00 shown as the dotted line (***P≤0.01).

5.3.10 Effect of CaMKII siRNAi on Adult Worm Motility

Whilst observing the siRNA-treated worms it became apparent that their movement appeared to have been compromised. To enable quantification of the effect, 30 s movies of both adult male and female worms which had been treated with either the scrambled control or the pooled CaMKII siRNAs were captured. Worm movement was then analysed visually on day 4 and scored according to the WHO-TDR Scoring system; 4 = normally active; 3 = slowed activity; 2 = minimal activity, occasional movement of head and tail; 1 = absence of motility apart from gut movements; 0 = total absence of mobility (Ramirez et al., 2007). For the scrambled negative control treatments, all male and female worms displayed either normal movement or slowed activity with ≥80% normal movement observed in the two groups (Figures 5.29, 5.30). In contrast, CaMKII knockdown reduced the proportion of worms displaying normal movement considerably, with a striking ~75% reduction in females. In both sexes, siRNA treatment produced worms with TDR-Score phenotypes of 0 and 2 (Figures 5.29, 5.30). When the TDR scores were averaged for worms within each treatment, a significant 31% and 58% reduction in motility between scrambled and pooled CaMKII siRNAs was seen for males ($P \leq 0.05$) and females, respectively ($P \leq 0.001$) (Figure 5.31).

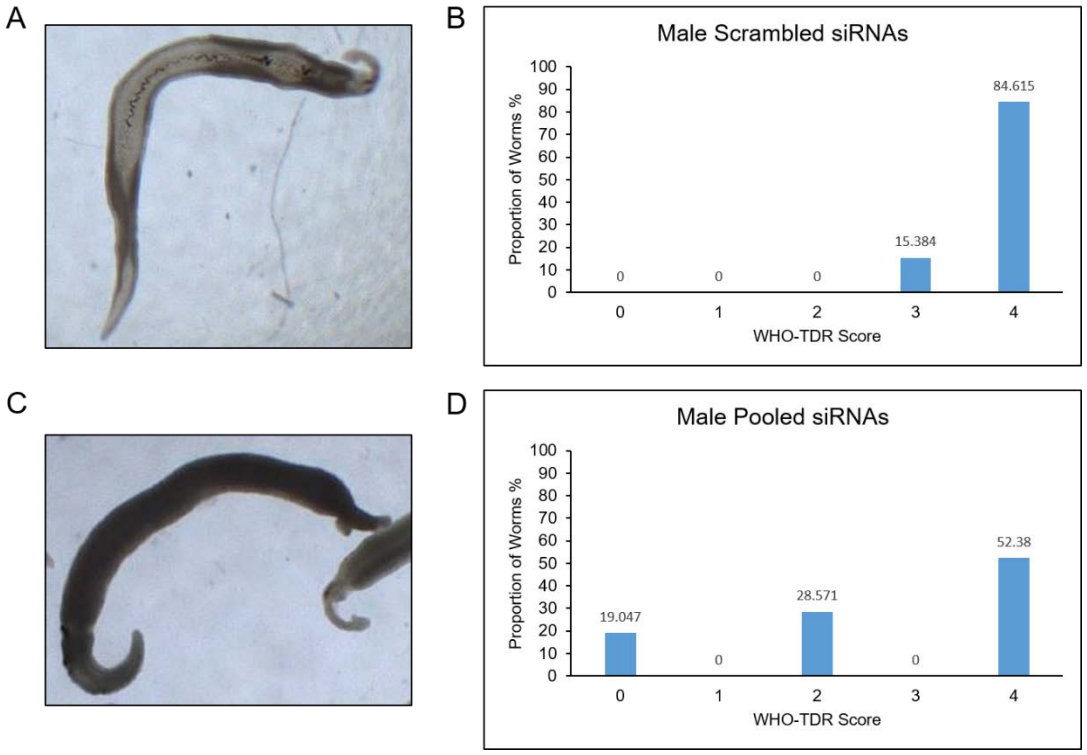

Figure 5.29. Motility of adult male *S. mansoni* after CaMKII knockdown. (A) Still shot from movie of males treated with scrambled control siRNAs. (B) Proportion of males treated with scrambled control siRNAs worms scored 0-4 according to the WHO-TDR scoring system. (C) Still shot from movie of males treated with pooled siRNAs. (D) Proportion of males treated with pooled siRNAs worms scored 0-4 according to the WHO-TDR scoring system**.** A total of 34 worms were analysed for each treatment.

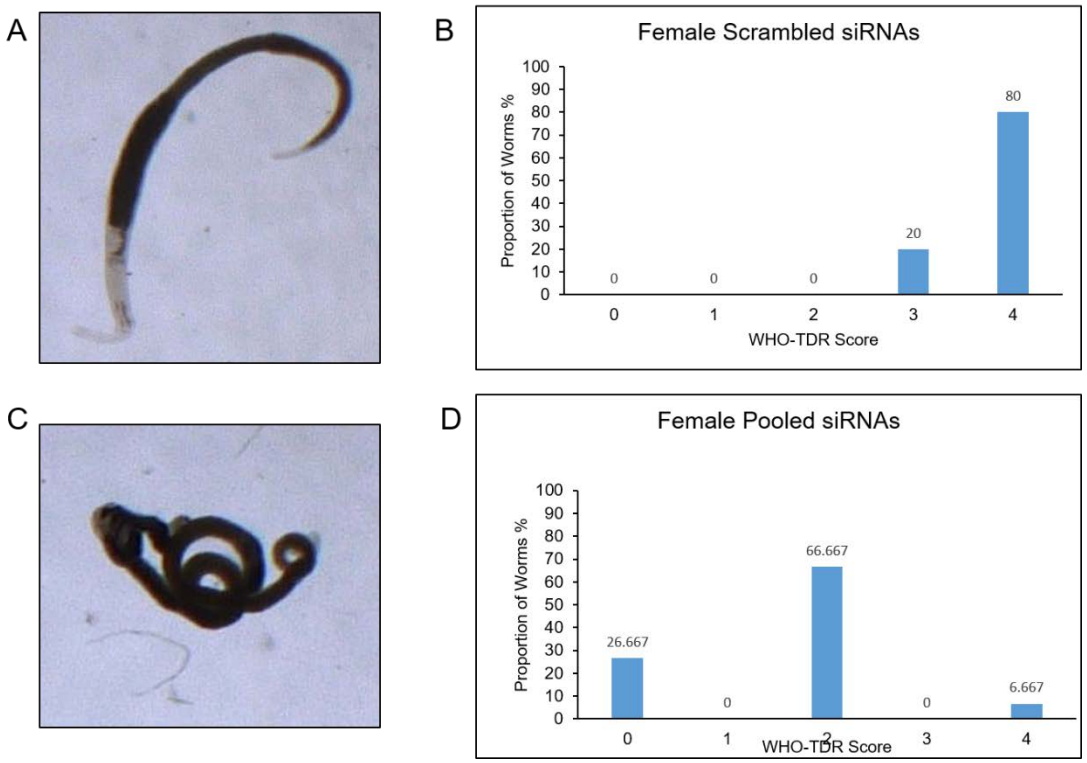

Figure 5.30. Motility of adult female *S. mansoni* after CaMKII knockdown. (A) Still shot from movie of females treated with scrambled control siRNAs. (B) Proportion of females treated with scrambled control siRNAs worms scored 0-4 according to the WHO-TDR scoring system. (C) Still shot from movie of females treated with pooled siRNAs. (D) Proportion of females treated with pooled siRNAs worms scored 0-4 according to the WHO-TDR scoring system. A total of 30 worms were analysed for each treatment.

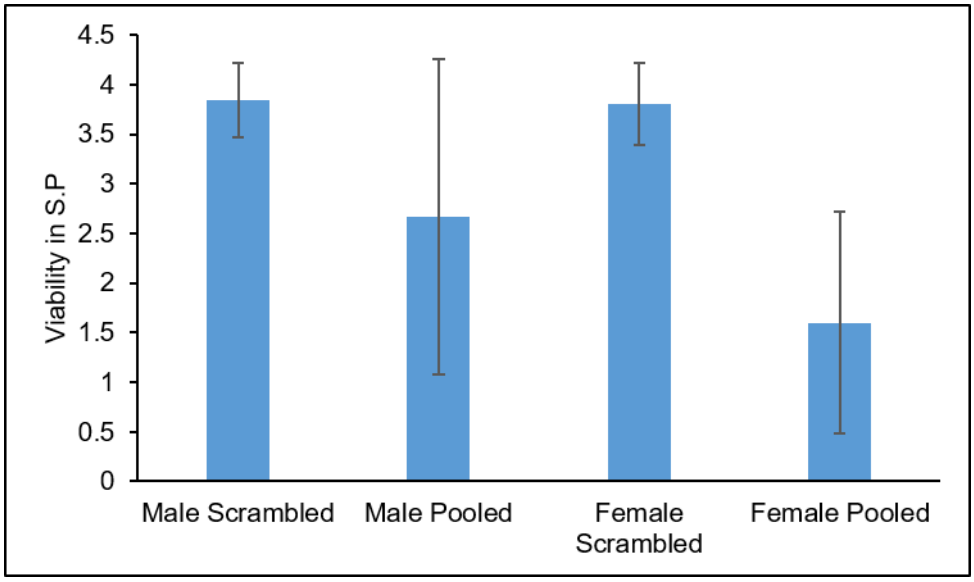

Figure 5.31. Global effects of CaMKII siRNA on adult *S. mansoni* movement. Average WHO-TDR scores (Viability Score Point) for each treatment: male scrambled control, male pooled CaMKII siRNAs, female scrambled control, female pooled CaMKII siRNAs. A total of 64 worms were analysed for each treatment.

5.4 Discussion

Calcium/calmodulin dependent protein kinase II signalling has been characterised in a number of eukaryotes, including humans in which it has been found to play a fundamental role in key organs including the brain, muscle and heart (Huberfeld et al., 2007; Maier et al., 2003; Wagner et al., 2006; Wehrens et al., 2004). Yet in parasites there has been little research on this kinase. One study demonstrated a role for CaMKII in the proliferation of the epimastigote stage of the parasite *Trypanasoma cruzi*, which causes Chagas' disease (Nogueira et al., 2011). As previously discussed, CaMKII transcription levels were found to be elevated after exposure to PZQ in *S. japonicum*, establishing CaMKII's potential role in the mode of action of PZQ, which is as yet unknown (You et al., 2013). These results, which highlight CaMKII as a potential drug target, alongside the lack of knowledge of CaMKII within schistosomes provided the premise to undertake an evaluation of CaMKII in *S. mansoni*.

In this study, commercially available anti-phospho CaMKII-(Thr286) antibodies were validated to enable the detection of activated CaMKII in the cercariae, somule and adult worm life stages of *S. mansoni*. This is the first reported use of anti-phospho-CaMKII (Thr286) antibodies in any parasite. The antibodies were employed to determine the effects of pharmacological agents and PZQ on CaMKII signalling within *S. mansoni* and were also used to functionally localize activated CaMKII in *S. mansoni* cercariae, somules and adult worms.

5.4.1 Detection of Activated CaMKII in schistosomes

Initially, bioinformatics were performed whereby the protein sequence for each human CaMKII isoform was BLASTed against the *S. mansoni* genome, which highlighted that Smp_011660.2 had the highest identity (77%) to human CaMKIIβ; the predicted autophosphorylation site (Thr284) was also conserved. Smp_011660 was described as a 'protein kinase' on the GeneDB/WormBase Parasite databases, and searches of the term CaMKII (or Ca^{2+}/Calmodulin dependant kinase II) did not identify any 'hits', therefore CaMKII was not definitely annotated in the genome.

Anti-phospho antibodies are raised against peptides which normally comprise the phosphorylated (target) amino acid and -7/+7 residues either side of the phosphorylated site. This region was highly conserved between human CaMKIIβ and Smp_011660, with 13/15 of the amino acids being identical including the crucial Thr residue; such conservation is usually sufficient to ensure immunoreactivity. Next the antibody was tested using somule extracts and a single ~57 kDa band was detected, close to the predicted MWs of two Smp_011660 variants listed on WormBase Parasite. Furthermore, a lambda phosphatase assay was performed demonstrating that the anti-phospho-CaMKII (Thr286) antibody is capable of detecting only the phosphorylated (activated) form of the kinase in schistosomes as anticipated. The conservation of antibody detection site, broad agreement of apparent to predicted MW, behaviour in lambda phosphatase assay, and response of protein phosphorylation to the CaMKII inhibitor KN93 (below) support that the antibody is specifically detecting phosphorylated (activated) *S. mansoni* CaMKII.

Activated CaMKII was found in all life stages investigated, cercariae, somules, adult male and females, although it is unclear which stage had the greatest activation due to the lack of protein determination. Meta Schisto however reports CaMKII (Smp_011660) gene expression present across all life stages (except the eggs), which was highest in sporocysts. Normalised gene expression in adult males and females, however, was 2 – 3 times less than in cercariae and somules. A total CaMKII antibody was sourced to enable the determination of the levels of total CaMKII across life stages; this antibody detected a band at a similar molecular weight as the anti-phospho antibody on a comparative Western blot of ~1000 cercariae, ~1000 somules, 1 adult female and 1 adult male, with varying levels of immunoreactivity across each of the life stages. Typically, in our laboratory, 1000 somules generates similar amounts of protein to an adult male worm, so it could tentatively be concluded that the adult worms express less of the detected CaMKII, which is in agreement with the gene expression data.

5.4.2 Immunolocalization of Activated CaMKII in Schistosomes

Confocal laser scanning microscopy was employed to ascertain where activated CaMKII was localised within cercariae, somules and adult worms. Activated CaMKII was predominantly found in the nervous system of all life stages of schistosomes investigated. For instance, activation at the longitudinal nerves was prominent in each life stage, with further CaMKII activation seen in the nerve projections, particularly in the adults, culminating in nerve endings towards the surface of the parasite. In cercariae and somules there was a significant association of activated CaMKII in the cephalic ganglion, which is the nerve centre of the parasite. These results are intriguing as research in other organisms (*Xenopus, M. musculus* and *H. sapiens*) has shown the link between CaMKII

and the nervous system where it has been shown to play a role in neuronal development, synaptic plasticity as well as the regulation of gene transcription and protein synthesis needed for neuronal development (Wayman et al., 2008). One of the most fascinating advances in CaMKII research is discovery of its involvement in learning and memory through synaptic plasticity (Matsuzaki et al., 2004). Thus, the findings here have implications for future research questions such as "do schistosomes learn and have memory (e.g. for pairing between males and females)?" and, if so, "could such behaviour be targetable for schistosome control?" These are not necessarily the most conventional questions to be asked but nevertheless they could lead to new ways of thinking about schistosome biology.

Activated CaMKII was also associated with the tegument of adult worms, in particular the tubercles of the males. This finding could support a role for activated CaMKII in the neuromuscular system of the adult worms, given the location of activated CaMKII not only in the tegument, but in the nervous system, as well as the ventral sucker. CaMKII has been located in both cardiac and skeletal muscle, where the activated form is involved in signalling pathways resulting in contractile movements (Chin, 2005; Rose et al., 2006). There is also a potential role for CaMKII in host-parasite communication through the activation of receptors in the tegument by host molecules, which may be the source of localised activated CaMKII in this region. Research in our laboratory has found that human EGF was capable of activating extracellular signal-regulated kinase (ERK) and protein kinase C (PKC) signalling pathways in somules (Ressurreição et al., 2016). These activated kinases were both localised to the tegument, displaying the ability a human growth factor has to regulate signalling in schistosomes, at least *in vitro*.

The cercariae displayed activated CaMKII at putative sensory structures which were located at the anterior tip of the head, and therefore could be involved in host location. Investigations with cercariae found they respond to linoleic acid, which is an essential fatty acid found in the human skin (Shiff & Graczyk, 1994), as well as changing their swim behaviour by increasing the frequency of shifts in swim direction in response to skin surface molecules including free fatty acids, and L-arginine (Haeberlein & Haas, 2008). L-arginine has also been shown to be the strongest chemical stimulus in the human skin for the attachment of *S. mansoni* cercariae (Haas et al., 2001). Furthermore, research in our laboratory has found that linoleic acid plays a role alongside PKC, ERK and p38 mitogen-activated protein kinase (p38 MAPK) signalling pathways in the release of enzymes essential for host invasion from the cercarial acetabular glands (Ressurreição et al., 2015). In addition, activated CaMKII localized to structures in cercariae that may be flame cells, these could also be seen in the somules. Flame cells participate in the excretory and osmoregulatory systems of schistosomes (Skelly & Shoemaker, 2001), they are tubule shaped structures filled with microtubules and myosin which suggests they function as a contractile structure (Bahia et al., 2006). In some mammals CaMKII has been shown to transduce intracellular signals in the enteric nervous system which controls the functions of the muscles in the gastrointestinal tract (Gao et al., 2012), this includes circular muscles which can also be found in flame cells of the parasite.

In female worms a large portion of the posterior half of the worm is filled with tissue known as the vitellaria. This tissue is made up of thousands of follicles which contain stem cells that will differentiate in mature vitellocytes (Erasmus, 1975). Vitellocytes supply the developing zygotes with nutrition as well as parts of the eggshell that protect it (Shinn, 1993). Although CaMKII activation was not observed in reproductive structures

such as the male testes and female ovary, it was significantly associated with the vitellaria, where not only each follicle attached to the vitelline duct could be seen, but the individual stem cells could also be distinguished. This finding supports a role for CaMKII in the production of schistosome eggs further highlighting CaMKII as a potential therapeutic target in the development of anti-schistosomal drugs.

Immunolocalization of activated CaMKII in cercariae, somules and adult males and females has enabled functional mapping of the kinase in the parasite. Overall, it has been localized to the nervous, neuromuscular, excretory, and egg production systems, all of which could be as potential targets for development of drugs against schistosomes.

5.4.3 Modulation of Activated CaMKII in *S. mansoni*

KN93 has been widely used to inhibit CaMKII and is thought to do this through binding to Ca^{2+}/CaM, preventing Ca^{2+}/CaM from binding to CaMKII, in turn causing inhibition of CaMKII phosphorylation and activation (Wong et al., 2019). When KN93 was employed here it was found to significantly reduce levels of CaMKII phosphorylation (activation) in 24 h *in vitro* cultured somules. This was also the case when using KN93 with somule homogenates. Overall, KN93 reduced levels of activated CaMKII in a dose and time dependant manner. Also, CaMKII was localized to a number of key organ systems within schistosomes. Already, KN93 is being considered as a therapeutic tool against cardiovascular disease such as heart failure and arrhythmia and improving myocardial function in patients with type 2 diabetes (Daniels et al., 2018; Pellicena & Schulman, 2014). Moreover, KN93 has been shown to prevent breast cancer cell migration and invasion through inhibition of CaMKII (Chi et al., 2016). The inhibition

profile of KN93 seen in the current work indicates that the principal mechanisms of CaMKII signalling, which include phosphorylation of Thr286, are conserved between schistosomes and humans. The above examples illustrate how KN93 could be developed as a therapeutic drug, and therefore investigation into using KN93 as an anti-schistosomal therapy warrants further research.

In comparison to inhibition, stimulation of CaMKII phosphorylation in *S. mansoni* proved challenging. Therefore, assays were performed to determine the effect of PMA on CaMKII phosphorylation in 24 h *in vitro* cultured somules, but initial assays found no significant effect. This could be due to the apparently high levels of basal CaMKII phosphorylation found in untreated parasites across the life stages, indicating that CaMKII is already highly activated. To circumvent this, assays were performed by firstly inhibiting CaMKII phosphorylation in parasites with KN93 before stimulating with PMA. However, CaMKII phosphorylation did not increase. It might be that, by firstly inhibiting CaMKII, the levels of Ca^{2+}/CaM in the sample were insufficient to allow for subsequent stimulation of CaMKII as recent research has shown that KN93 binds to CaM inhibiting CaMKII stimulation (Wong et al., 2019) or PMA may not be a good stimulant of CaMKII signalling in intact schistosomes, nevertheless PMA has been shown to stimulate PKC in *S. mansoni* (Ressurreição et al., 2014).

5.4.4 Effect of Praziquantel on Schistosomes – a link to CaMKII?

Studies in *S. japonicum* demonstrated that RNAi-mediated suppression of the delta-like form of CaMKII adversely effected adult worm movement. Moreover, when CaMKII expression was supressed and worms treated with PZQ, worm movement decreased even further (You et al., 2013). This points to CaMKII potentially playing a role in the mechanism of action of PZQ. Thus, studies aimed to define the effects of this drug on *S. mansoni* CaMKII over time in both somules and adult worms. In somules, CaMKII activation increased 30 min after exposure, but not after 15 min; whereas in adult worms a significant effect on CaMKII phosphorylation was observed only after 60 min. CaMKII is likely to be influenced by the influx of Ca^{2+} associated with exposure to PZQ reported by others (Greenberg, 2005). Although the Ca^{2+} influx is thought to be rapid, the duration of effect on CaMKII in these life stages seems to differ, indicating that PZQ's mechanism of action may even differ between the two life stages (Pica-Mattoccia & Cioli, 2004). PZQ is less effective on juvenile somules, whereas adult worms are more susceptible to its schistosomicidal activity, which could explain the difference in activation of CaMKII between the two life stages (Silva et al., 2003; Wang et al., 2012; Xiao et al., 1985). Nonetheless, PZQ seems to activate CaMKII in both stages of the parasite warranting further research to determine the role PZQ plays in CaMKII signalling. One further possible cause for the difference in activation of CaMKII in the life stages may be parasite physiology as the somules are smaller and their tegument is not as well developed as in adults which may hinder passage of PZQ across the tegument. Treatment of worms with PZQ results in an influx of extracellular Ca^{2+} possibly mediated by effects on the Ca^{2+}channel (Cavß); in addition, there is also a disruption of the Ca^{2+} homeostasis (Cioli & Pica-Mattoccia, 2003; Doenhoff et al., 2008; Jeziorski & Greenberg, 2006). In conclusion, PZQ significantly increases levels of activated CaMKII in both somules and adult worms, and therefore CaMKII is possibly integral to the mechanism of action of

PZQ; however, further research is needed to specifically determine how CaMKII is involved in the specific effects of PZQ.

5.4.5 Reduced CaMKII and its effect on *S. mansoni*

As previously mentioned, studies using *S. japonicum* found that RNAi-mediated suppression of the delta-like form of CaMKII reduced motility in adult worms especially in conjunction with PZQ. In accordance this study found a significant reduction in CaMKII levels of expression when exposed to siRNAs targeting the length of SmCaMKII's sequence. The effect was more pronounced in males, with CaMKII expression levels decreased by 66%, compared to a 52% decrease in females. Gene expression levels of CaMKII are higher in adult males than in adult females (Figure 5.8), and this could explain the difference in expression of the protein between sexes. Adult males are physically larger and are comprised larger amounts of muscle than female worms (Biolchini et al. 2006). Morphological studies of female worms have concluded their muscle mass has atrophied, and dependence for locomotion is reliant on the muscular male (Basch, 1990). CaMKII has been implicated in muscle movement within mammalian species (Eilers, et al., 2014; Kim et al., 2000), and despite *S. mansoni* isolated muscle fibres showing a Ca^{2+}-dependent contractility (Day et al., 1994) along with reduced movement in *S. japonicum* after suppression of CaMKII levels, there has been no link between CaMKII and movement in *S. mansoni*. Motility assays performed on adult male and female *S. mansoni* worms post reduction of CaMKII levels using RNAi highlighted a significant reduction in motility with a 31% and 58% reduction in motility in males and females respectively. Reasons for this may be down to the muscle mass of

each sex, males have significantly more muscle and hence only a complete knockdown of CaMKII could potentially disable their movement completely. However, the females muscle mass is reduced to prioritise reproductive genes (Biolchini et al., 2006), and motility is easily lost when CaMKII is knocked down. Thus, this assay found CaMKII can definitively be linked to movement in *S. mansoni*, whether it is CaMKII or downstream signalling pathways of CaMKII that ultimately halt movement is yet to be understood, but as CaMKII presents as an enticing target for the next generation of anti-schistosomicidal therapeutics.

6 CONCLUSION

Protein phosphorylation is one of the most prevalent and significant post translational modification across species, acting as a mechanism of regulation over vital processes in the cell encompassing protein synthesis, cell division, signal transduction, cell growth and development (Li et al., 2013; Sacco et al., 2012). Kinases and phosphatases consist of 2–4% of eukaryotic proteomes (Moorhead et al., 2009), and the elucidation of the phosphosites, amounts, and the roles they play in a biological sample presents a challenge which the advent of LC-MS/MS technologies have advanced (Grimsrud et al., 2010). Using results achieved through LC-MS/MS, this study identified and quantified the phosphoproteins, their phosphorylation sites, and potential roles they play within mixed adult *S. mansoni*, providing a novel global biological insight into the parasite. Knowledge of the location of a phosphosite, and its potential role presents an area for targeted drug development towards the kinases which add a phosphate group to these phosphosites, altering the activity of the phosphoprotein and often acting as an 'on or off' switch for the relative signalling pathway. Indeed this is a route that has already been exploited in humans where mutations in the regulatory pathways kinases control can lead to activation of proliferation when not needed, resulting in oncogenesis and the development of cancer (Harsha & Pandey, 2010). The successful generation of drugs targeting kinases implicated in such un-regulated pathways, as has occurred with Gleevec a therapeutic agent for treatment of chronic myelogenous leukaemia, which is inhibitor of Abl tyrosine kinase (Lin et al., 2013), exhibits the potential application of knowledge gained during phosphoproteomic investigations such as the one carried out in this study. The information gathered in this study can also be transferred to similar species such as *S. japonicum* and *S. haematobium* due to the relatively conserved nature of kinase structure (Hanks, 2003), it was this fact that was the basis for the initial bioinformatics in the generation of a schistosome specific peptide array during this study which used

knowledge gained during a phosphoproteomic analysis in *S. japonicum* (Cheng et al., 2013).

This study presents the first schistosome specific kinase array chip using valuable data gathered during the phosphoproteomic study of mixed adult *S. mansoni*. A number of significantly different proteins between males and females have been identified which could represent potential drug/vaccine targets and certainly warrant further investigation. With further time this array could be employed across life stages, identifying phosphopeptides which may differ in activation, potentially discovering drug targets that could attack the parasite at earlier stages than the current drug of use PZQ can. Alternatively, the array could be used in conjunction with relevant biological substance and drugs such as PZQ to help identify kinases which may be involved in related signalling pathways. The array has the potential to be used in many differing scenarios which could be tailored to fit a laboratories needs with ease, enabling access to a large amount of information with a small amount of time an effort. As mentioned, the conserved nature of kinases between species could enable the use of this peptide array in conjunction with alternate schistosome species, or indeed parasite species to help identify their own potential drug targets. Peptide arrays often employ kinase consensus sequences in a standardised commercial array which is transferrable interspecies (Peppelenbosch, 2012). This type of high-throughput analysis is the mark of the future in cell signalling research and its evolution in the coming years looks to provide much integral knowledge which could change the way we tackle life changing diseases.

Knowledge gained during this study indicated CaMKII was a protein of interest which warranted further research, in *S. japonicum* CaMKII had already been identified as playing a role in PZQ signalling mechanisms (You et al., 2013). The identification of this protein of interest during the phosphoproteomic and schistosome specific peptide array validate the use of these techniques in the search for novel therapeutic candidates. This study discovered CaMKII was involved in worm motility during the reduction of CaMKII levels in adult worms, presenting CaMKII as a viable drug target as the ability to cause cessation of movement within the worms would ensure they could not feed, pair or produce eggs which causes the pathologies associated with schistosomiasis, ultimately resulting in death. Of course, further research is needed to clarify exactly how CaMKII affects worm motility, to determine the best target within its signalling pathway for the development of a drug and ensure the drug target would be usable in humans. Identification of CaMKII in movement also has implications across species, it has already been found in mammalian skeletal muscle (Eilers et al., 2014),

In conclusion this study has presented a successful pipeline, from identify the overarching phosphoproteomics of *S. mansoni* identifying and quantifying a large number of phosphoproteins and their potential mechanisms of action. Following this came the consolidation of the most key phosphopeptide identifications and their inclusion onto the first generation of a schistosome specific kinase array, the use of which highlighted vital differences between proteins levels in male and female worms and corroborated the recognition of CaMKII as a protein of interest. This evolved into a in depth study of CaMKIIs signalling pathway across *S. mansoni* life stages demonstrating evidence to suggest CaMKII could be a developed as a therapeutic drug target in the ongoing search for novel drug discovery to treat schistosomiasis. In the future, this research could be

expanded on in a number of interesting ways. Firstly, the kinase array could be honed and improved, allowing for the use across all life stages and sexes within *S. mansoni*, finding differences between key kinase peptides could identify potential therapeutic targets for development of drugs against schistosomiasis. Furthermore, improvement of this array could make the way in which we study kinases within parasites significantly easier, allowing us to screen many targets using one small and simple assay. Further future work to be expanded on would be the identification of CaMKII's role within the parasite, it has been highlighted as a potential candidate involved in the movement of these worms, this could present as a highly druggable target and therefore warrants a deeper insight into its full signalling pathway. Finally, CaMKII was only one of a number of potentially important proteins identified during the PTM scan, it is imperative that this highly useful dataset is interrogated closely and more of these proteins are investigated in depth to deepen our knowledge of the signalling within schistosoma, allowing us to move every closer to the identification and development of a drug against this debilitating disease.

References

Acevedo, N., Ding, J., & Smith, G. D. (2007). Insulin Signaling in Mouse Oocytes1. *Biology of Reproduction*, *77*(5), 872–879. https://doi.org/10.1095/biolreprod.107.060152

Ahmad, G., Zhang, W., Torben, W., Noor, Z., & Siddiqui, A. A. (2010). Protective effects of Sm-p80 in the presence of resiquimod as an adjuvant against challenge infection with Schistosoma mansoni in mice. *International Journal of Infectious Diseases*, *14*(9), e781–e787. https://doi.org/10.1016/j.ijid.2010.02.2266

Allocco, J. J., Donald, R., Zhong, T., Lee, A., Tang, Y. S., Hendrickson, R. C., … Nare, B. (2006). Inhibitors of casein kinase 1 block the growth of Leishmania major promastigotes in vitro. *International Journal for Parasitology*, *36*(12), 1249–1259. https://doi.org/10.1016/j.ijpara.2006.06.013

Alonso, D., Muñoz, J., Gascón, J., Valls, M. E., & Corachan, M. (2006). Failure of standard treatment with praziquantel in two returned travelers with Schistosoma haematobium infection. *The American Journal of Tropical Medicine and Hygiene*, *74*(2), 342–344. Retrieved from http://www.ncbi.nlm.nih.gov/pubmed/16474094

Altschul, S. F., Gish, W., Miller, W., Myers, E. W., & Lipman, D. J. (1990). Basic local alignment search tool. *Journal of Molecular Biology*, *215*(3), 403–410. https://doi.org/10.1016/S0022-2836(05)80360-2

Alves, C. C., Araujo, N., dos Santos, V. C. F., Couto, F. B., Assis, N. R. G., Morais, S. B., … Fonseca, C. T. (2015). Sm29, but Not Sm22.6 Retains its Ability to Induce a Protective Immune Response in Mice Previously Exposed to a Schistosoma mansoni Infection. *PLOS Neglected Tropical Diseases*, *9*(2), e0003537. https://doi.org/10.1371/journal.pntd.0003537

Amanchy, R., Periaswamy, B., Mathivanan, S., Reddy, R., Tattikota, S. G., & Pandey, A. (2007). A curated compendium of phosphorylation motifs. *Nature Biotechnology*, *25*(3), 285–286. https://doi.org/10.1038/nbt0307-285

Andrade, L. F., Nahum, L. a, Avelar, L. G. a, Silva, L. L., Zerlotini, A., Ruiz, J. C., & Oliveira, G. (2011). Eukaryotic protein kinases (ePKs) of the helminth parasite Schistosoma mansoni. *BMC Genomics*, *12*(1), 215. https://doi.org/10.1186/1471-2164-12-215

Angeli, V., Faveeuw, C., Roye, O., Fontaine, J., Teissier, E., Capron, A., … Trottein, F. (2001). Role of the parasite-derived prostaglandin D2 in the inhibition of epidermal Langerhans cell migration during schistosomiasis infection. *The Journal of Experimental Medicine*, *193*(10),

1135–1147. Retrieved from http://www.ncbi.nlm.nih.gov/pubmed/11369785

Ardito, F., Giuliani, M., Perrone, D., Troiano, G., & Lo Muzio, L. (2017). The crucial role of protein phosphorylation in cell signaling and its use as targeted therapy (Review). *International Journal of Molecular Medicine*, *40*(2), 271–280. https://doi.org/10.3892/ijmm.2017.3036

Arsenault, R., Griebel, P., & Napper, S. (2011). Peptide arrays for kinome analysis: New opportunities and remaining challenges. *PROTEOMICS*, *11*(24), 4595–4609. https://doi.org/10.1002/pmic.201100296

Avelar, L. G. A., Nahum, L. A., Andrade, L. F., & Oliveira, G. (2011). Functional Diversity of the Schistosoma mansoni Tyrosine Kinases. *Journal of Signal Transduction*, *2011*, 603290. https://doi.org/10.1155/2011/603290

Bahia, D, Avelar, L. G. A., Vigorosi, F., Cioli, D., Oliveira, G. C., & Mortara, R. A. (2006). The distribution of motor proteins in the muscles and flame cells of the Schistosoma mansoni miracidium and primary sporocyst. *Parasitology*, *133*(Pt 3), 321–329. https://doi.org/10.1017/S0031182006000400

Bahia, Diana, Andrade, L. F., Ludolf, F., Mortara, R. A., & Oliveira, G. (2006). Protein tyrosine kinases in Schistosoma mansoni. *Memórias Do Instituto Oswaldo Cruz*, *101 Suppl*, 137–143. Retrieved from http://www.ncbi.nlm.nih.gov/pubmed/17308761

Bahia, Diana, Avelar, L., Mortara, R. A., Khayath, N., Yan, Y., Noël, C., … Oliveira, G. (2006). SmPKC1, a new protein kinase C identified in the platyhelminth parasite Schistosoma mansoni. *Biochemical and Biophysical Research Communications*, *345*(3), 1138–1148. https://doi.org/10.1016/j.bbrc.2006.05.025

Bahia, Diana, Mortara, R. A., Kusel, J. R., Andrade, L. F., Ludolf, F., Kuser, P. R., … Oliveira, G. (2007). Schistosoma mansoni: expression of Fes-like tyrosine kinase SmFes in the tegument and terebratorium suggests its involvement in host penetration. *Experimental Parasitology*, *116*(3), 225–232. https://doi.org/10.1016/j.exppara.2007.01.009

Barsoum, R. S. (2013). Urinary schistosomiasis: review. *Journal of Advanced Research*, *4*(5), 453–459. https://doi.org/10.1016/j.jare.2012.08.004

Basch, P. F. (1990). Why do schistosomes have separate sexes? *Parasitology Today (Personal Ed.)*, *6*(5), 160–163. Retrieved from http://www.ncbi.nlm.nih.gov/pubmed/15463329

Bayer, K. U., Löhler, J., Schulman, H., & Harbers, K. (1999). Developmental expression of the CaM kinase II isoforms: ubiquitous gamma- and delta-CaM kinase II are the early isoforms and most abundant in the developing nervous system. *Brain Research. Molecular Brain*

Research, *70*(1), 147–154. Retrieved from http://www.ncbi.nlm.nih.gov/pubmed/10381553

Beall, M. J., McGonigle, S., & Pearce, E. J. (2000). Functional conservation of Schistosoma mansoni Smads in TGF-beta signaling. *Molecular and Biochemical Parasitology*, *111*(1), 131–142. Retrieved from http://www.ncbi.nlm.nih.gov/pubmed/11087923

Beckmann, S., & Grevelding, C. G. (2010). Imatinib has a fatal impact on morphology, pairing stability and survival of adult Schistosoma mansoni in vitro. *International Journal for Parasitology*, *40*(5), 521–526. https://doi.org/10.1016/j.ijpara.2010.01.007

Beckmann, Svenja, Buro, C., Dissous, C., Hirzmann, J., & Grevelding, C. G. (2010). The Syk kinase SmTK4 of Schistosoma mansoni is involved in the regulation of spermatogenesis and oogenesis. *PLoS Pathogens*, *6*(2), e1000769. https://doi.org/10.1371/journal.ppat.1000769

Beckmann, Svenja, Hahnel, S., Cailliau, K., Vanderstraete, M., Browaeys, E., Dissous, C., & Grevelding, C. G. (2011). Characterization of the Src/Abl hybrid kinase SmTK6 of Schistosoma mansoni. *The Journal of Biological Chemistry*, *286*(49), 42325–42336. https://doi.org/10.1074/jbc.M110.210336

Beckmann, Svenja, Quack, T., Dissous, C., Cailliau, K., Lang, G., & Grevelding, C. G. (2012). Discovery of Platyhelminth-Specific α/β-Integrin Families and Evidence for Their Role in Reproduction in Schistosoma mansoni. *PLoS ONE*, *7*(12), e52519. https://doi.org/10.1371/journal.pone.0052519

Beenstock, J., Mooshayef, N., & Engelberg, D. (2016). How Do Protein Kinases Take a Selfie (Autophosphorylate)? *Trends in Biochemical Sciences*, *41*(11), 938–953. https://doi.org/10.1016/j.tibs.2016.08.006

Berriman, M., Haas, B. J., LoVerde, P. T., Wilson, R. A., Dillon, G. P., Cerqueira, G. C., … El-Sayed, N. M. (2009). The genome of the blood fluke Schistosoma mansoni. *Nature*, *460*(7253), 352–358. https://doi.org/10.1038/nature08160

Berry, A., Moné, H., Iriart, X., Mouahid, G., Aboo, O., Boissier, J., … Magnaval, J.-F. (2014). Schistosomiasis haematobium, Corsica, France. *Emerging Infectious Diseases*, *20*(9), 1595–1597. https://doi.org/10.3201/eid2009.140928

Biolchini, C. de L., Neves, R. H., Hulstijn, M., Gomes, D. C., & Machado-Silva, J. R. (2006). Development of Schistosoma mansoni worms in mice analyzed by bright field and confocal microscopy. *Memórias Do Instituto Oswaldo Cruz*, *101*(suppl 1), 261–265. https://doi.org/10.1590/S0074-02762006000900040

Blach, O., Rai, B., Oates, K., Franklin, G., & Bramwell, S. (2012). An outbreak of schistosomiasis

in travellers returning from endemic areas: the importance of rigorous tracing in peer groups exposed to risk of infection. *Journal of Public Health*, *34*(1), 32–36. https://doi.org/10.1093/pubmed/fdr099

Boekhorst, J., van Breukelen, B., Heck, A. J., & Snel, B. (2008). Comparative phosphoproteomics reveals evolutionary and functional conservation of phosphorylation across eukaryotes. *Genome Biology*, *9*(10), R144. https://doi.org/10.1186/gb-2008-9-10-r144

Bogitsh, B. J., & Carter, O. S. (1977). Schistosoma mansoni: ultrastructural studies on the esophageal secretory granules. *The Journal of Parasitology*, *63*(4), 681–686. Retrieved from http://www.ncbi.nlm.nih.gov/pubmed/196065

Boissier, J., Grech-Angelini, S., Webster, B. L., Allienne, J.-F., Huyse, T., Mas-Coma, S., … Mitta, G. (2016). Outbreak of urogenital schistosomiasis in Corsica (France): an epidemiological case study. *The Lancet Infectious Diseases*, *16*, 971–979. https://doi.org/10.1016/S1473-3099(16)00175-4

Boissier, J., Moné, H., Mitta, G., Bargues, M. D., Molyneux, D., & Mas-Coma, S. (2015). Schistosomiasis reaches Europe. *The Lancet. Infectious Diseases*, *15*(7), 757–758. https://doi.org/10.1016/S1473-3099(15)00084-5

Bonetta, L. (2005). Probing the kinome. *Nature Methods*, *2*(3), 225–232. https://doi.org/10.1038/nmeth0305-225

Bowick, G. C., Fennewald, S. M., Scott, E. P., Zhang, L., Elsom, B. L., Aronson, J. F., … Herzog, N. K. (2007). Identification of differentially activated cell-signaling networks associated with pichinde virus pathogenesis by using systems kinomics. *Journal of Virology*, *81*(4), 1923–1933. https://doi.org/10.1128/JVI.02199-06

Braschi, S., Curwen, R. S., Ashton, P. D., Verjovski-Almeida, S., & Wilson, A. (2006). The tegument surface membranes of the human blood parasite Schistosoma mansoni: a proteomic analysis after differential extraction. *Proteomics*, *6*(5), 1471–1482. https://doi.org/10.1002/pmic.200500368

Braschi, S., & Wilson, R. A. (2006). Proteins exposed at the adult schistosome surface revealed by biotinylation. *Molecular & Cellular Proteomics : MCP*, *5*(2), 347–356. https://doi.org/10.1074/mcp.M500287-MCP200

Braun, A. P., & Schulman, H. (1995). A non-selective cation current activated via the multifunctional Ca(2+)-calmodulin-dependent protein kinase in human epithelial cells. *The Journal of Physiology*, 37–55. Retrieved from http://www.ncbi.nlm.nih.gov/pubmed/8568664

Bui, J. D., bastien Calbo, S., Hayden-Martinez, K., Kane, L. P., Gardner, P., & Hedrick, S. M. (2000). *A Role for CaMKII in T Cell Memory induces high levels of kinase activity. Activated CaMKII phosphorylates various substrates including threonine A form of CaMKII found in human T cells is the B subtype*. *Cell* (Vol. 100). Retrieved from https://www.cell.com/cell/pdf/S0092-8674(00)80681-9.pdf

Capowski, E. E., & Tracy, J. W. (2003). Ribosomal RNA processing and the role of SmMAK16 in ribosome biogenesis in Schistosoma mansoni. *Molecular and Biochemical Parasitology*, *132*(2), 67–74. https://doi.org/10.1016/J.MOLBIOPARA.2003.08.006

Capron, A., Capron, M., Dombrowicz, D., & Riveau, G. (2001). Vaccine Strategies against Schistosomiasis: From Concepts to Clinical Trials. *International Archives of Allergy and Immunology*, *124*(1–3), 9–15. https://doi.org/10.1159/000053656

Carlo, J. M., Osman, A., Niles, E. G., Wu, W., Fantappie, M. R., Oliveira, F. M. B., & LoVerde, P. T. (2007). Identification and characterization of an R-Smad ortholog (SmSmad1B) from Schistosoma mansoni. *The FEBS Journal*, *274*(16), 4075–4093. https://doi.org/10.1111/j.1742-4658.2007.05930.x

Carmona, S. J., Nielsen, M., Schafer-Nielsen, C., Mucci, J., Altcheh, J., Balouz, V., … Agüero, F. (2015). Towards High-throughput Immunomics for Infectious Diseases: Use of Next-generation Peptide Microarrays for Rapid Discovery and Mapping of Antigenic Determinants. *Molecular & Cellular Proteomics*, *14*(7), 1871–1884. https://doi.org/10.1074/mcp.M114.045906

Castro-Borges, W., Dowle, A., Curwen, R. S., Thomas-Oates, J., & Wilson, R. A. (2011). Enzymatic shaving of the tegument surface of live schistosomes for proteomic analysis: a rational approach to select vaccine candidates. *PLoS Neglected Tropical Diseases*, *5*(3), e993. https://doi.org/10.1371/journal.pntd.0000993

Castro-Borges, W., Simpson, D. M., Dowle, A., Curwen, R. S., Thomas-Oates, J., Beynon, R. J., & Wilson, R. A. (2011). Abundance of tegument surface proteins in the human blood fluke Schistosoma mansoni determined by QconCAT proteomics. *Journal of Proteomics*, *74*(9), 1519–1533. https://doi.org/10.1016/j.jprot.2011.06.011

Cayla, M., Rachidi, N., Leclercq, O., Schmidt-Arras, D., Rosenqvist, H., Wiese, M., & Späth, G. F. (2014). Transgenic Analysis of the Leishmania MAP Kinase MPK10 Reveals an Auto-inhibitory Mechanism Crucial for Stage-Regulated Activity and Parasite Viability. *PLoS Pathogens*, *10*(9), e1004347. https://doi.org/10.1371/journal.ppat.1004347

Chan, J. D., Cupit, P. M., Gunaratne, G. S., McCorvy, J. D., Yang, Y., Stoltz, K., … Marchant, J. S. (2017). The anthelmintic praziquantel is a human serotoninergic G-protein-coupled

receptor ligand. *Nature Communications*, *8*(1), 1910. https://doi.org/10.1038/s41467-017-02084-0

Cheng, G., Luo, R., Hu, C., Lin, J., Bai, Z., Zhang, B., & Wang, H. (2013). TiO2-based phosphoproteomic analysis of schistosomes: characterization of phosphorylated proteins in the different stages and sex of Schistosoma japonicum. *Journal of Proteome Research*, *12*(2), 729–742. https://doi.org/10.1021/pr3007864

Cheng, W., Curti, E., Rezende, W. C., Kwityn, C., Zhan, B., Gillespie, P., … Bottazzi, M. E. (2013). Biophysical and formulation studies of the *Schistosoma mansoni* TSP-2 extracellular domain recombinant protein, a lead vaccine candidate antigen for intestinal schistosomiasis. *Human Vaccines & Immunotherapeutics*, *9*(11), 2351–2361. https://doi.org/10.4161/hv.25788

Chi, M., Evans, H., Gilchrist, J., Mayhew, J., Hoffman, A., Pearsall, E. A., … Skelding, K. A. (2016). Phosphorylation of calcium/calmodulin-stimulated protein kinase II at T286 enhances invasion and migration of human breast cancer cells. *Scientific Reports*, *6*(1), 33132. https://doi.org/10.1038/srep33132

Chin, E. R. (2005). Role of Ca^{2+} /calmodulin-dependent kinases in skeletal muscle plasticity. *Journal of Applied Physiology*, *99*(2), 414–423. https://doi.org/10.1152/japplphysiol.00015.2005

Chitsulo, L., Loverde, P., & Engels, D. (2004). Focus: Schistosomiasis. *Nature Reviews Microbiology*, *2*(1), 12–13. https://doi.org/10.1038/nrmicro801

Cioli, D., & Pica-Mattoccia, L. (2003). Praziquantel. *Parasitology Research*, *90 Supp 1*, S3-9. https://doi.org/10.1007/s00436-002-0751-z

Cioli, D., Pica-Mattoccia, L., Basso, A., & Guidi, A. (2014). Schistosomiasis control: praziquantel forever? *Molecular and Biochemical Parasitology*, *195*(1), 23–29. https://doi.org/10.1016/j.molbiopara.2014.06.002

Clark, D. A., & Coker, R. (1998). Transforming growth factor-beta (TGF-beta). *The International Journal of Biochemistry & Cell Biology*, *30*(3), 293–298. Retrieved from http://www.ncbi.nlm.nih.gov/pubmed/9611771

Coakley, G., Wright, M. D., & Borger, J. G. (2019). Schistosoma mansoni-Derived Lipids in Extracellular Vesicles: Potential Agonists for Eosinophillic Tissue Repair. *Frontiers in Immunology*, *10*, 1010. https://doi.org/10.3389/fimmu.2019.01010

Cohen, P. (2001). The role of protein phosphorylation in human health and disease. *European Journal of Biochemistry*, *268*(19), 5001–5010. https://doi.org/10.1046/j.0014-

2956.2001.02473.x

Colley, D. G., Bustinduy, A. L., Secor, W. E., & King, C. H. (2014). Human schistosomiasis. *The Lancet*, *383*(9936), 2253–2264. https://doi.org/10.1016/S0140-6736(13)61949-2

Collins, J. J., King, R. S., Cogswell, A., Williams, D. L., & Newmark, P. A. (2011). An Atlas for Schistosoma mansoni Organs and Life-Cycle Stages Using Cell Type-Specific Markers and Confocal Microscopy. *PLoS Neglected Tropical Diseases*, *5*(3), e1009. https://doi.org/10.1371/journal.pntd.0001009

Collins, J. J., Wang, B., Lambrus, B. G., Tharp, M. E., Iyer, H., & Newmark, P. a. (2013). Adult somatic stem cells in the human parasite Schistosoma mansoni. *Nature*, *494*(7438), 476–479. https://doi.org/10.1038/nature11924

Conesa, A., Götz, S., García-Gómez, J. M., Terol, J., Talón, M., & Robles, M. (2005). Blast2GO: a universal tool for annotation, visualization and analysis in functional genomics research. *Bioinformatics (Oxford, England)*, *21*(18), 3674–3676. https://doi.org/10.1093/bioinformatics/bti610

Correnti, J. M., Brindley, P. J., & Pearce, E. J. (2005). Long-term suppression of cathepsin B levels by RNA interference retards schistosome growth. *Molecular and Biochemical Parasitology*, *143*(2), 209–215. https://doi.org/10.1016/j.molbiopara.2005.06.007

Couto, F. F. B., Coelho, P. M. Z., Araújo, N., Kusel, J. R., Katz, N., Jannotti-Passos, L. K., & Mattos, A. C. A. (2011). Schistosoma mansoni: a method for inducing resistance to praziquantel using infected Biomphalaria glabrata snails. *Memorias Do Instituto Oswaldo Cruz*, *106*(2), 153–157. Retrieved from http://www.ncbi.nlm.nih.gov/pubmed/21537673

Crompton, P. D., Kayala, M. A., Traore, B., Kayentao, K., Ongoiba, A., Weiss, G. E., … Pierce, S. K. (2010). A prospective analysis of the Ab response to Plasmodium falciparum before and after a malaria season by protein microarray. *Proceedings of the National Academy of Sciences of the United States of America*, *107*(15), 6958–6963. https://doi.org/10.1073/pnas.1001323107

Curwen, R. S., Ashton, P. D., Johnston, D. A., & Wilson, R. A. (2004). The Schistosoma mansoni soluble proteome: a comparison across four life-cycle stages. *Molecular and Biochemical Parasitology*, *138*(1), 57–66. https://doi.org/10.1016/J.MOLBIOPARA.2004.06.016

Daniels, L. J., Wallace, R. S., Nicholson, O. M., Wilson, G. A., McDonald, F. J., Jones, P. P., … Erickson, J. R. (2018). Inhibition of calcium/calmodulin-dependent kinase II restores contraction and relaxation in isolated cardiac muscle from type 2 diabetic rats. *Cardiovascular Diabetology*, *17*(1), 89. https://doi.org/10.1186/s12933-018-0732-x

Dashatan, N. A., Tavirani, M. R., Zali, H., Koushki, M., & Ahmadi, N. (2018). Prediction of Leishmania Major Key Proteins via Topological Analysis of Protein-Protein Interaction Network. *Galen Medical Journal GMJ.*, *7*(0), e1129. Retrieved from https://www.gmj.ir/index.php/gmj/article/view/1129/html

Davies, S. J., Shoemaker, C. B., & Pearce, E. J. (1998). A divergent member of the transforming growth factor beta receptor family from Schistosoma mansoni is expressed on the parasite surface membrane. *The Journal of Biological Chemistry*, *273*(18), 11234–11240. Retrieved from http://www.ncbi.nlm.nih.gov/pubmed/9556614

Day, T. A., Bennett, J. L., & Pax, R. A. (1994). Serotonin and its requirement for maintenance of contractility in muscle fibres isolated from Schistosoma mansoni. *Parasitology*, *108 (Pt 4)*, 425–432. Retrieved from http://www.ncbi.nlm.nih.gov/pubmed/8008457

de Oliveira, P. S. L., Ferraz, F. A. N., Pena, D. A., Pramio, D. T., Morais, F. A., & Schechtman, D. (2016). Revisiting protein kinase-substrate interactions: Toward therapeutic development. *Science Signaling*, *9*(420), re3. https://doi.org/10.1126/scisignal.aad4016

de Paula, R. G., de Magalhães Ornelas, A. M., Morais, E. R., de Souza Gomes, M., de Paula Aguiar, D., Magalhães, L. G., & Rodrigues, V. (2015). Proteasome stress responses in Schistosoma mansoni. *Parasitology Research*, *114*(5), 1747–1760. https://doi.org/10.1007/s00436-015-4360-z

de Saram, P. S. R., Ressurreição, M., Davies, A. J., Rollinson, D., Emery, A. M., & Walker, A. J. (2013). Functional mapping of protein kinase A reveals its importance in adult Schistosoma mansoni motor activity. *PLoS Neglected Tropical Diseases*, *7*(1), e1988. https://doi.org/10.1371/journal.pntd.0001988

Deracinois, B., Flahaut, C., Duban-Deweer, S., Karamanos, Y., Deracinois, B., Flahaut, C., … Karamanos, Y. (2013). Comparative and Quantitative Global Proteomics Approaches: An Overview. *Proteomes*, *1*(3), 180–218. https://doi.org/10.3390/proteomes1030180

Dionne, U., Chartier, F. J. M., López de los Santos, Y., Lavoie, N., Bernard, D. N., Banerjee, S. L., … Bisson, N. (2018). Direct Phosphorylation of SRC Homology 3 Domains by Tyrosine Kinase Receptors Disassembles Ligand-Induced Signaling Networks. *Molecular Cell*, *70*(6), 995-1007.e11. https://doi.org/10.1016/j.molcel.2018.05.013

Dissous, C., Ahier, A., & Khayath, N. (2007). Protein tyrosine kinases as new potential targets against human schistosomiasis. *BioEssays*, *29*(12), 1281–1288. https://doi.org/10.1002/bies.20662

Doenhoff, M. J., Cioli, D., & Utzinger, J. (2008). Praziquantel: mechanisms of action, resistance and new derivatives for schistosomiasis. *Current Opinion in Infectious Diseases*, *21*(6),

659–667. https://doi.org/10.1097/QCO.0b013e328318978f

Doolan, D. L., Mu, Y., Unal, B., Sundaresh, S., Hirst, S., Valdez, C., … Felgner, P. L. (2008). Profiling humoral immune responses to P. falciparum infection with protein microarrays. *PROTEOMICS*, *8*(22), 4680–4694. https://doi.org/10.1002/pmic.200800194

Dorsey, C. H., Cousin, C. E., Lewis, F. a, & Stirewalt, M. a. (2002). Ultrastructure of the Schistosoma mansoni cercaria. *Micron (Oxford, England : 1993)*, *33*(3), 279–323. Retrieved from http://www.ncbi.nlm.nih.gov/pubmed/11742750

Dukic, A. R., Gerbaud, P., Guibourdenche, J., Thiede, B., Taskén, K., & Pidoux, G. (2018). Ezrin-anchored PKA phosphorylates serine 369 and 373 on connexin 43 to enhance gap junction assembly, communication, and cell fusion. *Biochemical Journal*, *475*(2), 455–476. https://doi.org/10.1042/BCJ20170529

Eglen, R. M., & Reisine, T. (2009). The Current Status of Drug Discovery Against the Human Kinome. *ASSAY and Drug Development Technologies*, *7*(1), 22–43. https://doi.org/10.1089/adt.2008.164

Eilers, W., Gevers, W., van Overbeek, D., de Haan, A., Jaspers, R. T., Hilbers, P. A., … Flück, M. (2014). Muscle-type specific autophosphorylation of CaMKII isoforms after paced contractions. *BioMed Research International*, *2014*, 943806. https://doi.org/10.1155/2014/943806

Eilers, W., Jaspers, R. T., de Haan, A., Ferrié, C., Valdivieso, P., & Flück, M. (2014). CaMKII content affects contractile, but not mitochondrial, characteristics in regenerating skeletal muscle. *BMC Physiology*, *14*(1), 7. https://doi.org/10.1186/s12899-014-0007-z

El Ridi, R., Mohamed, S. H., & Tallima, H. (2003). Incubation of Schistosoma mansoni Lung-Stage Schistosomula in Corn Oil Exposes Their Surface Membrane Antigenic Specificities. *Journal of Parasitology*, *89*(5), 1064–1067. https://doi.org/10.1645/GE-3122RN

Erasmus, D. A. (1975). Schistosoma mansoni: Development of the vitelline cell, its role in drug sequestration, and changes induced by Astiban. *Experimental Parasitology*, *38*(2), 240–256. https://doi.org/10.1016/0014-4894(75)90027-2

Erickson, J. R. (2014). Mechanisms of CaMKII Activation in the Heart. *Frontiers in Pharmacology*, *5*, 59. https://doi.org/10.3389/fphar.2014.00059

Erondu, N. E., & Kennedy, M. B. (1985). Regional distribution of type II Ca2+/calmodulin-dependent protein kinase in rat brain. *The Journal of Neuroscience : The Official Journal of the Society for Neuroscience*, *5*(12), 3270–3277. Retrieved from http://www.ncbi.nlm.nih.gov/pubmed/4078628

Esteves, A., Joseph, L., Paulino, M., & Ehrlich, R. (1997). Remarks on the phylogeny and structure of fatty acid binding proteins from parasitic platyhelminths. *International Journal for Parasitology*, *27*(9), 1013–1023. Retrieved from http://www.ncbi.nlm.nih.gov/pubmed/9363483

Evans, T. I. A., & Shea, M. A. (2009). Energetics of calmodulin domain interactions with the calmodulin binding domain of CaMKII. *Proteins*, *76*(1), 47–61. https://doi.org/10.1002/prot.22317

Fairfax, K., Nascimento, M., Ching, S., Huang, -Cheng, Everts, B., & Pearce, E. J. (2012). Th2 responses in schistosomiasis. *Semin Immunopathol*, *34*(6), 863–871. https://doi.org/10.1007/s00281-012-0354-4

Fallon, P. G., & Doenhoff, M. J. (1994). Drug-Resistant Schistosomiasis: Resistance to Praziquantel and Oxamniquine Induced in Schistosoma Mansoni in Mice is Drug Specific. *The American Journal of Tropical Medicine and Hygiene*, *51*(1), 83–88. https://doi.org/10.4269/ajtmh.1994.51.83

Fallon, P. G., Smith, P., & Dunne, D. W. (1998). Type 1 and type 2 cytokine-producing mouse CD4+ and CD8+ T cells in acuteSchistosoma mansoni infection. *European Journal of Immunology*, *28*(4), 1408–1416. https://doi.org/10.1002/(SICI)1521-4141(199804)28:04<1408::AID-IMMU1408>3.0.CO;2-H

Fernandes, R. S., Barbosa, T. C., Barbosa, M. M. F., Miyasato, P. A., Nakano, E., Leite, L. C. C., & Farias, L. P. (2017). Stage and tissue expression patterns of Schistosoma mansoni venom allergen-like proteins SmVAL 4, 13, 16 and 24. *Parasites & Vectors*, *10*(1), 223. https://doi.org/10.1186/s13071-017-2144-2

Fields, S., & Song, O. (1989). A novel genetic system to detect protein–protein interactions. *Nature*, *340*(6230), 245–246. https://doi.org/10.1038/340245a0

Figueiredo, B. C.-P., Ricci, N. D., de Assis, N. R. G., de Morais, S. B., Fonseca, C. T., & Oliveira, S. C. (2015). Kicking in the Guts: Schistosoma mansoni Digestive Tract Proteins are Potential Candidates for Vaccine Development. *Frontiers in Immunology*, *6*, 22. https://doi.org/10.3389/fimmu.2015.00022

Fire, A., Xu, S., Montgomery, M. K., Kostas, S. A., Driver, S. E., & Mello, C. C. (1998). Potent and specific genetic interference by double-stranded RNA in Caenorhabditis elegans. *Nature*, *391*(6669), 806–811. https://doi.org/10.1038/35888

Forrester, S. G., Warfel, P. W., & Pearce, E. J. (2004). Tegumental expression of a novel type II receptor serine/threonine kinase (SmRK2) in Schistosoma mansoni. *Molecular and Biochemical Parasitology*, *136*(2), 149–156.

https://doi.org/10.1016/j.molbiopara.2004.03.007

Frank, R. (1992). Spot-synthesis: an easy technique for the positionally addressable, parallel chemical synthesis on a membrane support. *Tetrahedron*, *48*(42), 9217–9232. https://doi.org/10.1016/S0040-4020(01)85612-X

Fujita-Yamaguchi, Y., Bagramyan, K., Yamaguchi, Y., Ikeda, A., Dohmae, N., Hong, T. B., & Kalkum, M. (2018). Mass spectrometric revival of an l-rhamnose– and d-galactose–specific lectin from a lost strain of *Streptomyces*. *Journal of Biological Chemistry*, *293*(1), 368–378. https://doi.org/10.1074/jbc.M117.812719

Furlong, S. T. (1991). Unique roles for lipids in Schistosoma mansoni. *Parasitology Today (Personal Ed.)*, *7*(2), 59–62. Retrieved from http://www.ncbi.nlm.nih.gov/pubmed/15463424

Gaertner, T. R., Kolodziej, S. J., Wang, D., Kobayashi, R., Koomen, J. M., Stoops, J. K., & Waxham, M. N. (2004). Comparative Analyses of the Three-dimensional Structures and Enzymatic Properties of α, β, γ, and δ Isoforms of Ca $^{2+}$ -Calmodulin-dependent Protein Kinase II. *Journal of Biological Chemistry*, *279*(13), 12484–12494. https://doi.org/10.1074/jbc.M313597200

Gao, N., Luo, J., Uray, K., Qian, A., Yin, S., Wang, G., … Hu, H. (2012). CaMKII Is Essential for the Function of the Enteric Nervous System. *PLoS ONE*, *7*(8), e44426. https://doi.org/10.1371/journal.pone.0044426

Gerdes, F. (2007). *Focus Migration: Senegal*. Retrieved from http://focus-migration.hwwi.de/uploads/tx_wilpubdb/CP_10_Senegal.pdf

Gnad, F., Gunawardena, J., & Mann, M. (2011). PHOSIDA 2011: the posttranslational modification database. *Nucleic Acids Research*, *39*(Database issue), D253-60. https://doi.org/10.1093/nar/gkq1159

Gnad, F., Young, A., Zhou, W., Lyle, K., Ong, C. C., Stokes, M. P., … Hoeflich, K. P. (2013). Systems-wide Analysis of K-Ras, Cdc42, and PAK4 Signaling by Quantitative Phosphoproteomics. *Molecular & Cellular Proteomics*, *12*(8), 2070–2080. https://doi.org/10.1074/mcp.M112.027052

Gobert, G. N., Chai, M., & McManus, D. P. (2007). Biology of the schistosome lung-stage schistosomulum. *Parasitology*, *134*(Pt 4), 453–460. https://doi.org/10.1017/S0031182006001648

Godawska-Matysik, A., & Kieć-Kononowicz, K. (2006). Biotransformation of praziquantel by human cytochrome p450 3A4 (CYP 3A4). *Acta Poloniae Pharmaceutica*, *63*(5), 381–385.

Retrieved from http://www.ncbi.nlm.nih.gov/pubmed/17357589

Gouignard, N. (2011). Caractérisation moléculaire des Récepteurs Venus Kinase : étude fonctionnelle chez le parasite Schistosoma mansoni. *Http://Www.Theses.Fr*. Retrieved from http://www.theses.fr/2011LIL2S034

Graefe, G., Hohorst, W., & Drager, H. (1967). Forked Tail of the Cercaria of Schistosoma mansoni—a Rowing Device. *Nature*, *215*(5097), 207–208. https://doi.org/10.1038/215207a0

Gray, D. J., Ross, A. G., Li, Y.-S., & McManus, D. P. (2011). Diagnosis and management of schistosomiasis. *Bmj*, *342*(may17 1), d2651–d2651. https://doi.org/10.1136/bmj.d2651

Greenberg, R. M. (2005). Are Ca2+ channels targets of praziquantel action? *International Journal for Parasitology*, *35*(1), 1–9. https://doi.org/10.1016/j.ijpara.2004.09.004

Grevelding, C. G., Langner, S., & Dissous, C. (2018). Kinases: Molecular Stage Directors for Schistosome Development and Differentiation. *Trends in Parasitology*, *34*(3), 246–260. https://doi.org/10.1016/j.pt.2017.12.001

Griffith, L. C. (2004). Regulation of Calcium/Calmodulin-Dependent Protein Kinase II Activation by Intramolecular and Intermolecular Interactions. *Journal of Neuroscience*, *24*(39), 8394–8398. https://doi.org/10.1523/JNEUROSCI.3604-04.2004

Grimsrud, P. A., Swaney, D. L., Wenger, C. D., Beauchene, N. A., & Coon, J. J. (2010). Phosphoproteomics for the masses. *ACS Chemical Biology*, *5*(1), 105–119. https://doi.org/10.1021/cb900277e

Gryseels, B. Polman, K. Clerinx, J. Kestens, L. (2006). Human Schistosomiasis. The Lancet.

Gryseels, B. (2012). Schistosomiasis. *Infectious Disease Clinics of North America*, *26*(2), 383–397. https://doi.org/10.1016/j.idc.2012.03.004

Guillou, F., Roger, E., Moné, Y., Rognon, A., Grunau, C., Théron, A., … Gourbal, B. E. F. (2007). Excretory–secretory proteome of larval Schistosoma mansoni and Echinostoma caproni, two parasites of Biomphalaria glabrata. *Molecular and Biochemical Parasitology*, *155*(1), 45–56. https://doi.org/10.1016/J.MOLBIOPARA.2007.05.009

Haas, W, Diekhoff, D., Koch, K., Schmalfuss, G., & Loy, C. (1997). Schistosoma mansoni cercariae: stimulation of acetabular gland secretion is adapted to the chemical composition of mammalian skin. *The Journal of Parasitology*, *83*(6), 1079–1085. Retrieved from http://www.ncbi.nlm.nih.gov/pubmed/9406783

Haas, W, Grabe, K., Geis, C., Päch, T., Stoll, K., Fuchs, M., … Loy, C. (2001). Recognition and invasion of human skin by Schistosoma mansoni cercariae: the key-role of L-arginine.

Parasitology, *124*(Pt 2), 153–167. Retrieved from http://www.ncbi.nlm.nih.gov/pubmed/11860033

Haas, Wilfried, Beran, B., & Loy, C. (2008). Selection of the Host's Habitat by Cercariae: From Laboratory Experiments to the Field. *Journal of Parasitology*, *94*(6), 1233–1238. https://doi.org/10.1645/GE-1192.1

Haeberlein, S., & Haas, W. (2008). Chemical attractants of human skin for swimming Schistosoma mansoni cercariae. *Parasitology Research*, *102*(4), 657–662. https://doi.org/10.1007/s00436-007-0807-1

Haider, M., Haselgrübler, T., Sonnleitner, A., Aberger, F., & Hesse, J. (2016). A Double-Hybridization Approach for the Transcription- and Amplification-Free Detection of Specific mRNA on a Microarray. *Microarrays (Basel, Switzerland)*, *5*(1). https://doi.org/10.3390/microarrays5010005

Hams, E., Aviello, G., & Fallon, P. G. (2013). The schistosoma granuloma: friend or foe? *Frontiers in Immunology*, *4*, 89. https://doi.org/10.3389/fimmu.2013.00089

Hanks, S K, Quinn, A. M., & Hunter, T. (1988). The protein kinase family: conserved features and deduced phylogeny of the catalytic domains. *Science (New York, N.Y.)*, *241*(4861), 42–52. Retrieved from http://www.ncbi.nlm.nih.gov/pubmed/3291115

Hanks, Steven K. (2003). Genomic analysis of the eukaryotic protein kinase superfamily: a perspective. *Genome Biology*, *4*(5), 111. https://doi.org/10.1186/GB-2003-4-5-111

Hanson, P. I., Kapiloff, M. S., Lou, L. L., Rosenfeld, M. G., Schulman, H., Bennett, M. K., … Smith, M. (1989). Expression of a multifunctional Ca2+/calmodulin-dependent protein kinase and mutational analysis of its autoregulation. *Neuron*, *3*(1), 59–70. https://doi.org/10.1016/0896-6273(89)90115-3

Hanson, P. I., Meyer, T., Stryer, L., & Schulman, H. (1994). Dual role of calmodulin in autophosphorylation of multifunctional CaM kinase may underlie decoding of calcium signals. *Neuron*, *12*(5), 943–956. Retrieved from http://www.ncbi.nlm.nih.gov/pubmed/8185953

Harnett, W., & Kusel, J. R. (1986). Increased exposure of parasite antigens at the surface of adult male Schistosoma mansoni exposed to praziquantel in vitro. *Parasitology*, *93 (Pt 2)*, 401–405. Retrieved from http://www.ncbi.nlm.nih.gov/pubmed/2431374

Harsha, H. C., & Pandey, A. (2010). Phosphoproteomics in cancer. *Molecular Oncology*, *4*(6), 482–495. https://doi.org/10.1016/j.molonc.2010.09.004

Hayashi, M., Fearns, C., Eliceiri, B., Yang, Y., & Lee, J.-D. (2005). Big Mitogen-Activated

Protein Kinase 1/Extracellular Signal-Regulated Kinase 5 Signaling Pathway Is Essential for Tumor-Associated Angiogenesis. *Cancer Research*, *65*(17), 7699–7706. https://doi.org/10.1158/0008-5472.CAN-04-4540

He, Y.-X., Chen, L., & Ramaswamy, K. (2002). Schistosoma mansoni, S. haematobium, and S. japonicum: early events associated with penetration and migration of schistosomula through human skin. *Experimental Parasitology*, *102*(2), 99–108. https://doi.org/10.1016/S0014-4894(03)00024-9

Hem, S., Gherardini, P. F., Fortéa, J. O. y, Hourdel, V., Morales, M. A., Watanabe, R., … Späth, G. F. (2010). Identification of Leishmania-specific protein phosphorylation sites by LC-ESI-MS/MS and comparative genomics analyses. *PROTEOMICS*, *10*(21), 3868–3883. https://doi.org/10.1002/pmic.201000305

Herbert, D. R., Hölscher, C., Mohrs, M., Arendse, B., Schwegmann, A., Radwanska, M., … Brombacher, F. (2004). Alternative macrophage activation is essential for survival during schistosomiasis and downmodulates T helper 1 responses and immunopathology. *Immunity*, *20*(5), 623–635. Retrieved from http://www.ncbi.nlm.nih.gov/pubmed/15142530

Herwaldt, B. L., Tao, L. F., van Pelt, W., Tsang, V. C., & Bruce, J. I. (1995). Persistence of Schistosoma haematobium infection despite multiple courses of therapy with praziquantel. *Clinical Infectious Diseases : An Official Publication of the Infectious Diseases Society of America*, *20*(2), 309–315. Retrieved from http://www.ncbi.nlm.nih.gov/pubmed/7742435

Hirst, N. L., Lawton, S. P., & Walker, A. J. (2016). Protein kinase A signalling in Schistosoma mansoni cercariae and schistosomules. *International Journal for Parasitology*, *46*(7), 425–437. https://doi.org/10.1016/j.ijpara.2015.12.001

Ho, M. W., Kaetzel, M. A., Armstrong, D. L., & Shears, S. B. (2001). Regulation of a human chloride channel. a paradigm for integrating input from calcium, type ii calmodulin-dependent protein kinase, and inositol 3,4,5,6-tetrakisphosphate. *The Journal of Biological Chemistry*, *276*(22), 18673–18680. https://doi.org/10.1074/jbc.M101128200

Hockley, D., & McLaren, D. (1973). Schistosoma mansoni: Changes in the outer membrane of the tegument during development from cercaria to adult worm. *International Journal for Parasitology*, *3*, 13–25.

Holtfreter, M. C., Moné, H., Müller-Stöver, I., Mouahid, G., & Richter, J. (2014). Schistosoma haematobium infections acquired in Corsica, France, August 2013. *Euro Surveillance : Bulletin Europeen Sur Les Maladies Transmissibles = European Communicable Disease Bulletin*, *19*(22). Retrieved from http://www.ncbi.nlm.nih.gov/pubmed/24925456

Huberfeld, G., Wittner, L., Clemenceau, S., Baulac, M., Kaila, K., Miles, R., & Rivera, C. (2007).

Perturbed Chloride Homeostasis and GABAergic Signaling in Human Temporal Lobe Epilepsy. *Journal of Neuroscience*, *27*(37), 9866–9873. https://doi.org/10.1523/JNEUROSCI.2761-07.2007

Hudmon, A., & Schulman, H. (2002). Structure-function of the multifunctional Ca2+/calmodulin-dependent protein kinase II. *The Biochemical Journal*, *364*(Pt 3), 593–611. https://doi.org/10.1042/BJ20020228

Hunter, T. (2002). Tyrosine phosphorylation in cell signaling and disease. *The Keio Journal of Medicine*, *51*(2), 61–71. Retrieved from http://www.ncbi.nlm.nih.gov/pubmed/12125907

Huttlin, E. L., Jedrychowski, M. P., Elias, J. E., Goswami, T., Rad, R., Beausoleil, S. A., … Gygi, S. P. (2010). A tissue-specific atlas of mouse protein phosphorylation and expression. *Cell*, *143*(7), 1174–1189. https://doi.org/10.1016/j.cell.2010.12.001

Huyse, T., Webster, B. L., Geldof, S., Stothard, J. R., Diaw, O. T., Polman, K., & Rollinson, D. (2009). Bidirectional Introgressive Hybridization between a Cattle and Human Schistosome Species. *PLoS Pathogens*, *5*(9), e1000571. https://doi.org/10.1371/journal.ppat.1000571

Ingram, J. R., Rafi, S. B., Eroy-Reveles, A. A., Ray, M., Lambeth, L., Hsieh, I., … McKerrow, J. H. (2012). Investigation of the proteolytic functions of an expanded cercarial elastase gene family in Schistosoma mansoni. *PLoS Neglected Tropical Diseases*, *6*(4), e1589. https://doi.org/10.1371/journal.pntd.0001589

Ishida, A., Kameshita, I., Okuno, S., Kitani, T., & Fujisawa, H. (1995). A Novel Highly Specific and Potent Inhibitor of Calmodulin-Dependent Protein Kinase II. *Biochemical and Biophysical Research Communications*, *212*(3), 806–812. https://doi.org/10.1006/bbrc.1995.2040

Ismail, M. M., Taha, S. A., Farghaly, A. M., & el-Azony, A. S. (1994). Laboratory induced resistance to praziquantel in experimental schistosomiasis. *Journal of the Egyptian Society of Parasitology*, *24*(3), 685–695. Retrieved from http://www.ncbi.nlm.nih.gov/pubmed/7844435

Ismail, M., Metwally, A., Farghaly, A., Bruce, J., Tao, L. F., & Bennett, J. L. (1996). Characterization of isolates of Schistosoma mansoni from Egyptian villagers that tolerate high doses of praziquantel. *The American Journal of Tropical Medicine and Hygiene*, *55*(2), 214–218. Retrieved from http://www.ncbi.nlm.nih.gov/pubmed/8780463

Jankovic, D., Cheever, A. W., Kullberg, M. C., Wynn, T. A., Yap, G., Caspar, P., … Sher, A. (1998). CD4+ T cell-mediated granulomatous pathology in schistosomiasis is downregulated by a B cell-dependent mechanism requiring Fc receptor signaling. *The Journal of Experimental Medicine*, *187*(4), 619–629. Retrieved from

http://www.ncbi.nlm.nih.gov/pubmed/9463412

Jeziorski, M. C., & Greenberg, R. M. (2006). Voltage-gated calcium channel subunits from platyhelminths: potential role in praziquantel action. *International Journal for Parasitology*, *36*(6), 625–632. https://doi.org/10.1016/j.ijpara.2006.02.002

Jones, M. K., Lustigman, S., & Loukas, A. (2008). Tracking the odysseys of juvenile schistosomes to understand host interactions. *PLoS Neglected Tropical Diseases*, *2*(7), e257. https://doi.org/10.1371/journal.pntd.0000257

Kapp, K, Schüssler, P., Kunz, W., & Grevelding, C. G. (2001). Identification, isolation and characterization of a Fyn-like tyrosine kinase from Schistosoma mansoni. *Parasitology*, *122*(Pt 3), 317–327. Retrieved from http://www.ncbi.nlm.nih.gov/pubmed/11289068

Kapp, Katja, Knobloch, J., Schüssler, P., Sroka, S., Lammers, R., Kunz, W., & Grevelding, C. G. (2004). The Schistosoma mansoni Src kinase TK3 is expressed in the gonads and likely involved in cytoskeletal organization. *Molecular and Biochemical Parasitology*, *138*(2), 171–182. https://doi.org/10.1016/j.molbiopara.2004.07.010

Kersey, P. J., Allen, J. E., Christensen, M., Davis, P., Falin, L. J., Grabmueller, C., … Staines, D. M. (2014). Ensembl Genomes 2013: scaling up access to genome-wide data. *Nucleic Acids Research*, *42*(Database issue), D546-52. https://doi.org/10.1093/nar/gkt979

Khayath, N., Vicogne, J., Ahier, A., BenYounes, A., Konrad, C., Trolet, J., … Dissous, C. (2007). Diversification of the insulin receptor family in the helminth parasite Schistosoma mansoni. *The FEBS Journal*, *274*(3), 659–676. https://doi.org/10.1111/j.1742-4658.2006.05610.x

Kim, I., Je, H. D., Gallant, C., Zhan, Q., Riper, D. V, Badwey, J. A., … Morgan, K. G. (2000). Ca2+-calmodulin-dependent protein kinase II-dependent activation of contractility in ferret aorta. *The Journal of Physiology*, *526 Pt 2*(Pt 2), 367–374. https://doi.org/10.1111/j.1469-7793.2000.00367.x

Kinoshita-Kikuta, E., Kinoshita, E., & Koike, T. (2016). Phosphopeptide Detection with Biotin-Labeled Phos-tag. In *Methods in molecular biology (Clifton, N.J.)* (Vol. 1355, pp. 17–29). https://doi.org/10.1007/978-1-4939-3049-4_2

Kinoshita, E., Kinoshita-Kikuta, E., & Koike, T. (2013). Phos-tag-Based Microarray Techniques Advance Phosphoproteomics. *Journal of Proteomics & Bioinformatics*, *01*(S6). https://doi.org/10.4172/jpb.S6-008

Kinoshita, E., Kinoshita-Kikuta, E., Sugiyama, Y., Fukada, Y., Ozeki, T., & Koike, T. (2012). Highly sensitive detection of protein phosphorylation by using improved Phos-tag Biotin. *PROTEOMICS*, *12*(7), 932–937. https://doi.org/10.1002/pmic.201100639

Kjetland, E. F., Ndhlovu, P. D., Gomo, E., Mduluza, T., Midzi, N., Gwanzura, L., … Gundersen, S. G. (2006). Association between genital schistosomiasis and HIV in rural Zimbabwean women. *AIDS*, *20*(4), 593–600. https://doi.org/10.1097/01.aids.0000210614.45212.0a

Knobloch, J., Beckmann, S., Burmeister, C., Quack, T., & Grevelding, C. G. (2007). Tyrosine kinase and cooperative TGFβ signaling in the reproductive organs of Schistosoma mansoni. *Experimental Parasitology*, *117*(3), 318–336. https://doi.org/10.1016/j.exppara.2007.04.006

Knobloch, J., Winnen, R., Quack, M., Kunz, W., & Grevelding, C. G. (2002). A novel Syk-family tyrosine kinase from Schistosoma mansoni which is preferentially transcribed in reproductive organs. *Gene*, *294*(1–2), 87–97. https://doi.org/10.1016/S0378-1119(02)00760-6

Kohn, A. B., Anderson, P. A., Roberts-Misterly, J. M., & Greenberg, R. M. (2001). Schistosome calcium channel beta subunits. Unusual modulatory effects and potential role in the action of the antischistosomal drug praziquantel. *The Journal of Biological Chemistry*, *276*(40), 36873–36876. https://doi.org/10.1074/jbc.C100273200

Kosako, H., & Nagano, K. (2011). Quantitative phosphoproteomics strategies for understanding protein kinase-mediated signal transduction pathways. *Expert Review of Proteomics*, *8*(1), 81–94. https://doi.org/10.1586/epr.10.104

Krautz-Peterson, G., Simoes, M., Faghiri, Z., Ndegwa, D., Oliveira, G., Shoemaker, C. B., & Skelly, P. J. (2010). Suppressing glucose transporter gene expression in schistosomes impairs parasite feeding and decreases survival in the mammalian host. *PLoS Pathogens*, *6*(6), e1000932. https://doi.org/10.1371/journal.ppat.1000932

Kreegipuu, A., Blom, N., Brunak, S., & Järv, J. (1998). Statistical analysis of protein kinase specificity determinants. *FEBS Letters*, *430*(1–2), 45–50. https://doi.org/10.1016/S0014-5793(98)00503-1

Krishnamurthy, D., Katsikis, G., Bhargava, A., & Prakash, M. (2017). Schistosoma mansoni cercariae swim efficiently by exploiting an elastohydrodynamic coupling. *Nature Physics*, *13*, 266–271. https://doi.org/10.1038/NPHYS3924

Kunz, W. (2001). Schistosome male–female interaction: induction of germ-cell differentiation. *Trends in Parasitology*, *17*(5), 227–231. https://doi.org/10.1016/S1471-4922(01)01893-1

Kwon, S., Kim, H., & Kim, H. S. (2017). Identification of Pharmacologically Tractable Protein Complexes in Cancer Using the R-Based Network Clustering and Visualization Program MCODER. *BioMed Research International*, *2017*, 1–8. https://doi.org/10.1155/2017/1016305

Lai, Y., Nairn, A. C., & Greengard, P. (1986). Autophosphorylation reversibly regulates the Ca2+/calmodulin-dependence of Ca2+/calmodulin-dependent protein kinase II. *Proceedings of the National Academy of Sciences of the United States of America*, *83*(12), 4253–4257. Retrieved from http://www.ncbi.nlm.nih.gov/pubmed/3012560

Lasonder, E., Green, J. L., Camarda, G., Talabani, H., Holder, A. A., Langsley, G., & Alano, P. (2012). The Plasmodium falciparum schizont phosphoproteome reveals extensive phosphatidylinositol and cAMP-protein kinase A signaling. *Journal of Proteome Research*, *11*(11), 5323–5337. https://doi.org/10.1021/pr300557m

Lewit-Bentley, A., & Réty, S. (2000). EF-hand calcium-binding proteins. *Current Opinion in Structural Biology*, *10*(6), 637–643. https://doi.org/10.1016/S0959-440X(00)00142-1

Li, H.-J., Liang, Y.-S., Dai, J.-R., Wang, W., Qu, G.-L., Li, Y.-Z., … Wei, J.-Y. (2011). Studies on resistance of Schistosoma to praziquantel XIV experimental comparison of susceptibility to praziquantel between PZQ-resistant isolates and PZQ-susceptible isolates of Schistosoma japonicum in stages of adult worms, miracidia and cercariae. *Zhongguo Xue Xi Chong Bing Fang Zhi Za Zhi = Chinese Journal of Schistosomiasis Control*, *23*(6), 611–619. Retrieved from http://www.ncbi.nlm.nih.gov/pubmed/22379813

Li, X., Wilmanns, M., Thornton, J., & Kohn, M. (2013). Elucidating Human Phosphatase-Substrate Networks. *Science Signaling*, *6*(275), rs10–rs10. https://doi.org/10.1126/scisignal.2003203

Lin, Y.-L., Meng, Y., Jiang, W., & Roux, B. (2013). Explaining why Gleevec is a specific and potent inhibitor of Abl kinase. *Proceedings of the National Academy of Sciences*, *110*(5), 1664–1669. https://doi.org/10.1073/pnas.1214330110

Linding, R., Jensen, L. J., Ostheimer, G. J., van Vugt, M. A. T. M., Jørgensen, C., Miron, I. M., … Pawson, T. (2007). Systematic discovery of in vivo phosphorylation networks. *Cell*, *129*(7), 1415–1426. https://doi.org/10.1016/j.cell.2007.05.052

Lisman, J., Yasuda, R., & Raghavachari, S. (2012). Mechanisms of CaMKII action in long-term potentiation. *Nature Reviews. Neuroscience*, *13*(3), 169–182. https://doi.org/10.1038/nrn3192

Liu, F., Lu, J., Hu, W., Wang, S.-Y., Cui, S.-J., Chi, M., … Han, Z.-G. (2006). New perspectives on host-parasite interplay by comparative transcriptomic and proteomic analyses of Schistosoma japonicum. *PLoS Pathogens*, *2*(4), e29. https://doi.org/10.1371/journal.ppat.0020029

Logan-Klumpler, F. J., De Silva, N., Boehme, U., Rogers, M. B., Velarde, G., McQuillan, J. A., … Berriman, M. (2012). GeneDB--an annotation database for pathogens. *Nucleic Acids*

Research, *40*(Database issue), D98-108. https://doi.org/10.1093/nar/gkr1032

Loker, E. S., & Brant, S. V. (2006). Diversification, dioecy and dimorphism in schistosomes. *Trends in Parasitology*, *22*(11), 521–528. https://doi.org/10.1016/j.pt.2006.09.001

Long, T., Vanderstraete, M., Cailliau, K., Morel, M., Lescuyer, A., Gouignard, N., … Dissous, C. (2012). SmSak, the Second Polo-Like Kinase of the Helminth Parasite Schistosoma mansoni: Conserved and Unexpected Roles in Meiosis. *PLoS ONE*, *7*(6), e40045. https://doi.org/10.1371/journal.pone.0040045

Loukas, A., Tran, M., & Pearson, M. S. (2007). Schistosome membrane proteins as vaccines. *International Journal for Parasitology*, *37*(3–4), 257–263. https://doi.org/10.1016/j.ijpara.2006.12.001

Loverde, P. T., Osman, A., & Hinck, A. (2007). Schistosoma mansoni: TGF-beta signaling pathways. *Experimental Parasitology*, *117*(3), 304–317. https://doi.org/10.1016/j.exppara.2007.06.002

Löwenberg, M., Tuynman, J., Scheffer, M., Verhaar, A., Vermeulen, L., van Deventer, S., … Peppelenbosch, M. (2006). Kinome Analysis Reveals Nongenomic Glucocorticoid Receptor-Dependent Inhibition of Insulin Signaling. *Endocrinology*, *147*(7), 3555–3562. https://doi.org/10.1210/en.2005-1602

Löwenberg, M., Verhaar, A. P., Bilderbeek, J., Marle, J. van, Buttgereit, F., Peppelenbosch, M. P., … Hommes, D. W. (2006). Glucocorticoids cause rapid dissociation of a T-cell-receptor-associated protein complex containing LCK and FYN. *EMBO Reports*, *7*(10), 1023–1029. https://doi.org/10.1038/sj.embor.7400775

Ludtmann, M. H. R., Rollinson, D., Emery, A. M., & Walker, A. J. (2009). Protein kinase C signalling during miracidium to mother sporocyst development in the helminth parasite, Schistosoma mansoni. *International Journal for Parasitology*, *39*(11), 1223–1233. https://doi.org/10.1016/J.IJPARA.2009.04.002

Luo, R., Zhou, C., Lin, J., Yang, D., Shi, Y., & Cheng, G. (2012). Identification of in vivo protein phosphorylation sites in human pathogen Schistosoma japonicum by a phosphoproteomic approach. *Journal of Proteomics*, *75*(3), 868–877. https://doi.org/10.1016/j.jprot.2011.10.003

Macarron, R., Banks, M. N., Bojanic, D., Burns, D. J., Cirovic, D. A., Garyantes, T., … Sittampalam, G. S. (2011). Impact of high-throughput screening in biomedical research. *Nature Reviews Drug Discovery*, *10*(3), 188–195. https://doi.org/10.1038/nrd3368

Machado-Silva, J. R., Lanfredi, R. M., & Gomes, D. C. (1997). Morphological Study of Adult

Male Worms of Schistosoma mansoni Sambon, 1907 by Scanning Electron Microscopy. *Memórias Do Instituto Oswaldo Cruz*, *92*(5), 647–653. https://doi.org/10.1590/S0074-02761997000500016

Mahajan, N. P., Whang, Y. E., Mohler, J. L., & Earp, H. S. (2005). Activated tyrosine kinase Ack1 promotes prostate tumorigenesis: role of Ack1 in polyubiquitination of tumor suppressor Wwox. *Cancer Research*, *65*(22), 10514–10523. https://doi.org/10.1158/0008-5472.CAN-05-1127

Maier, L. S., Zhang, T., Chen, L., DeSantiago, J., Brown, J. H., & Bers, D. M. (2003). Transgenic CaMKIIδ $_{C}$ Overexpression Uniquely Alters Cardiac Myocyte Ca $^{2+}$ Handling. *Circulation Research*, *92*(8), 904–911. https://doi.org/10.1161/01.RES.0000069685.20258.F1

Mair, G. R., Maule, A. G., Day, T. A., & Halton, D. W. (2000). A confocal microscopical study of the musculature of adult Schistosoma mansoni. *Parasitology*, *121 (Pt 2)*, 163–170. Retrieved from http://www.ncbi.nlm.nih.gov/pubmed/11085236

Maksimov, P., Zerweck, J., Maksimov, A., Hotop, A., Gross, U., Pleyer, U., … Schares, G. (2012). Peptide microarray analysis of in silico-predicted epitopes for serological diagnosis of Toxoplasma gondii infection in humans. *Clinical and Vaccine Immunology : CVI*, *19*(6), 865–874. https://doi.org/10.1128/CVI.00119-12

Manning, G., Whyte, D. B., Martinez, R., Hunter, T., & Sudarsanam, S. (2002). The Protein Kinase Complement of the Human Genome. *Science*, *298*(5600), 1912–1934. https://doi.org/10.1126/science.1075762

Martin, J., Anamika, K., & Srinivasan, N. (2010). Classification of protein kinases on the basis of both kinase and non-kinase regions. *PloS One*, *5*(9), e12460. https://doi.org/10.1371/journal.pone.0012460

Maskos, U., & Southern, E. M. (1992). Parallel analysis of oligodeoxyribonucleotide (oligonucleotide) interactions. I. Analysis of factors influencing oligonucleotide duplex formation. *Nucleic Acids Research*, *20*(7), 1675–1678. https://doi.org/10.1093/nar/20.7.1675

Matsuzaki, M., Honkura, N., Ellis-Davies, G. C. R., & Kasai, H. (2004). Structural basis of long-term potentiation in single dendritic spines. *Nature*, *429*(6993), 761–766. https://doi.org/10.1038/nature02617

Mayya, V., & Han, D. K. (2009). Phosphoproteomics by mass spectrometry: insights, implications, applications and limitations. *Expert Review of Proteomics*, *6*(6), 605–618. https://doi.org/10.1586/epr.09.84

McKenzie, M. (2017) Akt signalling in the human parasite *Schistosoma mansoni*. (PhD thesis), Kingston University

McKenzie, M., Kirk, R. S., & Walker, A. J. (2018). Glucose Uptake in the Human Pathogen Schistosoma mansoni Is Regulated Through Akt/Protein Kinase B Signaling. *The Journal of Infectious Diseases*, *218*(1), 152–164. https://doi.org/10.1093/infdis/jix654

McKerrow, J. H., & Salter, J. (2002). Invasion of skin by Schistosoma cercariae. *Trends in Parasitology*, *18*(5), 193–195. Retrieved from http://www.ncbi.nlm.nih.gov/pubmed/11983589

Mclaren, D. J., & Hockley, D. J. (1977). Blood flukes have a double outer membrane. *Nature*, *269*(5624), 147–149. Retrieved from http://www.ncbi.nlm.nih.gov/pubmed/71658

McManus, D. P., Dunne, D. W., Sacko, M., Utzinger, J., Vennervald, B. J., & Zhou, X.-N. (2018). Schistosomiasis. *Nature Reviews Disease Primers*, *4*(1), 13. https://doi.org/10.1038/s41572-018-0013-8

McWilliam, H. E., Driguez, P., Piedrafita, D., McManus, D. P., & Meeusen, E. N. (2014). Discovery of novel Schistosoma japonicum antigens using a targeted protein microarray approach. *Parasites & Vectors*, *7*(1), 290. https://doi.org/10.1186/1756-3305-7-290

Meister, I., Ingram-Sieber, K., Cowan, N., Todd, M., Robertson, M. N., Meli, C., … Keiser, J. (2014). Activity of praziquantel enantiomers and main metabolites against Schistosoma mansoni. *Antimicrobial Agents and Chemotherapy*, *58*(9), 5466–5472. https://doi.org/10.1128/AAC.02741-14

Merrifield, M., Hotez, P. J., Beaumier, C. M., Gillespie, P., Strych, U., Hayward, T., & Bottazzi, M. E. (2016). Advancing a vaccine to prevent human schistosomiasis. *Vaccine*, *34*(26), 2988–2991. https://doi.org/10.1016/j.vaccine.2016.03.079

Meuleman, E. A., Holzmann, P. J., & Peet, R. C. (1980). The development of daughter sporocysts inside the mother sporocyst of Schistosoma mansoni with special reference to the ultrastructure of the body wall. *Zeitschrift Fur Parasitenkunde (Berlin, Germany)*, *61*(3), 201–212. Retrieved from http://www.ncbi.nlm.nih.gov/pubmed/7368772

Meyer, T., Hanson, P. I., Stryer, L., & Schulman, H. (1992). Calmodulin trapping by calcium-calmodulin-dependent protein kinase. *Science (New York, N.Y.)*, *256*(5060), 1199–1202. Retrieved from http://www.ncbi.nlm.nih.gov/pubmed/1317063

Mollapour, M., & Neckers, L. (2012). Post-translational modifications of Hsp90 and their contributions to chaperone regulation. *Biochimica et Biophysica Acta*, *1823*(3), 648–655. https://doi.org/10.1016/j.bbamcr.2011.07.018

Moorhead, G. B. G., De Wever, V., Templeton, G., & Kerk, D. (2009). Evolution of protein phosphatases in plants and animals. *Biochemical Journal*, *417*(2), 401–409. https://doi.org/10.1042/BJ20081986

Morais, E. R., Oliveira, K. C., Paula, R. G. de, Ornelas, A. M. M., Moreira, É. B. C., Badoco, F. R., … Rodrigues, V. (2017). Effects of proteasome inhibitor MG-132 on the parasite Schistosoma mansoni. *PLOS ONE*, *12*(9), e0184192. https://doi.org/10.1371/journal.pone.0184192

Morales, M. E., Rinaldi, G., Gobert, G. N., Kines, K. J., Tort, J. F., & Brindley, P. J. (2008). RNA interference of Schistosoma mansoni cathepsin D, the apical enzyme of the hemoglobin proteolysis cascade. *Molecular and Biochemical Parasitology*, *157*(2), 160–168. https://doi.org/10.1016/j.molbiopara.2007.10.009

Morel, M., Vanderstraete, M., Cailliau, K., Lescuyer, A., Lancelot, J., & Dissous, C. (2014a). Compound library screening identified Akt/PKB kinase pathway inhibitors as potential key molecules for the development of new chemotherapeutics against schistosomiasis. *International Journal for Parasitology. Drugs and Drug Resistance*, *4*(3), 256–266. https://doi.org/10.1016/j.ijpddr.2014.09.004

Morel, M., Vanderstraete, M., Cailliau, K., Lescuyer, A., Lancelot, J., & Dissous, C. (2014b). Compound library screening identified Akt/PKB kinase pathway inhibitors as potential key molecules for the development of new chemotherapeutics against schistosomiasis. *International Journal for Parasitology: Drugs and Drug Resistance*, *4*(3), 256–266. https://doi.org/10.1016/J.IJPDDR.2014.09.004

Mostafa, M. H., Sheweita, S. A., & O'Connor, P. J. (1999). Relationship between schistosomiasis and bladder cancer. *Clinical Microbiology Reviews*, *12*(1), 97–111. Retrieved from http://www.ncbi.nlm.nih.gov/pubmed/9880476

Mulcahy, L. A., Pink, R. C., & Carter, D. R. F. (2014). Routes and mechanisms of extracellular vesicle uptake. *Journal of Extracellular Vesicles*, *3*. https://doi.org/10.3402/jev.v3.24641

Muth, S., Sayasone, S., Odermatt-Biays, S., Phompida, S., Duong, S., & Odermatt, P. (2010). Schistosoma mekongi in Cambodia and Lao People's Democratic Republic (pp. 179–203). https://doi.org/10.1016/S0065-308X(10)72007-8

Naguib, F. N. M., & el Kouni, M. H. (2014). Nucleoside kinases in adult Schistosoma mansoni: Phosphorylation of pyrimidine nucleosides. *Molecular and Biochemical Parasitology*, *194*(1–2), 53–55. https://doi.org/10.1016/j.molbiopara.2014.04.007

Naula, C., Parsons, M., & Mottram, J. C. (2005). Protein kinases as drug targets in trypanosomes and Leishmania. *Biochimica et Biophysica Acta (BBA) - Proteins and Proteomics*, *1754*(1–

2), 151–159. https://doi.org/10.1016/j.bbapap.2005.08.018

Nett, I. R. E., Martin, D. M. A., Miranda-Saavedra, D., Lamont, D., Barber, J. D., Mehlert, A., & Ferguson, M. A. J. (2009). The phosphoproteome of bloodstream form Trypanosoma brucei, causative agent of African sleeping sickness. *Molecular & Cellular Proteomics : MCP*, *8*(7), 1527–1538. https://doi.org/10.1074/mcp.M800556-MCP200

Newton, A. C. (1995). Protein kinase C: structure, function, and regulation. *The Journal of Biological Chemistry*, *270*(48), 28495–28498. https://doi.org/10.1074/JBC.270.48.28495

Nishi, H., Hashimoto, K., & Panchenko, A. R. (2011). Phosphorylation in protein-protein binding: effect on stability and function. *Structure (London, England : 1993)*, *19*(12), 1807–1815. https://doi.org/10.1016/j.str.2011.09.021

Nogi, T., Zhang, D., Chan, J. D., & Marchant, J. S. (2009). A Novel Biological Activity of Praziquantel Requiring Voltage-Operated Ca2+ Channel β Subunits: Subversion of Flatworm Regenerative Polarity. *PLoS Neglected Tropical Diseases*, *3*(6), e464. https://doi.org/10.1371/journal.pntd.0000464

Nogueira, N. P. de A., Souza, C. F. de, Saraiva, F. M. de S., Sultano, P. E., Dalmau, S. R., Bruno, R. E., … Paes, M. C. (2011). Heme-Induced ROS in Trypanosoma Cruzi Activates CaMKII-Like That Triggers Epimastigote Proliferation. One Helpful Effect of ROS. *PLoS ONE*, *6*(10), e25935. https://doi.org/10.1371/journal.pone.0025935

Nowacki, F. C., Swain, M. T., Klychnikov,O. I., Niazi,U., Ivens, A., Quintana,J. F., Hensbergen, P. J., Hokke,C. H., Buck, A. H., and Hoffmann, K. F. (2015) Protein and small non-coding RNA-enriched extracellular vesicles are released by the pathogenic blood fluke *Schistosoma mansoni*. *J Extracell Vesicle*, 4: 10.3402/jev.v4.28665

Nolen, B., Taylor, S., & Ghosh, G. (2004). Regulation of protein kinases; controlling activity through activation segment conformation. *Molecular Cell*, *15*(5), 661–675. https://doi.org/10.1016/j.molcel.2004.08.024

Obenauer, J. C., Cantley, L. C., & Yaffe, M. B. (2003). Scansite 2.0: proteome-wide prediction of cell signaling interactions using short sequence motifs. Retrieved August 24, 2015, from http://scansite3.mit.edu/#faq2

Oliveira, S. C., Figueiredo, B. C., Cardoso, L. S., & Carvalho, E. M. (2016). A double edged sword: Schistosoma mansoni Sm29 regulates both Th1 and Th2 responses in inflammatory mucosal diseases. *Mucosal Immunology*, *9*(6), 1366–1371. https://doi.org/10.1038/mi.2016.69

Olliaro, P., Delgado-Romero, P., & Keiser, J. (2014). The little we know about the

pharmacokinetics and pharmacodynamics of praziquantel (racemate and R-enantiomer). *Journal of Antimicrobial Chemotherapy*, *69*(4), 863–870. https://doi.org/10.1093/jac/dkt491

Osman, A., Niles, E. G., & LoVerde, P. T. (2001). Identification and characterization of a Smad2 homologue from Schistosoma mansoni, a transforming growth factor-beta signal transducer. *The Journal of Biological Chemistry*, *276*(13), 10072–10082. https://doi.org/10.1074/jbc.M005933200

Parikh, K., Diks, S. H., Tuynman, J. H. B., Verhaar, A., Löwenberg, M., Hommes, D. W., … Peppelenbosch, M. P. (2009). Comparison of Peptide Array Substrate Phosphorylation of c-Raf and Mitogen Activated Protein Kinase Kinase Kinase 8. *PLoS ONE*, *4*(7), e6440. https://doi.org/10.1371/journal.pone.0006440

Pax, R., Bennett, J. L., & Fetterer, R. (1978). A benzodiazepine derivative and praziquantel: effects on musculature of Schistosoma mansoni and Schistosoma japonicum. *Naunyn-Schmiedeberg's Archives of Pharmacology*, *304*(3), 309–315. Retrieved from http://www.ncbi.nlm.nih.gov/pubmed/714190

Pearce, E. J., & MacDonald, A. S. (2002a). The immunobiology of schistosomiasis. *Nature Reviews. Immunology*, *2*(7), 499–511. https://doi.org/10.1038/nri843

Pearce, E. J., & MacDonald, A. S. (2002b). The immunobiology of schistosomiasis. *Nature Reviews Immunology*, *2*(7), 499–511. https://doi.org/10.1038/nri843

Pease, B. N., Huttlin, E. L., Jedrychowski, M. P., Talevich, E., Harmon, J., Dillman, T., … Chakrabarti, D. (2013a). Global analysis of protein expression and phosphorylation of three stages of Plasmodium falciparum intraerythrocytic development. *Journal of Proteome Research*, *12*(9), 4028–4045. https://doi.org/10.1021/pr400394g

Pease, B. N., Huttlin, E. L., Jedrychowski, M. P., Talevich, E., Harmon, J., Dillman, T., … Chakrabarti, D. (2013b). Global Analysis of Protein Expression and Phosphorylation of Three Stages of *Plasmodium falciparum* Intraerythrocytic Development. *Journal of Proteome Research*, *12*(9), 4028–4045. https://doi.org/10.1021/pr400394g

Pellicena, P., & Schulman, H. (2014). CaMKII inhibitors: from research tools to therapeutic agents. *Frontiers in Pharmacology*, *5*. https://doi.org/10.3389/FPHAR.2014.00021

Peppelenbosch, M. P. (2012). Kinome profiling. *Scientifica*, *2012*, 306798. https://doi.org/10.6064/2012/306798

Pereira, A. S. A., Padilha, R. J. R., Lima-Filho, J. L., & Chaves, M. E. C. (2011). Scanning electron microscopy of the human low-density lipoprotein interaction with the tegument of

Schistosoma mansoni. *Parasitology Research*, *109*(5), 1395–1402. https://doi.org/10.1007/s00436-011-2386-4

Pica-Mattoccia, L., & Cioli, D. (2004). Sex- and stage-related sensitivity of Schistosoma mansoni to in vivo and in vitro praziquantel treatment. *International Journal for Parasitology*, *34*(4), 527–533. https://doi.org/10.1016/j.ijpara.2003.12.003

Pica-Mattoccia, L., Orsini, T., Basso, A., Festucci, A., Liberti, P., Guidi, A., … Valle, C. (2008). Schistosoma mansoni: Lack of correlation between praziquantel-induced intra-worm calcium influx and parasite death. *Experimental Parasitology*, *119*(3), 332–335. https://doi.org/10.1016/J.EXPPARA.2008.03.012

Protasio, A. V, Tsai, I. J., Babbage, A., Nichol, S., Hunt, M., Aslett, M. A., … Berriman, M. (2012). A systematically improved high quality genome and transcriptome of the human blood fluke Schistosoma mansoni. *PLoS Neglected Tropical Diseases*, *6*(1), e1455. https://doi.org/10.1371/journal.pntd.0001455

Queiroz, R. M. L., Charneau, S., Motta, F. N., Santana, J. M., Roepstorff, P., & Ricart, C. A. O. (2013). Comprehensive Proteomic Analysis of *Trypanosoma cruzi* Epimastigote Cell Surface Proteins by Two Complementary Methods. *Journal of Proteome Research*, *12*(7), 3255–3263. https://doi.org/10.1021/pr400110h

Ramachandran, H., Skelly, P. J., & Shoemaker, C. B. (1996). The Schistosoma mansoni epidermal growth factor receptor homologue, SER, has tyrosine kinase activity and is localized in adult muscle. *Molecular and Biochemical Parasitology*, *83*(1), 1–10. Retrieved from http://www.ncbi.nlm.nih.gov/pubmed/9010837

Ramirez, B., Bickle, Q., Yousif, F., Fakorede, F., Mouries, M.-A., & Nwaka, S. (2007). Schistosomes: challenges in compound screening. *Expert Opinion on Drug Discovery*, *2*(sup1), S53–S61. https://doi.org/10.1517/17460441.2.S1.S53

Reinders, J., & Sickmann, A. (2005). State-of-the-art in phosphoproteomics. *PROTEOMICS*, *5*(16), 4052–4061. https://doi.org/10.1002/pmic.200401289

Ressurreição, M., De Saram, P., Kirk, R. S., Rollinson, D., Emery, A. M., Page, N. M., … Walker, A. J. (2014). Protein kinase C and extracellular signal-regulated kinase regulate movement, attachment, pairing and egg release in Schistosoma mansoni. *PLoS Neglected Tropical Diseases*, *8*(6), e2924. https://doi.org/10.1371/journal.pntd.0002924

Ressurreição, M., Elbeyioglu, F., Kirk, R. S., Rollinson, D., Emery, A. M., Page, N. M., & Walker, A. J. (2016). Molecular characterization of host-parasite cell signalling in Schistosoma mansoni during early development OPEN. *Nature Publishing Group*. https://doi.org/10.1038/srep35614

Ressurreição, M., Kirk, R. S., Rollinson, D., Emery, A. M., Page, N. M., & Walker, A. J. (2015). Sensory Protein Kinase Signaling in Schistosoma mansoni Cercariae: Host Location and Invasion. *The Journal of Infectious Diseases*, *212*(11), 1787. https://doi.org/10.1093/INFDIS/JIV464

Ressurreição, M., Rollinson, D., Emery, A. M., & Walker, A. J. (2011a). A role for p38 MAPK in the regulation of ciliary motion in a eukaryote. *BMC Cell Biology*, *12*(1), 6. https://doi.org/10.1186/1471-2121-12-6

Ressurreição, M., Rollinson, D., Emery, A. M., & Walker, A. J. (2011b). A role for p38 mitogen-activated protein kinase in early post-embryonic development of Schistosoma mansoni. *Molecular and Biochemical Parasitology*, *180*(1), 51–55. https://doi.org/10.1016/j.molbiopara.2011.07.002

Rezende, C. M. F., Coitinho, J. B., Costa, M., Silva, M. R., Giusta, M., Oliveira-Prado, R., … Goes, A. M. (2018). Biochemical analysis and identification of linear B-cell epitopes from recombinant Sm21.7 antigen from Schistosoma mansoni. *Molecular Immunology*, *101*, 29–37. https://doi.org/10.1016/J.MOLIMM.2018.05.019

Rich, R. C., & Schulman, H. (1998). Substrate-directed function of calmodulin in autophosphorylation of Ca2+/calmodulin-dependent protein kinase II. *The Journal of Biological Chemistry*, *273*(43), 28424–28429. Retrieved from http://www.ncbi.nlm.nih.gov/pubmed/9774470

Rinaldi, G., Morales, M. E., Alrefaei, Y. N., Cancela, M., Castillo, E., Dalton, J. P., … Brindley, P. J. (2009). RNA interference targeting leucine aminopeptidase blocks hatching of Schistosoma mansoni eggs. *Molecular and Biochemical Parasitology*, *167*(2), 118–126. https://doi.org/10.1016/j.molbiopara.2009.05.002

Ritsema, T., Joore, J., van Workum, W., & Pieterse, C. M. (2007). Kinome profiling of Arabidopsis using arrays of kinase consensus substrates. *Plant Methods*, *3*(1), 3. https://doi.org/10.1186/1746-4811-3-3

Ritsema, T., & Peppelenbosch, M. P. (2009). Kinome profiling of sugar signaling in plants using multiple platforms. *Plant Signaling & Behavior*, *4*(12), 1169–1173. https://doi.org/10.4161/psb.4.12.10022

Ritsema, T., van Zanten, M., Leon-Reyes, A., Voesenek, L. A. C. J., Millenaar, F. F., Pieterse, C. M. J., & Peeters, A. J. M. (2010). Kinome Profiling Reveals an Interaction Between Jasmonate, Salicylate and Light Control of Hyponastic Petiole Growth in Arabidopsis thaliana. *PLoS ONE*, *5*(12), e14255. https://doi.org/10.1371/journal.pone.0014255

Robertson, A. J., Trost, B., Scruten, E., Robertson, T., Mostajeran, M., Connor, W., … Napper,

S. (2014). Identification of developmentally-specific kinotypes and mechanisms of Varroa mite resistance through whole-organism, kinome analysis of honeybee. *Frontiers in Genetics*, *5*, 139. https://doi.org/10.3389/fgene.2014.00139

Robinson, D. R., Wu, Y.-M., & Lin, S.-F. (2000). The protein tyrosine kinase family of the human genome. *Oncogene*, *19*(49), 5548–5557. https://doi.org/10.1038/sj.onc.1203957

Rofatto, H. K., Parker-Manuel, S. J., Barbosa, T. C., Tararam, C. A., Alan Wilson, R., Leite, L. C. C., & Farias, L. P. (2012). Tissue expression patterns of Schistosoma mansoni Venom Allergen-Like proteins 6 and 7. *International Journal for Parasitology*, *42*(7), 613–620. https://doi.org/10.1016/j.ijpara.2012.04.008

Rose, A. J., Kiens, B., & Richter, E. A. (2006). Ca^{2+} -calmodulin-dependent protein kinase expression and signalling in skeletal muscle during exercise. *The Journal of Physiology*, *574*(3), 889–903. https://doi.org/10.1113/jphysiol.2006.111757

Rosenberg, O. S., Deindl, S., Sung, R.-J., Nairn, A. C., & Kuriyan, J. (2005). Structure of the Autoinhibited Kinase Domain of CaMKII and SAXS Analysis of the Holoenzyme. *Cell*, *123*(5), 849–860. https://doi.org/10.1016/j.cell.2005.10.029

Ross, A. G., Vickers, D., Olds, G. R., Shah, S. M., & Mcmanus, D. P. (2007). Katayama syndrome. *Infection.Thelancet.Com*, *7*. https://doi.org/10.1016/S1473-3099(07)70053-1

Rueden, C. T., Schindelin, J., Hiner, M. C., DeZonia, B. E., Walter, A. E., Arena, E. T., & Eliceiri, K. W. (2017). ImageJ2: ImageJ for the next generation of scientific image data. *BMC Bioinformatics*, *18*(1), 529. https://doi.org/10.1186/s12859-017-1934-z

Sacco, F., Perfetto, L., Castagnoli, L., & Cesareni, G. (2012). The human phosphatase interactome: An intricate family portrait. *FEBS Letters*, *586*(17), 2732–2739. https://doi.org/10.1016/j.febslet.2012.05.008

Salter, J. P., Lim, K.-C., Hansell, E., Hsieh, I., & McKerrow, J. H. (2000). Schistosome Invasion of Human Skin and Degradation of Dermal Elastin Are Mediated by a Single Serine Protease. *Journal of Biological Chemistry*, *275*(49), 38667–38673. https://doi.org/10.1074/jbc.M006997200

Samoil, V., Dagenais, M., Ganapathy, V., Aldridge, J., Glebov, A., Jardim, A., & Ribeiro, P. (2018). Vesicle-based secretion in schistosomes: Analysis of protein and microRNA (miRNA) content of exosome-like vesicles derived from Schistosoma mansoni. *Scientific Reports*, *8*(1), 3286. https://doi.org/10.1038/s41598-018-21587-4

Samuelson, J. C., Quinn, J. J., & Caulfield, J. P. (1984). Hatching, chemokinesis, and transformation of miracidia of Schistosoma mansoni. *The Journal of Parasitology*, *70*(3),

321–331. Retrieved from http://www.ncbi.nlm.nih.gov/pubmed/6541688

Santos, J., Fernandes, E., Ferreira, J. A., Lima, L., Tavares, A., Peixoto, A., … Santos, L. L. (2014). P53 and Cancer-Associated Sialylated Glycans Are Surrogate Markers of Cancerization of the Bladder Associated with Schistosoma haematobium Infection. *PLoS Neglected Tropical Diseases*, *8*(12), e3329. https://doi.org/10.1371/journal.pntd.0003329

Schopf, F. H., Biebl, M. M., & Buchner, J. (2017). The HSP90 chaperone machinery. *Nature Reviews Molecular Cell Biology*, *18*(6), 345–360. https://doi.org/10.1038/nrm.2017.20

Schüssler, P., Grevelding, C. G., & Kunz, W. (1997). Identification of Ras, MAP kinases, and a GAP protein in Schistosoma mansoni by immunoblotting and their putative involvement in male-female interaction. *Parasitology*, *115 (Pt 6)*, 629–634. Retrieved from http://www.ncbi.nlm.nih.gov/pubmed/9488874

Scott, J. K., & Smith, G. P. (1990). Searching for peptide ligands with an epitope library. *Science (New York, N.Y.)*, *249*(4967), 386–390. Retrieved from http://www.ncbi.nlm.nih.gov/pubmed/1696028

Shalaby, K. A., Yin, L., Thakur, A., Christen, L., Niles, E. G., & LoVerde, P. T. (2003). Protection against Schistosoma mansoni utilizing DNA vaccination with genes encoding Cu/Zn cytosolic superoxide dismutase, signal peptide-containing superoxide dismutase and glutathione peroxidase enzymes. *Vaccine*, *22*(1), 130–136. Retrieved from http://www.ncbi.nlm.nih.gov/pubmed/14604580

Sharma, K., D'Souza, R. C. J., Tyanova, S., Schaab, C., Wiśniewski, J. R., Cox, J., & Mann, M. (2014). Ultradeep Human Phosphoproteome Reveals a Distinct Regulatory Nature of Tyr and Ser/Thr-Based Signaling. *Cell Reports*, *8*(5), 1583–1594. https://doi.org/10.1016/j.celrep.2014.07.036

Shaw, M. K., & Erasmus, D. A. (1987). Schistosoma mansoni: structural damage and tegumental repair after in vivo treatment with praziquantel. *Parasitology*, *94 (Pt 2)*, 243–254. Retrieved from http://www.ncbi.nlm.nih.gov/pubmed/3108831

Shebel, H. M., Elsayes, K. M., Abou El Atta, H. M., Elguindy, Y. M., & El-Diasty, T. A. (2012). Genitourinary Schistosomiasis: Life Cycle and Radiologic-Pathologic Findings. *RadioGraphics*, *32*(4), 1031–1046. https://doi.org/10.1148/rg.324115162

Shiff, C. J., & Graczyk, T. K. (1994). A chemokinetic response in Schistosoma mansoni cercariae. *The Journal of Parasitology*, *80*(6), 879–883. Retrieved from http://www.ncbi.nlm.nih.gov/pubmed/7799158

Shinn, G. L. (1993). Formation of Egg Capsules by Flatworms (Phylum Platyhelminthes).

Transactions of the American Microscopical Society, *112*(1), 18. https://doi.org/10.2307/3226779

Shioda, N., & Fukunaga, K. (2017). Physiological and Pathological Roles of CaMKII-PP1 Signaling in the Brain. *International Journal of Molecular Sciences*, *19*(1). https://doi.org/10.3390/ijms19010020

Shuford, K. V., Turner, H. C., & Anderson, R. M. (2016). Compliance with anthelmintic treatment in the neglected tropical diseases control programmes: a systematic review. *Parasites & Vectors*, *9*(1), 29. https://doi.org/10.1186/s13071-016-1311-1

Siddiqui, A. A., Siddiqui, B. A., & Ganley-Leal, L. (2011). Schistosomiasis vaccines. *Human Vaccines*, *7*(11), 1192–1197. https://doi.org/10.4161/hv.7.11.17017

Sikkema, A. H., den Dunnen, W. F. A., Diks, S. H., Peppelenbosch, M. P., & de Bont, E. S. J. M. (2012). Optimizing targeted cancer therapy: Towards clinical application of systems biology approaches. *Critical Reviews in Oncology/Hematology*, *82*(2), 171–186. https://doi.org/10.1016/j.critrevonc.2011.05.002

Silva, I. M. da, Thiengo, R., Conceição, M. J., Rey, L., Lenzi, H. L., Pereira Filho, E., & Ribeiro, P. C. (2005). Therapeutic failure of praziquantel in the treatment of Schistosoma haematobium infection in Brazilians returning from Africa. *Memorias Do Instituto Oswaldo Cruz*, *100*(4), 445–449. https://doi.org//S0074-02762005000400018

Silva, L. M., Menezes, R. M. C., Oliveira, S. A. de, & Andrade, Z. A. (2003). Chemotherapeutic effects on larval stages of Schistosoma mansoni during infection and re-infection of mice. *Revista Da Sociedade Brasileira de Medicina Tropical*, *36*(3), 335–341. https://doi.org/10.1590/S0037-86822003000300004

Skelly, P J, & Shoemaker, C. B. (1996). Rapid appearance and asymmetric distribution of glucose transporter SGTP4 at the apical surface of intramammalian-stage Schistosoma mansoni. *Proceedings of the National Academy of Sciences of the United States of America*, *93*(8), 3642–3646. Retrieved from http://www.pubmedcentral.nih.gov/articlerender.fcgi?artid=39664&tool=pmcentrez&rendertype=abstract

Skelly, P J, & Shoemaker, C. B. (2001). Schistosoma mansoni proteases Sm31 (cathepsin B) and Sm32 (legumain) are expressed in the cecum and protonephridia of cercariae. *The Journal of Parasitology*, *87*(5), 1218–1221. https://doi.org/10.1645/0022-3395(2001)087[1218:SMPSCB]2.0.CO;2

Skelly, P J, Tielens, A. G., & Shoemaker, C. B. (1998). Glucose Transport and Metabolism in Mammalian-stage Schistosomes. *Parasitology Today (Personal Ed.)*, *14*(10), 402–406.

Retrieved from http://www.ncbi.nlm.nih.gov/pubmed/17040830

Skelly, Patrick J., & Alan Wilson, R. (2006). Making Sense of the Schistosome Surface. In *Advances in parasitology* (Vol. 63, pp. 185–284). https://doi.org/10.1016/S0065-308X(06)63003-0

Skelly, Patrick J., Da'dara, A. A., Li, X.-H., Castro-Borges, W., & Wilson, R. A. (2014). Schistosome Feeding and Regurgitation. *PLoS Pathogens*, *10*(8), e1004246. https://doi.org/10.1371/journal.ppat.1004246

Soderling, T. R., Chang, B., & Brickey, D. (2001). Cellular signaling through multifunctional Ca2+/calmodulin-dependent protein kinase II. *The Journal of Biological Chemistry*, *276*(6), 3719–3722. https://doi.org/10.1074/jbc.R000013200

Sotillo, J., Pearson, M., Becker, L., Mulvenna, J., & Loukas, A. (2015). A quantitative proteomic analysis of the tegumental proteins from Schistosoma mansoni schistosomula reveals novel potential therapeutic targets. *International Journal for Parasitology*, *45*(8), 505–516. https://doi.org/10.1016/j.ijpara.2015.03.004

Sotillo, J., Pearson, M., Potriquet, J., Becker, L., Pickering, D., Mulvenna, J., & Loukas, A. (2016). Extracellular vesicles secreted by Schistosoma mansoni contain protein vaccine candidates. *International Journal for Parasitology*, *46*(1), 1–5. https://doi.org/10.1016/J.IJPARA.2015.09.002

Sotillo, J., Pearson, M. S., Becker, L., Mekonnen, G. G., Amoah, A. S., van Dam, G., … Loukas, A. (2019). In-depth proteomic characterization of Schistosoma haematobium: Towards the development of new tools for elimination. *PLOS Neglected Tropical Diseases*, *13*(5), e0007362. https://doi.org/10.1371/journal.pntd.0007362

Stavreva, D. A., Kawasaki, M., Dundr, M., Koberna, K., Müller, W. G., Tsujimura-Takahashi, T., … McNally, J. G. (2006). Potential roles for ubiquitin and the proteasome during ribosome biogenesis. *Molecular and Cellular Biology*, *26*(13), 5131–5145. https://doi.org/10.1128/MCB.02227-05

Steiner, F., Ignatius, R., Friedrich-Jaenicke, B., Dieckmann, S., Harms, G., Poppert, S., & Mockenhaupt, F. P. (2013). Acute Schistosomiasis in European Students Returning From Fieldwork at Lake Tanganyika, Tanzania: Table 1. *Journal of Travel Medicine*, *20*(6), 380–383. https://doi.org/10.1111/jtm.12069

Steinmann, P., Keiser, J., Bos, R., Tanner, M., & Utzinger, J. (2006). Schistosomiasis and water resources development: systematic review, meta-analysis, and estimates of people at risk. *The Lancet Infectious Diseases*, *6*(7), 411–425. https://doi.org/10.1016/S1473-3099(06)70521-7

Stelma, F. F., Talla, I., Sow, S., Kongs, A., Niang, M., Polman, K., … Gryseels, B. (1995). Efficacy and side effects of praziquantel in an epidemic focus of Schistosoma mansoni. *The American Journal of Tropical Medicine and Hygiene*, *53*(2), 167–170. Retrieved from http://www.ncbi.nlm.nih.gov/pubmed/7677219

Stokes, M., Farnsworth, C., Gu, H., Jia, X., Worsfold, C., Yang, V., … Silva, J. (2015). Complementary PTM Profiling of Drug Response in Human Gastric Carcinoma by Immunoaffinity and IMAC Methods with Total Proteome Analysis. *Proteomes*, *3*(3), 160–183. https://doi.org/10.3390/proteomes3030160

Strack, S., Barban, M. A., Wadzinski, B. E., & Colbran, R. J. (1997). Differential inactivation of postsynaptic density-associated and soluble Ca2+/calmodulin-dependent protein kinase II by protein phosphatases 1 and 2A. *Journal of Neurochemistry*, *68*(5), 2119–2128. Retrieved from http://www.ncbi.nlm.nih.gov/pubmed/9109540

Strehl, C., Gaber, T., Löwenberg, M., Hommes, D. W., Verhaar, A. P., Schellmann, S., … Buttgereit, F. (2011). Origin and functional activity of the membrane-bound glucocorticoid receptor. *Arthritis & Rheumatism*, *63*(12), 3779–3788. https://doi.org/10.1002/art.30637

Sugawara, T., Hisatsune, C., Miyamoto, H., Ogawa, N., & Mikoshiba, K. (2017). Regulation of spinogenesis in mature Purkinje cells via mGluR/PKC-mediated phosphorylation of CaMKIIβ. *Proceedings of the National Academy of Sciences of the United States of America*, *114*(26), E5256–E5265. https://doi.org/10.1073/pnas.1617270114

Sumi, M., Kiuchi, K., Ishikawa, T., Ishii, A., Hagiwara, M., Nagatsu, T., & Hidaka, H. (1991). The newly synthesized selective Ca2+calmodulin dependent protein kinase II inhibitor KN-93 reduces dopamine contents in PC12h cells. *Biochemical and Biophysical Research Communications*, *181*(3), 968–975. https://doi.org/10.1016/0006-291X(91)92031-E

Sung, M.-K., Reitsma, J. M., Sweredoski, M. J., Hess, S., & Deshaies, R. J. (2016). Ribosomal proteins produced in excess are degraded by the ubiquitin-proteasome system. *Molecular Biology of the Cell*, *27*(17), 2642–2652. https://doi.org/10.1091/mbc.E16-05-0290

Swierczewski, B. E., & Davies, S. J. (2009). A schistosome cAMP-dependent protein kinase catalytic subunit is essential for parasite viability. *PLoS Neglected Tropical Diseases*, *3*(8), e505. https://doi.org/10.1371/journal.pntd.0000505

Swierczewski, B. E., & Davies, S. J. (2010a). Conservation of protein kinase a catalytic subunit sequences in the schistosome pathogens of humans. *Experimental Parasitology*, *125*(2), 156–160. https://doi.org/10.1016/j.exppara.2010.01.012

Swierczewski, B. E., & Davies, S. J. (2010b). Developmental regulation of protein kinase A expression and activity in Schistosoma mansoni. *International Journal for Parasitology*,

40(8), 929–935. https://doi.org/10.1016/j.ijpara.2010.01.001

Swulius, M. T., & Waxham, M. N. (2008). Ca2+/Calmodulin-dependent Protein Kinases. *Cellular and Molecular Life Sciences*, *65*(17), 2637–2657. https://doi.org/10.1007/s00018-008-8086-2

Szklarczyk, D., Franceschini, A., Wyder, S., Forslund, K., Heller, D., Huerta-Cepas, J., … von Mering, C. (2015). STRING v10: protein-protein interaction networks, integrated over the tree of life. *Nucleic Acids Research*, *43*(Database issue), D447-52. https://doi.org/10.1093/nar/gku1003

Tchuem Tchuenté, L. A., Southgate, V. R., Combes, C., & Jourdane, J. (1996). Mating behaviour in schistosomes: Are paired worms always faithful? *Parasitology Today*, *12*(6), 231–236. https://doi.org/10.1016/0169-4758(96)10020-X

Tebeje, B. M., Harvie, M., You, H., Loukas, A., & McManus, D. P. (2016). Schistosomiasis vaccines: where do we stand? *Parasites & Vectors*, *9*(1), 528. https://doi.org/10.1186/s13071-016-1799-4

Tendler, M., Almeida, M., Vilar, M., Pinto, P., & Limaverde-Sousa, G. (2018). Current Status of the Sm14/GLA-SE Schistosomiasis Vaccine: Overcoming Barriers and Paradigms towards the First Anti-Parasitic Human(itarian) Vaccine. *Tropical Medicine and Infectious Disease*, *3*(4), 121. https://doi.org/10.3390/tropicalmed3040121

Tendler, M., & Simpson, A. J. G. (2008). The biotechnology-value chain: Development of Sm14 as a schistosomiasis vaccine. *Acta Tropica*, *108*(2–3), 263–266. https://doi.org/10.1016/j.actatropica.2008.09.002

Tombes, R. M., Faison, M. O., & Turbeville, J. M. (2003). Organization and evolution of multifunctional Ca(2+)/CaM-dependent protein kinase genes. *Gene*, *322*, 17–31. Retrieved from http://www.ncbi.nlm.nih.gov/pubmed/14644494

Trieu, A., Kayala, M. A., Burk, C., Molina, D. M., Freilich, D. A., Richie, T. L., … Doolan, D. L. (2011). Sterile Protective Immunity to Malaria is Associated with a Panel of Novel *P. falciparum* Antigens. *Molecular & Cellular Proteomics*, *10*(9), M111.007948. https://doi.org/10.1074/mcp.M111.007948

Urbaniak, M. D. (2009). Casein kinase 1 isoform 2 is essential for bloodstream form Trypanosoma brucei. *Molecular and Biochemical Parasitology*, *166*(2), 183–185. https://doi.org/10.1016/j.molbiopara.2009.03.001

Urbaniak, M. D., Martin, D. M. A., & Ferguson, M. A. J. (2013). Global quantitative SILAC phosphoproteomics reveals differential phosphorylation is widespread between the

procyclic and bloodstream form lifecycle stages of Trypanosoma brucei. *Journal of Proteome Research*, *12*(5), 2233–2244. https://doi.org/10.1021/pr400086y

Vale, N., Gouveia, M. J., Rinaldi, G., Brindley, P. J., Gärtner, F., & Correia da Costa, J. M. (2017). Praziquantel for Schistosomiasis: Single-Drug Metabolism Revisited, Mode of Action, and Resistance. *Antimicrobial Agents and Chemotherapy*, *61*(5), e02582-16. https://doi.org/10.1128/AAC.02582-16

van Balkom, B. W. M., van Gestel, R. A., Brouwers, J. F. H. M., Krijgsveld, J., Tielens, A. G. M., Heck, A. J. R., & van Hellemond, J. J. (2005). Mass spectrometric analysis of the Schistosoma mansoni tegumental sub-proteome. *Journal of Proteome Research*, *4*(3), 958–966. https://doi.org/10.1021/pr050036w

Van Hellemond, J. J., Retra, K., Brouwers, J. F. H. M., van Balkom, B. W. M., Yazdanbakhsh, M., Shoemaker, C. B., & Tielens, A. G. M. (2006). Functions of the tegument of schistosomes: Clues from the proteome and lipidome. *International Journal for Parasitology*, *36*(6), 691–699. https://doi.org/10.1016/j.ijpara.2006.01.007

van Veelen, W., Korsse, S. E., van de Laar, L., & Peppelenbosch, M. P. (2011). The long and winding road to rational treatment of cancer associated with LKB1/AMPK/TSC/mTORC1 signaling. *Oncogene*, *30*(20), 2289–2303. https://doi.org/10.1038/onc.2010.630

van Vliet, M. T. H., Vögele, S., & Rübbelke, D. (2013). Water constraints on European power supply under climate change: impacts on electricity prices. *Environmental Research Letters*, *8*(3), 035010. https://doi.org/10.1088/1748-9326/8/3/035010

Vanderstraete, M., Gouignard, N., Cailliau, K., Morel, M., Hahnel, S., Leutner, S., … Dissous, C. (2014). Venus Kinase Receptors Control Reproduction in the Platyhelminth Parasite Schistosoma mansoni. *PLoS Pathogens*, *10*(5), e1004138. https://doi.org/10.1371/journal.ppat.1004138

Vercruysse, J., Albonico, M., Behnke, J. M., Kotze, A. C., Prichard, R. K., McCarthy, J. S., … Levecke, B. (2011). Is anthelmintic resistance a concern for the control of human soil-transmitted helminths? *International Journal for Parasitology: Drugs and Drug Resistance*, *1*(1), 14–27. https://doi.org/10.1016/J.IJPDDR.2011.09.002

Vicogne, J., Pin, J. P., Lardans, V., Capron, M., Noël, C., & Dissous, C. (2003). An unusual receptor tyrosine kinase of Schistosoma mansoni contains a Venus Flytrap module. *Molecular and Biochemical Parasitology*, *126*(1), 51–62. Retrieved from http://www.ncbi.nlm.nih.gov/pubmed/12554084

Villén, J., Beausoleil, S. A., Gerber, S. A., & Gygi, S. P. (2007). Large-scale phosphorylation analysis of mouse liver. *Proceedings of the National Academy of Sciences of the United*

States of America, *104*(5), 1488–1493. https://doi.org/10.1073/pnas.0609836104

Volkmer, R. (2009). Synthesis and Application of Peptide Arrays: Quo Vadis SPOT Technology. *ChemBioChem*, *10*(9), 1431–1442. https://doi.org/10.1002/cbic.200900078

Vos, T., Flaxman, A. D., Naghavi, M., Lozano, R., Michaud, C., Ezzati, M., … Murray, C. J. (2012). Years lived with disability (YLDs) for 1160 sequelae of 289 diseases and injuries 1990–2010: a systematic analysis for the Global Burden of Disease Study 2010. *The Lancet*, *380*(9859), 2163–2196. https://doi.org/10.1016/S0140-6736(12)61729-2

Wagner, S., Dybkova, N., Rasenack, E. C. L., Jacobshagen, C., Fabritz, L., Kirchhof, P., … Maier, L. S. (2006). Ca2+/calmodulin-dependent protein kinase II regulates cardiac Na+ channels. *Journal of Clinical Investigation*, *116*(12), 3127–3138. https://doi.org/10.1172/JCI26620

Walker, Anthony J, Ressurreição, M., & Rothermel, R. (2014). Exploring the function of protein kinases in schistosomes: perspectives from the laboratory and from comparative genomics. *Frontiers in Genetics*, *5*, 229. https://doi.org/10.3389/fgene.2014.00229

Walker, Anthony John. (2011). Insights into the functional biology of schistosomes. *Parasites & Vectors*, *4*(1), 203. https://doi.org/10.1186/1756-3305-4-203

Wang, J., Zhong, J., Chen, G., Li, M., Wu, F., & Pan, Y. (2015). ClusterViz: A Cytoscape APP for Cluster Analysis of Biological Network. *IEEE/ACM Transactions on Computational Biology and Bioinformatics*, *12*(4), 815–822. https://doi.org/10.1109/TCBB.2014.2361348

Wang, W., Wang, L., & Liang, Y.-S. (2012a). Susceptibility or resistance of praziquantel in human schistosomiasis: a review. *Parasitology Research*, *111*(5), 1871–1877. https://doi.org/10.1007/s00436-012-3151-z

Wang, W., Wang, L., & Liang, Y.-S. (2012b). Susceptibility or resistance of praziquantel in human schistosomiasis: a review. *Parasitology Research*, *111*(5), 1871–1877. https://doi.org/10.1007/s00436-012-3151-z

Ward, P., Equinet, L., Packer, J., & Doerig, C. (2004). Protein kinases of the human malaria parasite Plasmodium falciparum : the kinome of a divergent eukaryote. *BMC Genomics*, *5*(1), 79. https://doi.org/10.1186/1471-2164-5-79

Warren, K. S., Mahmoud, A. A., Cummings, P., Murphy, D. J., & Houser, H. B. (1974). Schistosomiasis mansoni in Yemeni in California: duration of infection, presence of disease, therapeutic management. *The American Journal of Tropical Medicine and Hygiene*, *23*(5), 902–909. Retrieved from http://www.ncbi.nlm.nih.gov/pubmed/4451230

Wayman, G. A., Lee, Y.-S., Tokumitsu, H., Silva, A., & Soderling, T. R. (2008). Calmodulin-Kinases: Modulators of Neuronal Development and Plasticity. *Neuron*, *59*(6), 914–931.

https://doi.org/10.1016/j.neuron.2008.08.021

Webster, B. L., Diaw, O. T., Seye, M. M., Webster, J. P., & Rollinson, D. (2013). Introgressive Hybridization of Schistosoma haematobium Group Species in Senegal: Species Barrier Break Down between Ruminant and Human Schistosomes. *PLoS Neglected Tropical Diseases*, *7*(4), e2110. https://doi.org/10.1371/journal.pntd.0002110

Webster, B. L., Southgate, V. R., Timothy, D., & Littlewood, J. (2006). A revision of the interrelationships of Schistosoma including the recently described Schistosoma guineensis. *International Journal for Parasitology*, *36*(8), 947–955. https://doi.org/10.1016/j.ijpara.2006.03.005

Wehrens, X. H. T., Lehnart, S. E., Reiken, S. R., & Marks, A. R. (2004). Ca $^{2+}$ /Calmodulin-Dependent Protein Kinase II Phosphorylation Regulates the Cardiac Ryanodine Receptor. *Circulation Research*, *94*(6). https://doi.org/10.1161/01.RES.0000125626.33738.E2

WHO. (2006). Preventive in human helminthiasis chemotherapy Coordinated use of anthelminthic drugs in control interventions: a manual for health professionals and programme managers in human helminthiasis. Retrieved from http://apps.who.int/iris/bitstream/handle/10665/43545/9241547103_eng.pdf;jsessionid=895C7F0FB5EF668A1922DD25C77ABF28?sequence=1

Wilson, R. A., Li, X.-H., & Castro-Borges, W. (2016). Do schistosome vaccine trials in mice have an intrinsic flaw that generates spurious protection data? *Parasites & Vectors*, *9*(1), 89. https://doi.org/10.1186/s13071-016-1369-9

Witczak, C. A., Jessen, N., Warro, D. M., Toyoda, T., Fujii, N., Anderson, M. E., … Goodyear, L. J. (2010). CaMKII regulates contraction- but not insulin-induced glucose uptake in mouse skeletal muscle. *American Journal of Physiology-Endocrinology and Metabolism*, *298*(6), E1150–E1160. https://doi.org/10.1152/ajpendo.00659.2009

Wong, M. H., Samal, A. B., Lee, M., Vlach, J., Novikov, N., Niedziela-Majka, A., … Papalia, G. A. (2019). The KN-93 Molecule Inhibits Calcium/Calmodulin-Dependent Protein Kinase II (CaMKII) Activity by Binding to Ca2+/CaM. *Journal of Molecular Biology*. https://doi.org/10.1016/J.JMB.2019.02.001

Wu, W., Wang, W., & Huang, Y. (2011). New insight into praziquantel against various developmental stages of schistosomes. *Parasitology Research*, *109*(6), 1501–1507. https://doi.org/10.1007/s00436-011-2670-3

Xiao, S. H., Catto, B. A., & Webster, L. T. (1985). Effects of praziquantel on different developmental stages of Schistosoma mansoni in vitro and in vivo. *The Journal of Infectious Diseases*, *151*(6), 1130–1137. Retrieved from

http://www.ncbi.nlm.nih.gov/pubmed/3998507

Xiao, S., Xue, J., & Zhang, H. (2012). Further studies on mefloquine and praziquantel alone or interaction of both drugs against Schistosoma japonicum in vitro. *Parasitology Research*, *110*(3), 1239–1248. https://doi.org/10.1007/s00436-011-2621-z

Yan, J.-Z., Xu, Z., Ren, S.-Q., Hu, B., Yao, W., Wang, S.-H., … Lu, W. (2011). Protein Kinase C Promotes *N* -Methyl-d-aspartate (NMDA) Receptor Trafficking by Indirectly Triggering Calcium/Calmodulin-dependent Protein Kinase II (CaMKII) Autophosphorylation. *Journal of Biological Chemistry*, *286*(28), 25187–25200. https://doi.org/10.1074/jbc.M110.192708

Yan, Y., Tulasne, D., Browaeys, E., Cailliau, K., Khayath, N., Pierce, R. J., … Dissous, C. (2007). Molecular cloning and characterisation of SmSLK, a novel Ste20-like kinase in Schistosoma mansoni. *International Journal for Parasitology*, *37*(14), 1539–1550. https://doi.org/10.1016/j.ijpara.2007.06.001

Yang, M.-R., Zhang, Y., Wu, X.-X., & Chen, W. (2016). Critical genes of hepatocellular carcinoma revealed by network and module analysis of RNA-seq data. *European Review for Medical and Pharmacological Sciences*, *20*(20), 4248–4256. Retrieved from http://www.ncbi.nlm.nih.gov/pubmed/27831650

You, H., Gobert, G. N., Jones, M. K., Zhang, W., & McManus, D. P. (2011). Signalling pathways and the host-parasite relationship: putative targets for control interventions against schistosomiasis: signalling pathways and future anti-schistosome therapies. *BioEssays : News and Reviews in Molecular, Cellular and Developmental Biology*, *33*(3), 203–214. https://doi.org/10.1002/bies.201000077

You, H., & McManus, D. P. (2018). Vaccines and diagnostics for zoonotic schistosomiasis japonica. https://doi.org/10.1017/S0031182014001310

You, H., McManus, D. P., Hu, W., Smout, M. J., Brindley, P. J., & Gobert, G. N. (2013a). Transcriptional responses of in vivo praziquantel exposure in schistosomes identifies a functional role for calcium signalling pathway member CamKII. *PLoS Pathogens*, *9*(3), e1003254. https://doi.org/10.1371/journal.ppat.1003254

You, H., McManus, D. P., Hu, W., Smout, M. J., Brindley, P. J., & Gobert, G. N. (2013b). Transcriptional responses of in vivo praziquantel exposure in schistosomes identifies a functional role for calcium signalling pathway member CamKII. *PLoS Pathogens*, *9*(3), e1003254. https://doi.org/10.1371/journal.ppat.1003254

You J. Q., Yue W. J., Xiao X. H. (1986) Effect of praziquantel *in vitro* on different developmental stages of *Schistosoma japonicum*. *Acta Pharmacol Sin* 7:82–84

Young, N. D., Jex, A. R., Li, B., Liu, S., Yang, L., Xiong, Z., … Gasser, R. B. (2012). Whole-genome sequence of Schistosoma haematobium. *Nature Genetics*, *44*(2), 221–225. https://doi.org/10.1038/ng.1065

Yu, Y., Anjum, R., Kubota, K., Rush, J., Villen, J., & Gygi, S. P. (2009). A site-specific, multiplexed kinase activity assay using stable-isotope dilution and high-resolution mass spectrometry. *Proceedings of the National Academy of Sciences*, *106*(28), 11606–11611. https://doi.org/10.1073/pnas.0905165106

Zhang, M., Hong, Y., Han, Y., Han, H., Peng, J., Qiu, C., … Lin, J. (2013). Proteomic Analysis of Tegument-Exposed Proteins of Female and Male Schistosoma japonicum Worms. *Journal of Proteome Research*, *12*(11), 5260–5270. https://doi.org/10.1021/pr400476a

Zhang, X., & Zeng, Y. (2011). Performing Custom MicroRNA Microarray Experiments. *Journal of Visualized Experiments*, (56), e3250. https://doi.org/10.3791/3250

Zhao, Y., & Jensen, O. N. (2009). Modification-specific proteomics: strategies for characterization of post-translational modifications using enrichment techniques. *Proteomics*, *9*(20), 4632–4641. https://doi.org/10.1002/pmic.200900398

Zhou, Y. Zheng, H. Liu, F. Hu, W. (2009). The Schistosoma japonicum genome reveals features of host-parasite interplay. *Nature*, *460*(7253), 345–351. https://doi.org/10.1038/nature08140